Immune inhibitory receptors in blood and barrier tissues

conveyers of context

Helen J. von Richthofen

Immune inhibitory receptors in blood and barrier tissues

conveyers of context

Helen Juliette von Richthofen

Immune inhibitory receptors in blood and barrier tissues
conveyers of context

Remmende immuun receptoren in bloed en barrièreweefsels
(met een samenvatting in het Nederlands)

Proefschrift

ter verkrijging van de graad van doctor aan de
Universiteit Utrecht
op gezag van de
rector magnificus, prof.dr. H.R.B.M. Kummeling,
ingevolge het besluit van het college voor promoties
in het openbaar te verdedigen op

woensdag 28 juni 2023 des middags te 12.15 uur

door

Helen Juliette von Richthofen

geboren op 16 februari 1989
te Berlin-Wilmersdorf, Duitsland

Promotor

Prof. dr. L. Meyaard

Beoordelingscommissie

Prof. dr. J.C. Clevers
Prof. M.G. Netea
Prof. dr. B. Oldenburg (voorzitter)
Prof. dr. J.A.G. van Strijp
Prof. dr. F. van Wijk

Table of contents

CHAPTER **1**

General introduction

The basis of an appropriate immune response lies in the ability of the immune system to distinguish between self and non-self, or between safety and danger (1, 2). Danger can comprise an invading pathogen, excessive tissue damage, or the formation of malignant cells. These events are signaled by pathogen- or danger-associated molecular patterns (PAMPs/DAMPs) or by cognate antigens, which are respectively recognized by pattern recognition receptors (PRRs) of the innate immune system or by antigen-specific T or B cell receptors of the adaptive immune system. On the other hand, safety can comprise the presence of commensal microbes, homeostatic tissue renewal, or an intact extracellular matrix. An incorrect distinction between danger and safety has detrimental consequences, as indicated by a variety of immunological disorders: for example, in case of cancer, the immune system fails to recognize dangerous, malignant cells. Conversely, in case of autoimmune disease, the immune system is activated despite a safe situation, and immune-mediated pathology becomes the primary disease symptom (3). Thus, a correct distinction between danger and safety is of pivotal importance to maintain health.

One might argue that the distinction between danger and safety could be made by only regulating the signaling strength of activating immune receptors. For example, immune activating receptors will sense an increase in PAMPs when a pathogen invades host tissue, which in turn induces an immune response to eradicate the pathogen. Still, there are situations in which the distinction between danger and safety is not so easily made. For instance, a pathogenic and a commensal microbe both express PAMPs that bind to immune-activating PRRs, but the continuous colonization of host barrier tissues with commensal microbes should not lead to inflammation (4). This suggests that additional mechanisms are in place to regulate immune responses during situations of safety. Indeed, some of these mechanisms include the expression of MHC-I on host cells to prevent killing by NK cells (5) or the secretion of anti-inflammatory cytokines by regulatory T cells to actively suppress the immune response against commensal bacteria (6, 7). Together, this exemplifies that signaling of safety is an active process, rather than a mere absence of danger signaling.

Nonetheless, a knowledge gap exists on how the immune system makes the distinction between safety and danger, and on how this information is translated to a dampened immune response. One mechanism through which the immune system inhibits immune responses is via the expression of immune inhibitory receptors (8). These receptors are transmembrane proteins that usually contain one or more immunoreceptor tyrosine-based inhibitory motifs (ITIMs) in their intracellular tail, with V/L/I/SxYxxV/L/I as consensus sequence. Upon receptor ligation, the tyrosine within

the ITIM is phosphorylated by Src family kinases (SFKs). This, in turn, allows docking and activation of inhibitory effectors that contain a Src homology 2 (SH2) domain, such as SH2 domain-containing phosphatases 1 and 2 (SHP-1, SHP-2), SH2 domain-containing inositol phosphatase (SHIP1) or C-terminal Src kinase (Csk) (9-11). These effectors deactivate the signaling components of activating receptors and thereby dampen immune activation (Fig 1).
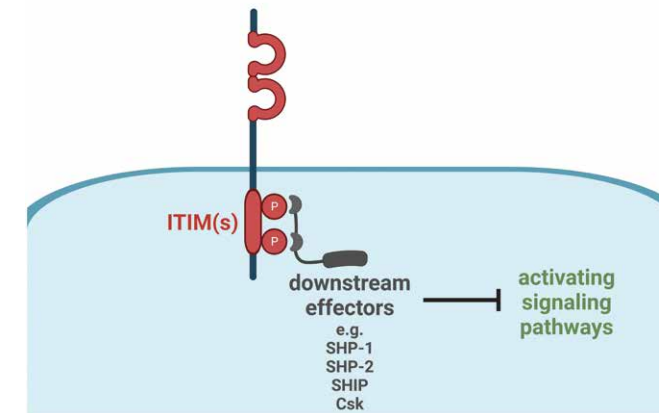
Figure 1. Signaling pathway of inhibitory receptors.
Upon receptor ligation, the central tyrosine(s) within the ITIM(s) of an inhibitory receptor become(s) phosphorylated. This leads to recruitment of downstream effectors such as SHP-1, SHP-2, SHIP or Csk, which in turn inhibit the signaling pathways of other (activating) receptors. Created with BioRender.com .

Our group recently proposed that inhibitory receptors can be divided in functional categories based on receptor expression, and used mathematical modeling to test the benefit of these inhibitory receptor categories compared to a system without inhibitory receptors (12). In brief, these models suggest that receptors which are upregulated after immune activation (so called negative feedback receptors) can mediate pathogen clearance with less effector functions due to timely inhibition of the activation signal. Receptors that are constitutively expressed (so called threshold receptors) set a threshold for immune activation, and in this way distinguish signal from noise to prevent unnecessary immune response. Lastly, receptors that are downregulated upon activation (so called disinhibition receptors) mediate faster pathogen clearance by allowing a cell to respond more strongly after the initial activation threshold has been exceeded. Even though these functional outcomes

remain to be confirmed experimentally, they suggest that the expression pattern of an inhibitory receptor can give important clues towards its biological function.

The importance of inhibitory receptors as immune regulators is illustrated by the finding that some pathogens and malignancies express ligands of inhibitory receptors to evade eradication by the immune system (13, 14). This characteristic forms the basis for the therapeutic effect of checkpoint inhibitors, which are (mostly) antagonistic antibodies that block inhibitory receptors to restore the antitumor response of the immune system (14). Checkpoint inhibitors have revolutionized anti-cancer therapy in the last decade, although many types of malignancies remain poorly responsive to checkpoint inhibitors. In addition, many patients develop severe immune-related adverse events as a result of the treatment (15). This again underscores the importance of a balanced immune response for health.

As of now, more than sixty inhibitory receptors have been characterized (12). One of these is Signal inhibitory receptor on leukocytes-1 (SIRL-1), which is expressed on human monocytes and granulocytes in peripheral blood (16, 17). SIRL-1 has two intracellular ITIMs, which recruit SHP-1 and SHP-2 upon receptor ligation (16). Antibody-mediated ligation of SIRL-1 dampens antimicrobial functions, such as production of reactive oxygen species (ROS) (17-19) and NETosis (19, 20). The gene encoding SIRL-1, *VSTM1*, contains the polymorphism rs612529T/C in its promoter region. In individuals homozygous for the minor allele (C/C) of this polymorphism, SIRL-1 expression on monocytes is almost completely absent, while SIRL-1 expression on granulocytes does not associate with rs612529 (17). Importantly, the genotype of rs612529 directly correlates with the function of SIRL-1 on monocytes: in individuals with rs612529C/C genotype, SIRL-1-mediated inhibition of ROS production by monocytes is strongly hampered compared to individuals with rs612529 T/T genotype (17). Notably, rs612529 also associates with a modest but significantly increased risk of the inflammatory skin disease atopic dermatitis (AD) (17), suggestive that absence of SIRL-1 on monocytes may contribute to skin inflammation in AD. SIRL-1 also has potential soluble forms: SIRL-1 is rapidly downregulated upon cell activation *in vitro*, which might be the result of ectodomain shedding (18). In addition, SIRL-1 has a soluble splice isoform named VSTM1-v2 (21, 22). Recombinant VSTM1-v2 has been shown to enhance Th17 cell differentiation of purified CD4^{+} T cells (22), but direct binding of VSTM1-v2 to CD4^{+} T cells has not yet been assessed. Many aspects of the biology of SIRL-1 remain unidentified, such as its expression in tissues, the identity of its ligands, and the context in which it meets its ligands.

Many questions also remain on the function of inhibitory receptors as a collective. In which contexts or tissues does regulation by inhibitory receptors primarily play a role? And can inhibitory receptors be used to distinguish safety from danger, and if so, how?

Aim and scope of this thesis

In the first part of this thesis we focus on different aspects of the biology of SIRL-1. In **Chapter 2**, we investigate the expression of SIRL-1 on phagocyte subsets in barrier tissues, including the skin, intestine and lungs. In addition, we test the influence of rs612529 on SIRL-1 expression in these immune cell subsets. In **Chapter 3**, we identify a group of endogenous ligands for SIRL-1 and show the functional relevance of this interaction. In **Chapter 4**, we identify microbial and endogenous ligands for SIRL-1 with high structural similarity. On the basis of these findings, we conclude that SIRL-1 is an inhibitory receptor that recognizes molecular patterns. In **Chapter 5**, we delve into the release of SIRL-1 from activated cells, and show that this involves the cleavage of SIRL-1 via ectodomain shedding. In **Chapter 6**, we follow up on the findings that VSTM1-v2 induces Th17 differentiation, and investigate whether VSTM1-v2 can bind directly to T cells.

Then, we proceed to address the characteristics of inhibitory receptors more collectively. Prompted by the finding that SIRL-1 recognizes molecular patterns, we review literature in **Chapter 7** to explore the recognition of molecular patterns by inhibitory receptors. We also formulate a hypothesis on tissue-dependent regulation by inhibitory receptors. In **Chapter 8**, we review the functions of inhibitory receptors outside of the immune system, leading to the proposal that inhibitory receptors provide context to non-hematopoietic cells. In **Chapter 9**, we discuss the overall findings of this thesis and give directions for future research.

References

1. Matzinger P. The danger model: a renewed sense of self. Science. 2002;296(5566):301-5.

2. Medzhitov R, Janeway CA, Jr. Decoding the patterns of self and nonself by the innate immune system. Science. 2002;296(5566):298-300.

3. Sakowska J, Arcimowicz L, Jankowiak M, Papak I, Markiewicz A, Dziubek K, et al. Autoimmunity and Cancer-Two Sides of the Same Coin. Front Immunol. 2022;13:793234.

4. McClure R, Massari P. TLR-Dependent Human Mucosal Epithelial Cell Responses to Microbial Pathogens. Front Immunol. 2014;5:386.

5. Yokoyama WM, Kim S. How do natural killer cells find self to achieve tolerance? Immunity. 2006;24(3):249-57.

6. Vignali DAA, Collison LW, Workman CJ. How regulatory T cells work. Nat Rev Immunol. 2008;8(7):523-32.

7. Nutsch KM, Hsieh CS. T cell tolerance and immunity to commensal bacteria. Curr Opin Immunol. 2012;24(4):385-91.

8. Ravetch JV, Lanier LL. Immune inhibitory receptors. Science. 2000;290(5489):84-9.

9. Daeron M, Jaeger S, Du Pasquier L, Vivier E. Immunoreceptor tyrosine-based inhibition motifs: a quest in the past and future. Immunol Rev. 2008;224:11-43.

10. Verbrugge A, Rijkers ES, de Ruiter T, Meyaard L. Leukocyte-associated Ig-like receptor-1 has SH2 domain-containing phosphatase-independent function and recruits C-terminal Src kinase. Eur J Immunol. 2006;36(1):190-8.

11. Sayos J, Martinez-Barriocanal A, Kitzig F, Bellon T, Lopez-Botet M. Recruitment of C-terminal Src kinase by the leukocyte inhibitory receptor CD85j. Biochem Biophys Res Commun. 2004;324(2):640-7.

12. Rumpret M, Drylewicz J, Ackermans LJE, Borghans JAM, Medzhitov R, Meyaard L. Functional categories of immune inhibitory receptors. Nat Rev Immunol. 2020;20(12):771-80.

13. Van Avondt K, van Sorge NM, Meyaard L. Bacterial immune evasion through manipulation of host inhibitory immune signaling. PLoS Pathog. 2015;11(3):e1004644.

14. Ribas A, Wolchok JD. Cancer immunotherapy using checkpoint blockade. Science. 2018;359(6382):1350-5.

15. Johnson DB, Nebhan CA, Moslehi JJ, Balko JM. Immune-checkpoint inhibitors: long-term implications of toxicity. Nat Rev Clin Oncol. 2022;19(4):254-67.

16. Steevels TAM, Lebbink RJ, Westerlaken GHA, Coffer PJ, Meyaard L. Signal Inhibitory Receptor on Leukocytes-1 (SIRL-1) is a novel functional inhibitory immune receptor expressed on human phagocytes. J Immunol. 2010;184:4741-8.

17. Kumar D, Puan KJ, Andiappan AK, Lee B, Westerlaken GH, Haase D, et al. A functional SNP associated with atopic dermatitis controls cell type-specific methylation of the VSTM1 gene locus. Genome Med. 2017;9(1):18.

18. Steevels TA, van Avondt K, Westerlaken GH, Walk J, Bont L, Coffer PJ, et al. Signal Inhibitory Receptor on Leukocytes-1 (SIRL-1) negatively regulates the oxidative burst in human phagocytes. Eur J Immunol. 2013;43:1297-308.

19. Besteman SB, Callaghan A, Hennus MP, Westerlaken GHA, Meyaard L, Bont LL. Signal inhibitory receptor on leukocytes (SIRL)-1 and leukocyte- associated immunoglobulin-like receptor (LAIR)-1 regulate neutrophil function in infants. Clin Immunol. 2020;211:108324.

20. Van Avondt K, van der Linden M, Naccache PH, Egan DA, Meyaard L. Signal Inhibitory Receptor on Leukocytes-1 Limits the Formation of Neutrophil Extracellular Traps, but Preserves Intracellular Bacterial Killing. J Immunol. 2016;196(9):3686-94.

21. Wang D, Li Y, Liu Y, He Y, Shi G. Expression of VSTM1-v2 Is Increased in Peripheral Blood Mononuclear Cells from Patients with Rheumatoid Arthritis and Is Correlated with Disease Activity. PLoS One. 2016;11(1):e0146805.

22. Guo X, Zhang Y, Wang P, Li T, Fu W, Mo X, et al. VSTM1-v2, a novel soluble glycoprotein, promotes the differentiation and activation of Th17 cells. Cell Immunol. 2012;278(1-2):136-42.

CHAPTER **2**

Signal Inhibitory Receptor on Leukocytes-1 is highly expressed on lung monocytes, but absent on mononuclear phagocytes in skin and colon

Helen J. von Richthofen[1,2], **Doron Gollnast**[1,2], **Toni M.M. van Capel**[3],
Barbara Giovannone[1,4], **Geertje H.A. Westerlaken**[1,2],
Lisanne Lutter[1,5], **Bas Oldenburg**[5], **DirkJan Hijnen**[1,4,6,7],
Michiel van der Vlist[1,2], **Esther C. de Jong**[3], **Linde Meyaard**[1,2,]

[1] Center for Translational Immunology, University Medical Center Utrecht,
   Lundlaan 6, 3584 EA, Utrecht, The Netherlands
[2] Oncode Institute, University Medical Center Utrecht, Lundlaan 6,
   3584 EA, Utrecht, The Netherlands
[3] Department of Experimental Immunology, Amsterdam University Medical
   Center, Meibergdreef 15, 1105 AZ Amsterdam, The Netherlands
[4] Department of Dermatology and Allergology, University Medical Center
   Utrecht, Heidelberglaan 100, 3584 CX, Utrecht, The Netherlands
[5] Department of Gastroenterology and Hepatology, University Medical
   Center Utrecht, Heidelberglaan 100, 3584 CX, Utrecht, The Netherlands
[6] Department of Dermatology, Diakonessenhuis Utrecht, Bosboomstraat 1,
   3582 KE, Utrecht, The Netherlands
[7] Present address: Department of Dermatology, Erasmus MC,
   Dr. Molewaterplein 40, 3015 GD, Rotterdam, The Netherlands

14   CHAPTER 2

15   SIGNAL INHIBITORY RECEPTOR ON LEUKOCYTES-1 IS HIGHLY EXPRESSED ON LUNG
   MONOCYTES, BUT ABSENT ON MONONUCLEAR PHAGOCYTES IN SKIN AND COLON

Abstract

Signal Inhibitory Receptor on Leukocytes-1 (SIRL-1) is expressed on human blood monocytes and granulocytes and inhibits myeloid effector functions. On monocytes, but not granulocytes, SIRL-1 expression is low or absent in individuals with the single nucleotide polymorphism (SNP) rs612529C. The expression of SIRL-1 in tissue and the influence of rs612529 hereon is currently unknown. Here, we used flow cytometry to determine SIRL-1 expression on immune cells in human blood and three barrier tissues; skin, colon and lung. SIRL-1 was expressed by virtually all neutrophils and eosinophils in these tissues. In contrast, SIRL-1 was not expressed by monocyte-derived cells in skin and colon, whereas it was highly expressed by lung classical monocytes. Lung monocytes from individuals with a rs612529C allele had decreased SIRL-1 expression, consistent with the genotype association in blood. Within the different monocyte subsets in blood and lung, SIRL-1 expression was highest in classical monocytes and lowest in nonclassical monocytes. SIRL-1 was not expressed by dendritic cells in blood and barrier tissues. Together, these results indicate that SIRL-1 is differentially expressed on phagocyte subsets in blood and barrier tissues, and that its expression on monocytes is genotype- and tissue-specific. Immune regulation of monocytes by SIRL-1 may be of particular importance in the lung.

Introduction

Phagocytes, a heterogeneous cell population including mononuclear phagocytes and polymorphonuclear granulocytes, play a crucial role in the host defense at barrier tissues. Phagocytes internalize and process invading pathogens, and thereby contribute directly to pathogen clearance as well as to activation of the adaptive immune response via antigen presentation (1, 2). However, the defense mechanisms of phagocytes can also be harmful to the host. For example, excessive production of Reactive Oxygen Species (ROS) by phagocytes causes tissue injury and has been implicated in the pathogenesis of several inflammatory diseases, such as pulmonary fibrosis, atherosclerosis and atopic dermatitis (AD) (3, 4). Therefore, the activity of phagocytes needs to be tightly regulated.

Phagocytes are regulated, among others, by inhibitory receptors, also known as immune checkpoints. These receptors inhibit several phagocyte effector functions, including ROS production, cytokine production and phagocytosis (5). Most inhibitory receptors relay inhibitory signals via immunoreceptor tyrosine-based inhibitory motifs (ITIMs) in the intracellular tail (6). The expression pattern of immune inhibitory receptors varies: receptors can be widely expressed or restricted to specific cell types, tissues or activation states. For example, the inhibitory collagen receptor LAIR-1 is constitutively expressed on most lymphocytes (7), but on neutrophils it is only expressed upon activation and in inflamed tissue (8). The expression pattern of a receptor is pivotal for its biology, as it dictates where and when the receptor can exert its function.

We have previously identified Signal Inhibitory Receptor on Leukocytes-1 (SIRL-1) as an ITIM-bearing inhibitory receptor that is expressed on circulating human monocytes and granulocytes, but absent on lymphoid cells (9-11). Crosslinking of SIRL-1 with an agonistic antibody inhibits Fc Receptor (FcR) induced ROS production (10, 12, 13) and neutrophil extracellular trap (NET) formation (12, 14). The gene encoding SIRL-1, *VSTM1*, contains a single nucleotide polymorphism (SNP) rs612529T/C in its promoter region that dictates expression (Frequency of C-allele: in Caucasians 15.8%, in Chinese 36.7%, in Japanese 25.6% (10)). In individuals with rs612529C/C genotype, SIRL-1 expression on monocytes is almost completely absent, whereas SIRL-1 expression on granulocytes does not associate with rs612529 (10). rs612529C also associates with an increased risk at AD (10).

Even though SIRL-1 expression has been well characterized on peripheral blood granulocytes and monocytes, SIRL-1 expression in barrier tissues and the influence of rs612529 hereon is currently unknown. In this study, we used flow cytometry, cell sorting and qRT-PCR to examine SIRL-1 expression on human phagocytes in peripheral blood and in the barrier tissues skin, colon, and lung. We show that SIRL-1 is expressed on granulocytes in these tissues, but that SIRL-1 expression on mononuclear phagocytes differs between tissues and cell types.

Materials and methods

Tissue source
Peripheral blood was obtained from healthy volunteers. Healthy skin from Caucasian donors was obtained from discarded material after cosmetic abdominal or breast reduction surgery. AD patient skin was obtained from 4 mm punch biopsies from lesional skin, non-lesional skin, and non-lesional skin 24h after the initiation of an atopy patch test (APT). APT was performed by application of house dust mite extract to the patients' back, as previously described (15). Colon biopsies were obtained from Ulcerative Colitis or Crohn's disease patients who were in remission for at least four years. Lung tissue was obtained from lung cancer patients during surgical tumor removal; for this study a piece of non-malignant tissue was used. All samples were collected in accordance with the Institutional Review Board of the University Medical Center (UMC) Utrecht and Amsterdam UMC.

PBMC isolation
PBMCs were isolated by density gradient centrifugation of sodium-heparinized peripheral blood over Ficoll-Paque (Amersham Biosciences). PBMCs were washed and suspended in PBS containing 2% (v/v) heat-inactivated fetal calf serum (FCS; Sigma-Aldrich) before further use.

Digestion of skin tissue
For flow cytometric analysis, healthy whole skin was digested with a Whole Skin Dissociation Kit (Miltenyi) according to manufacturer's instructions, using overnight incubation without Enzyme P.

For qRT-PCR analysis of sorted healthy skin cell populations, dermis and epidermis were digested separately. Skin was shaved with a dermatome to get the upper 0.3 mm, washed with PBS, and incubated 5 minutes with 100 mg/mL gentamycin (Duchefa) to kill bacteria. Skin was incubated overnight at 4°C with 0.2% (w/v) dispase II (Roche)

to separate dermis and epidermis. Dermis was digested for 1.5h in IMDM (Lonza) supplemented with 0.5% (w/v) collagenase D (Sigma-Aldrich), 30 U/mL DNAse-I (Roche) and 1% (v/v) FCS. Epidermis was digested for 0.5h in PBS supplemented with 0.25% (w/v) Trypsin (Invitrogen) and 0.2% EDTA (Invitrogen). Both digestions were performed at 37°C under gentle agitation, and quenched by adding FCS. Single cell suspensions were obtained by thorough vortexing and filtering of the cells over a single cell filter chamber and a 70 μm cell strainer. Next, epidermal cells were treated with 12 U/mL DNAse-I and again filtered over a 70 μm cell strainer, followed by Ficoll gradient centrifugation and harvesting of cells from the interphase. Finally, epidermal and dermal cells were washed and suspended in FACS buffer (PBS supplemented with 2% (v/v) FSC, 1% (w/v) bovine serum albumin (BSA; Sigma-Aldrich), 1% (v/v) human serum (HS; Sigma-Aldrich) and 0.1% (v/v) sodium azide) before further use.

Digestion of colon tissue
Biopsies from the colon were collected in ice-cold Hank's Balanced Salt Solution (HBSS; Gibco) supplemented with 2% (v/v) FCS, 1% (v/v) penicillin-streptomycin (PS; Gibco) and 1% (v/v) Amphotericin B (Gibco). Next, 1 mM DTT (Sigma-Aldrich) was added to the solution and the biopsy was incubated 10 minutes at 4°C under gentle agitation. After thorough vortexing and one wash with supplemented HBSS, the biopsy was digested with 1 mg/mL collagenase IV (Sigma-Aldrich) in supplemented RPMI 1640 (10% FCS, 1% PS, 1% Amphotericin B), for 1h at 37°C under gentle agitation. The biopsy was suspended by pressing it through a 18.5-19G needle and a 70 μm cell strainer. Cells were then washed and suspended in supplemented RPMI 1640 before further use.

Digestion of lung tissue
Lung biopsies were rinsed with PBS, cut thoroughly, and digested in IMDM supplemented with 125 ug/mL liberase (Roche), 100 ug/mL DNAse-I and 5% (v/v) HS, for 45 minutes at 37°C or overnight at 4°C. The digestion was quenched with FCS, and a single cell suspension was obtained by vortexing and filtering of the cells over a 70 μm cell strainer. Erythrocytes were lysed by incubation with erythrocyte lysis buffer (containing 0.155 mM NH_4Cl (Sigma-Aldrich), 1 mM $KHCO_3$ (Merck KGaA), and 80 μM EDTA) for 10 minutes on ice. After one wash with PBS and one wash with MACS buffer (PBS supplemented with 0.5% BSA, 2% FCS, 1% HS and 2 mM EDTA), cells were frozen in HBSS with 50% (v/v) FCS and 10% (v/v) DMSO (Sigma-Aldrich) and stored in liquid N_2. Before flow cytometry, cells were thawed by drop wise addition of HBSS with 10% (v/v) FCS and washing with MACS buffer.

Flow cytometry and cell sorting

Cells were incubated with 5% (v/v) mouse serum (Equitech-Bio) in PBS to block aspecific binding by Fc receptors. For cells from digested tissue, this incubation was combined with viability dye APC-eFluor 780 (eBioscience). Subsequently, cells were stained with fluorochrome-conjugated antibodies diluted in Brilliant Stain buffer (BD Biosciences), see Supplementary Table 1 for an overview of the antibodies used. Flow cytometry was performed on an LSRFortessa (BD Biosciences); cell sorting was performed on a FACSAria III (BD Biosciences). Data were analyzed using FlowJo software (Treestar, Ashland, OR). Cell subsets were gated based on their typical surface marker expression ((1, 16, 17), see Supplementary Fig 1-4 for the gating strategy used)

qRT-PCR

Sorted cells from the skin were collected in FACS buffer, centrifuged and taken up in 350 µl RTL buffer (Qiagen) supplemented with 0.14 M 2-mercaptoethanol (Sigma-Aldrich). RNA was isolated with the RNeasy mini KiT (Qiagen) and cDNA was synthesized with the iScript reverse transcription kit (Bio-Rad). Subsequently, qRT-PCR was performed with SYBR Select Master Mix (Life Technologies) on 10 ng cDNA input per reaction on a QuantStudio 12K Flex (Applied Biosystems). Primers were used that specifically amplify VSTM1-v1, the primary splice form that encodes membrane-bound SIRL-1. SIRL-1 mRNA expression was represented relative to GAPDH expression, using the formula 'relative expression = $2^{\wedge}(Ct(average\ of\ reference\ genes)-Ct(target))$.

Target	Forward primer	Reverse primer
VSTM1-v1 (SIRL-1)	gacaacagcctcccatgagt	tgaagatggcgacaaagatg
GAPDH	agaaggctggggctcattt	gaggcattgctgatgatcttg

Genotyping

DNA was isolated with the DNA Extract All Reagents Kit (Thermo Fisher Scientific). The genotype of rs612529 was determined using a TaqMan SNP Genotyping Assay and TaqMan GTXpress Master mix (Thermo Fisher Scientific). All procedures were performed according to manufacturer's instructions.

Immunohistochemistry

Whole skin cryosections (7 µm) were fixed by immersion in 10% (v/v) Neutral Buffered Formalin (Sigma-Aldrich). Next, slides were incubated for 10 minutes in 0.03% (v/v) hydrogen peroxide (Sigma-Aldrich) and blocked for 20 minutes with 2.5% (v/v) horse serum (ImmPress kit, Vector Laboratories). Slides were stained by a 1h incubation with anti-SIRL-1 (clone 1A5, produced in house (9)), anti-elastase (clone NP57, DAKO) or an isotype control (SouthernBiotech), followed by a 30 minute incubation with horse anti-mouse IgG-HRP (ImmPress kit, Vector Laboratories) and a 10 minute incubation with AEC+ Substrate-Chromogen (DAKO). Slides were counterstained with Mayer's Hematoxylin solution (Sigma-Aldrich) and mounted with Entellan (VWR). Between each step, slides were washed extensively with PBS 0.05% (v/v) Tween-20. All procedures were performed at room temperature. Images were acquired on a Zeiss Axiovision.

Data analysis

Statistical analysis was performed using GraphPad Prism software (version 8.3.0). A mixed-effects model with Sidak's correction for multiple testing was used to compare SIRL-1 expression between peripheral blood mononuclear phagocytes subsets of donors with rs612529T/T genotype. The same test was used to compare SIRL-1 expression between donors with rs612529T/T and rs612529T/C genotypes in each lung phagocyte subset. P values of <0.05 were considered statistically significant. Statistics in the text indicate the percentage of SIRL-1^{+} cells as compared to the isotype control and are reported as mean ± standard deviation.

Results

Monocyte subsets, but not pDCs and cDCs, express SIRL-1 in peripheral blood

We have previously shown that SIRL-1 is highly and homogeneously expressed on peripheral blood neutrophils and eosinophils (8-10, 12, 13, 18). Here, we used flow cytometry to measure SIRL-1 expression on mononuclear phagocyte subsets in peripheral blood (For gating strategy see Supplementary Fig 1). SIRL-1 was expressed by all monocyte subsets, with highest expression on classical (c) monocytes (CD14$^+$CD16$^-$), intermediate expression on intermediate (i) monocytes (CD14$^+$CD16$^+$), and lowest expression on nonclassical (nc) monocytes (CD14^{dim}CD16$^+$) and slanMonocytes, a subset of ncMonocytes (Fig 1A, B). SIRL-1 was absent on plasmacytoid dendritic cells (pDC), CD141$^+$ DCs ('cDC1') and CD1c$^+$ DCs ('cDC2') (Fig 1A, C). However, a subset of CD141$^-$CD1c$^-$ DCs expressed SIRL-1 in all donors (Fig 1A, D). As CD141$^-$CD1c$^-$ DCs are not well described, we backgated these SIRL-1$^+$ DCs (data not shown) and confirmed their correct gating as CD3$^-$CD19$^-$C56$^-$HLA-DR$^+$CD14$^-$CD16$^-$CD11c$^+$CD141$^-$CD1c$^-$ cells (Supplementary Fig 1).

In line with our previous findings (10), we found that SIRL-1 expression was lower on monocytes from a donor with rs612529T/C genotype and absent on monocytes from a donor with rs612529C/C genotype (Fig 1B). The percentage of SIRL-1$^+$ CD141$^-$CD1c$^-$ DCs was not clearly affected by rs612529 (Fig 1D). Taken together, these data show that SIRL-1 is expressed by all monocyte subsets in peripheral blood, but not by cDCs and pDCs.

SIRL-1 is expressed by very few mononuclear phagocytes in the skin

We previously reported that rs612529C associates with an increased risk at AD (10), which led to the hypothesis that low SIRL-1 expression on monocytes or monocyte-derived cells in the skin predisposes for AD. Therefore, we used flow cytometry to examine SIRL-1 expression in healthy human skin (For gating strategy see Supplementary Fig 2). SIRL-1 was not detected on autofluorescent dermal macrophages (MΦ), CD1c$^+$ DCs or CD141$^+$ DCs in the skin (Fig 2A). Low SIRL-1 expression was found on a very small percentage of CD14$^+$ monocyte-derived macrophages (Mo-MΦ) in all four donors with rs612529T/T genotype (2.13 ± 0.54% SIRL-1$^+$ cells). Of note, in CD14$^+$ Mo-MΦ from an individual with rs612529T/C genotype, an even lower percentage of cells expressed SIRL-1 (0.42% SIRL-1$^+$ cells).

Tissue digestion may have altered surface receptor expression, so to validate these results we used qRT-PCR to determine SIRL-1 mRNA levels in sorted mononuclear phagocytes from the skin. Compared to PBMC, SIRL-1 mRNA levels
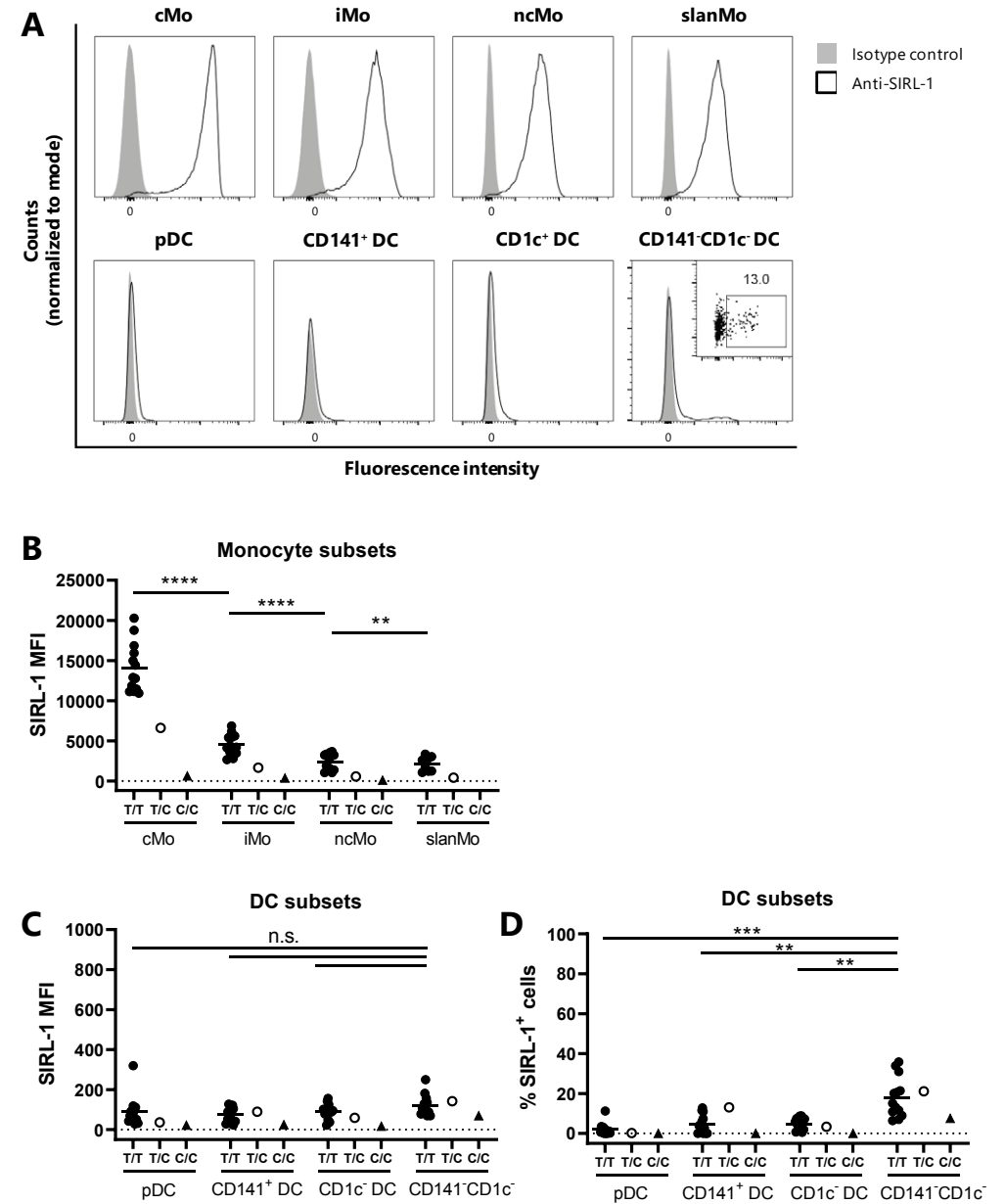
Figure 1. SIRL-1 is expressed on monocyte subsets, but not on pDCs and cDCs in peripheral blood.

PBMCs were isolated from peripheral blood of healthy human donors and analyzed by flow cytometry (See Supplementary Fig. 1 for the gating strategy). **(A)** Panels show representative histograms of the fluorescence intensity of mononuclear phagocyte subsets stained with a SIRL-1 antibody (open histogram) or an isotype control (closed histogram). The dot plot insert of CD141⁻CD1c⁻ DCs shows the fluorescence intensity of anti-SIRL-1 stained cells on the x-axis, and SSC-A on the y-axis. The gate shows the percentage of SIRL-1⁺ cells compared to the isotype control. The donor's genotype is rs612529T/T (n=8-13). **(B-C)** Median fluorescence intensity (MFI) of monocyte subsets (B) and DC subsets (C) stained with a SIRL-1 antibody. **(D)** Percentage of SIRL-1⁺ cells in DC subsets. **(B-D)** Each symbol represents one donor, the bar indicates the mean. Genotypes of rs612529 are indicated with filled circles (T/T, n=13), open circles (T/C, n=1) or filled triangles (C/C, n=1). SlanMo's were analyzed in less donors: T/T, n=8; T/C, n=1; C/C, n=0. A mixed-effects model with Sidak's correction for multiple testing was used to compare SIRL-1 expression between cell subsets of donors with T/T genotype, ****p<0.0001, ***p<0.001, **p<0.01. cMo, classical monocytes; iMo, intermediate monocytes; ncMo, nonclassical monocytes; slanMo, slan monocytes; pDC, plasmacytoid DC.

were approximately 100-fold lower in CD14⁺ Mo-MΦ from donors with rs612529T/T genotype, and levels were 500-1000-fold lower or undetectable in CD14⁺ Mo-MΦ from donors with rs612529T/C genotype and in MΦ, dermal DCs and Langerhans cells (LCs) (Fig 2B). Together, this confirmed that SIRL-1 expression on mononuclear phagocytes in healthy skin is very low or absent, and is lower in CD14⁺ Mo-MΦ from donors with rs612529T/C genotype.

Lastly, we used immunohistochemistry (IHC) to examine SIRL-1 expression in AD skin. No SIRL-1 staining was detectable in healthy skin, AD non-lesional skin, and AD lesional skin, compared to isotype control (Fig 2C). In contrast, several SIRL-1⁺ cells and elastase⁺ granulocytes were found in skin from an AD patient who received an atopy patch test (15) (Fig 2C), suggesting that SIRL-1 may be expressed by skin infiltrating granulocytes.

In summary, we show that SIRL-1 is expressed on a very low number of cells in healthy skin and AD skin.
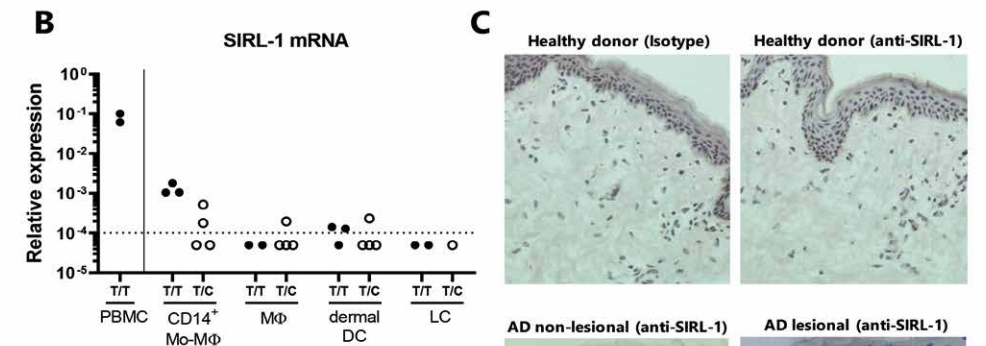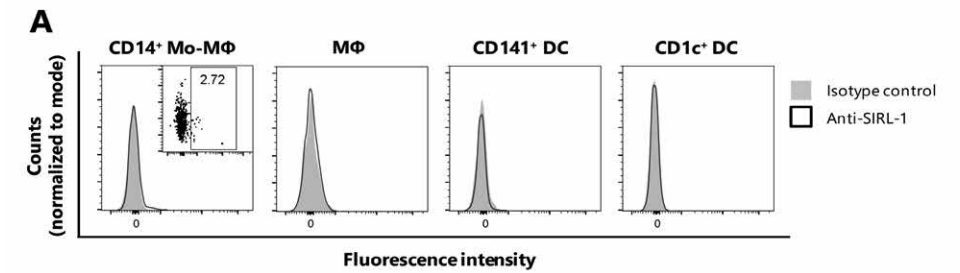

Figure 2. SIRL-1 expression on mononuclear phagocytes in skin is very low or absent.

(A) Healthy human skin biopsies were digested and analyzed by flow cytometry (See Supplementary Fig. 2 for the gating strategy). Panels show representative histograms of the fluorescence intensity of mononuclear phagocyte subsets stained with a SIRL-1 antibody (open histogram) or an isotype control (closed histogram). The dot plot insert of CD14⁺ Mo-MΦ shows the fluorescence intensity of anti-SIRL-1 stained cells on the x-axis, and SSC-A on the y-axis. The gate shows the percentage of SIRL-1⁺ cells compared to the isotype control. The donor's genotype is rs612529T/T (n=4). **(B)** Human skin biopsies were separated into dermis and epidermis, followed by digestion and FACS sorting. mRNA was isolated from the sorted cell subsets and SIRL-1 mRNA expression was analyzed by qRT-PCR. Expression was normalized to GAPDH expression, and expression below the detection limit was set at a value below 10⁻⁴. Each symbol represents one donor. Genotypes of rs612529 are indicated with filled circles (T/T) or open circles (T/C). PBMC, n=2; CD14⁺ Mo-MΦ, n=7; MΦ, n=6, dermal DCs, n=7; LCs, n=3. The vertical line indicates that PBMCs were collected from different donors and used for reference. **(C)** Human skin cryosections were stained for presence of SIRL-1 or elastase. The sections derived from donors with rs612529T/T genotype and include healthy donor skin (upper panels), atopic dermatitis (AD) non-lesional skin (middle left panel), AD lesional skin (middle right panel) or skin from an AD patient that underwent an atopy patch test (APT, lower panels). Shown are representative images of ≥3 donors. Magnification: upper and lower panel 200x, middle panel 400x. PBMC, peripheral blood mononuclear cell; MΦ, macrophage, Mo-MΦ, monocyte-derived macrophage; LC, Langerhans cell.

Eosinophils in the colon express SIRL-1

To investigate SIRL-1 expression in another human barrier tissue, we analyzed cells from a colon biopsy by flow cytometry (For gating strategy see Supplementary Fig 3). Because of varying degrees of background signal in tissue cells, the MFI of anti-SIRL-1 stained cells was normalized by subtracting the MFI of isotype stained cells. As in skin, SIRL-1 was completely absent on CD11c+ DCs and lowly expressed on a small percentage of mature CD206+ MΦ and immature CD206- Mo-MΦ (Fig 3A). More SIRL-1+ cells were found in immature CD206- Mo-MΦ from two donors with rs612529T/T genotype (8.29% and 11.90% SIRL-1+ cells) compared to two donors with rs612529T/C genotype (1.28% and 0% SIRL-1+ cells)

Eosinophils reside in the colon under homeostatic conditions (19). In contrast to mononuclear phagocytes in the colon, SIRL-1 was highly expressed on these colonic eosinophils. This expression was unaffected by rs612529C (Fig 3B), which corresponds with our earlier findings that SIRL-1 expression on blood granulocytes does not associate with rs612529C (10). Together, these results show that in the colon, SIRL-1 is mostly absent on mononuclear phagocytes, but highly expressed on eosinophils.

Lung monocytes express SIRL-1

Lastly, we determined SIRL-1 expression on immune cells in human lung by flow cytometry (for gating strategy see Supplementary Fig 4). In contrast to mononuclear phagocytes in skin and colon, SIRL-1 was highly expressed on lung cMonocytes (CD206- CD14+CD16-) (Fig 4A, B). Similar to blood, SIRL-1 expression was intermediate on iMonocytes and lowest on ncMonocytes (Fig 4B). SIRL-1 expression was significantly lower on lung cMonocytes and ncMonocytes from donors with rs612529T/C genotype compared to donors with rs612529T/T genotype (Fig 4B). SIRL-1 was also expressed by a subset of interstitial macrophages (12.54 ± 10.77% SIRL-1+ cells), but absent on alveolar macrophages, pDCs and CD11c+ DCs (Fig 4A, B).

SIRL-1 was undetectable on mast cells in the lung, but highly expressed by neutrophils and, although at more variable levels, by eosinophils (Fig 4A, C). In line with findings from blood (10) and colon, there was no effect of rs612529C on SIRL-1 expression by neutrophils and eosinophils (Fig 4C). In summary, these results show that SIRL-1 is expressed by subsets of mononuclear phagocytes and granulocytes in the lung.
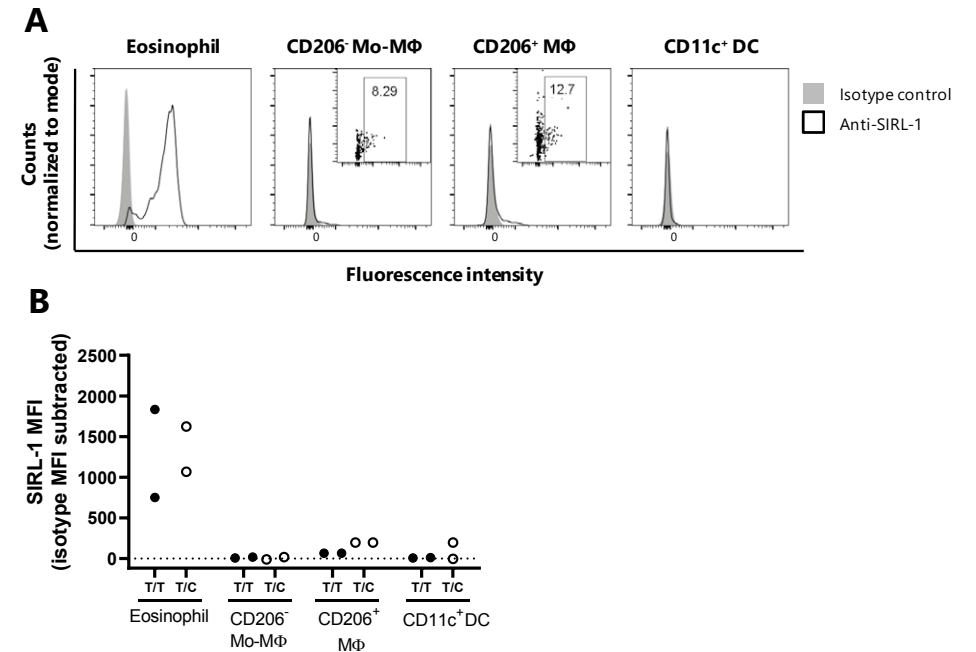
Figure 3. SIRL-1 is expressed by eosinophils in the colon.

Human colon biopsies were digested and analyzed by flow cytometry (See Supplementary Fig. 3 for the gating strategy). **(A)** Panels show representative histograms of the fluorescence intensity of immune cells stained with a SIRL-1 antibody (open histogram) or an isotype control (closed histogram). The dot plot inserts of CD206- Mo-MΦ and CD206+ MΦ show the fluorescence intensity of anti-SIRL-1 stained cells on the x-axis, and SSC-A on the y-axis. The gate shows the percentage of SIRL-1+ cells compared to the isotype control. The donor's genotype is rs612529T/T (n=2). **(B)** Median fluorescence intensity (MFI) of immune cells stained with a SIRL-1 antibody, minus the MFI of cells stained with an isotype control. Each symbol represents one donor, the bar indicates the mean. Genotypes of rs612529 are indicated with filled circles (T/T, n=2) or open circles (T/C, n=2). Mo-MΦ, monocyte-derived macrophage.

SIRL-1 is differentially expressed between non-diseased tissues from the GTEx consortium

The lung tissue in which we examined SIRL-1 expression was derived from lung cancer patients, and malignant tissue might affect SIRL-1 expression in healthy adjacent tissue. Therefore we used the Genotype-Tissue Expression (GTEx) RNA sequencing database of gene expression in non-diseased tissues to analyze *VSTM1* expression (20). *VSTM1* mRNA expression was highest in blood, pituitary gland, spleen, lung and testis, whereas it was mostly absent in colon and skin (Supplementary Fig 5). This corresponds to the SIRL-1 protein expression we found on mononuclear phagocytes in blood, skin, colon and lung, suggesting that the SIRL-1 expression we report is representative for SIRL-1 expression in healthy tissues.
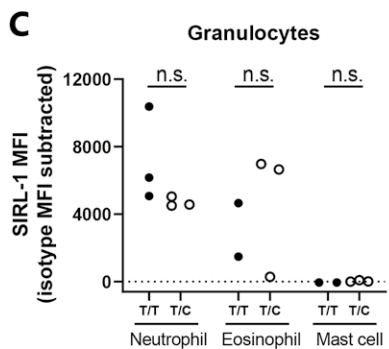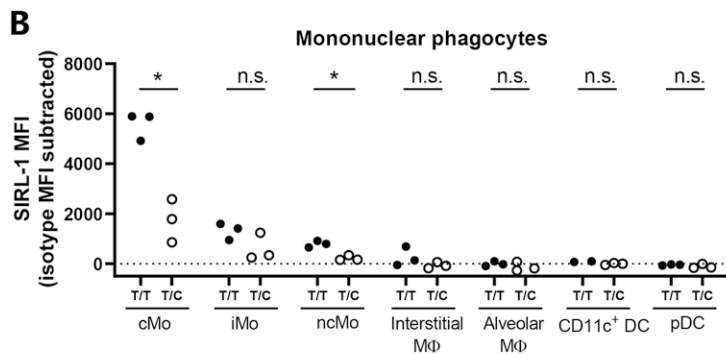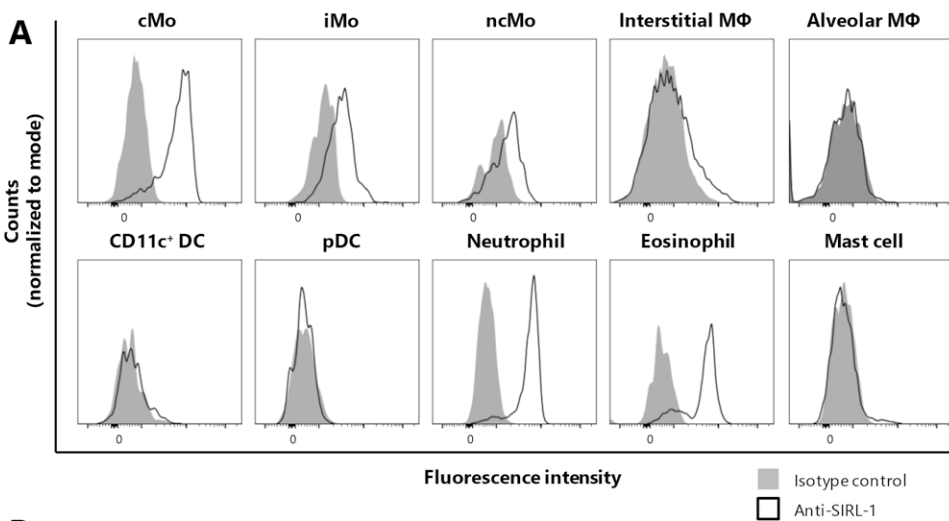
A

cMo | iMo | ncMo | Interstitial MΦ | Alveolar MΦ

CD11c⁺ DC | pDC | Neutrophil | Eosinophil | Mast cell

Counts (normalized to mode)

Fluorescence intensity

Isotype control
Anti-SIRL-1

Figure 4. SIRL-1 is expressed by lung monocytes.

Human lung biopsies were digested and analyzed by flow cytometry (See Supplementary Fig. 4 for the gating strategy). **(A)** Panels show representative histograms of the fluorescence intensity of mononuclear phagocytes and granulocytes stained with a SIRL-1 antibody (open histogram) or an isotype control (closed histogram). The donor's genotype is rs612529T/T (n=3). **(B-C)** Median fluorescence intensity (MFI) of mononuclear phagocytes (B) and granulocytes (C) stained with a SIRL-1 antibody, minus the MFI of the same cell type stained with an isotype control. Each symbol represents one donor, the bar indicates the mean. Genotypes of rs612529 are indicated with filled circles (T/T, n=3) or open circles (T/C, n=3). A mixed-effects model with Sidak's correction for multiple testing was used to compare SIRL-1 expression between donors with rs612529T/T and rs612529T/C genotype in each cell subset, $*p<0.05$. cMo, classical monocytes; iMo, intermediate monocytes; ncMo, nonclassical monocytes; MΦ, macrophage.

B

Mononuclear phagocytes

SIRL-1 MFI (isotype MFI subtracted)

C

Granulocytes

SIRL-1 MFI (isotype MFI subtracted)

Discussion

Phagocytes are pivotal players in host defense, but excessive use of their effector mechanisms can cause immunopathology. Therefore, phagocyte activity is controlled by several mechanisms, including the expression of inhibitory receptors (5). SIRL-1 is a functional inhibitory receptor that is expressed on circulating monocytes and granulocytes (9, 10). Here, SIRL-1 expression was examined in peripheral blood and barrier tissues, including skin, colon and lung. SIRL-1 was expressed by virtually all neutrophils and eosinophils in these barrier tissues. In contrast, SIRL-1 was expressed by few mononuclear phagocytes in skin and colon, yet highly expressed by lung classical monocytes.

SIRL-1 was not expressed on pDCs and cDC subsets in peripheral blood and barrier tissues (Fig 1A, 2A, 3A, 4A). This is in apparent conflict with a previous report, in which we showed SIRL-1 expression by 30% of peripheral blood DCs (9). These outcomes can be explained by different gating strategies that were used to identify DCs. At the time, DCs were defined as HLA-DR$^+$CD14$^-$, without excluding CD16$^+$ cells. However, in recent protein and RNA single-cell analyses, CD16$^+$ DCs were found to be more similar to ncMonocytes (21, 22). Therefore, cells that were previously gated as SIRL-1 positive CD16$^+$ DCs were in this study defined as ncMonocytes. Remarkably, a small subset of CD141$^-$CD1c$^-$ DCs did express SIRL-1 in all donors examined (Fig 1D). These 'double negative' DCs are poorly described in literature, but a single cell RNA sequencing study described a CD141$^-$CD1c$^-$ DC subset in peripheral blood, which were named DC4s (23). However, DC4s expressed CD16 and were therefore in later studies also described as ncMonocytes (21, 22). In contrast, the CD141$^-$CD1c$^-$ DCs we describe here are CD16 negative. Further research is warranted to clarify whether SIRL-1 expressing CD141$^-$CD1c$^-$ DCs are a distinct subset.

We previously reported that rs612529C associates with low SIRL-1 expression on monocytes (10). Here, we extended this into tissue. SIRL-1 expression was significantly lower in lung cMonocytes and ncMonocytes from individuals carrying a rs612529C allele (Fig 4B). A similar trend was observed in CD14$^+$ Mo-MΦ in the skin and immature CD206$^-$ Mo-MΦ in the colon, even though SIRL-1 levels were overall very low in these cells. On eosinophils and neutrophils in colon and lung, SIRL-1 expression was not affected by the genotype of rs612529 (Fig 3B, 4C), which is in correspondence with findings from peripheral blood granulocytes (10).

Notably, rs612529C also associates with an increased risk at AD (10). This association suggests a relationship between rs612529C, abrogated SIRL-1 expression on monocytic

cells, and AD pathogenesis. We hypothesized that SIRL-1 is expressed by skin-resident mononuclear phagocytes, and that abrogation of this expression in individuals with rs612529C genotype leads to lack of inhibitory signaling via SIRL-1. This, in turn, could lead to hyperactivation of skin-resident mononuclear phagocytes and thereby contribute to skin inflammation in AD. However, mononuclear phagocytes in the skin expressed no or very low levels of SIRL-1, in donors from all rs612529 genotypes, which argues against a major role of SIRL-1 in the regulation of these cells in the skin (Fig 2A). Therefore it remains to be elucidated if and how the absence of SIRL-1 expression on monocytes in individuals with rs612529C genotype contributes to the development of AD. Possibly, monocytes that are recruited to inflamed skin express SIRL-1, and abrogation of SIRL-1 expression in this time frame could predispose for AD. Alternatively, mononuclear phagocytes with abrogated SIRL-1 expression could play a role in AD pathogenesis in a different location than in the skin, for example in the lymph nodes. Of note, CD14$^+$ Mo-MΦ in the skin expressed SIRL-1 mRNA, albeit at very low levels compared to PBMCs, indicating that these cells have the potential to express SIRL-1 protein (Fig 2B). In the flow cytometry analysis, this protein expression may have been partially lost by the tissue digestion.

This study is limited by the availability of healthy human tissue. Firstly, the sample size of tissue biopsies is relatively small. Secondly, colon and lung tissue were derived from patients with (former) disease: colon biopsies were taken from Ulcerative Colitis or Crohn's disease patients that were in remission for at least four years, and lung biopsies were obtained from non-malignant tissue of lung cancer patients. Because these disease states might alter SIRL-1 expression, we compared our data to SIRL-1 mRNA expression found in the GTEx dataset, which contains RNA sequencing data of human non-diseased tissues (20). In the GTEx dataset, SIRL-1 expression was relatively high in blood and lung, and absent in colon and skin (Fig 5), resembling the SIRL-1 protein expression we found on mononuclear phagocytes in these tissues. This supports that the SIRL-1 expression we measured in this study is representative for SIRL-1 expression in healthy tissues. SIRL-1 expression was absent in the GTEx analysis of the colon, whereas we detected SIRL-1 expression on colon eosinophils. Granulocytes contain low total transcript levels (24), and therefore the SIRL-1 transcripts of eosinophils may have been underrepresented in the RNA sequencing analysis.

Mononuclear phagocyte subsets have distinct ontogenies. For example, macrophages can originate either from circulating monocytes that extravasate into the tissue, or from yolk-sac or fetal liver-derived cells that already populate the tissue during

embryonic development (1). We show that most macrophages in tissues do not express SIRL-1. However, a small percentage of macrophages expressed low levels of SIRL-1, including CD14+ Mo-MΦ in the skin, immature CD206- Mo-MΦ and mature CD206- MΦ in the colon, and interstitial MΦ in the lung. These macrophage subsets are all considered to be of monocytic origin (1, 17, 25-27). In contrast, autofluorescent dermal MΦ and alveolar MΦ, both considered to be of fetal origin (1, 25), did not express SIRL-1. Even though we cannot confirm the development of SIRL-1 expression over time, these results suggest that monocytes downregulate SIRL-1 expression when they enter the tissue and differentiate into macrophages.

We can only speculate as to why monocytes in lung express SIRL-1, whereas mononuclear phagocytes in colon and skin do not. Mechanistically, SIRL-1 expression may be directly maintained by a factor specifically present in the lung. Alternatively, SIRL-1 may be predominantly expressed by undifferentiated monocytes, and a factor in the lung keeps monocytes in this state. Indeed, even though it has long been thought that all monocytes which enter the tissue differentiate into MΦ or DCs, healthy human lungs contain undifferentiated monocytes in steady state (28). Of note, lung interstitial macrophages, which are at least partially monocyte-derived (reviewed by (27), express very low levels of SIRL-1 (Fig 4A, B). This argues that it is not the lung environment per se which maintains SIRL-1 expression on mononuclear phagocytes, but rather the differentiation status of the monocytes.

Functionally, SIRL-1 may inhibit ROS production in lung monocytes and granulocytes, as it has been described for these cells from healthy donor peripheral blood (10, 13) and sputum from infants with severe Respiratory Syncytial Virus bronchiolitis (12). In addition, SIRL-1 may have yet unexplored effects on the regulatory function of monocytes, for example cytokine production. Based on intravital imaging in mice, lung monocytes were suggested to be mainly involved in scavenging of particles to clean up airways and blood (29). Lungs are continuously exposed to inhaled particles, many of which are non-pathogenic. Inhibiting the immune response to such particles, for example by inhibitory receptor signaling, is therefore likely to be beneficial to the host.

In conclusion, we show that SIRL-1 is differentially expressed on human phagocyte subsets in barrier tissues. SIRL-1 is ubiquitously expressed on granulocytes, whereas expression on monocytes is genotype- and tissue-specific. Identification of the ligand of SIRL-1 will add to the understanding of the context in which SIRL-1 exerts its biological functions.

References

1. Haniffa M, Bigley V, Collin M. Human mononuclear phagocyte system reunited. Semin Cell Dev Biol. 2015;41:59-69.
2. Scott CL, Henri S, Guilliams M. Mononuclear phagocytes of the intestine, the skin, and the lung. Immunol Rev. 2014;262(1):9-24.
3. Mittal M, Siddiqui MR, Tran K, Reddy SP, Malik AB. Reactive oxygen species in inflammation and tissue injury. Antioxid Redox Signal. 2014;20(7):1126-67.
4. Ji H, Li XK. Oxidative Stress in Atopic Dermatitis. Oxid Med Cell Longev. 2016;2016:2721469.
5. Steevels TA, Meyaard L. Immune inhibitory receptors: essential regulators of phagocyte function. Eur J Immunol. 2011;41(3):575-87.
6. Vivier E, Daeron M. Immunoreceptor tyrosine-based inhibition motifs. Immunol Today. 1997;18:286-91.
7. Meyaard L. The inhibitory collagen receptor LAIR-1 (CD305). J Leukoc Biol. 2008;83(4):799-803.
8. Geerdink RJ, Hennus MP, Westerlaken GHA, Abrahams AC, Albers KI, Walk J, et al. LAIR-1 limits neutrophil extracellular trap formation in viral bronchiolitis. The Journal of allergy and clinical immunology. 2018;141(2):811-4.
9. Steevels TAM, Lebbink RJ, Westerlaken GHA, Coffer PJ, Meyaard L. Signal Inhibitory Receptor on Leukocytes-1 (SIRL-1) is a novel functional inhibitory immune receptor expressed on human phagocytes. J Immunol. 2010;184:4741-8.
10. Kumar D, Puan KJ, Andiappan AK, Lee B, Westerlaken GH, Haase D, et al. A functional SNP associated with atopic dermatitis controls cell type-specific methylation of the VSTM1 gene locus. Genome Med. 2017;9(1):18.
11. Xie M, Li T, Li N, Li J, Yao Q, Han W, et al. VSTM-v1, a potential myeloid differentiation antigen that is downregulated in bone marrow cells from myeloid leukemia patients. J Hematol Oncol. 2015;8(1):25.
12. Besteman SB, Callaghan A, Hennus MP, Westerlaken GHA, Meyaard L, Bont LL. Signal inhibitory receptor on leukocytes (SIRL)-1 and leukocyte- associated immunoglobulin-like receptor (LAIR)-1 regulate neutrophil function in infants. Clin Immunol. 2020;211:108324.
13. Steevels TA, van Avondt K, Westerlaken GH, Walk J, Bont L, Coffer PJ, et al. Signal Inhibitory Receptor on Leukocytes-1 (SIRL-1) negatively regulates the oxidative burst in human phagocytes. Eur J Immunol. 2013;43:1297-308.
14. Van Avondt K, van der Linden M, Naccache PH, Egan DA, Meyaard L. Signal Inhibitory Receptor on Leukocytes-1 Limits the Formation of Neutrophil Extracellular Traps, but Preserves Intracellular Bacterial Killing. J Immunol. 2016;196(9):3686-94.
15. Landheer J, Giovannone B, Mattson JD, Tjabringa S, Bruijnzeel-Koomen CA, McClanahan T, et al. Epicutaneous application of house dust mite induces thymic stromal lymphopoietin in nonlesional skin of patients with atopic dermatitis. J Allergy Clin Immunol. 2013;132(5):1252-4.
16. Yu YR, Hotten DF, Malakhau Y, Volker E, Ghio AJ, Noble PW, et al. Flow Cytometric Analysis of Myeloid Cells in Human Blood, Bronchoalveolar Lavage, and Lung Tissues. Am J Respir Cell Mol Biol. 2016;54(1):13-24.
17. Bain CC, Schridde A. Origin, Differentiation, and Function of Intestinal Macrophages. Front Immunol. 2018;9:2733.
18. Van Avondt K, Fritsch-Stork R, Derksen RH, Meyaard L. Ligation of signal inhibitory receptor on leukocytes-1 suppresses the release of neutrophil extracellular traps in systemic lupus erythematosus. PLoS One. 2013;8(10):e78459.

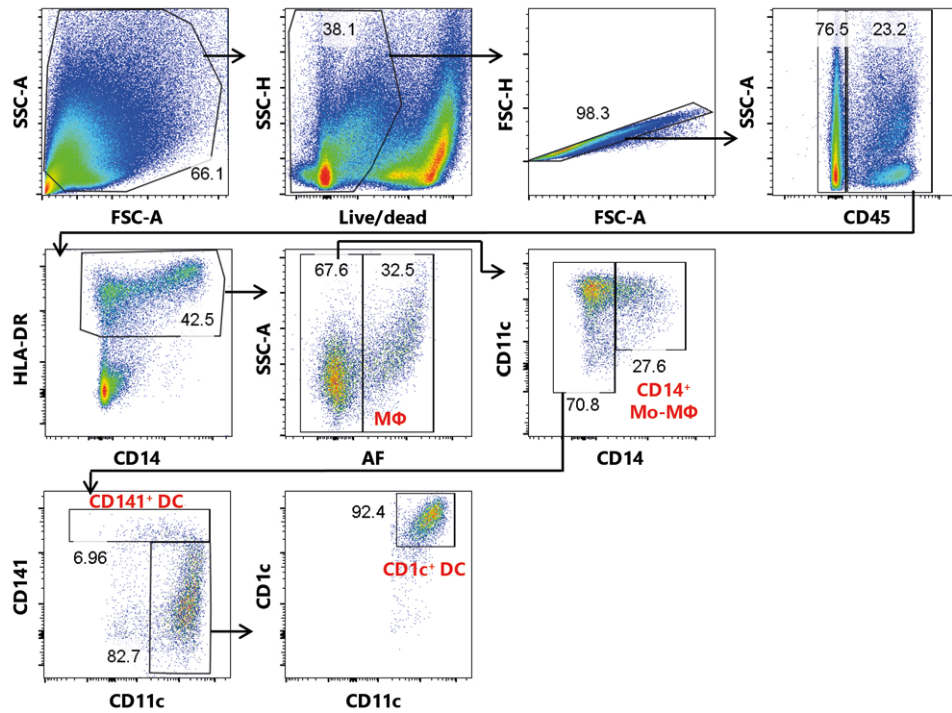32   CHAPTER 2

33   SIGNAL INHIBITORY RECEPTOR ON LEUKOCYTES-1 IS HIGHLY EXPRESSED ON LUNG MONOCYTES, BUT ABSENT ON MONONUCLEAR PHAGOCYTES IN SKIN AND COLON

19. Loktionov A. Eosinophils in the gastrointestinal tract and their role in the pathogenesis of major colorectal disorders. World J Gastroenterol. 2019;25(27):3503-26.

20. Carithers LJ, Ardlie K, Barcus M, Branton PA, Britton A, Buia SA, et al. A Novel Approach to High-Quality Postmortem Tissue Procurement: The GTEx Project. Biopreserv Biobank. 2015;13(5):311-9.

21. Dutertre CA, Becht E, Irac SE, Khalilnezhad A, Narang V, Khalilnezhad S, et al. Single-Cell Analysis of Human Mononuclear Phagocytes Reveals Subset-Defining Markers and Identifies Circulating Inflammatory Dendritic Cells. Immunity. 2019;51(3):573-89 e8.

22. Günther P, Cirovic B, Baßler K, Händler K, Becker M, Dutertre CA, et al. A rule-based data-informed cellular consensus map of the human mononuclear phagocyte cell space. bioRxiv. 2019.

23. Villani AC, Satija R, Reynolds G, Sarkizova S, Shekhar K, Fletcher J, et al. Single-cell RNA-seq reveals new types of human blood dendritic cells, monocytes, and progenitors. Science. 2017;356(6335).

24. Monaco G, Lee B, Xu W, Mustafah S, Hwang YY, Carre C, et al. RNA-Seq Signatures Normalized by mRNA Abundance Allow Absolute Deconvolution of Human Immune Cell Types. Cell Rep. 2019;26(6):1627-40 e7.

25. Gomez Perdiguero E, Klapproth K, Schulz C, Busch K, Azzoni E, Crozet L, et al. Tissue-resident macrophages originate from yolk-sac-derived erythro-myeloid progenitors. Nature. 2015;518(7540):547-51.

26. McGovern N, Schlitzer A, Gunawan M, Jardine L, Shin A, Poyner E, et al. Human dermal CD14(+) cells are a transient population of monocyte-derived macrophages. Immunity. 2014;41(3):465-77.

27. Schyns J, Bureau F, Marichal T. Lung Interstitial Macrophages: Past, Present, and Future. J Immunol Res. 2018;2018:5160794.

28. Baharom F, Thomas S, Rankin G, Lepzien R, Pourazar J, Behndig AF, et al. Dendritic Cells and Monocytes with Distinct Inflammatory Responses Reside in Lung Mucosa of Healthy Humans. J Immunol. 2016;196(11):4498-509.

29. Rodero MP, Poupel L, Loyher PL, Hamon P, Licata F, Pessel C, et al. Immune surveillance of the lung by migrating tissue monocytes. Elife. 2015;4:e07847.

30. Goldman M, Craft B, Hastie M, Repečka K, McDade F, Kamath A, et al. The UCSC Xena platform for public and private cancer genomics data visualization and interpretation. bioRxiv. 2019:326470.

Supplementary Information
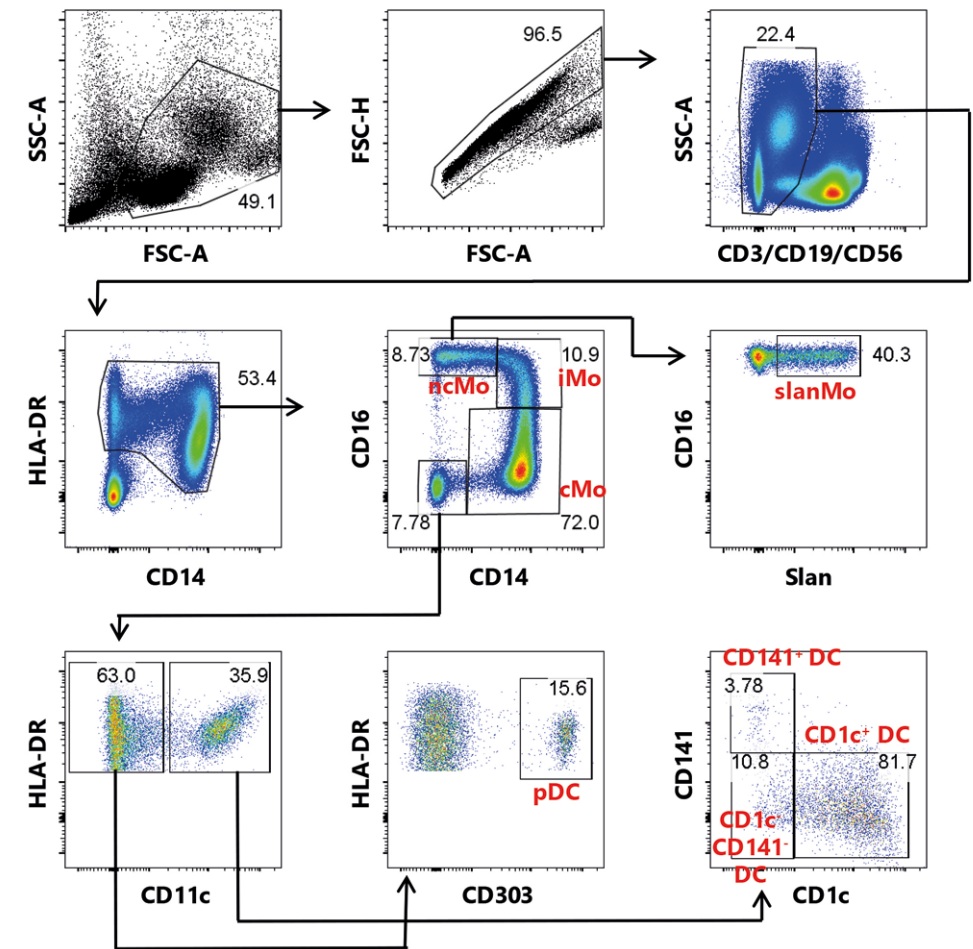
Supplementary Figure 1. Gating strategy of mononuclear phagocytes in human peripheral blood.

Single, viable cells from human peripheral blood were gated using forward scatter (FSC) and sideward scatter (SSC). Mononuclear phagocytes were selected as cells negative for lineage markers CD3, CD19 and CD56, followed by gating of HLA-DR$^{dim/+}$ cells. Monocytes were divided into classical monocytes (cMo, CD14$^+$CD16$^-$), intermediate monocytes (iMo, CD14$^+$CD16$^+$) and nonclassical monocytes (ncMo, CD14^{dim}CD16$^+$). Expression of slan was used to identify slanMo's, a subset of ncMo's. DCs were defined as CD14$^-$CD16$^-$, followed by division into plasmacytoid DCs (pDC, CD11c$^-$CD303$^+$) and 3 types of CD11c$^+$ conventional DCs (CD141$^+$ DCs, CD1c$^+$ DCs and CD141$^-$CD1c$^-$ DCs).

34   CHAPTER 2

35   SIGNAL INHIBITORY RECEPTOR ON LEUKOCYTES-1 IS HIGHLY EXPRESSED ON LUNG MONOCYTES, BUT ABSENT ON MONONUCLEAR PHAGOCYTES IN SKIN AND COLON
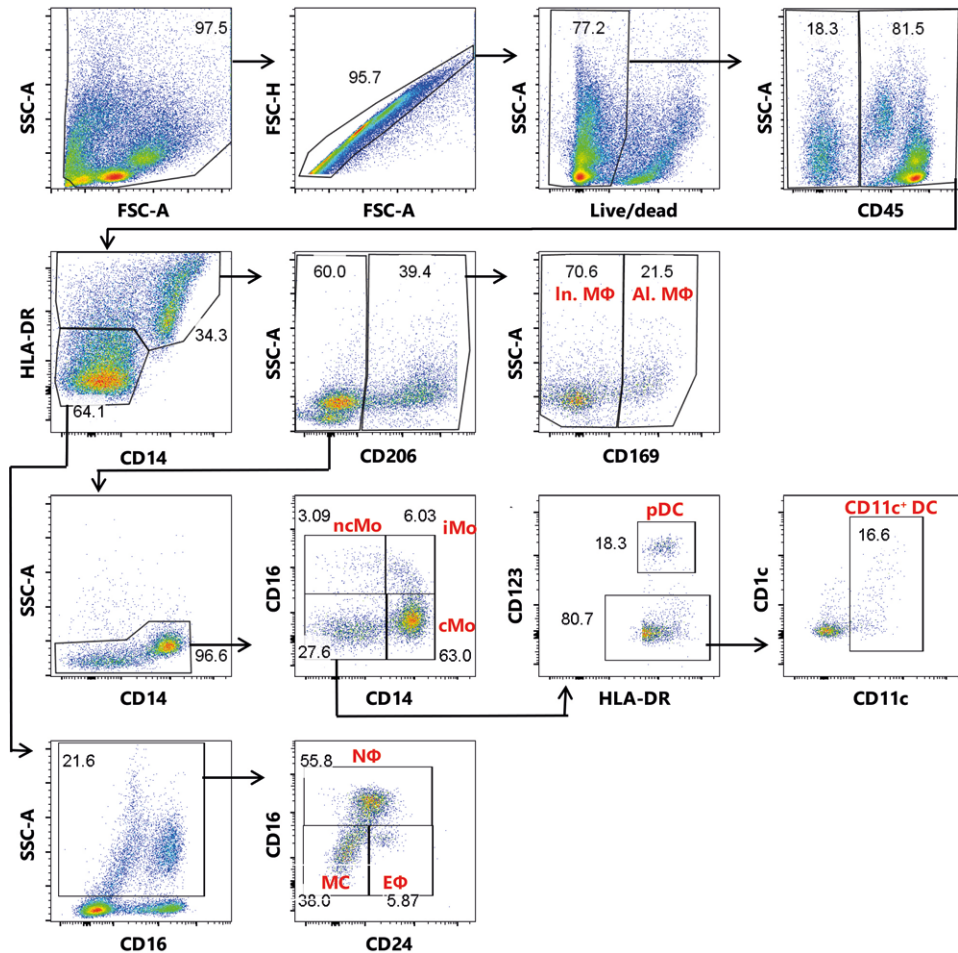
Supplementary Figure 2. Gating strategy of mononuclear phagocytes in human skin.

Single, viable cells from a human skin biopsy were selected using forward scatter (FSC), sideward scatter (SSC) and a live/dead stain, followed by gating of dermal mononuclear phagocytes (CD45$^+$HLA-DR$^+$). Macrophages were divided into autofluorescent macrophages (MΦ) derived from embryonic yolk sack and in macrophages of monocytic origin (AF$^-$CD14$^+$ Mo-MΦ). Dermal DCs were selected from the AF$^-$CD14$^-$ gate and divided into CD141$^+$ DCs and CD1c$^+$ DCs.
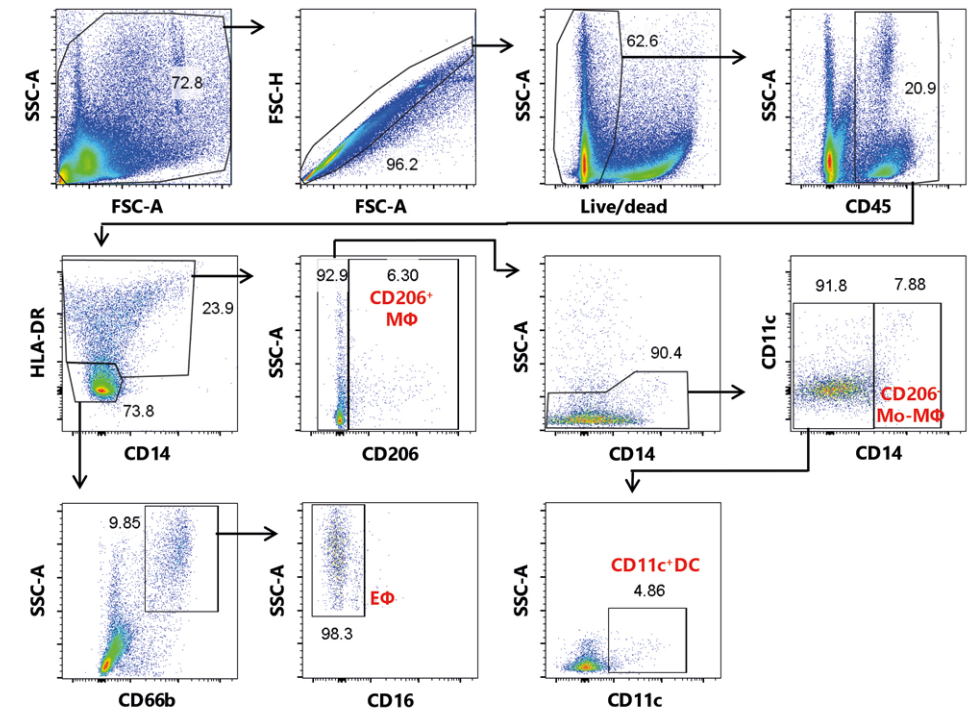
Supplementary Figure 3. Gating strategy of mononuclear phagocytes and eosinophils in human colon.

Single, viable leukocytes from a human colonic biopsy were gated using forward scatter (FSC), sideward scatter (SSC), a live/dead marker and CD45 expression. Mature macrophages (CD206$^+$ MΦ) were gated as HLA-DR$^+$ CD206$^+$, whereas immature monocyte-derived macrophages (CD206$^-$ Mo-MΦ) were defined as HLA-DR$^+$CD206$^-$CD14$^+$. Selection of DCs was done by gating on CD11c$^+$ cells within the HLA-DR$^+$CD206$^-$CD14$^-$ population. Eosinophils (EΦ) were defined as HLA-DR$^-$SSC^{high}CD66b$^+$CD16$^-$.

Supplementary Figure 4. Gating strategy of mononuclear phagocyte and granulocytes in human lung.

Single, viable leukocytes from a human lung biopsy were gated using forward scatter (FSC), sideward scatter (SSC), a live/dead marker and CD45 expression. Macrophages were selected as HLA-DR$^{dim/+}$CD206$^+$, followed by subdivision into alveolar macrophages (Al. MΦ, CD169$^+$) and interstitial macrophages (In. MΦ, CD169$^-$). Monocytes and DCs were gated as HLA-DR$^{dim/+}$CD206$^-$ SSC^{low}. Monocytes were further divided into classical monocytes (cMo, CD14$^+$CD16$^-$), intermediate monocytes (iMo, CD14$^+$CD16$^+$) and nonclassical monocytes (ncMo, CD14^{dim}CD16$^+$). DCs were selected from the CD14$^-$CD16$^-$ gate, followed by division into plasmacytoid DCs (pDC, CD123$^+$) and CD11c$^+$ DCs (CD123$^-$CD11c$^+$). Granulocytes were defined as HLA-DR$^-$ SSC^{high} and further divided into neutrophils (NΦ, CD16$^+$), eosinophils (EΦ, CD16$^-$CD24$^+$) and mast cells (MC, CD16$^-$CD24$^-$).
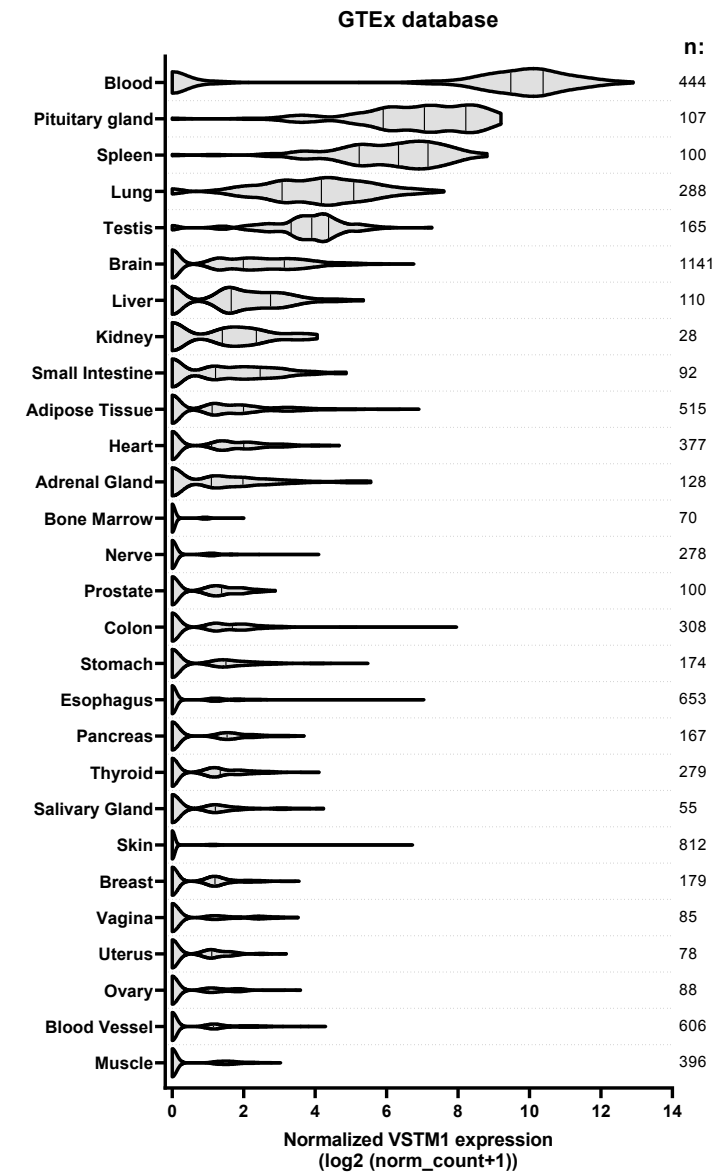
Supplementary Figure 5. *VSTM1*, the gene encoding SIRL-1, is differentially expressed in non-diseased tissues.

The violin plots show normalized mRNA expression of *VSTM1*. The dataset derives from the Genotype-Tissue Expression (GTEx) project, in which RNA from postmortem non-diseased tissues was analyzed by RNA-sequencing (20). Data were obtained with the UCSC Xena Platform (30). Null values were excluded, as well as tissues with n<20 (fallopian tube, cervix uteri and bladder). The n for each tissue is indicated on the right side of the graph.

Supplementary Table 1. Antibodies used for flow cytometry.

This table describes the properties of each antibody that was used for flow cytometry staining, including recognized antigen, conjugated fluorochrome, antibody clone and manufacturer, categorized per tissue.

Tissue	Antigen	Fluorochrome	Antibody clone	Manufacturer
all	SIRL-1	AF647	1A5	In house (Steevels et al., 2010)
	IgG1 k Isotype	AF647	MOPC-21	Biolegend
peripheral blood	HLA-DR	BV421	L243	Biolegend
	CD16	BV510	3G8	BD Biosciences
	CD141	BV711	1A4	BD Biosciences
	Slan	FITC	DD-1	Miltenyi
	CD1c	PE	AD5-8E7	Miltenyi
	CD11c	PE-CF594	B-LY6	BD Biosciences
	CD303	PE-Cy7	201A	Biolegend
	CD3	AF700	UCHT1	Biolegend
	CD19	AF700	HIB19	eBioscience
	CD56	AF700	B159	BD Biosciences
	CD14	eF780	61D3	eBioscience
skin	CD1c	BV421	L161	Biolegend
	CD14	V500	M5E2	BD Biosciences
	HLA-DR	BV605	G46-6	BD Biosciences
	CD141	BV711	1A4	BD Biosciences
	CD16	BV785	3G8	Sony Biotechnology
	CD117	PerCP-Cy5.5	104D2	Biolegend
	CD209	PE	9E9A8	Biolegend
	CD45	PE-Cy7	HI30	BD Biosciences
	CD11c	AF700	3.9	eBioscience
	Viability dye	APC-eF780	-	eBioscience
colon	CD45	PB	T29/33	Dako
	HLA-DR	BV711	G46-6	BD Biosciences
	CD14	BV785	M5E2	Biolegend
	CD66b	FITC	80H3	Beckman Coulter
	CD11c	PerCP-Cy5.5	Bu15	Biolegend
	CD206	PE-CF594	19.2	BD Biosciences
	Viability dye	APC-eF780	-	eBioscience
lung	HLA-DR	BV421	G46-6	BD Biosciences
	CD16	BV510	3G8	Biolegend
	CD45	BV650	HI30	Biolegend
	CD14	BV785	M5E2	Biolegend
	CD1c	AF488	L161	Sony Biotechnology
	CD24	PerCP-Cy5.5	ML5	BD Biosciences
	CD169	PE	7-239	eBioscience
	CD206	PE-CF594	19.2	BD Biosciences
	CD123	PE-Cy7	6H6	Biolegend
	CD11c	AF700	3.9	eBioscience
	Viability dye	APC-eF780	-	eBioscience

CHAPTER 3

Recognition of S100 proteins by Signal Inhibitory Receptor on Leukocytes-1 negatively regulates human neutrophils

Matevž Rumpret[1,2], **Helen J. von Richthofen**[1,2] *,
Maarten van der Linden[1] *, **Geertje H. A. Westerlaken**[1,2],
Cami Talavera Ormeño[2,3], **Teck Y. Low**[4,5],
Huib Ovaa[2,3] †, **Linde Meyaard**[1,2]

[1] Center for Translational Immunology, University Medical Center Utrecht, Utrecht University, Utrecht, The Netherlands
[2] Oncode Institute, Utrecht, The Netherlands
[3] Department of Cell and Chemical Biology, Leiden University Medical Center, Leiden, The Netherlands
[4] Biomolecular Mass Spectrometry and Proteomics, Bijvoet Center for Biomolecular Research and Utrecht Institute for Pharmaceutical Sciences and Netherlands Proteomics Center, Utrecht University, Utrecht, The Netherlands
[5] Current address: UKM Medical Molecular Biology Institute (UMBI), Universiti Kebangsaan Malaysia, 56000 Kuala Lumpur, Malaysia

* equal contributions
† Deceased

Abstract

Signal inhibitory receptor on leukocytes-1 (SIRL-1) is an inhibitory receptor with a hitherto unknown ligand, and is expressed on human monocytes and neutrophils. SIRL-1 inhibits myeloid effector functions such as reactive oxygen species (ROS) production. In this study, we identify S100 proteins as SIRL-1 ligands. S100 proteins are composed of two calcium-binding domains. Various S100 proteins are damage-associated molecular patterns (DAMPs) released from damaged cells, after which they initiate inflammation by ligating activating receptors on immune cells. We now show that the inhibitory SIRL-1 recognizes individual calcium-binding domains of all tested S100 proteins. Blocking SIRL-1 on human neutrophils enhanced S100 protein S100A6-induced ROS production, showing that S100A6 suppresses neutrophil ROS production via SIRL-1. Taken together, SIRL-1 is an inhibitory receptor recognizing the S100 protein family of DAMPs. This may help limit tissue damage induced by activated neutrophils.

Introduction

Inhibitory immune receptors set thresholds for immune cell activation and ensure prompt cessation of immune responses, preventing immunopathology (1). Signal inhibitory receptor on leukocytes-1 (SIRL-1, VSTM1) is an inhibitory receptor without known ligands, expressed on human granulocytes and monocytes (2). It dampens Fc-receptor-mediated reactive oxygen species (ROS) production in neutrophils and monocytes and neutrophil extracellular trap formation *in vitro* (3-5).

S100 proteins are small proteins with member-specific functions (6). The human genome encodes twenty-one S100s (7, 8). Although functionally diverse, S100s share a conserved structure comprising two Ca^{2+}-binding EF-hand domains, one S100 protein-specific and the other common to other Ca^{2+}-binding proteins. Each EF-hand domain is composed of two α-helices connected by a short Ca^{2+}-binding loop, giving rise to a helix–loop–helix motif, and the two EF-hand domains are joined by a short hinge region to form a full S100 protein (9). Some S100s are damage-associated molecular patterns (DAMPs) released from damaged cells (10, 11). Additionally, S100s such as S100A8 and S100A9 are also actively secreted from activated immune cells. After release into extracellular space, many S100s interact with pattern recognition receptors such as TLR4 and RAGE and promote inflammation (12-14). Here, we show that some S100s engage SIRL-1 to suppress S100-induced ROS in neutrophils.

Materials and Methods

Recombinant protein cloning, expression, and purification

SIRL-1 and LAIR-1 ectodomains (containing their native signal sequences) were PCR-amplified and cloned into pJet2.blunt. Inserts were cut out from the plasmid using PCR primer-encoded restriction enzymes and ligated into pcDNA3.1 expression vector (ThermoFisher) in frame with C-terminal 2×HA and 2×Flag tags. HEK293T cells were transiently (PEI)-transfected with newly generated plasmids. After one day, cells were transferred from RPMI 1640 supplemented with 10% (v/v) heat-inactivated fetal bovine serum and 50 U/ml penicillin–streptomycin to serum-free OptiMEM (ThermoFisher) and incubated for five days at 37°C and 5% CO_2. Afterward, the supernatant was collected by centrifugation, and the recombinant proteins were purified by incubation of the clarified supernatant with anti-FLAG (M2) agarose on a rotatory incubator at 4°C overnight. The next day, anti-FLAG (M2) agarose loaded with the SIRL-1-(2×HA-2×Flag) or LAIR-1-(2×HA-2×Flag) ectodomains was washed five times with PBS, and pull-down experiments were performed.

Monocyte isolation

All samples were collected after obtaining informed consent and with the approval of the Medical Research Ethics Committee Utrecht. Human monocytes were isolated from the freshly drawn peripheral blood of healthy donors. Whole blood was centrifuged over a Ficoll (GE Healthcare) gradient, and isolated PBMCs were further centrifuged over a Percoll (GE Healthcare) gradient. Purified monocytes were then lysed immediately, as described below.

Cell lysis, pull-down assays, and mass spectrometry

Isolated monocytes and mouse RAW cells were lysed by incubation in 50 mM Tris pH 8, 150 mM NaCl, 1% NP-40, and protease inhibitor cocktail (Roche) at 4°C for 30 min. Following lysis, the lysate was cleared by centrifugation at 12,000 g and 4°C for 20 min. Cleared lysates (protein content around 1 mg/ml) were incubated with SIRL-1-HA-Flag or LAIR-1-HA-Flag recombinant proteins bound to anti-FLAG agarose (Sigma) at 4°C overnight. The next day, anti-FLAG agarose was washed six times with PBS, and proteins were eluted with 100 µg/ml FLAG peptide (Sigma). The eluate was then incubated with anti-HA agarose (Sigma) at 4°C overnight. The next day, anti-HA agarose was washed six times with PBS, protease digestion was performed, and samples were submitted to mass spectrometric analysis as described before (15).

Peptide synthesis

EF-hand domains of S100s A6, A8, A9, and A12 (Table 1) were synthesized as described (16), with some modifications. Peptide synthesis was performed on a Syro II Multisyntech automated synthesizer with a TIP module. We applied standard 9-fluoronylmethoxycarbonyl (Fmoc) based solid-phase peptide chemistry at a 2 µmol scale, using fourfold excess of amino acids relative to pre-loaded Fmoc amino acid wang-type resin (0.2 mmol/g Rapp Polymere) (16)?. For all cycles, double couplings in NMP for 25 min using PyBOP (4 equiv) and DiPEA (8 equiv) were performed. After each coupling, the resin was washed five times with NMP. In between cycles, Fmoc removal was performed with 20% piperidine in NMP for 2×2 min and 1×5 min. After Fmoc removal, the resin was washed three times with NMP. Resins were then washed with ethoxyethane and dried on air. Peptides were cleaved from resins and deprotected with TFA/H_2O/phenol/iPr$_3$SiH (90.5/5/2.5/2 v/v/v/v) for 3 h. After resines were washed with 3×100 µL TFA/H_2O/phenol/iPr$_3$SiH (90.5/5/2.5/2 v/v/v/v), peptides were precipitated with cold Et$_2$O/n-pentane 3:1 v/v. Precipitated peptides were washed 3× with Et$_2$O, dissolved in H_2O/CH$_3$CN/HOAc (75/24/1 v/v/v), and lyophilized (16).

Table 1. List of S100 fragment peptides.

EF-hand domains: 1 = S100-specific, 2 = canonical

S100A5_1	METPLEKALTTMVTTFHKYSGREGSKLTLSRKELKELIKKELCLGE
S100A5_2	MKESSIDDLMKSLDKNSDQEIDFKEYSVFLTMLCMAYNDFFLEDNK
S100A6_1	MACPLDQAIGLLVAIFHKYSGREGDKHTLSKKELKELIQKELTIGS
S100A6_2	KLQDAEIARLMEDLDRNKDQEVNFQEYVTFLGALALIYNEALKG
S100A8_1	MLTELEKALNSIIDVYHKYSLIKGNFHAVYRDDLKKLLETECPQY
S100A8_2	IRKKGADVWFKELDINTDGAVNFQEFLILVIKMGVAAHKKSHEESHKE
S100A9_1	MTCKMSQLERNIETIINTFHQYSVKLGHPDTLNQGEFKELVRKDLQNFLK
S100A9_2	KENKNEKVIEHIMEDLDTNADKQLSFEEFIMLMARLTWASHEKMHEGDEGPGHHHKPGLGEGTP
S100A12_1	TKLEEHLEGIVNIFHQYSVRKGHFDTLSKGELKQLLTKELANTIKN
S100A12_2	KDKAVIDEIFQGLDANQDEQVDFQEFISLVAIALKAAHYHTHKE

Construction of 2B4 NFAT–GFP reporter cells

2B4 NFAT–GFP cell line is a T cell hybridoma cell line in which GFP expression is controlled by the transcriptional factor NFAT. LAIR-1–CD3ζ construction has been described (17), and SIRL-1–CD3ζ construction was performed similarly, yielding a 269 AA chimera comprising the SIRL-1 signal peptide and ectodomain (MTAEFLSLLC… APSMKTDQFK) fused to the CD3ζ transmembrane and cytoplasmic domains (LCYLLDGILF…ALHMQALPPR). The construct was transduced into a 2B4 NFAT–GFP cell line, in which ligation of the chimera by an antibody or a ligand results in NFAT promoter-driven GFP expression (18). Three days after transduction, cells were sorted for high SIRL-1 surface expression and subcloned by limiting dilution. We selected one clone with high surface SIRL-1 expression and high GFP expression levels after SIRL-1 ligation ("2B4 NFAT–GFP reporter cell assay" below) for further experiments. All cells were maintained in RPMI 1640 with 10% heat-inactivated fetal bovine serum (FBS) and 50 U/ml penicillin–streptomycin (culture medium) unless stated otherwise.

2B4 NFAT–GFP reporter cell assay

We assessed SIRL-1 activation using SIRL-1–CD3ζ 2B4 NFAT–GFP T cell hybridoma reporter cells with wt and LAIR-1–CD3ζ 2B4 NFAT–GFP cells as controls (17). MaxiSorp Nunc (Figures 1 and 3) or Greiner (Figure 2) 96-well flat-bottom plates were coated overnight at 4°C with 10 µM S100 proteins (Prospec) or fragments (own production), or 5 µg/ml collagen I (Sigma), unless stated otherwise. Mouse-anti-SIRL-1 mAb (clone 1A5, own production; 10 µg/ml), mouse-anti-LAIR-1 mAb (clone 8A8, own production; 10 µg/ml), and Armenian hamster-anti-mouse-CD3 mAb (clone 145-2C11, BD; 10 µg/ml) were coated as controls. After washing the wells with PBS, we seeded $0.5×10^5$ cells/

well in the culture medium and incubated them overnight at 37°C. Where indicated, cells were pre-incubated with anti-SIRL-1 F(ab')$_2$ or control F(ab')$_2$ for 30 min before seeding. For anti-CD3 control in reporter assays with pre-incubation with F(ab')$_2$, 1 µg/ml anti-mouse-CD3 was coated to the plate. The following day, GFP expression was measured by flow cytometry (LSR Fortessa; BD Bioscience) following the "Guidelines for the use of flow cytometry and cell sorting in immunological studies" (19). Results were analyzed with FlowJo 10.0.7r2.

Neutrophil isolation and ROS assay

We collected all samples after obtaining informed consent and with the approval of the Medical Research Ethics Committee Utrecht. Neutrophils were isolated from peripheral blood of healthy donors by Ficoll gradient centrifugation (20), with modifications. After erythrocyte lysis, neutrophils were washed with RPMI 1640 with 2% FBS. Neutrophils were then washed and suspended in HEPES buffer (20 mM HEPES, 132 mM NaCl, 6 mM KCl, 1 mM CaCl$_2$, 1 mM MgSO$_4$, 1.2 mM KH$_2$PO$_4$, 5 mM D-glucose and 0.5% (w/v) bovine serum albumin, pH 7.4) with 4% FBS. Isolated neutrophils were incubated for 30 minutes at room temperature with 20 µg/ml control F(ab')$_2$ (Southern Biotech) or mouse-anti-SIRL-1 F(ab')$_2$ (own production). We generatead F(ab')$_2$ fragments using Pierce™ Mouse IgG1 Fab and F(ab')$_2$ Preparation Kit (ThermoFisher Scientific #44980). ROS production upon stimulation with or without 10 µM peptide S100A6-1 coated to a Microfluor® 2 white-bottom 96-well plate (ThermoFisher) was determined by AmplexRed assay (3). Fluorescence was measured in a 96-well plate reader (Clariostar, BMG Labtech) every two minutes for 150 minutes (λ Ex/Em = 526.5–97 / 650–100 nm). We corrected the measurement for spontaneous ROS production by subtracting the signal of PBS-treated cells.

Statistical analysis

Student's *t*-test with the Holm–Šidák multiple comparison correction, or paired Student's *t*-test were performed as indicated. P-values lower than 0.05 were considered statistically significant (* p<0.05; ** p<0.01; *** p<0.001). Statistical analysis was performed with GraphPad Prism 8.

Results and discussion

S100 proteins activate SIRL-1

To identify SIRL-1 ligands, we performed pull-downs with recombinant SIRL-1 and LAIR-1 ectodomains from human monocyte and mouse RAW cell line lysates. We identified enriched proteins by mass spectrometry (MS, data available in jPOSTrepo). We used LAIR-1, an inhibitory receptor for collagen (17), as a specificity control. Human collagen II was enriched in LAIR-1 pull-downs. No proteins were significantly enriched in SIRL-1 pull-downs, but we did detect several S100 proteins in increased quantity. Despite S100s commonly appearing as non-specific hits in such experiments, we validated them further.

We tested multiple S100s as ligands for SIRL-1 in a reporter assay, in which ligation of SIRL-1–CD3ζ or LAIR-1–CD3ζ chimera by an antibody or a ligand results in GFP expression (Figure 1). SIRL-1–CD3ζ cells selectively responded to plate-coated anti-SIRL-1 mAb and S100A6 (Figure 1A shows selected scatter plots, and Figure 1B shows quantification). We next investigated additional members of the S100 protein family—A2, A5–A9, and A16—for SIRL-1 activation. All selectively activated the SIRL-1 reporter (Figure 1C), indicating SIRL-1 recognizes S100s. To investigate which S100 protein domains activate SIRL-1, we synthesized peptides spanning individual EF-hand domains of S100s A6, A8, A9, and A12. A sequence alignment (21) indicating EF-hand domains is shown in Figure 2A, and peptide sequences are listed in Table 1. We tested these fragments (Figure 2B) and found that one EF-hand domain was sufficient for SIRL-1 reporter cell activation and that both canonical and S100-specific EF-hand domains of selected S100s engaged SIRL-1. Such broad recognition of ligands is reminiscent of LAIR-1 recognizing different types of extracellular and membrane collagens (22).
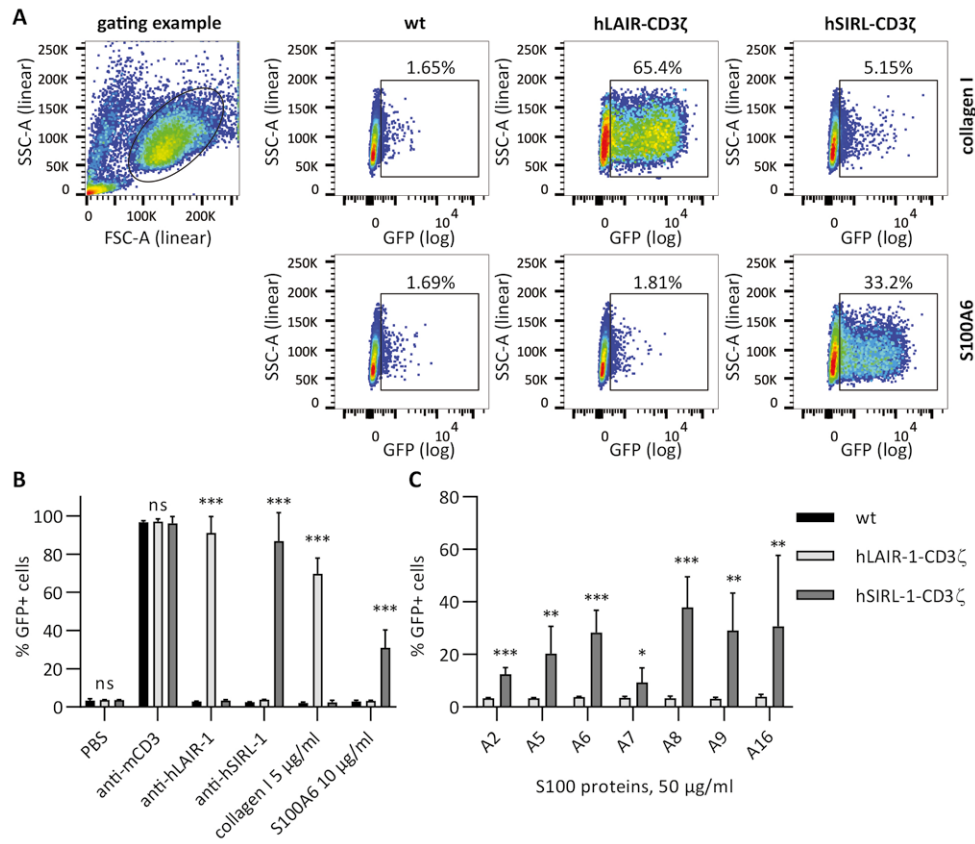
Figure 1. S100 proteins activate SIRL-1 reporter cells.

Reporter cells were incubated with antibodies, collagen I, and S100s coated to a MaxiSorp 96-well plate. We assessed receptor activation by measuring GFP expression by flow cytometry. **(A)** Representative dot plots and gating examples are shown. **(B)** Reporter cells stimulated with anti-CD3 mAb, anti-hLAIR-1 mAb, collagen I (a known LAIR-1 ligand), anti-hSIRL-1 mAb and S100A6. **(C)** Reporter cells stimulated with different S100 proteins. Mean and SD of three independent experiments are displayed. Student's *t*-test with the Holm–Šidák multiple comparison correction. * p<0.05; ** p<0.01; *** p<0.001; ns = not significant. Significance levels for comparison hLAIR-1–CD3ζ to hSIRL-1–CD3ζ are shown.
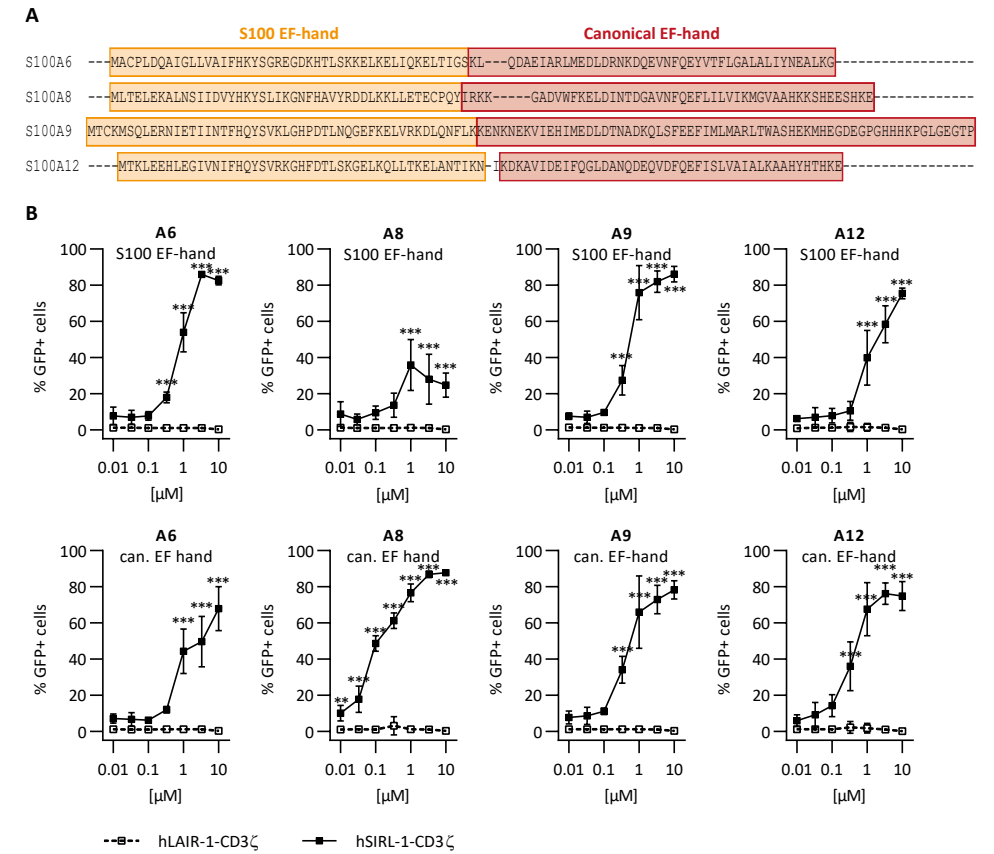

Figure 2. EF-hand domains of S100 proteins activate SIRL-1.

(A) Sequence alignment of selected S100s. S100-specific (orange) and canonical (red) EF-hand domains are indicated. **(B)** Reporter cells were incubated with EF-hand domains of S100A6, S100A8, S100A9, and S100A12 coated to Greiner 96-well plates. We assessed receptor activation by measuring GFP expression by flow cytometry. Mean and SD of three independent experiments are displayed. Student's *t*-test with the Holm–Šidák multiple comparison correction. * p<0.05; ** p<0.01; *** p<0.001.

Anti-SIRL-1 mAb blocks activation of SIRL-1 by S100 proteins

We next performed the reporter assay in the presence of anti-SIRL-1 F(ab')$_2$ or control F(ab')$_2$ (Figure 3A). We used anti-SIRL-1 F(ab')$_2$ instead of the full-length mAb to prevent Fc-receptor engagement, in the experiments where we block SIRL-1. Anti-SIRL-1 F(ab')$_2$, but not control F(ab')$_2$, concentration-dependently blocked S100-induced SIRL-1 reporter cell activation. Thus, S100 protein EF-hand domain recognition by SIRL-1 depends on SIRL-1 ectodomain accessibility. In the case of S100A9, the blockade was not significant, possibly due to the low GFP signal. Upon anti-CD3 stimulation, we observed no blockade by anti-SIRL-1 F(ab')$_2$, excluding steric hindrance by F(ab')$_2$ as the reason for anti-SIRL-1 F(ab')$_2$-specific blockade of S100-induced GFP (Figure 3A).

SIRL-1 blockade enhances S100-instigated ROS production in human neutrophils

SIRL-1 is a negative regulator of FcR-induced ROS production (3), and some S100s induce ROS in neutrophils (23). Thus, we investigated whether SIRL-1 inhibits S100-induced ROS production. We stimulated freshly isolated human neutrophils with SIRL-1-activating EF-hand domains of S100A5, S100A6, S100A8, S100A9, and S100A12. Of these, only the S100-specific EF-hand of S100A6 induced neutrophil ROS production (Supplementary Figure 1). Upon neutrophil stimulation with the S100-specific EF-hand of S100A6, anti-SIRL-1 F(ab')$_2$ pre-incubated neutrophils exhibited significantly higher ROS production than control F(ab')$_2$ pre-incubated neutrophils (Figure 3B, C), showing SIRL-1 dampens S100A6-induced ROS production in neutrophils. We observed a slight increase in ROS production upon SIRL-1 blockage in the absence of S100A6. This could indicate the presence of S100s or other SIRL-1 ligands in medium with serum, of which recognition was also blocked by anti-SIRL-1 F(ab')$_2$. In agreement with this, the NFAT–GFP SIRL-1–CD3ζ reporter cells typically show slightly higher background GFP levels than wt and LAIR-1–CD3ζ reporter cells.

We could not show a direct interaction between S100s and SIRL-1 (Supplementary figures 2 and 3), even though we initially identified S100s by SIRL-1 pull-down from cell lysates. Additional molecules could be needed for SIRL-1–S100 interaction, which is not uncommon—for instance, TLR4 binds LPS in complex with MD2 and CD14 (24). Alternatively, the SIRL-1–S100 interaction affinity might be too low for detection in a purified system. Lastly, S100s frequently appear as non-specific hits in MS experiments. The initial SIRL-1 pull-down of S100s might thus have been a chance finding, of which follow-up experiments showed that S100s specifically activate SIRL1.
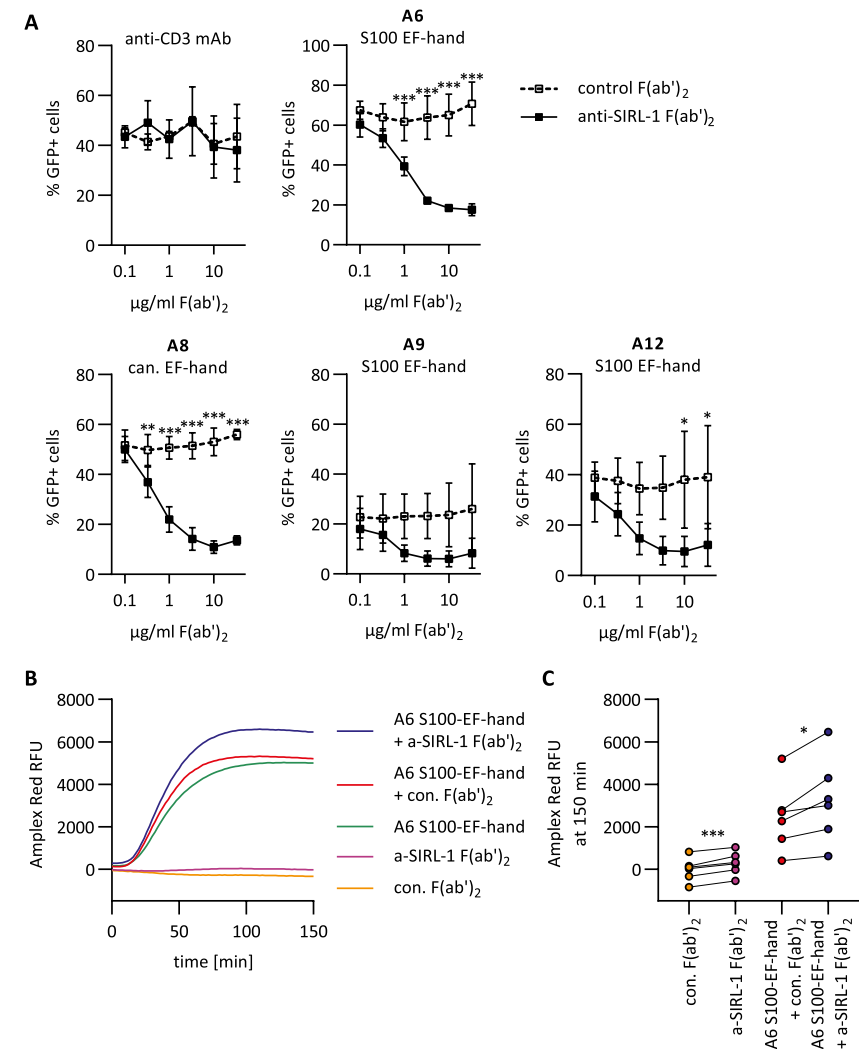

Figure 3: SIRL-1 blockade with anti-SIRL-1 F(ab')$_2$ enhances S100A6-induced ROS in human neutrophils.

(A) SIRL-1 reporter cells were pre-incubated with varying concentrations of anti-SIRL-1 F(ab')$_2$ or a control F(ab')$_2$. Subsequently, they were incubated with S100 EF-hand domains of S100A6, S100A9, and S100A12, and the canonical EF-hand domain of S100A8 that had been coated to a MaxiSorp 96-well plate. 1 µg/ml coated anti-CD3 mAb was used as a control. We assessed receptor activation by measuring GFP expression by flow cytometry. Mean and SD of three independent experiments are displayed. Student's t-test with the Holm–Šidák multiple comparison correction. **(B, C)** Human neutrophils were pre-incubated with anti-SIRL-1 F(ab')2 or a control F(ab')2 and subsequently stimulated with S100-EF-hand of S100A6 coated to Microfluor 2 96-well plate. ROS production was monitored for 150 minutes. **(B)** ROS production over time, shown for one representative donor. **(C)** ROS production at 150 min for all six donors. Three independent experiments with neutrophils isolated from blood of six healthy donors are shown. Paired Student's t-test. * p<0.05; ** p<0.01; *** p<0.001.

Concluding Remarks

DAMPs can deliver activating as well as inhibitory signals to immune cells—the inhibitory receptor Siglec-10 recognizes high mobility group box 1, a prototypical DAMP, in complex with CD24 (25). The S100 DAMPs behave similarly: S100A9 binds the inhibitory receptor LILRB1 (CD85j) to modulate NK cell activity (26), and here we show that S100A6 induces SIRL-1-mediated inhibition. What is the benefit of SIRL-1 mediated negative regulation through DAMPs like S100s? When neutrophils first infiltrate the affected tissue to deploy effector mechanisms, the tissue has not been damaged by inflammatory processes and is devoid of DAMPS like S100s. Later in inflammation, effector cells will induce tissue damage and enhance DAMP release. We have previously shown that activated neutrophils gradually downregulate SIRL-1 expression (3). Incoming neutrophils, however, express high levels of SIRL-1, which can detect S100s and induce an inhibitory signal. This functions as negative feedback for further deployment of tissue-damaging effector mechanisms and reduces the chances of developing immunopathology. In conclusion, we identify the first known SIRL-1 ligands. We demonstrate that S100 proteins activate SIRL-1 and that blocking SIRL-1 with anti-SIRL-1 F(ab')$_2$ fragments enhances S100A6-induced ROS production in neutrophils. Similarly, S100s could modulate monocyte function through SIRL-1, which can be explored in the future. We propose that SIRL-1 broadly recognizes a yet unidentified feature of S100 proteins to help limit tissue damage by immune cells.

Acknowledgments

References

1. Rumpret M, Drylewicz J, Ackermans LJE, Borghans JAM, Medzhitov R, Meyaard L. Functional categories of immune inhibitory receptors. Nat Rev Immunol. 2020;20(12):771-80.

2. Steevels TA, Lebbink RJ, Westerlaken GH, Coffer PJ, Meyaard L. Signal inhibitory receptor on leukocytes-1 is a novel functional inhibitory immune receptor expressed on human phagocytes. J Immunol. 2010;184(9):4741-8.

3. Steevels TA, van Avondt K, Westerlaken GH, Stalpers F, Walk J, Bont L, et al. Signal inhibitory receptor on leukocytes-1 (SIRL-1) negatively regulates the oxidative burst in human phagocytes. Eur J Immunol. 2013;43(5):1297-308.

4. Van Avondt K, Fritsch-Stork R, Derksen RH, Meyaard L. Ligation of signal inhibitory receptor on leukocytes-1 suppresses the release of neutrophil extracellular traps in systemic lupus erythematosus. PLoS One. 2013;8(10):e78459.

5. Van Avondt K, van der Linden M, Naccache PH, Egan DA, Meyaard L. Signal Inhibitory Receptor on Leukocytes-1 Limits the Formation of Neutrophil Extracellular Traps, but Preserves Intracellular Bacterial Killing. J Immunol. 2016;196(9):3686-94.

6. Donato R, Sorci G, Giambanco I. S100A6 protein: functional roles. Cell Mol Life Sci. 2017;74(15):2749-60.

7. Zimmer DB, Eubanks JO, Ramakrishnan D, Criscitiello MF. Evolution of the S100 family of calcium sensor proteins. Cell Calcium. 2013;53(3):170-9.

8. Donato R, R. Cannon B, Sorci G, Riuzzi F, Hsu K, J. Weber D, et al. Functions of S100 Proteins. Current Molecular Medicine. 2012;13(1):24-57.

9. Kawasaki H, Nakayama S, Kretsinger RH. Classification and evolution of EF-hand proteins. Biometals. 1998;11(4):277-95.

10. Bianchi ME. DAMPs, PAMPs and alarmins: all we need to know about danger. J Leukoc Biol. 2007;81(1):1-5.

11. Yang, Han Z, Oppenheim JJ. Alarmins and immunity. Immunol Rev. 2017;280(1):41-56.

12. Holzinger D, Tenbrock K, Roth J. Alarmins of the S100-Family in Juvenile Autoimmune and Auto-Inflammatory Diseases. Front Immunol. 2019;10:182.

13. Pruenster M, Kurz AR, Chung KJ, Cao-Ehlker X, Bieber S, Nussbaum CF, et al. Extracellular MRP8/14 is a regulator of beta2 integrin-dependent neutrophil slow rolling and adhesion. Nat Commun. 2015;6:6915.

14. Fassl SK, Austermann J, Papantonopoulou O, Riemenschneider M, Xue J, Bertheloot D, et al. Transcriptome assessment reveals a dominant role for TLR4 in the activation of human monocytes by the alarmin MRP8. J Immunol. 2015;194(2):575-83.

15. Low TY, Peng M, Magliozzi R, Mohammed S, Guardavaccaro D, Heck AJ. A systems-wide screen identifies substrates of the SCFbetaTrCP ubiquitin ligase. Sci Signal. 2014;7(356):rs8.

16. El Oualid F, Merkx R, Ekkebus R, Hameed DS, Smit JJ, de Jong A, et al. Chemical synthesis of ubiquitin, ubiquitin-based probes, and diubiquitin. Angew Chem Int Ed Engl. 2010;49(52): 10149-53.

17. Lebbink RJ, de Ruiter T, Adelmeijer J, Brenkman AB, van Helvoort JM, Koch M, et al. Collagens are functional, high affinity ligands for the inhibitory immune receptor LAIR-1. J Exp Med. 2006;203(6):1419-25.

18. Voehringer D, Rosen DB, Lanier LL, Locksley RM. CD200 receptor family members represent novel DAP12-associated activating receptors on basophils and mast cells. J Biol Chem. 2004;279(52):54117-23.

19. Cossarizza A, Chang HD, Radbruch A, Acs A, Adam D, Adam-Klages S, et al. Guidelines for the use of flow cytometry and cell sorting in immunological studies (second edition). Eur J Immunol. 2019;49(10):1457-973.

20. Besteman SB, Callaghan A, Hennus MP, Westerlaken GHA, Meyaard L, Bont LL. Signal inhibitory receptor on leukocytes (SIRL)-1 and leukocyte- associated immunoglobulin-like receptor (LAIR)-1 regulate neutrophil function in infants. Clin Immunol. 2020;211:108324.

21. Sievers F, Wilm A, Dineen D, Gibson TJ, Karplus K, Li W, et al. Fast, scalable generation of high-quality protein multiple sequence alignments using Clustal Omega. Mol Syst Biol. 2011;7:539.

22. Lebbink RJ, Raynal N, de Ruiter T, Bihan DG, Farndale RW, Meyaard L. Identification of multiple potent binding sites for human leukocyte associated Ig-like receptor LAIR on collagens II and III. Matrix Biol. 2009;28(4):202-10.

23. Simard JC, Simon MM, Tessier PA, Girard D. Damage-associated molecular pattern S100A9 increases bactericidal activity of human neutrophils by enhancing phagocytosis. J Immunol. 2011;186(6):3622-31.

24. Ryu JK, Kim SJ, Rah SH, Kang JI, Jung HE, Lee D, et al. Reconstruction of LPS Transfer Cascade Reveals Structural Determinants within LBP, CD14, and TLR4-MD2 for Efficient LPS Recognition and Transfer. Immunity. 2017;46(1):38-50.

25. Chen GY, Tang J, Zheng P, Liu Y. CD24 and Siglec-10 selectively repress tissue damage-induced immune responses. Science. 2009;323(5922):1722-5.

26. Arnold V, Cummings JS, Moreno-Nieves UY, Didier C, Gilbert A, Barre-Sinoussi F, et al. S100A9 protein is a novel ligand for the CD85j receptor and its interaction is implicated in the control of HIV-1 replication by NK cells. Retrovirology. 2013;10:122.

Supplementary materials and methods

Cell-based binding assay

Recombinant S100 proteins, anti-SIRL-1, and anti-LAIR-1 antibodies were dissolved in PBS to a final concentration of 10 µg/ml. Collagen I was dissolved in PBS with 2 mM acetic acid to a final concentration of 25 µg/ml. 150 µl of the solutions were incubated in wells of a MaxiSorp 96-well plate at 4°C overnight to allow immobilization. The next day, wells were washed three times with PBS and incubated with 1% (w/v) BSA solution in PBS for 60 min at RT, and the plate was again washed three times with PBS. K562 is a human lymphoblast cell line, which we transduced with full-length SIRL-1 analogous to the LAIR-1-overexpressing K562 cells, described previously (1). K562 cells (wt, LAIR-1-overexpressing, and SIRL-1-overexpressing) were concentrated to 5×10^6 cells/ml and incubated with the fluorescent dye calcein dissolved in PBS for 30 min at 37°C in a cell culture incubator. Cells were then washed three times with RPMI 1640 + 1% fetal bovine serum (FBS), and 1.5×10^5 cells in 100 µl RPMI 1640 + 1% FBS were added to the microtiter plate and incubated for 6 h at 37°C in a cell culture incubator to allow adherence to the plate-coated proteins. After incubation, cells were washed 15 times with RPMI 1640 + 1% FBS, and calcein fluorescence was recorded (Ex/Em = 485/527 nm) in a plate reader before every wash step to measure the decrease in calcein fluorescence intensity as a consequence of cell detachment. Results are shown in supplementary figure 2.
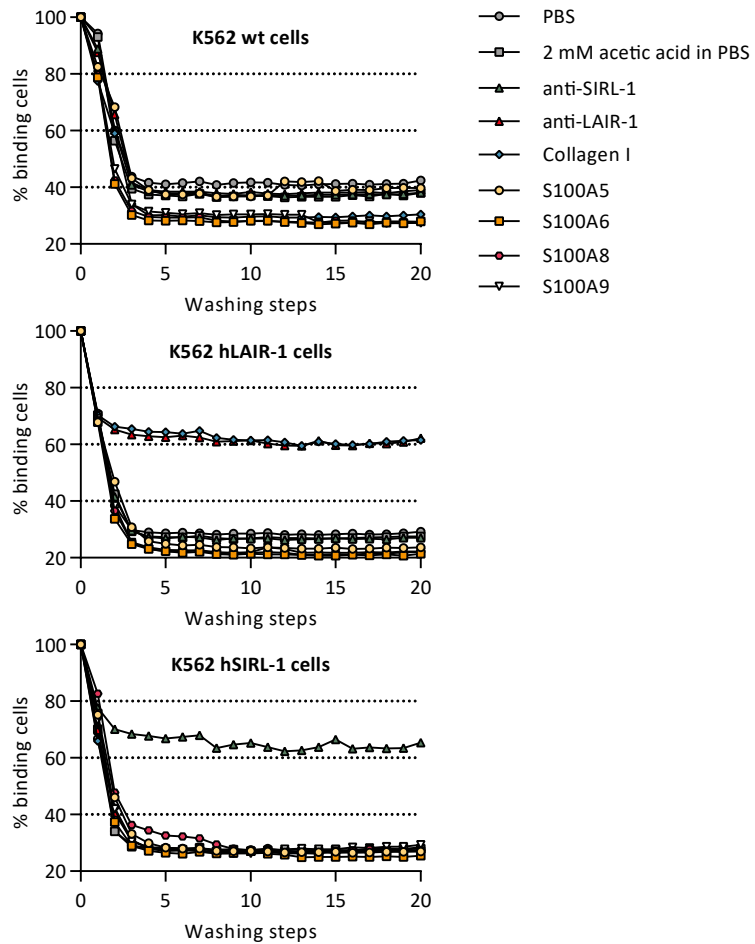
ELISA-based binding assay

Recombinant S100 proteins were dissolved in PBS to a final concentration of 10 µg/ml. Anti-SIRL-1 (clone 1A5, own production) and anti-LAIR-1 (clone 8A8, own production) antibodies and bovine serum albumin (BSA) were dissolved in PBS to a final concentration of 5 µg/ml. 100 µl of the solutions were incubated in wells of a MaxiSorp 96-well plate at 4°C overnight to allow immobilization. The next day, wells were washed three times with PBS and incubated with 3% (w/v) BSA solution in PBS for 60 min at RT. The plate was then washed five times with PBS. Fusion proteins containing ectodomains of SIRL-1 or LAIR-1 and the Fc dimerization tag, respectively SIRL-1-Fc or LAIR-1-Fc, were added to the wells to a concentration of 10 µg/ml in PBS + 1% BSA and incubated for 2 h at RT. Wells were washed five times with PBS. Anti-human-IgG-HPR Ab was added to 0.2 µg/ml in PBS + 1% BSA and incubated for 1 h at 4°C. Wells were washed five times with PBS, and ELISA was developed with TMB substrate and stopped with 1 M H_2SO_4. Absorbance was measured at 450 nm. Results are shown in supplementary figure 3.
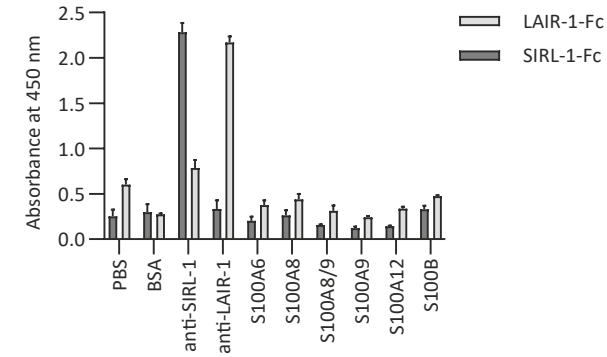
Supplementary figures
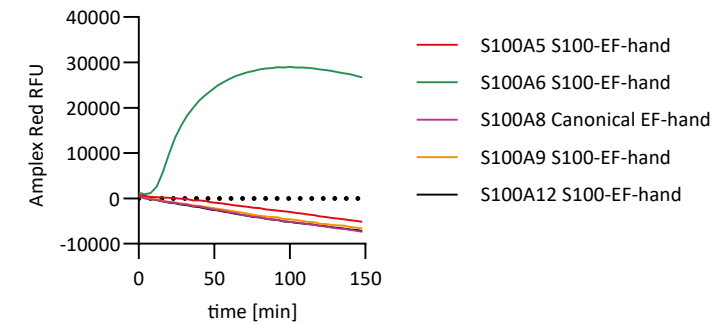
Supplementary figure 1.

EF-hand motifs of selected S100 proteins were tested for induction of ROS in human neutrophils. The S100-specific EF-hand of S100 protein A6 was the only one that induced ROS. Representative traces of one experiment.

Supplementary figure 3.

Recombinant SIRL-1-Fc fusion protein selectively bound to anti-SIRL-1, but not to plate-coated S100 proteins A6, A8, A8/9 heterodimer, A9, A12, or B. Recombinant LAIR-1-Fc fusion protein selectively bound to anti-LAIR-1, and was used as a control. Mean and SEM of one representative experiment are shown.

Supplementary references

1. Lebbink RJ, de Ruiter T, Adelmeijer J, Brenkman AB, van Helvoort JM, Koch M, et al. Collagens are functional, high affinity ligands for the inhibitory immune receptor LAIR-1. J Exp Med. 2006;203(6):1419-25.

Supplementary figure 2.

SIRL-1 overexpressing and control K562 cells were incubated with plate-coated S100 proteins as well as control antibodies and ligands. LAIR-1 overexpressing cells bound plate-coated collagen I and anti-LAIR-1 antibody. SIRL-1 overexpressing cells bound to plate-coated anti-SIRL-1 antibody, but no binding was observed to S100 proteins A5, A6, A8, and A9. A representative experiment is shown.

CHAPTER **4**

Signal Inhibitory Receptor on Leukocytes-1 recognizes bacterial and endogenous amphipathic α-helical peptides

Matevž Rumpret[1,2], **Helen J. von Richthofen**[1,2], **Maarten van der Linden**[1], **Geertje H. A. Westerlaken**[1,2], **Cami Talavera Ormeño**[2,3], **Jos A. G. van Strijp**[4], **Meytal Landau**[5], **Huib Ovaa**[2,3,†], **Nina M. van Sorg**e[4,*], **Linde Meyaard**[1,2]

[1] Center for Translational Immunology, University Medical Center Utrecht, Utrecht University, Utrecht, The Netherlands
[2] Oncode Institute, Utrecht, The Netherlands
[3] Department of Cell and Chemical Biology, Leiden University Medical Center, Leiden, The Netherlands
[4] Department of Medical Microbiology, University Medical Center Utrecht, Utrecht University, Utrecht, The Netherlands
[5] Department of Biology, Technion Israel Institute of Technology, Haifa, Israel

[†] Deceased
[*] Current affiliation: Department of Medical Microbiology and Infection Prevention, Netherlands Reference Laboratory for Bacterial Meningitis, Amsterdam Institute for Infection and Immunity, Amsterdam UMC, location Amsterdam Medical Center, University of Amsterdam, Amsterdam, The Netherlands

Abstract

Signal Inhibitory Receptor on Leukocytes-1 (SIRL-1) is a negative regulator of myeloid cell function and dampens antimicrobial responses. We here show that different species of the genus Staphylococcus secrete SIRL-1-engaging factors. By screening a library of single-gene transposon mutants in Staphylococcus aureus, we identified these factors as phenol-soluble modulins (PSMs). PSMs are amphipathic α-helical peptides involved in multiple aspects of staphylococcal virulence and physiology. They are cytotoxic and activate the chemotactic formyl peptide receptor 2 (FPR2) on immune cells. Human cathelicidin LL-37 is also an amphipathic α-helical peptide with antimicrobial and chemotactic activities, structurally and functionally similar to α-type PSMs. We demonstrate that α-type PSMs from multiple staphylococcal species as well as human cathelicidin LL-37 activate SIRL-1, suggesting that SIRL-1 recognizes α-helical peptides with an amphipathic arrangement of hydrophobicity although we were not able to show direct binding to SIRL-1. Upon rational peptide design, we identified artificial peptides in which the capacity to ligate SIRL-1 is segregated from cytotoxic and FPR2-activating properties, allowing specific engagement of SIRL-1. In conclusion, we propose staphylococcal PSMs and human LL-37 as a potential new class of natural ligands for SIRL-1.

Introduction

Our defense system typically recognizes microbes through pattern recognition receptors (PRRs), which interact with pathogen-associated molecular patterns (PAMPs) (1). Besides extrinsic stimuli such as bacteria, endogenous damage- or danger-associated molecular patterns (DAMPs) such as defensins, heat shock proteins, cathelicidin LL-37, and some S100 proteins also interact with PRRs and initiate or potentiate immune responses (2, 3). Nevertheless, excessive triggering of PRRs and other activating immune receptors can lead to immune system overactivation, induce immunopathology, and cause tissue damage. To prevent disproportionate activation, inhibitory immune receptors control the activation of immune cells. They dampen and provide context to activation signals that immune cells receive when encountering a microbial or endogenous trigger and raise the activation threshold (4).

Signal inhibitory receptor on leukocytes-1 (SIRL-1) is an inhibitory immune receptor expressed on granulocytes and monocytes in the blood (5) and monocytes in the lung (6). A genetic polymorphism regulating SIRL-1 expression levels on monocytes is associated with the inflammatory skin disease atopic dermatitis (7). Upon SIRL-1 engagement, two immunoreceptor tyrosine-based inhibitory motifs in its cytoplasmic domain become phosphorylated and recruit Src homology 2 domain-containing tyrosine phosphatases 1 and 2 to relay inhibitory signals (8). Neutrophils possess potent mechanisms for microbe recognition and clearance and are critical immune cells in the defense against bacteria. We have shown that SIRL-1 engagement on neutrophils dampens reactive oxygen species production and neutrophil extracellular trap formation (8-10). Recently, we have revealed that SIRL-1 is engaged by the endogenous S100 protein family of DAMPs (11). We have also demonstrated that SIRL-1 is downregulated on *in vitro*-activated neutrophils (8) and neutrophils present at the site of infection (12). Therefore, we have proposed that SIRL-1 acts as a disinhibition receptor: once the threshold for activation provided by SIRL-1 is passed, SIRL-1 downregulation allows for the rapid deployment of neutrophil effector mechanisms (4).

The human skin is covered with a variety of microbes that provide benefit to the host (13). However, potentially pathogenic microbes are also commonly present among healthy microbiota communities and can, depending on the location or context in which they appear, cause infections (14). To prevent infections, a robust first line of microbe-controlling mechanisms, such as the skin's acidity, low moisture content, and the production of antimicrobial peptides such as β-defensins, dermcidin, some S100

proteins, and cathelicidin LL-37, is established in the skin (15-19). The skin-residing Gram-positive bacteria of the genus *Staphylococcus* are particularly well-adapted to life under such conditions (15, 16). *Staphylococcus* comprises bacterial species with vastly different pathogenic potential. The well-characterized *S. aureus* can exhibit a commensal-like lifestyle, and commonly colonizes the human nares and skin (20, 21). It is often present on the skin of patients with atopic dermatitis (22). *S. aureus* is also a well-known pathogen (20), causing skin and soft tissue infections and even invasive systemic infections (23, 24). *S. epidermidis* fulfills a similar dual role in its interaction with the host. It is the most common colonizer of human skin, but can also cause disease, although generally in a hospital setting and not in healthy individuals (25-27). Many well-characterized virulence factors that increase staphylococcal pathogenicity and promote survival when encountering the host's defense mechanisms have been described, predominantly in *S. aureus* (28-31). In contrast, features or molecules that promote staphylococcal commensalism are less well understood. Similarly, host factors contributing to the maintenance of tolerance to microbes are mainly unknown. Multiple inhibitory immune receptors interact with microbes (32). Here, we investigated the SIRL-1 engagement by *Staphylococcus* and identified a new group of staphylococcal and endogenous ligands for SIRL-1.

Materials and methods

Bacterial strains and plasmids
Bacterial strains and plasmids used are described in Table 1 and Table 2, respectively. All strains were grown overnight in tryptic soy broth (T8907, Sigma–Aldrich, St. Louis, Missouri, USA) at 37°C with agitation. Plasmid-harboring strains were grown in tryptic soy broth supplemented with 25 µg/ml tetracycline (T7660, Sigma–Aldrich, St. Louis, Missouri, USA) overnight at 37°C with agitation. The next day, bacterial cultures were centrifuged for 3 min at 2700 g, and the supernatant was filtered through a 0.2 µm filter. Strains of the Nebraska transposon mutant library (NTML) screening array were grown in 900 µl tryptic soy broth supplemented with 5 µg/ml erythromycin (E5389, Sigma–Aldrich, St. Louis, Missouri, USA) in deep 96-well plates overnight at 37°C without agitation. The next day, bacterial cultures were centrifuged for 3 min at 2700 g, and the supernatant was collected without filtration.

Table 1. Bacterial strains used in this study.

Bacterial strains	Source
S. aureus LAC wt	(33)
S. aureus LAC Δ*agr*	(33)
S. aureus LAC ΔPSM	(34)
S. aureus LAC ΔPSMα1–4	(33)
S. aureus LAC ΔPSMβ1–2	(33)
S. aureus LAC Δ*hld*	(33)
S. aureus MW2 wt	(33)
S. aureus MW2 Δ*agr*	(33)
S. aureus MW2 ΔPSM	(35)
S. aureus MW2 ΔPSMα1–4	(33)
S. aureus MW2 ΔPSMβ1–2	(33)
S. aureus MW2 Δ*hld*	(33)
S. epidermidis ATCC 49134	Own
S. capitis ATCC 35661	Own
S. carnosus TM-300	Own
S. haemolyticus KV-116	Own
S. hominis KV-111	Own
S. warneri KV-112	Own
S. saprophyticus ATCC 35552	Own
S. lugdunensis M23590, HM-141[†]	NIAID, NIH
S. caprae C87, HM-246[‡]	NIAID, NIH
Nebraska transposon mutant library (NTML), NR-48501[§]	NIAID, NIH

Table 2. Plasmids used in this study.

Plasmids	Description	Source
pTXΔ16	tetracycline (Tet) resistance, control plasmid	(33)
pTXΔ16–PSMα	Tet resistance, *psmα1–4* genes constitutively expressed through xylose promoter	(33)
pTXΔ16–PSMβ	Tet resistance, *psmβ1–2* genes constitutively expressed through xylose promoter	(36)
pTXΔ16–*hld*	Tet resistance, *hld* gene constitutively expressed through xylose promoter	(37)

Peptide design and analysis

We designed twenty-eight 18 AA residue long peptides comprising only amino acids with the highest α-helical propensities: lysine as a positively charged, glutamic acid as a negatively charged, glutamine as a polar uncharged, and leucine as a hydrophobic amino acid (38). Sequence alignment was performed with Clustal Omega (39), secondary structure prediction was performed with Jpred4 (40), and screening of peptides for specific α-helical properties was performed with HeliQuest (41). The 28 designed peptides are shown in Table 3.

Peptide synthesis

S. aureus PSMα3, N'-formyl-PSMα3, C'–N' reversed sequence PSMα3, N'-formyl-δ-toxin, and N'-formyl-PSMβ1 (33) were custom synthesized by GenScript (Piscataway, New Jersey, USA) at 95% purity. Human cathelicidin LL-37 (42) was custom synthesized by GenScript (Piscataway, New Jersey, USA) at 95% purity or purchased from AnaSpec (AS-61302, AnaSpec, Fremont, California, USA). *S. aureus* PSMα1, PSMα2, PSMα4, PSMβ1–2, δ-toxin(33), δ-toxin allelic variant G10S (43), PSM-Mec (44), N-AgrD F20, N-AgrD F24 and N-AgrD D20 (45), *S. epidermidis* PSMα, PSMβ1–3, PSMγ/δ-toxin, PSMδ and PSMε (46, 47), *S. haemolyticus* PSMα and PSMβ1–3 (48), *S. lugdunensis* PSMε (49) and OrfX (50), *S. pseudintermedius* PSMε, *S. warneri* PSMε (49), and all 28 designed peptides were synthesized in-house precisely as described before (11). Peptide sequences are available in the listed references and Table 3.

Table 3. Sequences of the 28 designed peptides.

No. peptide	Sequence	No. peptide	Sequence
1	LQLLQQLLQQLQQLLQQL	15	LQLLKQLLKKLKKLLQKL
2	LQLQLQLQLQLQLQLQLQ	16	LQLLKQLLKKLQKLLQKL
3	LQLLEKLLEKLKELLKEL	17	LQLLKQLLKQLQKLLQKL
4	LQLELELKLKLELELKLK	18	LQLLKQLLKQLQQLLQKL
5	LKLLKKLLKKLKKLLKKL	19	LQLLKQLLQQLQQLLQKL
6	LKLKLKLKLKLKLKLKLK	20	LQLLKQLLQQLQQLLQQL
7	LELLEELLEELEELLEEL	21	LQLLEQLLQQLQQLLQQL
8	ELELELELELELELELEL	22	LQLLEQLLQQLQQLLQEL
9	QKQQKKQQKKQKKQQKKQ	23	LQLLEQLLEQLQQLLQEL
10	QKQKQKQKQKQKQKQKQK	24	LQLLEQLLEQLQELLQEL
11	QEQQEEQQEEQEEQQEEQ	25	LQLLEQLLEELQELLQEL
12	EQEQEQEQEQEQEQEQEQ	26	LQLLEQLLEELEELLQEL
13	LQLLKQLLKKLKKLLKKL	27	LQLLEELLEELEELLQEL
14	LQLLKQLLKKLKKLLQKL	28	LQLLEELLEELEELLEEL

Antibody generation

Mouse anti-human-SIRL-1 antibody clone 3D3 was generated as described previously (5). BALB/c mice were subcutaneously injected with 50 µg SIRL-1 ectodomain (in-house production, as described in (5)), and injections were repeated two and three weeks after the first injection. Mice were sacrificed three days after the final injection, and we fused splenic PBMCs with SP2/0 cells using standard hybridoma technology. We screened the resulting hybridoma clones for specific binding to SIRL-1-transfected RBL-2H3 cells. We obtained monoclonal hybridoma cells by performing limiting dilution, screened them again for SIRL-1 binding, and selected clone 3D3 as a prominent SIRL-1 binder. We purified the mAb clone 3D3 from the monoclonal hybridoma cell supernatant using a HiTrap Protein G HP column (17-0405-01, GE Life sciences, Fairfield, Connecticut, USA).

2B4 NFAT–GFP reporter cell assay

The 2B4 cell line is a T cell hybridoma cell line. In the 2B4 NFAT–GFP reporter cell lines, extracellular domains of human leukocyte-associated immunoglobulin-like receptor 1 (LAIR-1) and SIRL-1 are fused to the transmembrane and intracellular domains of human CD3ζ (11, 51). Ligation of either the cells' endogenous CD3ζ or a hLAIR-1–CD3ζ or hSIRL-1–CD3ζ chimera by an antibody or a ligand results in nuclear factor of activated T-cells (NFAT) promoter-driven GFP expression. Reporter cells were maintained in RPMI 1640 (52400-041, Life Technologies, Carlsbad, California, USA) supplemented

with 10% heat-inactivated fetal bovine serum (Biowest, Nuaillé, France) and 50 U/ml penicillin–streptomycin (11528876, Life Technologies, Carlsbad, California, USA) (referred to as culture medium hereafter). The NFAT–GPF reporter cell assay was performed with wt–CD3ζ, hSIRL-1–CD3ζ, or hLAIR-1–CD3ζ NFAT–GFP reporter cells. Nunc MaxiSorp (442404, ThermoFisher Scientific, Waltham, Massachusetts, USA) (Figures 1–4, 5A, B) or Greiner Bio-One (655101, Kremsmünster, Austria) (Figure 5C) 96-well flat-bottom plates were coated overnight at 4°C with overnight bacterial supernatants, synthetic peptides, and controls (50 µl per well). Mouse anti-human-SIRL1 mAb (clone 1A5, in-house; 10 µg/ml), mouse anti-human-LAIR-1 mAb (clone 8A8, in-house; 10 µg/ml), Armenian hamster anti-mouse-CD3 (clone 145-2C11; 10 µg/ml; BD, Franklin Lakes, New Jersey, USA) in PBS (D8537, Sigma–Aldrich, St. Louis, Missouri, USA) and human collagen I (CC050, Sigma–Aldrich, St. Louis, Missouri, USA) 2 mM acetic acid (A6283, Merck, Darmstadt, Germany); 5 µg/ml) were used as controls. The next day, wells were washed three times with PBS, and 0.5×10^4 reporter cells in 200 µl culture medium were seeded to each well. Plates were incubated overnight in a cell culture incubator at 37°C and 5% CO_2. Where indicated, reporter cells were pre-incubated with mouse-anti-SIRL-1 clones 1A5 or 3D3 or mouse-anti-LAIR-1 clone 8A8 for 30 min before seeding to the plate without washing. For the anti-CD3 mAb control in reporter assays with pre-incubation with antibodies, 1 µg/ml anti-mouse-CD3 was coated to the plate. The next day, GFP expression was measured by flow cytometry (LSR Fortessa; BD Bioscience, Franklin Lakes, New Jersey, USA) and analyzed with FlowJo software (version 10.0.7r2).

2B4 NFAT translocation assay
hSIRL-1–CD3ζ reporter cells were stimulated for 30 minutes on 96-well MaxiSorp flat-bottom plates coated overnight at 4°C with PSMα3, LL-37, or the same control antibodies as were used in the 2B4 NFAT–GFP reporter assay. In addition, cells were stimulated with 50 ng/ml phorbol 12-myristate 13-acetate (PMA; P8139, Sigma–Aldrich, St. Louis, Missouri, USA) and 3.75 µM ionomycin (I0634, Sigma–Aldrich, St. Louis, Missouri, USA). After 30 minutes, cells were fixed by a 15-minute incubation in 3.7% paraformaldehyde (F8773, Sigma–Aldrich, St. Louis, Missouri, USA). Cells were then washed three times with PBS with 1% bovine serum albumin (BSA; BSAV-RO, Roche, Basel, Switzerland) and stained with DRAQ5 (424101, BioLegend, San Diego, California, USA) and an anti-NFAT mAb (conjugated to Alexa Fluor488, clone D43B1; 14324S, Cell Signaling, Danvers, Massachusetts, USA), diluted in PBS with 1% BSA and 0.1% Triton X-100 (X100, Sigma–Aldrich, St. Louis, Missouri, USA). After three washes with PBS with 1% BSA, NFAT translocation was measured by imaging flow cytometry (Imagestream; Amnis, Austin, Texas, USA). Data were analyzed using the IDEAS software (Amnis, Austin, Texas, USA). Nuclear translocation of NFAT was assessed by analyzing the overlay between the nuclear signal (DRAQ5) and NFAT (Alexa Fluor488). We reported the percentage of the cells with a DRAQ5–Alexa Fluor488 similarity score above 2.5 (as assessed by the Similarity Feature in IDEAS software) as the percentage of cells with nuclear NFAT.

Lactate dehydrogenase (LDH) release cytotoxicity assay
Lactate dehydrogenase (LDH) release cytotoxicity assay was performed using the Pierce LDH Cytotoxicity Assay Kit (88953, ThermoFisher Scientific, Waltham, Massachusetts, USA). hSIRL-1–CD3ζ GFP reporter cells were routinely cultured as described above. For the LDH assay, cells were transferred to RPMI 1640 without phenol red (11835063, ThermoFisher Scientific, Waltham, Massachusetts, USA) supplemented with 5% heat-inactivated fetal bovine serum and seeded to a flat bottom 96-well plate at 20,000 cells per well in 100 µl medium. Cells were incubated overnight in a cell culture incubator at 37°C and 5% CO_2. The next day, 10 µl of peptides dissolved in water were added to the cells to a final concentration of 10 µM. Water and manufacturer-provided lysis buffer were used as controls. Cells were incubated in a cell culture incubator at 37°C and 5% CO_2 for 45 minutes. After incubation, supernatants were collected, and the detection of LDH was performed following the manufacturer's instructions. Absorbance at 490 and 680 nm was measured. The 680 nm absorbance values were subtracted from the 490 nm absorbance values. Values were normalized to water-treated cells as 0% cytotoxicity and lysis-buffer-treated cells as 100% cytotoxicity. The experiment was performed in duplicates.

Formyl peptide receptor 2 (FPR2)-mediated Ca^{2+} mobilization assay
HL-60 FPR2 cells (52) were routinely cultured in culture medium (described above). Prior to the assay, cells were transferred to RPMI 1640 without phenol red supplemented with 1% BSA and 50 U/ml penicillin–streptomycin (assay medium). To assess FPR2 activation, we measured FPR2-specific Ca^{2+} fluxes. HL-60 FPR2 cells were washed twice with assay medium. 1.5×10^6 cells in 1.5 ml medium were mixed with 5 µM Fluo-3-AM (F14218, Invitrogen, Waltham, Massachusetts, USA) dissolved in DMSO (472301, Sigma–Aldrich, St. Louis, Missouri, USA) and incubated in a cell culture incubator at 37°C and 5% CO_2 for 30 minutes. After incubation, cells were washed with assay medium and resuspended to a final concentration of 2×10^6 cells per ml. To block FPR2, we added 15 µM WRW4 peptide (2262/1, Tocris Bio-Techne, Minneapolis, Minnesota, USA) dissolved in H_2O to the cells. Five hundred µl of cell suspension were pipetted into FACS tubes. Ca^{2+} fluxes were recorded by FACS (FACSCanto II, BD Bioscience, Franklin Lakes, New Jersey, USA) using a 488 nm excitation laser and 530/30 nm filter. The

baseline signal was measured for 30 seconds. Next, peptides were added to the cells to a 1.5 µM final concentration, cells were very briefly vortexed, and Ca^{2+} fluxes were immediately recorded for up to 4 minutes. FlowJo (version 10.0.7r2) kinetics platform was used for initial data analysis. A time series of median fluorescence values were exported for every sample. Baseline (I_0) was established as the average signal of the first 25 seconds of measurement, and data were normalized using the formula $(I - I_0)/I_0$. Unless stated otherwise, maximum signals after stimulation are reported.

Statistical analysis

Student's *t*-test with the Holm–Šidák multiple comparison correction or one-way ANOVA followed by Dunnett's or Tukey's multiple comparisons test were performed as indicated. P-values lower than 0.05 were considered statistically significant (* p<0.05; ** p<0.01; *** p<0.001). Statistical analysis was performed with GraphPad Prism 8.

Results

SIRL-1 is engaged by a factor secreted by staphylococci

We used 2B4 NFAT–GFP reporter cells, additionally expressing a chimeric protein consisting of the extracellular domain of human SIRL-1 and the transmembrane region and intracellular domain of CD3ζ (hSIRL-1–CD3ζ) to screen for potential bacterial ligands for SIRL-1. As controls, we used non-transduced and hLAIR-1–CD3ζ-transduced 2B4 NFAT–GFP reporter cells. We stimulated all three NFAT–GFP reporter cell lines with plate-coated specific monoclonal antibodies against mouse CD3, hLAIR-1 (clone 8A8) or hSIRL-1 (clone 1A5), or collagen I. All three cell lines highly expressed GFP upon stimulation with anti-mouse CD3, which ligates the endogenous mouse CD3 protein expressed by the 2B4 NFAT–GFP cell line (Figure 1A). Stimulation with anti-LAIR-1 and anti-SIRL-1 antibodies induced high GFP expression only in the respective cell lines, demonstrating specificity (Figure 1A). Additionally, the hLAIR-1–CD3ζ reporter cell line was stimulated with plate-coated collagen I, one of many types of collagens that are natural ligands of LAIR1 (51)C , resulting in up to 70% GFP-positive cells (Figure 1A). Next, we stimulated the reporter cell lines with plate-coated overnight supernatants of *S. aureus* strains LAC and MW2. Supernatants from both strains induced GFP expression in hSIRL-1–CD3ζ reporter cells, resulting in around 60% GFP-positive cells (Figure 1A, B). We observed no response in hLAIR-1–CD3ζ reporter cells, indicating specificity for SIRL-1 (Figure 1A, B). The bacterial culture broth, tryptic soy broth, induced only minimal GFP expression in the hSIRL-1–CD3ζ line (Figure 1A, B). To determine whether the potential SIRL-1 ligand was conserved among other staphylococcal species, we stimulated the reporter cell lines with overnight supernatants of nine additional staphylococcal species (Figure 1C). All supernatants induced GFP expression in hSIRL-1–CD3ζ reporter cells, whereas none induced GFP expression in hLAIR-1–CD3ζ or wt reporter cells. This shows that a potential bacterial SIRL-1 ligand is conserved among staphylococci.

Staphylococcal agr operon controls expression of the SIRL-1-activating factor

S. aureus is the most intensely studied member of the genus *Staphylococcus*, with a wealth of research tools available to study its biology. To identify the staphylococcal SIRL-1 ligand, we screened the supernatants of all 1,920 arrayed *S. aureus* mutants from the Nebraska transposon mutant library (NTML) for their ability to activate SIRL-1 as measured by induction of GFP expression in the hSIRL-1–CD3ζ reporter cells (Figure 2A). Nineteen mutants induced percentages of GFP-positive hSIRL-1–CD3ζ reporter cells equal to or lower than the background levels (6.4% GFP-positive reporter cells)
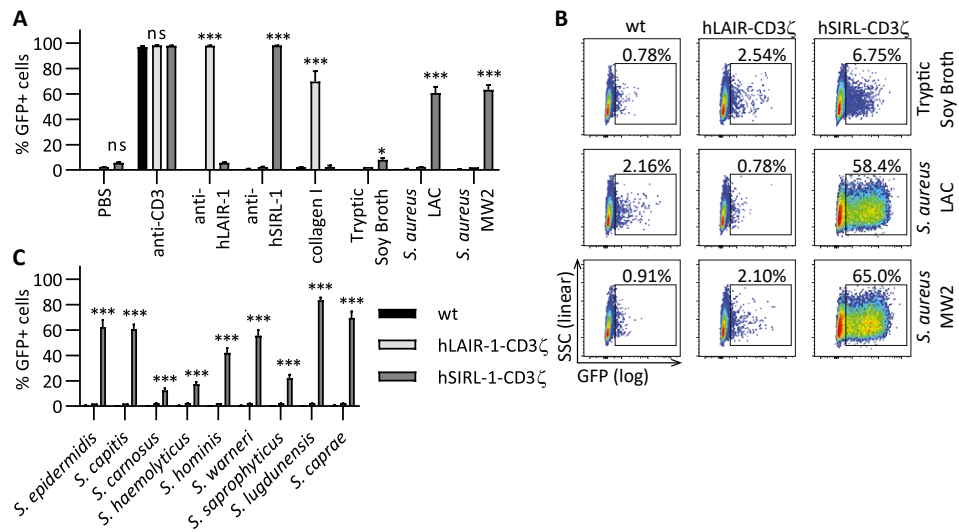
Figure 1. Supernatants of different staphylococcal species activate SIRL-1.

Wild type, hLAIR-1–CD3ζ or hSIRL-1–CD3ζ expressing NFAT–GFP reporter cells were stimulated overnight with plate-coated control antibodies, collagen, tryptic soy broth, or supernatants of overnight cultures of different *Staphylococcus sp.* grown in tryptic soy broth. GFP expression upon overnight stimulation was measured by flow cytometry. **(A)** The percentage of GFP-positive reporter cells in response to stimulation with plate-coated PBS (negative control), anti-mouse CD3, anti-LAIR-1 and anti-SIRL-1 specific antibodies, the LAIR-1 ligand collagen (positive controls) and overnight culture supernatants of the *S. aureus* strains LAC and MW2 and tryptic soy broth as control. **(B)** Representative dot plots showing the percentage of GFP-positive reporter cells after stimulation with *S. aureus* strains LAC and MW2, with tryptic soy broth as control. **(C)** The percentage of GFP-positive reporter cells in response to stimulation with plate-coated supernatants of nine other staphylococcal species. Mean and SD of three independent experiments are displayed. Student's *t*-test with the Holm–Šidák multiple comparison correction. Significance is indicated for the comparison of hLAIR-1–CD3ζ to hSIRL-1–CD3ζ. * p<0,05; ** p<0,01; *** p<0,001; ns = not significant.

induced by tryptic soy broth used to cultivate bacteria (Figure 2A, dashed line). Fifteen of these mutants are mutated in proteins normally not secreted from *S. aureus*, and one is a mutant of a putative membrane protein. These sixteen mutants are listed in the Appendix—Table 1, and we excluded them from further analysis. We next focused on the remaining three Tn-insertion mutants that induced percentages of GFP-positive cells lower than the background. Two of these Tn-insertion mutants were mutated in genes *agrB* and *agrC* (4.8% and 5.7% GFP-positive reporter cells, respectively; Figure 2A, red dots below background dashed line), which are part of the *agr* operon. The *agr* operon comprises four genes *agrA–agrD* (53). Additionally, a Tn-insertion mutant in the third gene of the *agr* operon, *agrA*, induced 7.2% GFP-positive reporter cells,

which is slightly above background (Figure 2A, red dot above background dashed line), whereas the fourth gene *agrD* is not present in the NTML. The third Tn-insertion mutant of interest was mutated in *sarA* (5.3% GFP-positive reporter cells; Figure 2A, green dot).

The *agr* operon encodes the *S. aureus* quorum sensing (QS) system, which consists of four cooperatively acting proteins AgrA–AgrD and controls the expression of accessory genes such as toxins, adhesins, and other proteins essential for biology and virulence of staphylococci (53). The gene *sarA* encodes the staphylococcal accessory regulator A (SarA), which controls the transcription of the *agr* operon (53). AgrD is a small peptide secreted through the cell wall-residing AgrB into the extracellular space, where it accumulates with the increasing density of bacterial population. High concentrations of AgrD activate the cell wall-residing receptor histidine kinase AgrC (54). Activated AgrC in turn phosphorylates the cytoplasmic response regulator AgrA, which in conjunction with SarA initiates transcription from *agr* promoters (55). Our data show that the *agr* system either regulates the secretion of a potential SIRL-1 ligand in *S. aureus* or that its components themselves induce GFP expression in the SIRL-1 reporter cell line. AgrD is the only one of the four Agr proteins that is not inactivated in the NTML but also the only secreted Agr protein, making it a likely candidate for SIRL-1 activation. In line with this, inactivation of AgrB, which is required for AgrD secretion, results in significant decrease in SIRL-1 activation. Nevertheless, inactivation of AgrA/C also results in abrogation of SIRL-1 activation, and secretion of AgrD is not dependent on AgrA/C. It is therefore unlikely that AgrD itself is the SIRL-1-activating molecule. Instead, the *agr*-encoded QS system components of *S. aureus* probably regulate the secretion of a SIRL-1 ligand. To test this hypothesis, we stimulated the hSIRL-1–CD3ζ reporter cells with supernatants of NTML mutants in regulatory proteins that are under control of the *agr* system. These included mutants in the pentose phosphate pathway-responsive regulator *rpiR*, repressor of toxins *rot*, endoribonuclease III *rnc*, and in two main staphylococcal protein secretion pathways—twin-arginine translocation system *tat/tatC* and the secretion system *secA/ secY*—which are responsible for the transmembrane transport of most *S. aureus* secreted proteins. Supernatants from all these mutants induced GFP expression in hSIRL-1–CD3ζ reporter cells, in contrast to the supernatants of *sarA*, *agrA*, *agrB*, and *agrC* NTML Tn-insertion mutants, which only induced minimal GFP-expression (Figure 2B). Our data show that the SIRL-1 ligand secreted by *S. aureus* is directly regulated by the *agr* system and not through an interconnected regulatory system downstream of the *agr* system. Further, it is not secreted via the major staphylococcal secretion systems Tat or Sec.
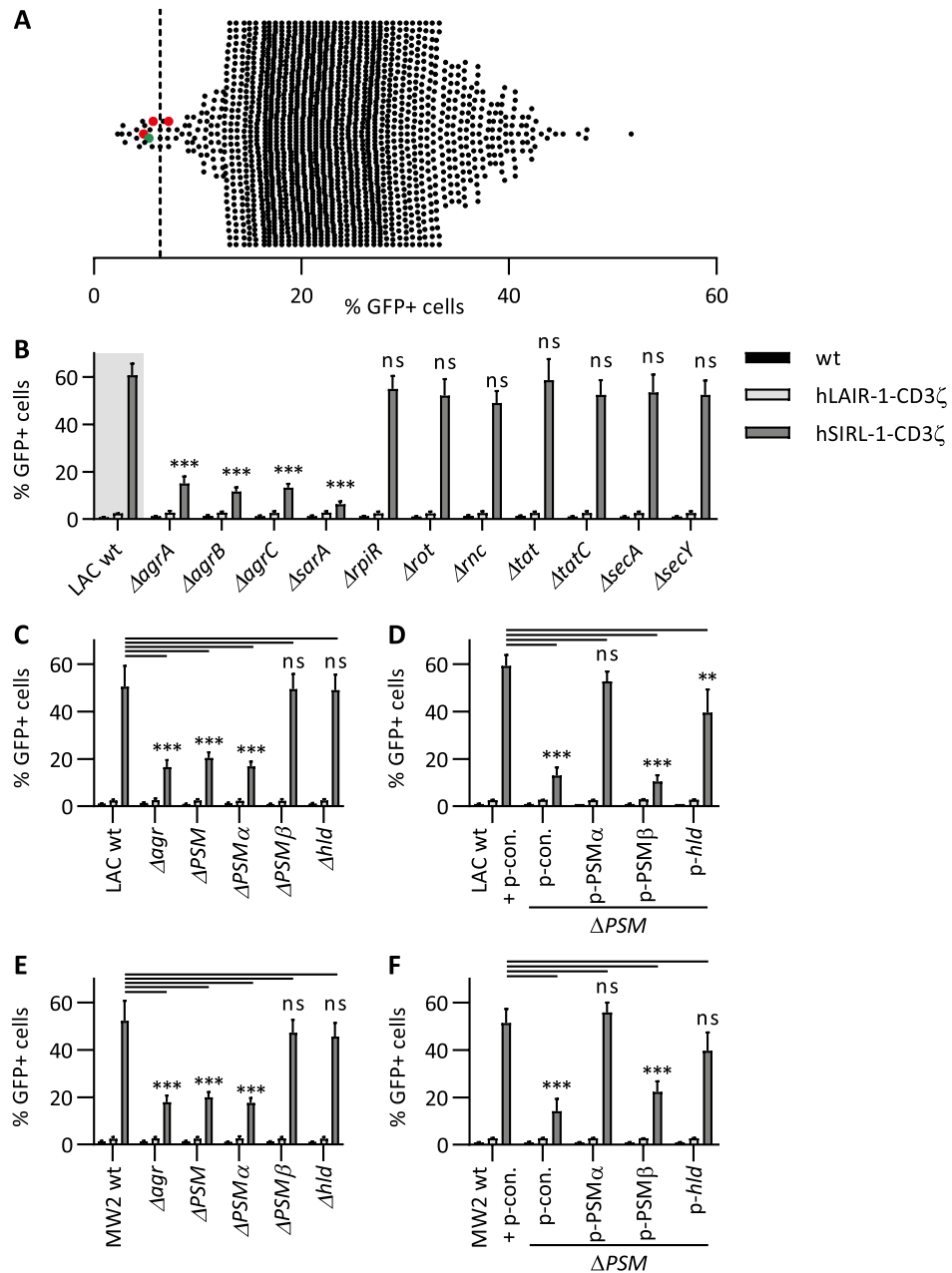
Figure 2. Inactivation of genes encoding phenol-soluble modulins (PSM) α1–4 and δ-toxin (*hld*) in *S. aureus* abrogates its ability to activate SIRL-1.

Wild type, hLAIR-1–CD3ζ or hSIRL-1–CD3ζ expressing NFAT–GFP reporter cells were stimulated overnight with plate-coated overnight supernatants of *S. aureus* strains. GFP expression upon overnight stimulation was measured by flow cytometry. **(A)** Supernatants of all *S. aureus* single-gene transposon (Tn) insertion mutants in the Nebraska transposon mutant library (NTML) were screened for activation of the hSIRL-1–CD3ζ reporter cell line. Each dot represents the GFP expression induced by the supernatant of an individual mutant in the library. Inactivation of *S. aureus* genes *agrABC* (red dots) and *sarA* (green dot) and tryptic soy broth-induced background (dashed line) are highlighted. **(B)** NTML Tn-insertion mutants of *sarA* and *agrAB*C, along with mutants of two major protein secretion systems: *tat/tatC* and *secA/secY*, and mutants of regulators of *S. aureus* gene expression *rpiR*, *rot*, and *rnc* were retested in the GFP reporter cell assay. Significance is indicated for the comparison of hSIRL-1–CD3ζ stimulated with supernatant of mutant bacteria to hSIRL-1–CD3ζ stimulated with supernatant of *S. aureus* LAC wt (result from Figure 1, here plotted for comparison and shaded grey). **(C, E)** Supernatants of isogenic deletion mutants in all four *agrABCD* quorum sensing system-encoding genes (Δ*agr*), the triple deletion mutant (ΔPSM) in all PSM-encoding genes (PSMα1–4, PSMβ1–2 and δ-toxin *hld*), and mutants in genes encoding α-type PSMs (ΔPSMα), β-type PSMs (ΔPSMβ), and δ-toxin (Δ*hld*) were tested in the GFP reporter cell assay. Deletion mutants in *S. aureus* LAC (C) and *S. aureus* MW2 (E) genetic backgrounds were used. **(D, F)** Supernatants of the triple PSM deletion strain (ΔPSM) with re-introduced plasmid-encoded PSMα1–4 (p-PSMα) or PSMβ1–2 (p-PSMβ) or δ-toxin (p-*hld*) genes were tested in the GFP reporter cell assay. Plasmid complementation was done in ΔPSM mutants of *S. aureus* LAC (D) and MW2 (F).

Significance is indicated for the comparison of hSIRL-1–CD3ζ stimulated with knockouts (C, E) or plasmid-complemented strains (D, F) to hSIRL-1–CD3ζ stimulated with wt strains (C, E) or strains complemented with control plasmid (D, F). Mean and SD of three independent experiments are displayed in panels B–F. One-way ANOVA followed by Dunnett's multiple comparisons test. * p<0,05; ** p<0,01; *** p<0,001; ns = not significant.

Staphylococcal α-type phenol-soluble modulins (PSMs) activate SIRL-1

The staphylococcal QS system also controls the expression of phenol-soluble modulins (PSMs), a family of peptides with distinct structural and functional characteristics, almost universally expressed by staphylococci. PSMs are amphipathic α-helical peptides, i.e., polar amino acids partition on one side of the helix and hydrophobic ones on the other (33). Many PSMs are cytotoxic to human cells (33, 46). PSMs are typically formylated on the N'-terminal methionine and can activate the chemotactic formyl peptide receptor 2 (FPR2) on immune cells (52). In *S. aureus*, the shorter α-type PSMs (20 to 26 amino acids) comprise PSMα1–4 and δ-toxin (*hld*), while the longer β-type PSMs comprise PSMβ1–2 (44 amino acids). The expression of *psm* genes is strictly controlled by the direct binding of AgrA to the *psm* promoter region (46). We tested overnight supernatants of the following independently-generated deletion mutants: a quadruple *agrABCD* mutant lacking all four QS genes (Δ*agr*) (33), a triple deletion mutant in PSMα1–4, PSMβ1–2 and δ-toxin *hld* (ΔPSM) (34), and single deletion mutants in either PSMα1–4 (ΔPSMα), PSMβ1–2 (ΔPSMβ) or δ-toxin (Δhld). To exclude

strain-specific effects, we used mutants in two different genetic backgrounds, *S. aureus* strains LAC and MW2. Δ*agr*, ΔPSM, and ΔPSMα1–4 in both genetic backgrounds showed significantly decreased SIRL-1 activation in the reporter cell line, while ΔPSMβ1–2 and Δ*hld* had no or very little (*hld*) effect on GFP expression, showing that PSMα1–4 are possibly the SIRL-1 ligands (Figure 2C and E).

To confirm that genes encoding PSMα1–4 confer SIRL-1 activating properties to *S. aureus* supernatants and exclude possible unwanted *in cis* effects of gene deletions, we performed a gene complementation study. Tetracycline resistance-bearing pTXΔ16 plasmids encoding either PSMα1–4 (p-PSMα), PSMβ1–2 (p-PSMβ) or δ-toxin (p-*hld*) under control of constitutively active staphylococcal xylose promoter were introduced into the ΔPSM strain. Empty pTXΔ16 plasmid backbone was introduced into wt and ΔPSM strains as a control. We performed the plasmid complementation in *S. aureus* LAC (Figure 2D) and *S. aureus* MW2 (Figure 2F) genetic backgrounds. Reintroduction of genes encoding PSMα1–4, but not PSMβ1–2, into ΔPSM mutants restored SIRL-1 reporter cell line activation to the levels induced by supernatants of wt strains. In contrast to our results with the *hld* deletion strains (Figures 2C, E), reintroduction of the gene encoding the δ-toxin (p-*hld*) restored the SIRL-1 activating phenotype exhibited by the wt strain (Figure 2D, F). Notably, in *S. aureus* LAC, p-*hld* complementation resulted in lower numbers of GFP-positive SIRL-1 reporter cells compared to the wt strain. In *S. aureus* MW2, this difference was not significant, which we attribute to slight variability in data. A possible explanation for the observed restoration of SIRL-1 activation in the p-*hld* complemented strains while the *hld* deletions showed no effect on SIRL-1 activation is that in overnight supernatants of wt strains, the amounts of PSMα1–4 may be higher than the amounts of δ-toxin and may compensate for the effect of *hld* deletion. Further, plasmid-encoded PSM genes are not controlled by their native promoter, but instead by a constitutively active xylose promoter. Additionally, the copy number of genes encoding PSMs on the plasmid is higher than on the chromosome. Both factors may result in higher supernatant concentrations of PSMs when expressed from the plasmid than when expressed from the chromosome. The empty vector backbone introduction into either wt or ΔPSM backgrounds did not have any noticeable effect on GFP expression (Figure 2D, F).

To verify that no other bacterial co-factors were required for SIRL-1 activation, we determined whether synthetic α-type PSMs activated the hSIRL-1–CD3ζ reporter cell line. Naturally-produced PSMs are predominantly N′-terminally formylated. We stimulated reporter cells with plate-coated *S. aureus* N′-formyl-PSMα3, N′-formyl-PSMβ1, N′-formyl-δ-toxin, and non-formylated PSMα3. The hSIRL-1–CD3ζ reporter

cell line was selectively activated by N′-formyl-PSMα3, non-formylated PSMα3, and N′-formyl δ-toxin, but not N′-formyl-PSMβ1, which is in line with our previous observations using bacterial gene knockouts (Figure 2C, E). The formylation status of PSMα3 did not affect SIRL-1 activation. Notably, the observed SIRL-1-activating effect was concentration-dependent (Figure 3A) and receptor-specific, since wt and hLAIR-1–CD3ζ reporter cell lines did not respond to any of the synthetic peptides (Figure 3B).

Human antimicrobial peptide cathelicidin LL-37 activates SIRL-1

Cathelicidin LL-37 is a human host defense peptide that shows biochemical, structural, and functional similarities to α-type PSMs (56, 57). It is a 37-AA long amphipathic α-helical peptide constitutively expressed by epithelial cells at barrier sites, such as the skin, and acts as a first defense against invading microbes (19). Additionally, activated immune cells secrete it in high amounts to promote the inflammatory process (17, 58-62). LL-37 is produced by cleavage of its precursor protein hCAP18 by kallikrein in keratinocytes (63) and proteinase 3 in neutrophils (64). It interacts with the membranes of bacteria and eukaryotic cells, impairing membrane integrity through pore formation, resulting in cytolysis (65, 66). In sub-cytolytic concentrations, LL-37 also regulates the immune system through binding to FPR2 (67), promoting immune cell activation to clear pathogens. We stimulated the hSIRL-1–CD3ζ reporter cells with increasing concentrations of plate-coated LL-37 and observed that this α-helical peptide activated the hSIRL-1–CD3ζ, but not wt or hLAIR-1–CD3ζ, reporter cells in a concentration-dependent manner (Figure 3C and D). This observation identifies a new endogenous candidate ligand for SIRL-1.

SIRL-1 activation by PSMs and LL-37 is blocked by specific antibodies

To further demonstrate that the observed GFP signal is SIRL-1 specific, we pre-incubated the hSIRL-1–CD3ζ reporter cells with two different anti-SIRL-1 antibodies (clones 1A5 and 3D3) or with the anti-LAIR-1 antibody (clone 8A8) before incubation on plate-coated PSMα3, LL-37, and anti-CD3 antibody as control (Figure 3E–H). Pre-incubation of hSIRL-1–CD3ζ reporter cells with anti-LAIR-1 or any of the anti-SIRL-1 antibodies did not affect the reporter cell activation by plate-coated anti-CD3 (Figure 3E). As an additional control, hLAIR-1–CD3ζ reporter cells were pre-incubated with anti-LAIR-1 and both anti-SIRL-1 antibodies and subsequently stimulated with plate-coated collagen I. While anti-LAIR-1 blocked collagen I-induced LAIR-1 activation, none of the anti-SIRL-1 antibodies did so (Figure 3F). Both anti-SIRL-1 antibodies blocked the interaction between PSMα3 or LL-37 and SIRL-1 in a concentration-dependent manner (Figure 3G, H). Thus, we have further confirmed that PMSα3- and LL-37-induced GFP expression is specific for SIRL-1 and requires the SIRL-1 ectodomain.
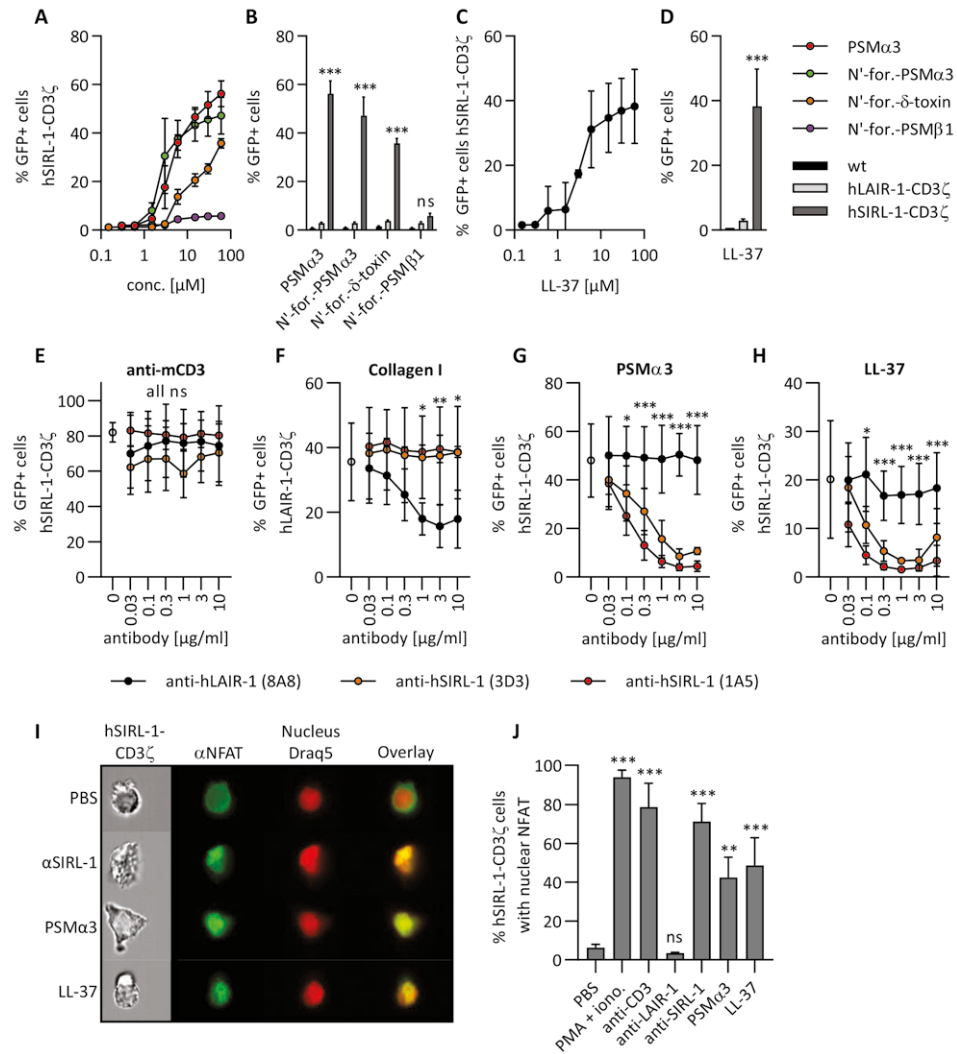
Figure 3. Synthetic *S. aureus* PSMα3 and δ-toxin and human cathelicidin LL37 selectively activate SIRL-1.

(A–D) Wild type, hLAIR-1–CD3ζ or hSIRL-1–CD3ζ expressing NFAT–GFP reporter cells were stimulated overnight with a concentration range up to 60 μM of plate-coated PSMα3, N'-formylated PSMα3, N'-formylated PSMβ1 and N'-formylated δ-toxin of *S. aureus* (A) and human cathelicidin LL-37 (C), as indicated. In B and D, only stimulations with 60 μM plate-coated peptides are shown for all three reporter cell lines. **(E–H)** hLAIR-1–CD3ζ or hSIRL-1–CD3ζ expressing NFAT–GFP reporter cells were pre-incubated with anti-hLAIR-1 and two different anti-hSIRL-1 antibodies, and then stimulated overnight with plate-coated anti-mCD3 (E), collagen I (F), PSMα3 (G) or LL-37 (H) as indicated. GFP expression upon stimulation was measured by flow cytometry (A–H). **(I, J)** Visualization (I) and quantification (J) of

NFAT translocation into the nucleus 30 minutes after stimulation of the hSIRL-1–CD3ζ GFP reporter cell line with PBS, phorbol 12-myristate 13-acetate and ionomycin (PMA + iono.), and plate-coated anti-CD3, anti-LAIR-1, anti-SIRL-1, PSMα3, and cathelicidin LL-37 was assessed by ImageStream. Mean and SD of three independent experiments are displayed. B, D–H) Student's *t*-test with the Holm–Šidák multiple comparison correction (no correction in D). **(B, D)** Significance is indicated for the comparison of hLAIR-1–CD3ζ to hSIRL-1–CD3ζ. **(E–H)** Significance is indicated for the comparison of anti-hLAIR-1 (8A8) to anti-hSIRL-1 (1A5) pre-incubation of reporter cells. **(J)** One-way ANOVA followed by Dunnett's multiple comparisons test. Significance is indicated for the comparison of PBS to all other conditions. * p<0,05; ** p<0,01; *** p<0,001; ns = not significant.

To further investigate whether PSMs and LL-37 directly activate SIRL-1, we sought to measure reporter cell activation in a transcription-independent manner. We visualized and quantified the translocation of NFAT from the cytoplasm to the nucleus 30 minutes after incubation of hSIRL-1–CD3ζ reporter cells with either PBS, PMA–ionomycin, anti-CD3, anti-SIRL-1, anti-LAIR-1, PSMα3, or cathelicidin LL-37 (Figure 3I shows visualization, and Figure 3J shows quantification). We observed NFAT translocation from the cytoplasm into the nucleus after incubation with PMA–ionomycin, anti-CD3, and anti-SIRL-1, but not PBS or anti-LAIR-1, showing specificity (Figure 3I). Incubation with both PSMα3 and cathelicidin LL-37 resulted in a substantial increase in nuclear NFAT (Figure 3J). These data strongly suggest that both *S. aureus* PSMα3 and human cathelicidin LL-37 directly activate SIRL-1.

SIRL-1 is broadly activated by staphylococcal PSMs

Virtually all staphylococcal species express PSMs. At least 12 different PSMs and similar peptides are identified in *S. aureus*: PSMα1–4, PSMβ1–2, δ-toxin, and its allelic variant G10S (33, 43). Furthermore, specific sub-types of methicillin-resistant *S. aureus* strains also possess PSM-Mec (44). Additionally, three N'-terminal fragments of the QS protein AgrD of *S. aureus*—N-AgrD F20, N-AgrD F24, and N-AgrD D20—have been identified (45) with properties remarkably similar to other PSMs. In *S. epidermidis*, PSMβ1–3, PSMα, PSMγ/δ-toxin, PSMδ and PSMε were identified (46, 47). Further, PSMβ1–3 and PSMα in *S. haemolyticus* (48), homologs of *S. epidermidis* PSMε in *S. lugdunensis*, *S. pseudintermedius* and *S. warneri* (49), and the OrfX peptide in *S. lugdunensis* (50) are described. We synthesized these PSMs and stimulated the reporter cell lines with them (Figure 4A–C). All shorter PSMα-type peptides of *S. aureus*, except for PSM-Mec and the N'-terminal fragments of AgrD, strongly activated the hSIRL-1–CD3ζ, but not wt or hLAIR-1–CD3ζ, reporter cell line (Figure 4A). The longer PSMβ-type peptides did not induce significant GFP expression in hSIRL-1–CD3ζ reporter cells (Figure 4A). Similarly, PSMα-type peptides of *S. epidermidis* and other staphylococci activated the hSIRL-1–CD3ζ, but not wt or hLAIR-1–CD3ζ, reporter cell line, while PSMβ-type peptides did not (Figure 4B, C). Therefore, we conclude that short, PSMα-like PSMs across the genus *Staphylococcus* activate SIRL-1.
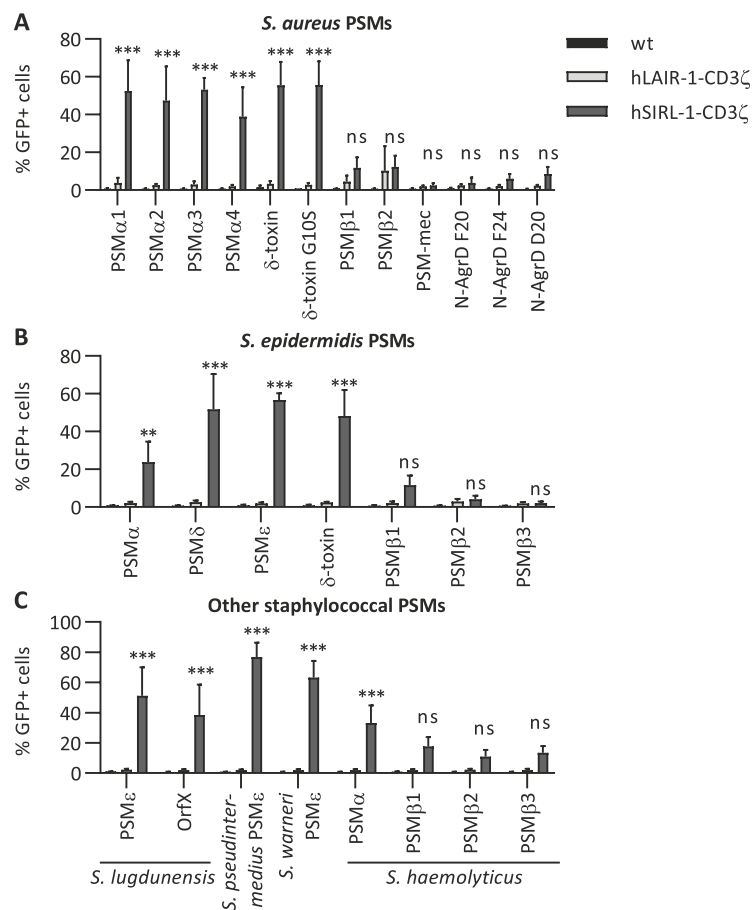
Figure 4. SIRL-1 is activated by α-type phenol-soluble modulins of multiple staphylococcal species.

Wild type, hLAIR-1–CD3ζ or hSIRL-1–CD3ζ expressing NFAT–GFP reporter cells were stimulated overnight with 10 μM plate-coated peptides as indicated. After overnight incubation, GFP expression was measured by flow cytometry. PSMs from **(A)** *S. aureus*, **(B)** *S. epidermidis* and **(C)** other staphylococci were used, as indicated. Mean and SD of three independent experiments are displayed. Student's *t*-test with the Holm–Šidák multiple comparison correction. Significance is indicated for the comparison of hLAIR-1–CD3ζ to hSIRL-1–CD3ζ. * p<0,05; ** p<0,01; *** p<0,001; ns = not significant.

SIRL-1 recognizes amphipathic α-helical peptides

Among staphylococcal PSMs, sequence identity is low. The pairwise sequence identities between SIRL-1-activating *S. aureus* PSMα3 and other SIRL-1-activating PSMs shown in Figure 4 range from 16% for *S. lugdunensis* OrfX to 41% for *S. aureus* PSMα2, and the average pairwise sequence identity is only 24%. On the other hand, general structural properties are much more conserved among PSMs. In these peptides, the alternating arrangement of charged and hydrophobic amino acids from the N' to the C' terminus results in their partitioning to the opposite sides of the α-helix, giving rise to amphipathicity. Further, an overall positive charge is seen in all SIRL-1-activating PSMs (except for *S. epidermidis* PSMα, which has a zero net charge but is still amphipathic). The same structural features are also recognized in the human cathelicidin LL-37, while its sequence identity to PSMs is low. To explore the structure–function relationship in SIRL-1-activating PSMs, we investigated how PSM-mediated SIRL-1 activation is affected by structural changes in PSMs such as change of chirality or C'–N' sequence reversal. We stimulated the hSIRL-1–CD3ζ reporter cell line with the all-D isomer of *S. aureus* PSMα3 or with C'–N' PSMα3 and observed that these peptides activated SIRL-1 in the GFP-reporter assay equally potently as the wt PSMα3 (Figure 5A and B). This observation supports the idea that SIRL-1 recognizes a general molecular feature of staphylococcal PSMs instead of a particular amino acid sequence.

To further explore the structural characteristics of SIRL-1 activating peptides, we designed a series of PSM- and LL-37-inspired peptides with differing properties and tested these in wt, hLAIR-1–CD3ζ, and hSIRL-1–CD3ζ reporter cells (Figure 5C, Table 3). We varied the amino acid composition and their positioning in the α-helix to vary: (1) overall/net charge of the helix; (2) partitioning of the charged and hydrophobic residues along the helix; and (3) overall hydrophobicity. We chose amino acids with the highest propensities to form α-helices (38): lysine to incorporate a positive charge, glutamic acid to incorporate a negative charge, glutamine as a polar uncharged amino acid, and leucine as a hydrophobic amino acid and performed secondary structure prediction for all designed peptides. Most peptides were strongly predicted to have α-helical secondary structure, except for peptides no. 2, 8, and 10-12, for which the α-helical secondary structure prediction was less reliable. The secondary structure of peptide no. 6 could not be confidently predicted. To illustrate the peptides' amphipathicity, we plotted them as helical wheels (Figure 5C, peptide no. 1 is an example of an amphipathic peptide). Using this panel of rationally designed artificial peptides, we observed that all peptides with a predicted α-helical secondary structure and amphipathic arrangement of hydrophobic residues activated SIRL-1 (Figure 5C). Notably, scrambling the positions of amino acids to disturb their separation to the
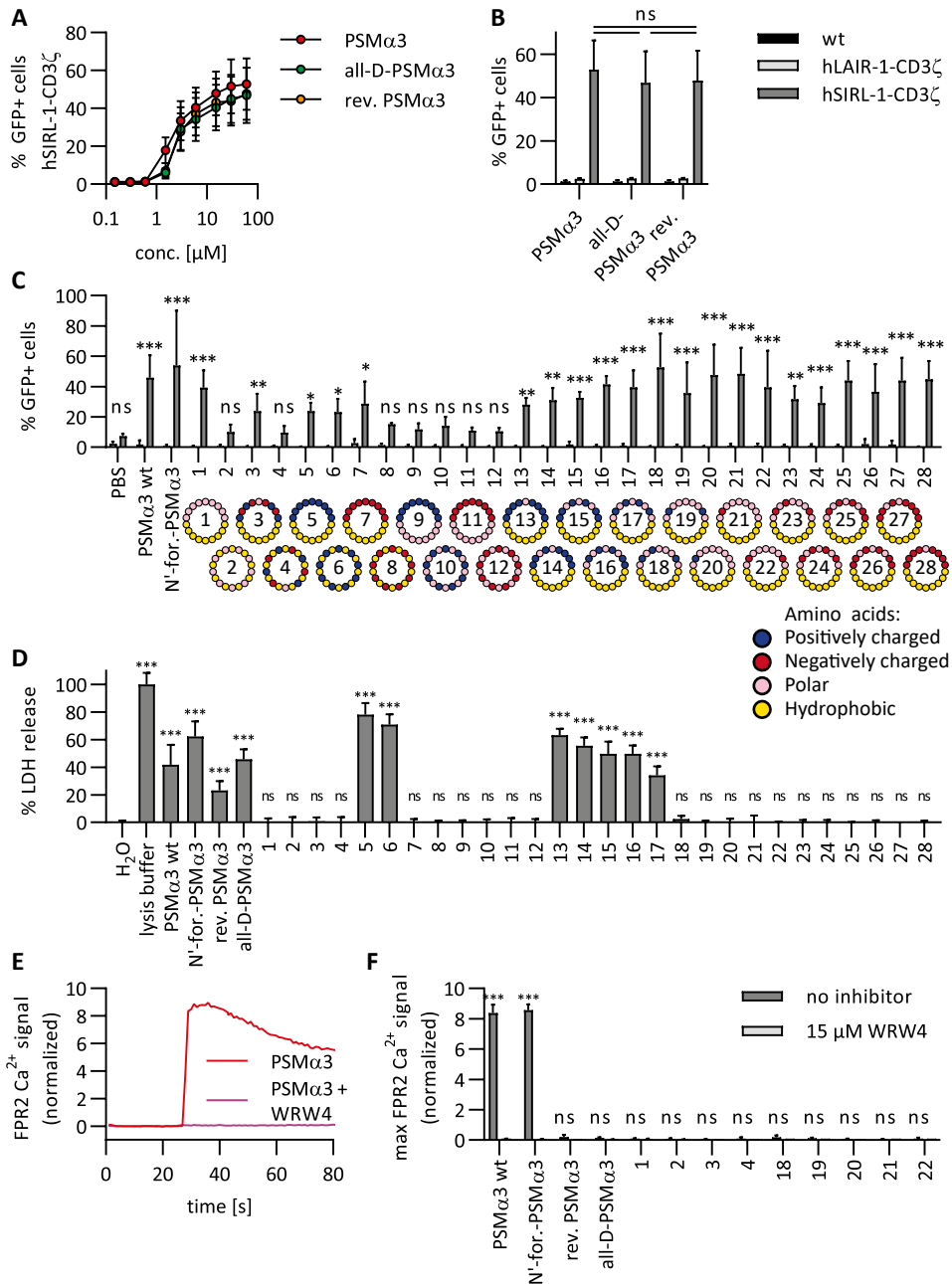
Figure 5. Artificial non-toxic amphipathic peptides specifically activate SIRL-1 and not FPR2.

Wild type, hLAIR-1–CD3ζ or hSIRL-1–CD3ζ expressing NFAT–GFP reporter cells were stimulated overnight with plate-coated peptides. After overnight incubation, GFP expression was measured by flow cytometry. **(A, B)** Reporter cells were stimulated with a concentration range up to 60 μM of plate-coated PSMα3, all-D-PSMα3 composed of D-isomers of amino acids in the same sequence as in the wt PSMα3, and reverse PSMα3 in which the amino acid sequence was reversed C'–N'. **(A)** concentration-dependent activation of hSIRL1–CD3ζ cell line. **(B)** Reporter cells stimulated with 60 μM plate-coated peptides from (A). One-way ANOVA followed by Tukey's multiple comparisons test. Significance is indicated for all comparisons between hSIRL-1–CD3ζ conditions. **(C)** Reporter cell lines were stimulated with a series of 28 artificially designed peptides with varying content and distribution of AA residues with different properties. Their helical wheel representations are shown. Amphipathic peptides contain hydrophobic residues (marked yellow) that partition to one side of the helix. Peptides were plate-coated from a 10 μM solution. Student's t-test with the Holm–Šidák multiple comparison correction. Significance is indicated for the comparison of hLAIR-1–CD3ζ to hSIRL-1–CD3ζ. **(D)** Cytotoxicity of 10 μM wt PSMα3, N'-formylated PSMα3, C'–N' reverse sequence PSMα3, all-D amino acid PSMα3, and all 28 artificial peptides against the hSIRL-1–CD3ζ reporter cells was assessed by measuring lactate dehydrogenase (LDH) release after a 45-minute incubation. One-way ANOVA followed by Dunnett's multiple comparisons test. Significance is indicated for the comparison of hSIRL-1–CD3ζ reporter cells treated with 10 μM peptides to hSIRL-1–CD3ζ reporter cells treated with H_2O. **(E, F)** HL-60 FPR2 cells were stimulated with PSMα3 and its derivatives, and with a selection of artificial SIRL-1 activating peptides that showed to be non-toxic (C, D). FPR2-mediated Ca^{2+} mobilization was monitored by flow cytometry. We stimulated the cells in presence or absence of a specific FPR2 inhibitor WRW4. **(E)** A representative Ca^{2+} signal induced by PSMα3 wt is shown. **(F)** Maximum Ca^{2+} signals with or without the FPR2 inhibitor are shown for all tested peptides. Student's t-test with the Holm–Šidák multiple comparison correction. Significance is indicated for the comparison of HL-60 FPR2 stimulated with the peptides in presence or absence of WRW4. **(A–D, F)** Mean and SD of three independent experiments are shown. * p<0,05; ** p<0,01; *** p<0,001; ns = not significant.

polar and hydrophobic faces, and consequently entirely disrupt the amphipathic character, while keeping the amino acid content unchanged, abrogated SIRL-1 activation (Figure 5C, peptide pairs 1–2, 3–4, and 7–8), except in the peptide pair 5–6 (Figure 5C). The specific composition of the helix's polar face had little effect on SIRL-1 activating properties of the peptides (Figure 5C, peptides 13–28).

Some artificial SIRL-1-activating peptides are non-toxic and do not activate FPR2

Most PSMs are highly cytotoxic and act pro-inflammatory by activating the chemotactic receptor FPR2 on immune cells (52). We tested if the cytotoxic and FPR2-activating properties of our panel of designed peptides could be segregated from the SIRL-1-engaging property. We first assessed the cytotoxicity of all designed peptides by measuring LDH release from hSIRL-1–CD3ζ reporter cells upon treatment with 10 μM peptides. All derivatives of *S. aureus* PSMα3 (PSMα3, N'-formyl-PSMα3, all-D-PSMα,

and C'–N' PSMα3) exhibited cytotoxicity (Figure 5D). In contrast, designed peptides 1–4, 7–12, and 18–22 were not cytotoxic at the same concentration (Figure 5D). We next screened a selection of non-toxic peptides for FPR2 activation by measuring Ca^{2+} mobilization in the HL-60 cell line overexpressing FPR2. *S aureus* PSMα3 and its naturally-occurring N'-formylated variant potently activated FPR2 (a representative transient Ca^{2+} signal induced by PSMα3 is shown in Figure 5E), and Ca^{2+} signaling was entirely inhibited when cells were pre-incubated with the FPR2 inhibitory peptide WRW4 (Figure 5E, F). The C'–N' PSMα3 and all-D-PSMα3 did not activate FPR2, in line with previously published data (52). None of the tested artificial SIRL-1 activating peptides activated FPR2 (Figure 5E, F). Therefore, cytotoxicity, FPR2 activation, and SIRL-1 engagement have different structural requirements. We here identified peptides 1, 3, and 18–22 as non-cytotoxic and non-FPR2-activating SIRL-1-specific agonists.

Discussion

Here, we demonstrate that secreted staphylococcal α-helical peptides, phenol-soluble modulins (PSMs) (46, 49), activate the human inhibitory receptor SIRL-1. Our data show that in *S. aureus*, PSMs are the primary SIRL-1-activating compound, as PSM-deficient mutant strains have considerably decreased SIRL-1-activating properties. Nevertheless, PSM-deficient mutants still weakly engage SIRL-1, hinting at possible additional SIRL-1-activating factors secreted by staphylococci. For instance, these could be additional not yet characterized PSMs or similar molecules. We show that synthetic PSMs from other staphylococcal species also activate SIRL-1, demonstrating that SIRL-1 broadly recognizes staphylococcal PSMs. We further demonstrate that SIRL-1 is activated by the human peptide cathelicidin LL-37, which has structural and functional similarities to staphylococcal PSMs (19). Taken together, we have identified a new group of bacterial and endogenous SIRL-1 ligands—the staphylococcal PSMs and the human cathelicidin LL-37.

PSMs are vital determinants of staphylococcal virulence: they are cytotoxic to different human cell types (33) and engage the chemotactic receptor FPR2 on human neutrophils (52). They can be secreted in high amounts; it has been shown that as much as 60% of total secreted proteins in wt *S. aureus* USA300 are PSMs (49). However, PSMs are not only virulence factors but perform multiple other functions. They promote the spreading of bacterial cells on the epithelial surface (49, 68) and facilitate the formation and structuring of biofilms (35, 69). PSMs also act as bacteriocins, cytotoxic bacterial products active against other bacterial species (34), helping to maintain staphylococci in their habitat and protecting them and their host from other invading bacterial species. Furthermore, PSMs have immunomodulatory and tolerance-inducing properties. For example, they modulate human dendritic cells to direct the development of regulatory T cells, leading to tolerogenic immune responses (70, 71). All these features identify PSMs not only as virulence factors but also as facilitators of a mutually beneficial relationship between staphylococci and their host.

The human antimicrobial peptide cathelicidin LL-37 structurally and functionally resembles the staphylococcal PSMs. It is an amphipathic α-helical peptide with cytotoxic and, through binding to FPR2, immunostimulatory properties (65-67). However, it also possesses a plethora of immunomodulatory functions; it decreases the production of pro-inflammatory and stimulates the production of anti-inflammatory cytokines in numerous cell types. For example, LL-37 decreases pro-inflammatory cytokine

production in epithelial cells pre-exposed to the bacterial TLR5 agonist flagellin (72), decreases TNF and nitric oxide production in macrophage cell lines stimulated with either LPS, LTA, or lipoarabinomannan PAMPs (73), and dampens the expression of IL-6, IL-8, and CXCL10 induced by LPS in human gingival fibroblasts (74). Future studies are needed to investigate the possibility that some of these modulatory functions are mediated by SIRL-1.

Recognition of PSMs and LL-37 by SIRL-1 does not require specific amino acid residues, which is evident from PSMs and LL-37 sharing little sequence identity. Instead, SIRL-1 may be activated by the general molecular features of these molecules. Based on the naturally occurring staphylococcal PSMs and the structurally and functionally similar human cathelicidin LL-37 that activate SIRL-1, we conclude that α-helical peptides with an amphipathic arrangement of hydrophobicity engage SIRL-1. Furthermore, structural rearrangements of PSMα3, such as in the all-D-PSMα3 isomer and the C'–N' reversed sequence PSMα3, in which α-helical secondary structure and amphipathic arrangement of hydrophobic amino acid residues are preserved, still activate SIRL-1. Similar to our observation that both L- and D-PSMα3 potently activate SIRL-1, both L-LL-37 and D-LL-37 equally induce IL-8 production in human keratinocytes, which could be blocked by surface-receptor-specific inhibitors (75). It has been suggested that the hydrophobic environment of the cell membrane might allow for specific peptide–peptide or peptide–protein interactions irrespectively of the peptide's chirality or helix sense (76). We could not demonstrate a direct interaction between PSMs or LL-37 and SIRL-1 in a purified system using recombinant proteins. This may indicate that a membrane component, which is absent in purified systems, is required for SIRL-1–PSM or SIRL-1–LL-37 complex formation. Our attempts to detect interaction may have additionally been hampered by the potent and irreversible tendency of these peptides to stack into amyloid-like fibrils (56, 57).

Based on the structural features of staphylococcal PSMs and the human LL-37, we rationally designed a series of peptides with predicted α-helical secondary structure and varying amphipathic character, charge, and charge distribution. We observed that the amphipathic character of these peptides is required for SIRL-1 activation, regardless of the detailed variations in their structure. Although we did not experimentally determine the secondary structure of these peptides, the predicted secondary structure, together with the peptides' SIRL-1-activating properties, support our idea that α-helical peptides with an amphipathic arrangement of hydrophobicity engage SIRL-1. Notably, scrambling the amino acids' positions to disturb their separation to the polar and hydrophobic faces, and consequently entirely disrupting

the amphipathic character of the designed peptides while keeping their amino acid content unchanged, abrogated SIRL-1 engagement in all but one peptide pair (Figure 5C, peptide pair 5–6). However, SIRL-1 engagement by both these peptides is much less prominent than with other peptides. Without further characterizing these peptides, we cannot adequately explain why peptide 6 still weakly engages SIRL-1. Finally, the charge distribution and overall charge of the artificial peptides did not have a notable effect on SIRL-1 activation.

General structural features of staphylococcal PSMs are formylation of the N'-terminal methionine, α-helical secondary structure, and amphipathic arrangement of amino acid residues. Functionally, PSMs are cytotoxic and FPR2-activating, and as we show here, they also engage SIRL-1. Using the series of designed peptides, we were able to decouple the cytotoxic and pro-inflammatory properties of these peptides from their SIRL-1-engaging function. As expected, all derivatives of PSMα3 (PSMα3, N'-formyl-PSMα3, all-D-PSMα, and C'–N' PSMα3) exhibited cytotoxicity, while peptides with a lower net charge showed decreased or no cytotoxicity. This is in line with the fact that antimicrobial or cytotoxic peptides are commonly amphipathic and positively charged (77). With regard to FPR2 activation, we confirm that C'–N' reversed and all-D-PSMα3 completely lost the FPR2-activating property, in line with previously published data (52). Thus, we have obtained a group of LL-37- and PSM-inspired SIRL-1 engaging peptides without FPR2-activating and cytotoxic properties, demonstrating that different structural features of PSMs and LL-37 mediate FPR2 activation, SIRL-1 activation, and cytotoxicity. Others previously showed that different epitopes of the LL-37 peptide mediate different functions and that segregation of the peptide's functions is possible (75). The ability to segregate the versatile properties of LL-37 and the PSMs is interesting from a therapeutic perspective, since inhibitory receptors are attractive targets for immunotherapy (78).

Microbes rapidly evolve and quickly change their molecular makeup. To achieve reliable recognition of microbes, the immune system employs PRRs, which recognize general structural patterns to ensure robust target recognition that is not perturbed by minor changes in the ligands. Many known PRRs recognize more than one structural pattern. For example, the receptors RAGE, TLR4, and TLR2 all recognize different patterns and bind diverse ligands (79, 80). SIRL-1 may employ a similar strategy to recognize its ligands. We previously showed that SIRL-1 is activated by the human S100 proteins (11). Here, we identify staphylococcal α-type PSMs and human cathelicidin LL-37 as an additional class of SIRL-1 ligands. Both cathelicidin LL-37 and the S100 family of proteins are DAMPs and are released from damaged cells

or activated immune cells to promote inflammatory processes. We have previously suggested that inhibitory receptors provide negative feedback on immune cell activation to prevent immunopathology (4). In this regard, the recognition of DAMPs such as LL-37 by SIRL-1 may enable prompt cessation of inflammatory processes and limit immunopathology. The interaction between SIRL-1 and its newly described exogenous ligands, staphylococcal PSMs, may serve a similar purpose. It may be in place to favor the commensal lifestyle of PSM-producing staphylococci over their potential to trigger host-damaging immune responses.

A genetic polymorphism causing reduced SIRL-1 expression levels on monocytes is associated with atopic dermatitis, a skin disease characterized by extensive inflammation and almost universal presence of *S. aureus* in atopic dermatitis skin lesions (7, 22). On the other hand, atopic dermatitis is correlated with significantly lower or even insufficient LL-37 expression, especially after skin injury (81-83), while in other inflammatory skin diseases, such as rosacea and psoriasis (84, 85), LL-37 expression is commonly increased. Together, this may suggest that the malfunction or absence of the PSM/LL-37–SIRL-1 regulatory axis, which would deliver inhibitory signals to immune cells, contributes to the development of inflammatory diseases like atopic dermatitis.

To conclude, we have demonstrated that SIRL-1 is activated by α-helical peptides with an amphipathic arrangement of hydrophobicity, namely the human cathelicidin LL-37 and the staphylococcal PSMs. We designed SIRL-1-specific activating peptides without cytotoxic and chemotactic properties. This will allow us to unravel the biology of SIRL-1 further and will facilitate the development of SIRL-1 agonists for possible therapeutic intervention in autoimmune and inflammatory diseases.

Acknowledgements

References

1. Akira S, Uematsu S, Takeuchi O. Pathogen recognition and innate immunity. Cell. 2006;124(4):783-801.

2. Yang, Han Z, Oppenheim JJ. Alarmins and immunity. Immunol Rev. 2017;280(1):41-56.

3. Bianchi ME. DAMPs, PAMPs and alarmins: all we need to know about danger. J Leukoc Biol. 2007;81(1):1-5.

4. Rumpret M, Drylewicz J, Ackermans LJE, Borghans JAM, Medzhitov R, Meyaard L. Functional categories of immune inhibitory receptors. Nat Rev Immunol. 2020;20(12):771-80.

5. Steevels TA, Lebbink RJ, Westerlaken GH, Coffer PJ, Meyaard L. Signal inhibitory receptor on leukocytes-1 is a novel functional inhibitory immune receptor expressed on human phagocytes. J Immunol. 2010;184(9):4741-8.

6. von Richthofen HJ, Gollnast D, van Capel TMM, Giovannone B, Westerlaken GHA, Lutter L, et al. Signal Inhibitory Receptor on Leukocytes-1 is highly expressed on lung monocytes, but absent on mononuclear phagocytes in skin and colon. Cell Immunol. 2020;357:104199.

7. Kumar D, Puan KJ, Andiappan AK, Lee B, Westerlaken GH, Haase D, et al. A functional SNP associated with atopic dermatitis controls cell type-specific methylation of the VSTM1 gene locus. Genome Med. 2017;9(1):18.

8. Steevels TA, van Avondt K, Westerlaken GH, Stalpers F, Walk J, Bont L, et al. Signal inhibitory receptor on leukocytes-1 (SIRL-1) negatively regulates the oxidative burst in human phagocytes. Eur J Immunol. 2013;43(5):1297-308.

9. Van Avondt K, Fritsch-Stork R, Derksen RH, Meyaard L. Ligation of signal inhibitory receptor on leukocytes-1 suppresses the release of neutrophil extracellular traps in systemic lupus erythematosus. PLoS One. 2013;8(10):e78459.

10. Van Avondt K, van der Linden M, Naccache PH, Egan DA, Meyaard L. Signal Inhibitory Receptor on Leukocytes-1 Limits the Formation of Neutrophil Extracellular Traps, but Preserves Intracellular Bacterial Killing. J Immunol. 2016;196(9):3686-94.

11. Rumpret M, von Richthofen HJ, van der Linden M, Westerlaken GHA, Talavera Ormeno C, Low TY, et al. Recognition of S100 proteins by Signal Inhibitory Receptor on Leukocytes-1 negatively regulates human neutrophils. Eur J Immunol. 2021;51(9):2210-7.

12. Besteman SB, Callaghan A, Hennus MP, Westerlaken GHA, Meyaard L, Bont LL. Signal inhibitory receptor on leukocytes (SIRL)-1 and leukocyte- associated immunoglobulin-like receptor (LAIR)-1 regulate neutrophil function in infants. Clin Immunol. 2020;211:108324.

13. Christensen GJ, Bruggemann H. Bacterial skin commensals and their role as host guardians. Benef Microbes. 2014;5(2):201-15.

14. Cogen AL, Nizet V, Gallo RL. Skin microbiota: a source of disease or defence? Br J Dermatol. 2008;158(3):442-55.

15. Glaser R, Harder J, Lange H, Bartels J, Christophers E, Schroder JM. Antimicrobial psoriasin (S100A7) protects human skin from Escherichia coli infection. Nat Immunol. 2005;6(1):57-64.

16. Schroder JM, Harder J. Human beta-defensin-2. Int J Biochem Cell Biol. 1999;31(6):645-51.

17. Lai Y, Gallo RL. AMPed up immunity: how antimicrobial peptides have multiple roles in immune defense. Trends Immunol. 2009;30(3):131-41.

18. Schittek B. The multiple facets of dermcidin in cell survival and host defense. J Innate Immun. 2012;4(4):349-60.

19. Vandamme D, Landuyt B, Luyten W, Schoofs L. A comprehensive summary of LL-37, the factotum human cathelicidin peptide. Cell Immunol. 2012;280(1):22-35.

20. Krismer B, Weidenmaier C, Zipperer A, Peschel A. The commensal lifestyle of Staphylococcus aureus and its interactions with the nasal microbiota. Nat Rev Microbiol. 2017;15(11):675-87.

21. Williams MR, Nakatsuji T, Gallo RL. Staphylococcus aureus: Master Manipulator of the Skin. Cell Host Microbe. 2017;22(5):579-81.

22. Geoghegan JA, Irvine AD, Foster TJ. Staphylococcus aureus and Atopic Dermatitis: A Complex and Evolving Relationship. Trends Microbiol. 2018;26(6):484-97.

23. Lowy FD. Staphylococcus aureus infections. N Engl J Med. 1998;339(8):520-32.

24. Edwards AM, Massey RC. How does Staphylococcus aureus escape the bloodstream? Trends Microbiol. 2011;19(4):184-90.

25. Becker K, Heilmann C, Peters G. Coagulase-negative staphylococci. Clin Microbiol Rev. 2014;27(4):870-926.

26. Brown MM, Horswill AR. Staphylococcus epidermidis-Skin friend or foe? PLoS Pathog. 2020;16(11):e1009026.

27. Byrd AL, Belkaid Y, Segre JA. The human skin microbiome. Nat Rev Microbiol. 2018;16(3):143-55.

28. O'Riordan K, Lee JC. Staphylococcus aureus capsular polysaccharides. Clin Microbiol Rev. 2004;17(1):218-34.

29. Foster TJ. Immune evasion by staphylococci. Nat Rev Microbiol. 2005;3(12):948-58.

30. de Jong NWM, van Kessel KPM, van Strijp JAG. Immune Evasion by Staphylococcus aureus. Microbiol Spectr. 2019;7(2).

31. Otto M, O'Mahoney DS, Guina T, Klebanoff SJ. Activity of Staphylococcus epidermidis phenol-soluble modulin peptides expressed in Staphylococcus carnosus. J Infect Dis. 2004;190(4):748-55.

32. Van Avondt K, van Sorge NM, Meyaard L. Bacterial immune evasion through manipulation of host inhibitory immune signaling. PLoS Pathog. 2015;11(3):e1004644.

33. Wang R, Braughton KR, Kretschmer D, Bach TH, Queck SY, Li M, et al. Identification of novel cytolytic peptides as key virulence determinants for community-associated MRSA. Nat Med. 2007;13(12):1510-4.

34. Joo HS, Cheung GY, Otto M. Antimicrobial activity of community-associated methicillin-resistant Staphylococcus aureus is caused by phenol-soluble modulin derivatives. J Biol Chem. 2011;286(11):8933-40.

35. Periasamy S, Joo HS, Duong AC, Bach TH, Tan VY, Chatterjee SS, et al. How Staphylococcus aureus biofilms develop their characteristic structure. Proc Natl Acad Sci U S A. 2012;109(4):1281-6.

36. Dastgheyb SS, Villaruz AE, Le KY, Tan VY, Duong AC, Chatterjee SS, et al. Role of Phenol-Soluble Modulins in Formation of Staphylococcus aureus Biofilms in Synovial Fluid. Infect Immun. 2015;83(7):2966-75.

37. Nakamura Y, Oscherwitz J, Cease KB, Chan SM, Munoz-Planillo R, Hasegawa M, et al. Staphylococcus delta-toxin induces allergic skin disease by activating mast cells. Nature. 2013;503(7476):397-401.

38. Nick Pace C, Martin Scholtz J. A Helix Propensity Scale Based on Experimental Studies of Peptides and Proteins. Biophysical Journal. 1998;75(1):422-7.

39. Sievers F, Wilm A, Dineen D, Gibson TJ, Karplus K, Li W, et al. Fast, scalable generation of high-quality protein multiple sequence alignments using Clustal Omega. Mol Syst Biol. 2011;7:539.

40. Drozdetskiy A, Cole C, Procter J, Barton GJ. JPred4: a protein secondary structure prediction server. Nucleic Acids Res. 2015;43(W1):W389-94.

41. Gautier R, Douguet D, Antonny B, Drin G. HELIQUEST: a web server to screen sequences with specific alpha-helical properties. Bioinformatics. 2008;24(18):2101-2.

42. Larrick JW, Hirata M, Balint RF, Lee J, Zhong J, Wright SC. Human CAP18: a novel antimicrobial lipopolysaccharide-binding protein. Infect Immun. 1995;63(4):1291-7.

43. Cheung GY, Yeh AJ, Kretschmer D, Duong AC, Tuffuor K, Fu CL, et al. Functional characteristics of the Staphylococcus aureus delta-toxin allelic variant G10S. Sci Rep. 2015;5:18023.

44. Qin L, McCausland JW, Cheung GY, Otto M. PSM-Mec-A Virulence Determinant that Connects Transcriptional Regulation, Virulence, and Antibiotic Resistance in Staphylococci. Front Microbiol. 2016;7:1293.

45. Schwartz K, Sekedat MD, Syed AK, O'Hara B, Payne DE, Lamb A, et al. The AgrD N-terminal leader peptide of Staphylococcus aureus has cytolytic and amyloidogenic properties. Infect Immun. 2014;82(9):3837-44.

46. Otto M. Phenol-soluble modulins. Int J Med Microbiol. 2014;304(2):164-9.

47. Wang R, Khan BA, Cheung GY, Bach TH, Jameson-Lee M, Kong KF, et al. Staphylococcus epidermidis surfactant peptides promote biofilm maturation and dissemination of biofilm-associated infection in mice. J Clin Invest. 2011;121(1):238-48.

48. Da F, Joo HS, Cheung GYC, Villaruz AE, Rohde H, Luo X, et al. Phenol-Soluble Modulin Toxins of Staphylococcus haemolyticus. Front Cell Infect Microbiol. 2017;7:206.

49. Cheung GY, Joo HS, Chatterjee SS, Otto M. Phenol-soluble modulins--critical determinants of staphylococcal virulence. FEMS Microbiol Rev. 2014;38(4):698-719.

50. Rautenberg M, Joo HS, Otto M, Peschel A. Neutrophil responses to staphylococcal pathogens and commensals via the formyl peptide receptor 2 relates to phenol-soluble modulin release and virulence. FASEB J. 2011;25(4):1254-63.

51. Lebbink RJ, de Ruiter T, Adelmeijer J, Brenkman AB, van Helvoort JM, Koch M, et al. Collagens are functional, high affinity ligands for the inhibitory immune receptor LAIR-1. J Exp Med. 2006;203(6):1419-25.

52. Kretschmer D, Gleske AK, Rautenberg M, Wang R, Koberle M, Bohn E, et al. Human formyl peptide receptor 2 senses highly pathogenic Staphylococcus aureus. Cell Host Microbe. 2010;7(6):463-73.

53. Novick RP, Geisinger E. Quorum sensing in staphylococci. Annu Rev Genet. 2008;42:541-64.

54. Lyon GJ, Mayville P, Muir TW, Novick RP. Rational design of a global inhibitor of the virulence response in Staphylococcus aureus, based in part on localization of the site of inhibition to the receptor-histidine kinase, AgrC. Proc Natl Acad Sci U S A. 2000;97(24):13330-5.

55. Cheung AL, Projan SJ. Cloning and sequencing of sarA of Staphylococcus aureus, a gene required for the expression of agr. J Bacteriol. 1994;176(13):4168-72.

56. Tayeb-Fligelman E, Tabachnikov O, Moshe A, Goldshmidt-Tran O, Sawaya MR, Coquelle N, et al. The cytotoxic Staphylococcus aureus PSMalpha3 reveals a cross-alpha amyloid-like fibril. Science. 2017;355(6327):831-3.

57. Engelberg Y, Landau M. The Human LL-37(17-29) antimicrobial peptide reveals a functional supramolecular structure. Nat Commun. 2020;11(1):3894.

58. Malm J, Sorensen O, Persson T, Frohm-Nilsson M, Johansson B, Bjartell A, et al. The human cationic antimicrobial protein (hCAP-18) is expressed in the epithelium of human epididymis, is present in seminal plasma at high concentrations, and is attached to spermatozoa. Infect Immun. 2000;68(7):4297-302.

59. Frohm M, Agerberth B, Ahangari G, Stahle-Backdahl M, Liden S, Wigzell H, et al. The expression of the gene coding for the antibacterial peptide LL-37 is induced in human keratinocytes during inflammatory disorders. J Biol Chem. 1997;272(24):15258-63.

60. Hase K, Eckmann L, Leopard JD, Varki N, Kagnoff MF. Cell differentiation is a key determinant of cathelicidin LL-37/human cationic antimicrobial protein 18 expression by human colon epithelium. Infect Immun. 2002;70(2):953-63.

61. Bals R, Wang X, Zasloff M, Wilson JM. The peptide antibiotic LL-37/hCAP-18 is expressed in epithelia of the human lung where it has broad antimicrobial activity at the airway surface. Proc Natl Acad Sci U S A. 1998;95(16):9541-6.

62. Xhindoli D, Pacor S, Benincasa M, Scocchi M, Gennaro R, Tossi A. The human cathelicidin LL-37--A pore-forming antibacterial peptide and host-cell modulator. Biochim Biophys Acta. 2016;1858(3):546-66.

63. Morizane S, Yamasaki K, Kabigting FD, Gallo RL. Kallikrein expression and cathelicidin processing are independently controlled in keratinocytes by calcium, vitamin D(3), and retinoic acid. J Invest Dermatol. 2010;130(5):1297-306.

64. Sorensen OE, Follin P, Johnsen AH, Calafat J, Tjabringa GS, Hiemstra PS, et al. Human cathelicidin, hCAP-18, is processed to the antimicrobial peptide LL-37 by extracellular cleavage with proteinase 3. Blood. 2001;97(12):3951-9.

65. Oren Z, Lerman JC, Gudmundsson GH, Agerberth B, Shai Y. Structure and organization of the human antimicrobial peptide LL-37 in phospholipid membranes: relevance to the molecular basis for its non-cell-selective activity. Biochem J. 1999;341 (Pt 3):501-13.

66. Thennarasu S, Tan A, Penumatchu R, Shelburne CE, Heyl DL, Ramamoorthy A. Antimicrobial and membrane disrupting activities of a peptide derived from the human cathelicidin antimicrobial peptide LL37. Biophys J. 2010;98(2):248-57.

67. Coffelt SB, Tomchuck SL, Zwezdaryk KJ, Danka ES, Scandurro AB. Leucine leucine-37 uses formyl peptide receptor-like 1 to activate signal transduction pathways, stimulate oncogenic gene expression, and enhance the invasiveness of ovarian cancer cells. Mol Cancer Res. 2009;7(6):907-15.

68. Tsompanidou E, Denham EL, Becher D, de Jong A, Buist G, van Oosten M, et al. Distinct roles of phenol-soluble modulins in spreading of Staphylococcus aureus on wet surfaces. Appl Environ Microbiol. 2013;79(3):886-95.

69. Schwartz K, Syed AK, Stephenson RE, Rickard AH, Boles BR. Functional amyloids composed of phenol soluble modulins stabilize Staphylococcus aureus biofilms. PLoS Pathog. 2012;8(6):e1002744.

70. Armbruster NS, Richardson JR, Schreiner J, Klenk J, Gunter M, Autenrieth SE. Staphylococcus aureus PSM peptides induce tolerogenic dendritic cells upon treatment with ligands of extracellular and intracellular TLRs. Int J Med Microbiol. 2016;306(8):666-74.

71. Richardson JR, Armbruster NS, Gunter M, Henes J, Autenrieth SE. Staphylococcus aureus PSM Peptides Modulate Human Monocyte-Derived Dendritic Cells to Prime Regulatory T Cells. Front Immunol. 2018;9:2603.

72. Pistolic J, Cosseau C, Li Y, Yu JJ, Filewod NC, Gellatly S, et al. Host defence peptide LL-37 induces IL-6 expression in human bronchial epithelial cells by activation of the NF-kappaB signaling pathway. J Innate Immun. 2009;1(3):254-67.

73. Scott MG, Davidson DJ, Gold MR, Bowdish D, Hancock RE. The human antimicrobial peptide LL-37 is a multifunctional modulator of innate immune responses. J Immunol. 2002;169(7):3883-91.

74. Into T, Inomata M, Shibata K, Murakami Y. Effect of the antimicrobial peptide LL-37 on Toll-like receptors 2-, 3- and 4-triggered expression of IL-6, IL-8 and CXCL10 in human gingival fibroblasts. Cell Immunol. 2010;264(1):104-9.

75. Braff MH, Hawkins MA, Di Nardo A, Lopez-Garcia B, Howell MD, Wong C, et al. Structure-function relationships among human cathelicidin peptides: dissociation of antimicrobial properties from host immunostimulatory activities. J Immunol. 2005;174(7):4271-8.

76. Tomasinsig L, Pizzirani C, Skerlavaj B, Pellegatti P, Gulinelli S, Tossi A, et al. The human cathelicidin LL-37 modulates the activities of the P2X7 receptor in a structure-dependent manner. J Biol Chem. 2008;283(45):30471-81.

77. Brogden KA. Antimicrobial peptides: pore formers or metabolic inhibitors in bacteria? Nat Rev Microbiol. 2005;3(3):238-50.

78. van der Vlist M, Kuball J, Radstake TR, Meyaard L. Immune checkpoints and rheumatic diseases: what can cancer immunotherapy teach us? Nat Rev Rheumatol. 2016;12(10):593-604.

79. Sims GP, Rowe DC, Rietdijk ST, Herbst R, Coyle AJ. HMGB1 and RAGE in inflammation and cancer. Annu Rev Immunol. 2010;28:367-88.

80. Erridge C. Endogenous ligands of TLR2 and TLR4: agonists or assistants? J Leukoc Biol. 2010;87(6):989-99.

81. Ong PY, Ohtake T, Brandt C, Strickland I, Boguniewicz M, Ganz T, et al. Endogenous antimicrobial peptides and skin infections in atopic dermatitis. N Engl J Med. 2002;347(15):1151-60.

82. Mallbris L, Carlen L, Wei T, Heilborn J, Nilsson MF, Granath F, et al. Injury downregulates the expression of the human cathelicidin protein hCAP18/LL-37 in atopic dermatitis. Exp Dermatol. 2010;19(5):442-9.

83. Kanda N, Hau CS, Tada Y, Sato S, Watanabe S. Decreased serum LL-37 and vitamin D3 levels in atopic dermatitis: relationship between IL-31 and oncostatin M. Allergy. 2012;67(6):804-12.

84. Yamasaki K, Di Nardo A, Bardan A, Murakami M, Ohtake T, Coda A, et al. Increased serine protease activity and cathelicidin promotes skin inflammation in rosacea. Nat Med. 2007;13(8):975-80.

85. Morizane S, Yamasaki K, Muhleisen B, Kotol PF, Murakami M, Aoyama Y, et al. Cathelicidin antimicrobial peptide LL-37 in psoriasis enables keratinocyte reactivity against TLR9 ligands. J Invest Dermatol. 2012;132(1):135-43.

4

Appendix

Appendix—Table 1. NTML screening hits that were excluded from further analysis.

NE number	% GFP-positive SIRL-1–CD3ζ cells	Gene	Gene product
NE169	4.1	*cap5P*	capsular polysaccharide biosynthesis protein Cap5P
NE352	5.6	*rsgA*	ribosome small subunit-dependent GTPase A
NE592	2.8	*atpA*	ATP synthase F1, alpha subunit
NE883	5.4	*xerC*	tyrosine recombinase XerC
NE974	6.4	*mutS*	DNA mismatch repair protein MutS
NE1048	4.7	*pyrP*	uracil permease
NE1205	6.4	*nrdG*	anaerobic ribonucleotide reductase, small subunit
NE1262	4.1	—	putative membrane protein (SAUSA300_1984)
NE1509	3.0	*mdlB*	ABC transporter, ATP-binding protein
NE1531	4.9	*pdxT*	glutamine amidotransferase subunit PdxT
NE1656	4.4	*ribD*	riboflavin biosynthesis protein
NE1713	4.9	*alr*	alanine racemase
NE1829	2.7	*acoB*	2-oxoisovalerate dehydrogenase, E1 component, beta subunit
NE1895	6.4	*argR*	arginine repressor
NE1896	2.3	*lpdA*	dihydrolipoamide dehydrogenase
NE1908	3.4	*ccmA*	ABC transporter, ATP-binding protein

CHAPTER **5**

Soluble Signal Inhibitory Receptor on Leukocytes-1 is released from activated neutrophils by proteinase 3 cleavage

Helen J. von Richthofen[1,2], **Geertje H.A. Westerlaken**[1,2], **Doron Gollnast**[1,2], **Sjanna Besteman**[1,3], **Eveline M. Delemarre**[1], **Karlijn Rodenburg**[1], **Petra Moerer**[1], **Daphne A.C. Stapels**[4], **Anand K. Andiappan**[5], **Olaf Rötzschke**[5], **Stefan Nierkens**[1], **Helen L. Leavis**[6], **Louis J. Bont**[1,3], **Suzan H.M. Rooijakkers**[4], **Linde Meyaard**[1,2]

[1] Center for Translational Immunology, University Medical Center Utrecht, Lundlaan 6, 3584 EA, Utrecht, The Netherlands
[2] Oncode Institute, University Medical Center Utrecht, Lundlaan 6, 3584 EA, Utrecht, The Netherlands
[3] Department of Pediatrics, Wilhelmina Children's Hospital, University Medical Centre Utrecht, Utrecht, Lundlaan 6, 3584, EA, Utrecht, The Netherlands
[4] Department of Medical Microbiology, University Medical Center Utrecht, Utrecht University, Utrecht, The Netherlands
[5] Singapore Immunology Network, Agency for Science, Technology and Research, Singapore
[6] Department of Rheumatology and Clinical Immunology, University Medical Center Utrecht, Utrecht University, Utrecht, The Netherlands

98   CHAPTER 5

99   SOLUBLE SIGNAL INHIBITORY RECEPTOR ON LEUKOCYTES-1 IS RELEASED FROM ACTIVATED NEUTROPHILS BY PROTEINASE 3 CLEAVAGE

Abstract

Signal inhibitory receptor on leukocytes-1 (SIRL-1) is an immune inhibitory receptor expressed on human granulocytes and monocytes which dampens antimicrobial functions. We previously showed that sputum neutrophils from infants with severe respiratory syncytial virus (RSV) bronchiolitis have decreased SIRL-1 surface expression compared to blood neutrophils, and that SIRL-1 surface expression is rapidly lost from *in vitro* activated neutrophils. This led us to hypothesize that activated neutrophils lose SIRL-1 by ectodomain shedding. Here, we developed an ELISA and measured the concentration of soluble SIRL-1 (sSIRL-1) in RSV bronchiolitis and hospitalized COVID-19 patients, which are both characterized by neutrophilic inflammation. In line with our hypothesis, sSIRL-1 concentration was increased in sputum compared to plasma of RSV bronchiolitis patients, and in serum of hospitalized COVID-19 patients compared to control serum. In addition, we show that *in vitro* activated neutrophils release sSIRL-1 by proteolytic cleavage, and that this diminishes the ability to inhibit neutrophilic ROS production via SIRL-1. Finally, we found that SIRL-1 shedding is prevented by proteinase 3 inhibition and by extracellular adherence protein (Eap) from S. aureus. Notably, we recently showed that SIRL-1 is activated by PSMα3 from *S. aureus*, suggesting that *S. aureus* may counteract SIRL-1 shedding to benefit from preserved inhibitory function of SIRL-1. In conclusion, we are the first to report that SIRL-1 is released from activated neutrophils by proteinase 3 cleavage and that endogenous sSIRL-1 protein is present *in vivo*.

Introduction

Immune inhibitory receptors (IIRs), also referred to as immune checkpoints, are pivotal in negative regulation of immune cells (1, 2). Although far less studied than the transmembrane form, many IIRs also have a soluble form or homologue (3). Soluble IIRs can arise from ectodomain shedding of the membrane-expressed receptor (4, 5), or can be a product of alternative splicing (6, 7) or a homologous gene (8). Soluble IIRs were found to be increased in the circulation of patients with several forms of cancer (reviewed by (3)), sepsis (9), and COVID-19 (10).

Signal inhibitory receptor on leukocytes-1 (SIRL-1), encoded by the *VSTM1* gene, is an IIR that is expressed on human monocytes and granulocytes in peripheral blood (11-13) and lung (14). On monocytes, but not granulocytes, SIRL-1 expression is associated with the single nucleotide polymorphism (SNP) rs612529T/C (13, 14). SIRL-1 inhibits innate effector functions such as Fc Receptor (FcR) induced production of reactive oxygen species (ROS) (13, 15, 16) and formation of neutrophil extracellular traps (NET) (16, 17). We recently showed that SIRL-1 recognizes amphipathic α-helical peptides, including cathelicidin LL-37 and *Staphylococcal* phenol-soluble modulins (PSMs) (18), as all well as several members of the S100 protein family (19), classifying SIRL-1 as an inhibitory pattern recognition receptor (20).

We previously showed that SIRL-1 surface expression on neutrophils and monocytes rapidly decreases after activation *in vitro* (15). Here, we hypothesized that activated neutrophils and monocytes shed the ectodomain of SIRL-1, thereby releasing soluble SIRL-1 (sSIRL-1). In addition, it has been described that *VSTM1* encodes the splice variant VSTM1-v2, which lacks the exon that encodes the transmembrane domain and is therefore predicted to give rise to a soluble form of SIRL-1 (21). Even though these potential sources of sSIRL-1 have been reported, presence of endogenous sSIRL-1 protein has not been demonstrated yet. In this study, we developed an ELISA to investigate the presence and release mechanism of sSIRL-1 protein.

Materials and methods

SIRL-1 antibodies

We previously described the production of the SIRL-1 specific monoclonal antibodies (mAbs) clone 1A5 (11) and 3D3 (18). The SIRL-1 specific mAb clone 3F5 (IgG2a isotype) was produced in a similar fashion, with the exception that mice were immunized with a SIRL-1 expressing cell line instead of Fc-labeled SIRL-1 ectodomain. The 1A5 and 3F5 mAbs were conjugated with Alexa Fluor 647 (AF647) (Thermo Fisher Scientific) for flow cytometry. The 3D3 mAb was conjugated with biotin (Thermo Scientific) for the sSIRL-1 ELISA.

For antibody competition assays, peripheral blood mononuclear cells (PBMCs) were pre-incubated for 2 hours at 37°C with respective mAb clones. Subsequently, 1A5-AF647 was added to the PBMCs and incubated for 20 minutes at 4°C, followed by two washes with FACS buffer (PBS containing 1% BSA and 0.01% NaN3). SIRL-1 expression was then measured by flow cytometry.

Biological samples

To isolate plasma for the ELISA spike experiment (Fig 1E) or for cell isolations, heparinized blood was obtained from healthy volunteers at the UMC Utrecht. For the rs612529T/C cohort, plasma and genotyping information was obtained from healthy volunteers from the Singapore Systems Immunology Cohort (SSIC) (22). For the RSV cohort, sputum, heparinized plasma and urine were obtained from infants with severe RSV bronchiolitis or control infants without infectious disease that were mechanically ventilated. These patients and the sputum isolation have been previously described (16). Briefly, sputum was collected by flushing tracheobronchial aspiration with a maximum of 2 mL normal saline. Sputum was then centrifuged 5 min at 500g to remove cells, and 30 minutes at 25000g to remove cellular debris. For the COVID-19 cohort, serum was used from SARS-CoV-2 infected patients that were hospitalized due to COVID-19 symptoms. As control, serum was obtained from healthy volunteers at the UMC Utrecht without COVID-19 symptoms. All samples were collected in accordance with the Institutional Review Board of the University Medical Center (UMC) Utrecht or the National University of Singapore.

Protease inhibitors

The protease inhibitor cocktail (cOmplete™, EDTA-free) was purchased from Roche and used at half of the recommended concentration for lysates. Pepstatin A was purchased from Fisher Scientific, E64 from Sanbio, GM6001 from Merck, Leupeptin from Roche, Eap, EapH1 and EapH2 were recombinantly produced as previously described (23). The proteinase 3 inhibitor Bt-PYDnVP (24) (compound 10, (O-C$_6$H$_4$-4-

Cl)$_2$,) was generously provided by Dr. Brice Korkmaz and Prof. Dr. Adam Lesner and used at a concentration of 10 µM.

Cloning and recombinant sSIRL-1 protein production

To produce cDNA constructs, gBlocks® (Integrated DNA Technologies) were ordered that encode VSTM1-v2 and sSIRL-1^{ecto} with a C-terminal His-tag (see Supplementary Fig 1 for the DNA sequence, and amino acid sequence of the recombinant proteins). The gBlocks were inserted into a pcDNA 3.1+ Zeocine plasmid using Gibson assembly master mix (New England Biolabs). The cDNA construct encoding LAIR-1 ectodomain (sLAIR-1^{ecto}) has been previously described (25).

Recombinant proteins were produced using the Freestyle™ 293 Expression System (Thermo Fisher Scientific) according to manufacturer's instructions. Four days after transfection, supernatants were collected and filtered through a 0.45 µM Minisart Filter (Sartorius). The His-tagged proteins in the supernatants were purified using HIStrap FF columns (GE Healthcare) according to manufacturer's instructions. Briefly, the columns were attached to an ÄKTAprime™ (GE Healthcare) and equilibrated with binding buffer (20 mM Na$_3$PO$_4$, 500 mM NaCl, 20 mM Imidazole, pH 7.4). Next, supernatants were mixed with binding buffer in a 1:1 ratio, filtered through a Stericup 0.22 µM filter (Millipore), and loaded onto the ÄKTAprime™. After loading, binding buffer was applied until a steady baseline was reached. Next, elution buffer (20 mM Na$_3$PO$_4$, 500 mM NaCl, 500 mM Imidazole, pH 7.4) was added for a one-step elution of the proteins. Protein-containing fractions were pooled and rebuffered to PBS using VIVAspin columns (5,000 MWCO PES; Sartorius). Protein yield was determined with a BCA protein assay (Pierce™; Thermo Scientific).

SDS-PAGE and Western blot

To remove N-linked glycosylation, recombinant proteins were treated with PNGase F (New England Biolabs) according to manufacturer's instructions. Next, the proteins were incubated 5 minutes at 95°C in Laemmli sample buffer (Bio-Rad laboratories), with or without addition of β-mercaptoethanol (Sigma-Aldrich Chemie). Proteins were separated by SDS-PAGE on Any kD Mini-PROTEAN TGX Precast Protein Gels (Bio-Rad Laboratories) and either stained directly with coomassie blue (Merck) or transferred onto 0.45 µm PVDF membranes (Merck) for western blot analysis.

For western blot analysis, membranes were blocked in TBS containing 0.05% Tween-20 (TBS-T) and 5% BSA, incubated with mAb 1A5 (2 µg/mL in TBS-T with 1% BSA), followed by staining with goat-anti-mouse IgG F(ab')2-HRP (Jackson ImmunoResearch; 1:5000 diluted in TBS-T with 1% BSA). All incubations were 1h at RT and followed by extensive washing with TBS-T. Finally, proteins were visualized using ECL Western blot reagent (Fisher Scientific) and the ChemiDoc™ imaging system (Bio-Rad).

To determine PR3 cleavage, 2 µg sSIRL-1^{ecto} or VSTM1-v2 was incubated with 0,2 µg PR3 in PBS with 0.5M NaCl and incubated 3h at 25°C, followed by SDS-PAGE and Western blot analysis as described above, except that rabbit-anti-mouse IgG-HRP (DAKO; 1:10.000 diluted in TBS-T with 1% BSA) was used as secondary antibody.

sSIRL-1 ELISA

To measure sSIRL-1 in cell supernatants, 96-wells flat-bottom MAXIsorp plates (Nunc) were coated overnight at 4°C with capture mAb 1A5 (5 µg/mL in PBS, 50 µL/well). After washing with PBS 0.05% (v/v) Tween-20, plates were blocked with 100 µL/well blocking buffer (1% (w/v) BSA, 3% (w/v) dry milk in PBS). Next, plates were washed and incubated with undiluted cell supernatants and the standard curve consisting of serially diluted sSIRL-1^{ecto} in PBS 1% BSA (50 µL/well), overnight at 4°C. The following day, plates were washed and incubated with biotinylated mAb 3D3 for 1 hour at RT, followed by washing and incubation with streptavidin poly-HRP (0.1 µg/mL; Sanquin) for 1 hour at RT. Finally, plates were washed and incubated with 100 µL/well TMB-substrate (Biolegend/ITK). The substrate reacted approximately 8 minutes, after which color development was stopped by adding 100 µL/well 1M H$_2$SO$_4$. Absorbance was measured at 450 nm on the CLARIOstar® (BMG Labtech). Absorbance at 570 nm was used for background correction. All incubations, except coating of the capture antibody, were done on a shaker.

The same procedure was used to measure sSIRL-1 in plasma, serum, urine or sputum samples, with two exceptions: a different blocking buffer was used (3% (w/v) BSA in PBS), and samples were pre-incubated 15 minutes on a shaker with 20 µg/mL HAMA blocking reagent (Fitzgerald) before adding the samples to the ELISA plate, to prevent a-specific interactions.

We expressed the concentration of sSIRL-1 in pM rather than pg/mL, because endogenous sSIRL-1 may have a different molecular weight than the recombinant sSIRL-1^{ecto} that was used for the standard curve.

Neutrophil stimulation with protease inhibitors

Neutrophils were isolated from peripheral blood using density gradient centrifugation on Ficoll (GE Healthcare). The neutrophil pellet was incubated with ammonium chloride buffer to lyse the erythrocytes. The remaining neutrophils were washed and suspended in RPMI 1640 containing 10% (v/v) FCS and 1% (v/v) PS. Neutrophils were then stimulated with 50-100 ng/mL tumor necrosis factor (TNF; Miltenyi) or 100 µg/mL of the Dectin-1 ligand Curdlan (Wako biochemical) in flatbottom plates (Nunc) at 37°C, with or without addition of protease inhibitors. After 2 to 4 hours, neutrophils were centrifuged 5 minutes at 500g to collect the supernatants. Cells were used for flow cytometry analysis. Supernatants were centrifuged once more for 30 minutes at 25000g at 4°C to remove cellular debris, followed by ELISA measurements.

ROS assay

ROS production by primary neutrophils was assessed by amplex red assay as previously described (15), with following changes: After isolation, neutrophils were first incubated for 1h at 37°C with or without 50 ng/mL TNF to induce SIRL-1 shedding. After two washes with HEPES buffer, ROS production was induced by plating cells on a Microfluor® 2 white-bottom 96-well plate (ThermoFisher) coated with 10 µg/mL anti-CD32 (clone IV.3, Stem cell) in combination with 15 µg/mL anti-SIRL-1 (clone 1A5; agonist) or an appropriate isotype control (BD Biosciences). Fluorescence was measured in a 96-well plate reader (Clariostar, BMG Labtech) every minute for 60 minutes (λ Ex/Em = 526.5–97 / 650–100 nm). Background ROS production was corrected by subtracting the signal of PBS-treated cells.

PLB-985 cell treatment with neutrophil serine proteases

The transduction and culture method of PLB-985 cells with SIRL-1 overexpression have been previously described (15). Cells were treated 2h at 37°C with neutrophil elastase (Elastin Products Company), cathepsin G (Biocentrum), or proteinase 3 (Elastin Products Company) (all 1 µM), followed by flow cytometry analysis.

Flow cytometry

To determine SIRL-1 expression, cells were washed once with FACS buffer and stained with mAb 1A5 or 3F5 conjugated to AF647 or appropriate isotype controls (BD Biosciences) for 20 minutes at 4°C. Subsequently, the cells were washed twice with FACS buffer and finally taken up in FACS buffer with addition of 7AAD (BD Bioscience) for viability staining. To assess neutrophil activation markers or mPR3 expression, cells were stained with antibodies against CD11b (conjugated to FITC; eBioscience), CD62L (conjugated to PE; BD Biosciences) or PR3 (Wieslab AB) for 20 minutes at 4°C, followed by washing. For the PR3 staining this was followed by incubation with a goat anti-mouse IgG antibody conjugated to PE (Southern Biotech.) Cells were analyzed using the BD FACS Canto II and FlowJo software (Treestar, Ashland, OR). Neutrophils were gated as in Supplementary Fig 3A. Neutrophil purity was always >90%, based on forward scatter (FSC) and sideward scatter (SSC).

Statistical analysis

Statistical analyses were performed using GrapPad Prism software (version 8.3.0). For each graph, the statistical test and number of biological replicates (n) are described in the figure legends.

Results

Development of sSIRL-1 ELISA

To develop a sSIRL-1 ELISA, we first produced recombinant His-tagged sSIRL-1 proteins: SIRL-1 ectodomain (sSIRL-1^{ecto}) and VSTM1-v2, representing products of ectodomain shedding and alternative splicing, respectively (See Fig 1A for a schematic representation of the proteins, and Supplementary Fig 1A for the amino acid sequences). Both proteins were N-glycosylated, as shown by a shift in molecular weight after PNGase-F treatment and SDS-PAGE and Western blot analysis (Fig 1B, C). Deglycosylated VSTM1-v2, with a predicted MW of 21.6 kDa, had an apparent size of 37 kDa, which is consistent with the MW found in a previous study (21). Deglycosylated sSIRL-1^{ecto}, with a predicted MW of 13.8 kDa, had an apparent size of 16 kDa. The size of the proteins was not affected by reduction with 2-mercaptoethanol, indicating the proteins did not form inter-molecular dimers with disulfide bonds.

For the ELISA, sSIRL-1^{ecto} was used as a standard, SIRL-1 mAb clone 1A5 as capture antibody and SIRL-1 mAb clone 3D3 as detection antibody. In a competition assay, clone 1A5 and 3D3 did not interfere with each other for binding to SIRL-1, and thus recognize different epitopes (Supplementary Fig 1B). The ELISA detected sSIRL-1^{ecto} and VSTM1-v2 equally well, with a lower limit of detection of 8 pM (Fig 1D). The ectodomain of the inhibitory receptor LAIR-1 (sLAIR-1^{ecto}), which has 31% sequence identity with sSIRL-1^{ecto}, was not detected in the ELISA, indicating specificity of the ELISA (Fig 1D). We spiked sSIRL-1^{ecto} into heparin plasmas that were sSIRL-1 negative in our ELISA. The spike was recovered in all plasma dilutions tested (Fig 1E), indicating that plasma is not interfering with the sSIRL-1 measurement. Next, we spiked sSIRL-1^{ecto} into human pooled serum (HPS) and subjected it to 10 freeze thaw cycles, or incubation at 37°C, 56°C or 65°C for 30 minutes or 1 hour. sSIRL-1 concentration was stable in all freeze thaw cycles but decreased after 30 minutes incubation at 65 °C (Supplementary Fig 1C). Taken together, we developed a sensitive and specific assay to measure sSIRL-1 protein concentration and showed that sSIRL-1 can be detected in presence of human plasma components and is stable during multiple freeze-thaw cycles.

sSIRL-1 is present *in vivo* and increased in respiratory inflammation

To investigate the presence of sSIRL-1 protein *in vivo*, we used the ELISA to measure sSIRL-1 in plasma of healthy individuals, stratified per genotype of the rs612529T/C SNP. rs612529C associates with decreased SIRL-1 expression on monocytes, but not on granulocytes (13, 14). sSIRL-1 was detectable in only a small percentage of plasma samples from healthy individuals (8 out of 53, 15.1%) (Fig 2A). There was a tendency
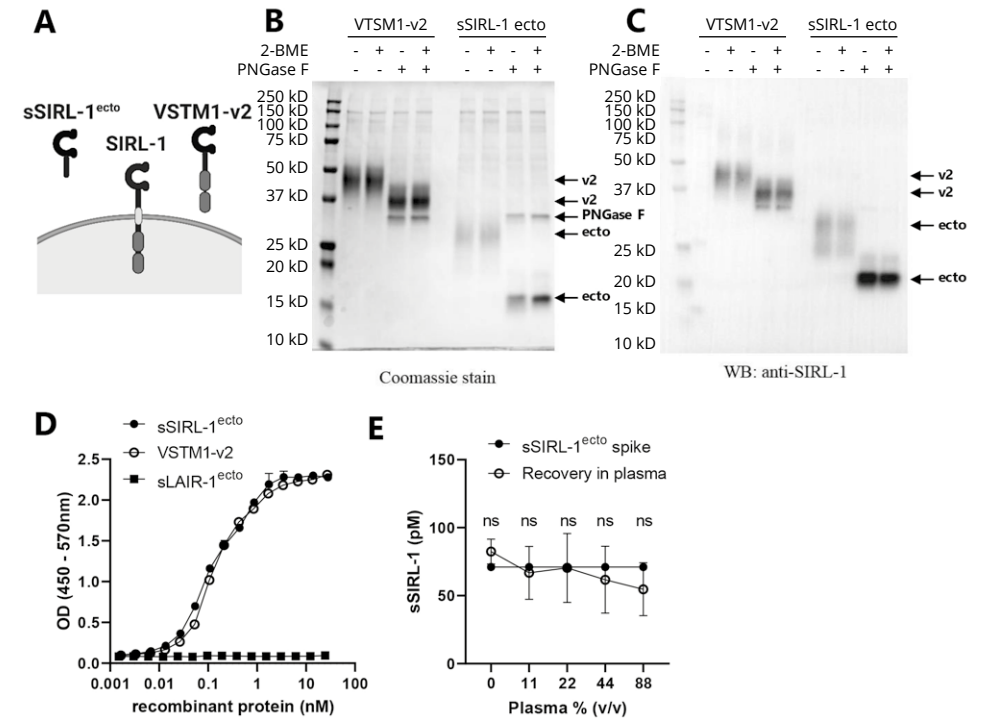

Figure 1. Development of sSIRL-1 ELISA.

(A) Schematic representation of SIRL-1 and its two potential soluble forms; VSTM1-v2 and sSIRL-1^{ecto}. **(B-C)** SDS-PAGE analysis of VSTM1-v2 and sSIRL-1^{ecto}, with or without pre-treatment with PNGase F or β-mercaptoethanol (2-BME). Proteins were either stained directly by coomassie (B) or transferred to a membrane and stained with SIRL-1 mAb clone 1A5 (C). Arrows indicate the position of VSTM1-v2 (v2), sSIRL-1^{ecto} (ecto) or PNGase F. **(D)** sSIRL-1^{ecto}, VSTM1-v2 and negative control sLAIR-1^{ecto} were titrated in an in-house developed sSIRL-1 ELISA (n≥3, one representative example is shown). **(E)** sSIRL-1 negative heparin plasmas (n=5) were titrated and spiked with 70 pM sSIRL-1^{ecto}. sSIRL-1 concentration was measured by ELISA, symbols represent the mean ± SD. The statistical difference between the spike and the recovery of sSIRL-1^{ecto} at different plasma dilutions was tested using an one sample Wilcoxon test, ns = not significant.

toward a lower percentage of samples with detectable sSIRL-1 in individuals with a rs612529 C allele, but these differences were not statistically significant (Fig 2B).

To investigate the presence of sSIRL-1 in an inflammatory context, we measured sSIRL-1 in patients with COVID-19 or RSV bronchiolitis, which are both characterized by excessive neutrophil recruitment and activation (reviewed in (26, 27). We detected sSIRL-1 in approximately 70% of sera drawn from hospitalized adult COVID-19 patients, and the mean sSIRL-1 concentration was significantly higher than in control serum (Fig 2C-D).

sSIRL-1 concentration in serum of COVID-19 patients was not affected by sex, age, nor the time since the start of symptoms or hospitalization (Supplementary Fig 2A, B, D, E). Within patients, sSIRL-1 concentration fluctuated in serum collected at two time points (Supplementary Fig 2C). Serum samples in this cohort were collected at non-standardized time points, and we had restricted availability to clinical data, thereby limiting further analysis on the correlation between sSIRL-1 concentration and disease activity.

We previously showed that RSV bronchiolitis patients have decreased SIRL-1 expression on sputum neutrophils compared to peripheral blood neutrophils (16, 28), which is in line with our hypothesis that activated neutrophils shed the ectodomain of SIRL-1. Indeed, in patients with severe RSV bronchiolitis, we detected sSIRL-1 in 15 out of 16 sputa, and the mean sSIRL-1 concentration in sputum was significantly increased compared to plasma (Fig 2E). We also detected sSIRL-1 in the urine of the RSV patients, in similar concentrations as in plasma (Fig 2F). In summary, we show that sSIRL-1 concentration is mostly undetectable in healthy individuals, but increased in hospitalized COVID-19 or severe RSV bronchiolitis patients.

Activated neutrophils shed sSIRL-1 via proteolytic cleavage

To test if activated neutrophils indeed shed SIRL-1, we stimulated neutrophils from healthy controls *in vitro* with TNF or curdlan, with or without addition of a broad-spectrum protease inhibitor cocktail. TNF treatment induced respectively up- and down-regulation of CD11b and CD62L, indicative of neutrophil activation (Supplementary Fig 3B, C). We then analyzed SIRL-1 expression on activated neutrophils by flow cytometry, and sSIRL-1 concentration in the supernatant by ELISA. In agreement with our previous work (15), the percentage of SIRL-1+ neutrophils decreased after activation (Fig 3A, B). Concomitantly, we detected sSIRL-1 in the supernatant (Fig 3C). Treatment with the protease inhibitor cocktail prevented this (Fig 3A-C), indicating that activated neutrophils release sSIRL-1 via proteolytic cleavage. We observed a trend of lower SIRL-1 expression on CD11b+ CD62L- cells compared to CD11bdim CD62L+ cells, suggesting a correlation between neutrophil activation markers and loss of SIRL-1 (Supplementary Fig 3D, E).

To determine whether SIRL-1 shedding by neutrophils has a functional consequence, we pre-treated neutrophils with TNF to induce SIRL-1 shedding and then tested the effect of SIRL-1 ligation on ROS production. To prevent that neutrophils would become unresponsive to stimulation by the pre-treatment, we stimulated with TNF for one hour, which induced SIRL-1 shedding albeit with variation between donors (Supplementary Fig 3F). As in our previous work (15), FcR stimulation with anti-CD32 induced ROS production, which was inhibited by SIRL-1 ligation (Fig 3D). However, in neutrophils which had shed SIRL-1, this inhibition was diminished (Fig 3D). Thus, SIRL-1 shedding limits the ability to dampen neutrophilic ROS production via SIRL-1.
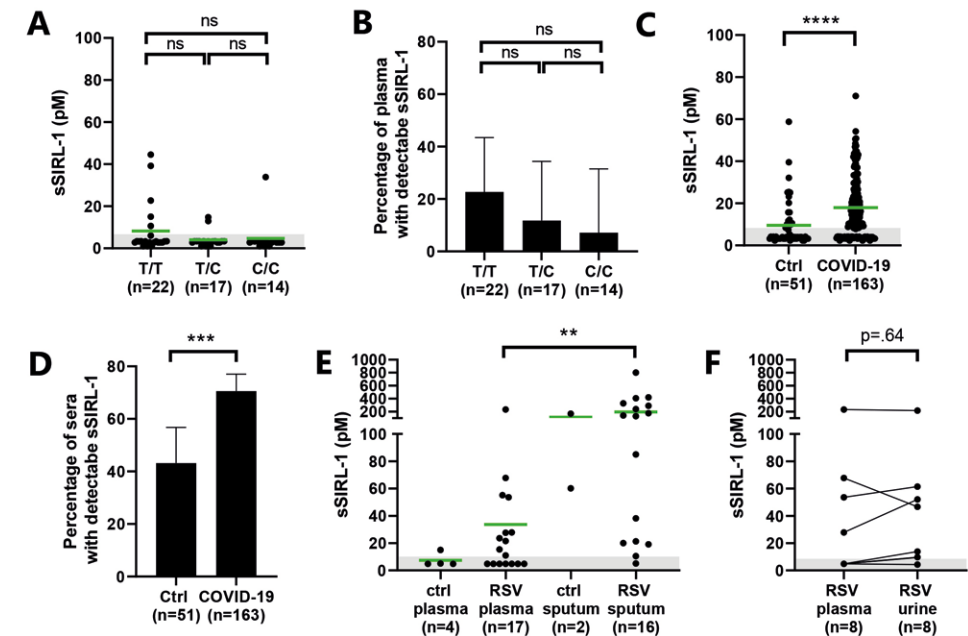

Figure 2. sSIRL-1 is increased in COVID-19 and RSV bronchiolitis patients.
sSIRL-1 was measured by ELISA in plasma, urine and sputum. **(A-B)** sSIRL-1 concentration in plasma from 53 healthy donors, stratified per genotype of the rs612529 SNP (T/T, n=22; T/C, n=17; C/C, n=14). **(C-D)** sSIRL-1 concentration in serum of hospitalized COVID-19 patients (n=163) and control serum (n=51). **(E)** sSIRL-1 concentration in heparin plasma or sputum of mechanically ventilated infants with severe RSV bronchiolitis or mechanically ventilated infants without infection (controls). Control plasma, n=4; RSV plasma, n=17; control sputum, n=2; RSV sputum, n= 16. **(F)** sSIRL-1 concentration in paired plasma and urine samples of infants with severe RSV bronchiolitis (n=8) **(A, C, E, F)** Each dot represents one donor, the green horizontal lines represent the mean. The shaded grey area indicates the lower limit of detection (LLOD). Samples with undetectable sSIRL-1 were given a value of 0.5 x LLOD. Statistical differences were calculated using a Kruskal-Wallis test with Dunn's correction (A, E), a Mann Whitney test (C), or a Wilcoxon test (F). **(B, D)** The percentage of samples with detectable sSIRL-1. The error bars indicate the 95% confidence interval, calculated with Wilson-Brown. The statistical differences were calculated using a Fisher's exact test (B, D), in combination with Bonferroni correction for multiple testing (B). ** $p \leq .01$, *** $p \leq .001$. **** $p \leq .0001$, ns = not significant.

sSIRL-1 is shed by proteinase 3

To examine which protease cleaves SIRL-1, we activated neutrophils with TNF in combination with inhibitors against major classes of proteases: pepstatin A for aspartic proteases, E64 for cysteine proteases, GM6001 for metalloproteases, leupeptin for serine and cysteine proteases, and aprotinin for serine proteases. Treatment with 10 μM aprotinin resulted in a small but significant increase in the percentage of SIRL-
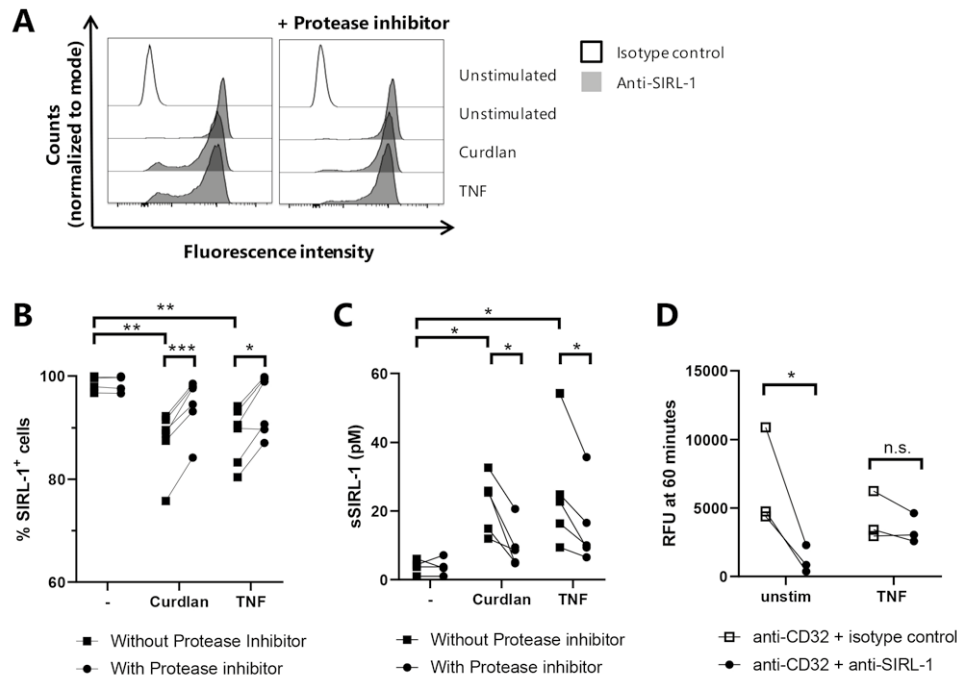
Figure 3. Activated neutrophils shed SIRL-1, which limits inhibition of ROS production via SIRL-1.

Neutrophils were isolated from healthy donors and stimulated 4h at 37 °C with curdlan (100 µg/mL) or TNF (100 ng/mL), with or without addition of a protease inhibitor cocktail. **(A-B)** SIRL-1 expression on neutrophils was analyzed by flow cytometry. Shown are representative histograms of the fluorescence intensity of cells stained with a SIRL-1 antibody (clone 1A5) (closed histogram) or an isotype control (open histogram) (A) and the quantification of the percentage of SIRL-1+ cells (B). Each symbol represents one donor, n=6. **(C)** Supernatants from stimulated neutrophils were analyzed by sSIRL-1 ELISA. Each symbol represents one donor, n=5. **(D)** Neutrophils were pre-incubated for 1h with or without 50 ng/mL TNF, upon which neutrophils were added to 96-well plates that were coated with mAb anti-CD32 in combination with anti-SIRL-1 (clone 1A5) or an isotype control. ROS was production was measured by amplex red assay. Shown is the relative fluorescent intensity (RFU) at 60 minutes. The background signal in unstimulated samples was subtracted from all samples. N=3. Statistical significance was determined using a two-way ANOVA with Geisser-Greenhouse correction and Holm-Sidak's multiple comparison test (B-D), * p ≤ .05, ** p ≤ .01, *** p ≤ .001.

1-expressing cells after TNF stimulation, suggesting that SIRL-1 is shed by a serine protease (Fig 4A). Thus, we further investigated SIRL-1 cleavage by the serine proteases that are predominantly secreted from activated neutrophils; cathepsin G, neutrophil elastase, and proteinase 3 (PR3) (29). Treatment of SIRL-1-overexpressing PLB-985 cells with PR3 resulted in a modest but consistent decrease in SIRL-1 expression,

whereas cathepsin G and elastase did not affect SIRL-1 expression on these cells (Fig 4B-C). To confirm that PR3 cleaves SIRL-1, we activated neutrophils with TNF in presence of a specific PR3 inhibitor. Indeed, the PR3 inhibitor partially prevented the loss of SIRL-1 expression on TNF-activated neutrophils in all donors tested (Fig 4D-E). TNF treatment induced expression of membrane-bound PR3 (mPR3) in part of the cell population (Supplementary Fig 4A, B), and neutrophils which upregulated mPR3 lost more SIRL-1 than neutrophils which remained mPR3 negative (Supplementary Fig 4C, D). Finally, treatment of sSIRL-1ecto and VSTM1-v2 with PR3 in a purified system resulted in proteolytic cleavage as assessed by SDS-PAGE and Western Blot (Fig 4F). Thus, we show that PR3 cleaves SIRL-1.

sSIRL-1 shedding can be prevented by Eap, a physiological PR3 inhibitor from *S. aureus*

Finally, we asked whether SIRL-1 shedding can also be prevented by a physiological PR3 inhibitor. For this we used extracellular adherence protein (Eap) and its homologues EapH1 and EapH2, which are *S. aureus*-derived inhibitors of neutrophil serine proteases, including PR3 (23). Remarkably, treatment with Eap almost completely prevented the loss of membrane-expressed SIRL-1 after TNF stimulation of neutrophils (Fig 5A, B). A similar trend was seen after treatment with EapH2, whereas treatment with EapH1 had no effect on membrane SIRL-1 expression. In PLB-985 cells, Eap and EapH1 both inhibited SIRL-1 cleavage by exogenous PR3 (Fig 5C). Together, these data indicate that SIRL-1 shedding can be prevented by natural PR3 inhibitors such as Eap.
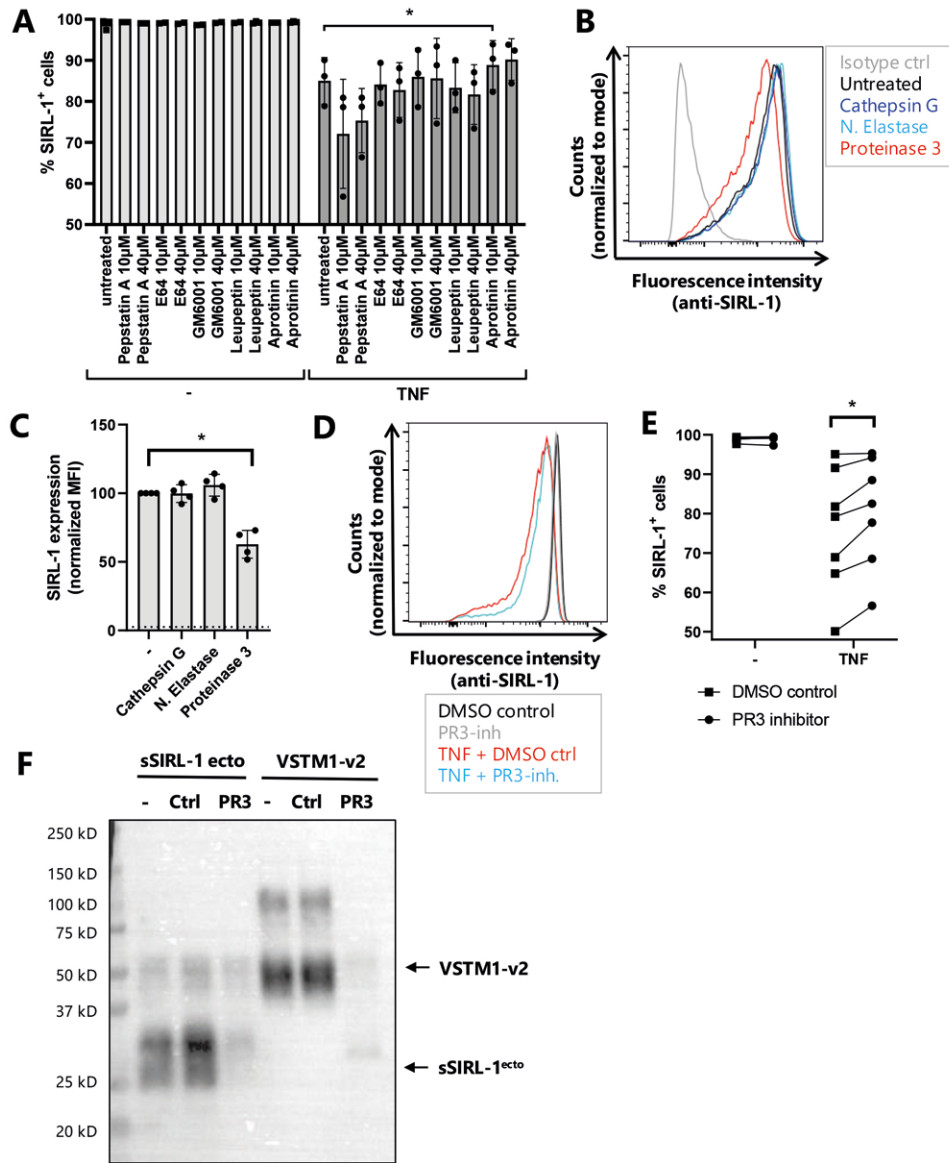
Figure 4. SIRL-1 is cleaved by PR3.

(A, D, E) Neutrophils were isolated from healthy donors and stimulated 2h at 37 °C with TNF (50 ng/mL), with or without addition of inhibitors against major protease classes (A; 10-40 μM) or a PR3 inhibitor (D-E; 10 μM). Cells were stained with a SIRL-1 antibody (clone 3F5) and analyzed by flow cytometry. **(A)** The bars indicate the percentage of SIRL-1⁺ cells (mean ± SD), each symbol represents a donor, n=3. **(D)** Representative histograms of the fluorescence intensity of cells stained with a SIRL-1 antibody and **(E)** the quantification of the percentage of SIRL-1⁺ cells (each symbol with connected line represents a donor),

n=7. **(B-C)** PLB-985 cells with SIRL-1 overexpression were treated 2h with neutrophil elastase, cathepsin G, or proteinase 3 (all 1 μM), followed by flow cytometry analysis (n=4). Shown are representative histograms of the fluorescence intensity of cells stained with a SIRL-1 antibody (clone 3F5) or isotype control (B) and the quantification of the median fluorescent intensity (MFI), normalized to the MFI of untreated cells (C; mean ± SD, each symbol represents one experiment, the dotted line represents the normalized MFI of the isotype control). **(F)** sSIRL-1^{ecto} and VSTM1-v2 were left untreated (-) or treated with buffer control (ctrl) or PR3 for 3h at 25 °C, and analyzed by SDS-PAGE and Western Blot. The membrane was stained with a SIRL-1 antibody (clone 1A5). The arrows indicate the position of VSTM1-v2 or sSIRL-1^{ecto}. One representative experiment of n=3 is shown. Statistical significance was determined using a mixed-effects model with Dunnett's multiple comparisons test (A; TNF treatment alone was compared to TNF treatment with each of the protease inhibitors), a 1-way ANOVA with Dunnett's multiple comparison test (C) or a mixed-effects model with Sidak's multiple comparisons test (E), all with Geisser-Greenhouse correction, * p ≤ .05.\
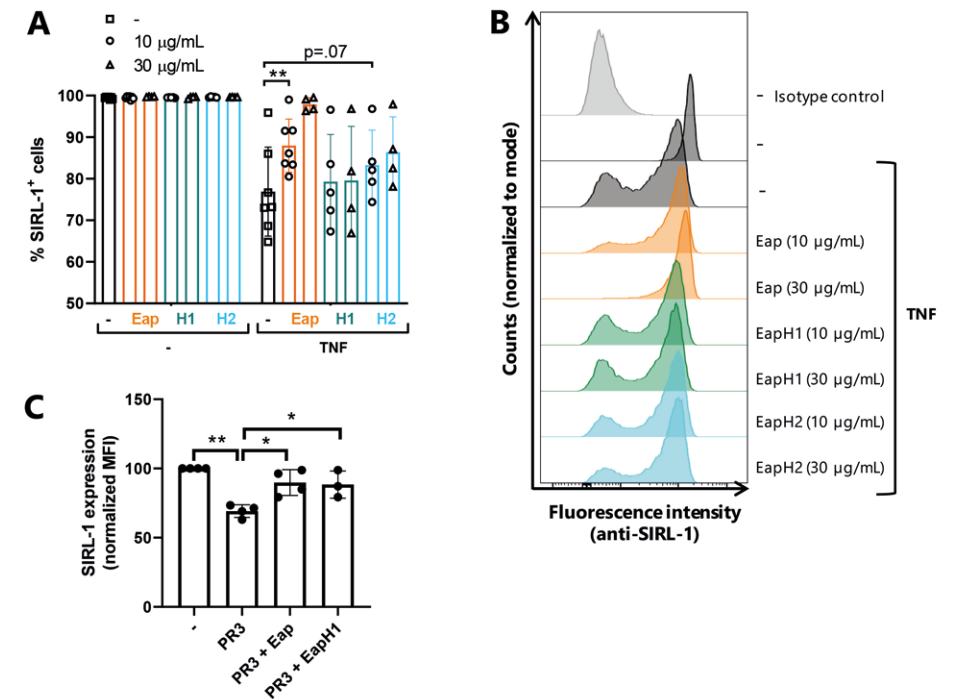

Figure 5. *S. aureus* protein Eap inhibits SIRL-1 shedding.

(A-B) Neutrophils were isolated from healthy donors and stimulated for 2h at 37 °C with TNF (50 ng/mL), with or without addition of 10-30 μg/mL Eap, EapH1, or EapH2 (indicated with H1 or H2, respectively). Cells were stained with a SIRL-1 mAb (clone 3F5) and analyzed by flow cytometry, n=4-6. **(A)** The percentage of SIRL-1⁺ cells (mean ± SD), each symbol represents a donor. **(B)** Representative histograms of the fluorescence intensity of cells stained with a SIRL-1 antibody. **(C)** PLB-985 cells with SIRL-1 overexpression were treated 2h with 1 μM proteinase 3, with or without addition of Eap or EapH1 (30 μg/mL). SIRL-1 expression was analyzed by flow cytometry. The bars indicate the percentage of SIRL-1⁺ cells (mean ± SD), each symbol represents an experiment, n=3-4. Statistical significance was determined using a mixed-effects model with Dunnett's multiple comparisons test (A) or Holm-Sidak's multiple comparisons test (C), both with Geisser-Greenhouse correction, * p ≤ .05, ** p ≤ .01.

Discussion

Here, we developed an ELISA to measure sSIRL-1 concentration (Fig 1) and are the first to show that sSIRL-1 protein is present *in vivo* (Fig 2).

sSIRL-1 concentration was increased in sputum of RSV bronchiolitis patients compared to plasma, suggesting release of sSIRL-1 at the site of infection (Fig 2E). sSIRL-1 was also detectable in sputum of control infants, which can be explained by previous observations that sputum neutrophils of these control patients are activated (16), possibly due to mechanical ventilation (30). From the site of infection, sSIRL-1 may leak into the circulation, as there was a trend of increased sSIRL-1 in RSV patient plasma compared to control plasma, although this comparison was limited by the low number of control plasmas (Fig 2E). Similarly, sSIRL-1 concentration was increased in serum of hospitalized COVID-19 patients compared to control serum (Fig 2C). Lastly, sSIRL-1 was also detectable in urine of RSV patients (Fig 2F), indicating that, similar to soluble LAIR-1 (25), sSIRL-1 is cleared by the kidneys.

Several studies have indicated a role of neutrophils in the pathophysiology of COVID-19 (reviewed in (27)). Using a machine learning algorithm on a broad panel of inflammatory markers, neutrophil-related markers predicted critical illness of COVID-19 patients most strongly (31). These markers included resistin, lipocalin-2 and hepatocyte growth factor, which are all released by degranulating neutrophils. Due to restricted availability of data and the collection of serum at non-standardized time points, we could not correlate sSIRL-1 concentration to COVID-19 disease progression, clinical parameters or inflammatory markers in our cohort. Future studies will have to clarify if sSIRL-1 may serve as a biomarker to predict COVID-19 disease severity, or other diseases characterized by high neutrophil activation. The presence of sSIRL-1 in urine at a similar concentration as in plasma (Fig 2F) indicates the potential usage of sSIRL-1 as a biomarker in urine, which is less invasive to obtain than plasma and sputum.

We found that SIRL-1 is cleaved from activated neutrophils by PR3 (Fig 3-4). In addition to secretion of soluble PR3, activated neutrophils can express PR3 on the plasma membrane on a subpopulation of cells (32). Membrane-bound PR3 (mPR3) has been suggested to bind to the plasma membrane via CD177, other membrane-expressed proteins, or directly to the lipid bilayer (33-35). We compared shedding of SIRL-1 on FACS-sorted CD177$^+$ versus CD177$^-$ neutrophils and found that CD177 expression did not affect sSIRL-1 shedding (unpublished observations). Still, we showed that SIRL-1 surface expression decreased in a subpopulation of neutrophils after activation *in*

vitro (Fig 3A, 4D, 5B), which may reflect cells with high mPR3 expression. Indeed, we found that, upon TNF treatment, mPR3 positive cells express significantly less SIRL-1 than mPR3 negative cells (Supplementary Fig 4D). Nonetheless, some mPR3 positive cells did not (yet) shed SIRL-1, suggesting that further activation is needed in these cells. For example, some of the mPR3 may still be in an inactive form (36). On the other hand, SIRL-1 expression was homogeneously low on neutrophils in sputum of RSV bronchiolitis patients (16, 28). We could not measure mPR3 expression on sputum neutrophils, because we only had access to frozen sputum in this study. However, others have shown that neutrophils of infectious disease patients have increased surface expression of PR3 (37). In addition, high concentrations of PR3 are found in sputum of patients with inflammatory airway disease, including COVID-19, COPD and cystic fibrosis (38-41), and its concentration predicts COVID-19 disease severity (42). Taken together, the relative contribution of soluble PR3 and mPR3 to SIRL-1 shedding remains to be determined.

Finally, we show that shedding of SIRL-1 by activated neutrophils can be prevented by physiological PR3 inhibitors such as Eap (Fig 5). This is relevant in the context of infections, as Eap is secreted by *S. aureus*. The homologues of Eap, EapH1 and EapH2, were less effective in preventing SIRL-1 shedding from activated neutrophils. In a previous study, using short peptide substrates, EapH1 and EapH2 also had a lower capacity to inhibit PR3 than Eap (Eap, K_i = 0.23 nM; EapH1, K_i = 1.0 nM; EapH2, K_i = 21 nM) (23) (Fig 5A, B). Alternatively, EapH1 and EapH2 may differ in their ability to inhibit mPR3, as mPR3 has been shown to be more resistant to PR3 inhibitors than soluble PR (43). The latter finding may also explain the partial effectiveness of the PR3 inhibitor used in this study, and the differential abilities of leupeptin and aprotinin to inhibit SIRL-1 shedding (Fig 4A, 5A).

In addition to ectodomain shedding, sSIRL-1 may derive from the splice variant VSTM1-v2 (21, 44). VSTM1-v2 mRNA expression was increased in PBMCs of Rheumatoid Arthritis patients compared to controls (44). However, it remains to be determined whether endogenous VSTM1-v2 protein is present *in vivo*. Both forms of sSIRL-1 were recognized by our ELISA (Fig 1D), thus not allowing for discrimination between these forms. Further research into VSTM1-v2 protein would benefit from the development of an antibody that recognizes the intracellular tail of SIRL-1, which is present in VSTM1-v2 but not in shed sSIRL-1.

We previously argued that IIRs that are constitutively expressed on a cell form a threshold to prevent unnecessary immune activation. Some of these threshold receptors, so-called disinhibition receptors, are downregulated after an activating

stimulus surpasses the initial threshold, to facilitate subsequent cellular activation (2). SIRL-1 is such an disinhibition receptor, based on its constitutive high expression on monocytes and granulocytes in peripheral blood and lung (11, 13, 14) and downregulation during inflammation (16, 28). We thus propose that the function of SIRL-1 shedding is to facilitate a strong anti-microbial response, once the threshold for activation is surpassed. In support, we show that SIRL-1 shedding limits the ability to dampen neutrophilic ROS production via SIRL-1 (Fig 3D).

Of course, the inhibitory function of SIRL-1 and hence the effect of SIRL-1 shedding also depends on expression of its ligands. We found that SIRL-1 is activated by S100 proteins (19), cathelicidin LL-37, and PSMs from Staphylococci (18). In inflammatory conditions with local tissue damage and DAMP release, neutrophil released LL-37 and S100 proteins may act mostly on newly incoming neutrophils with high SIRL-1 expression, to signal to these cells that no further immune activation is required.

PSMs are produced by both pathogenic and harmless Staphylococci (45). SIRL-1 ligation by PSMs may be beneficial for the host, for example by facilitating tolerance of resting neutrophils to harmless Staphylococci such as *S. epidermidis*, but still allowing for full neutrophil activation once SIRL-1 is shed in an inflammatory context. Interestingly, *S. aureus*, the most pathogenic member of the Staphylococcus family, is unique in its secretion of Eap proteins (23). *S. aureus* may use Eap to inhibit SIRL-1 shedding to benefit from the preserved inhibitory function of membrane-expressed SIRL-1. Of particular interest is a recent study showing that *S. aureus* also requires Eap to prevent degradation of PSMα3 by neutrophil serine proteases (46), indicating that Eap potentially preserves expression of SIRL-1 as well as its ligands.

In conclusion, we measured increased sSIRL-1 concentration in COVID-19 and RSV bronchiolitis patients and provided mechanistic insight into the loss of SIRL-1 from activated neutrophils. Future studies will have to further elucidate the implications of sSIRL-1 release, and its potential use as a biomarker.
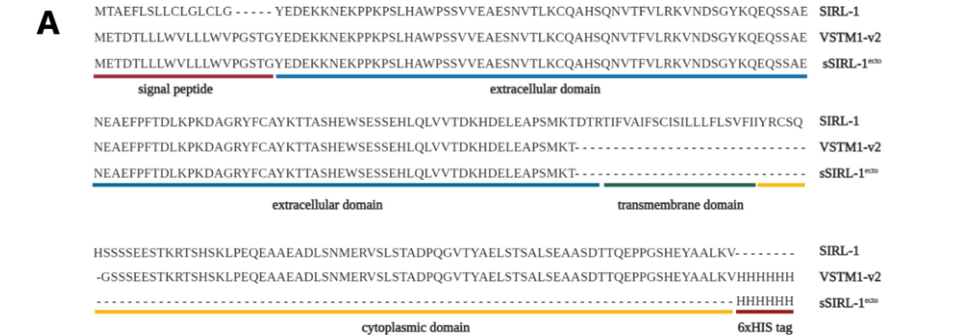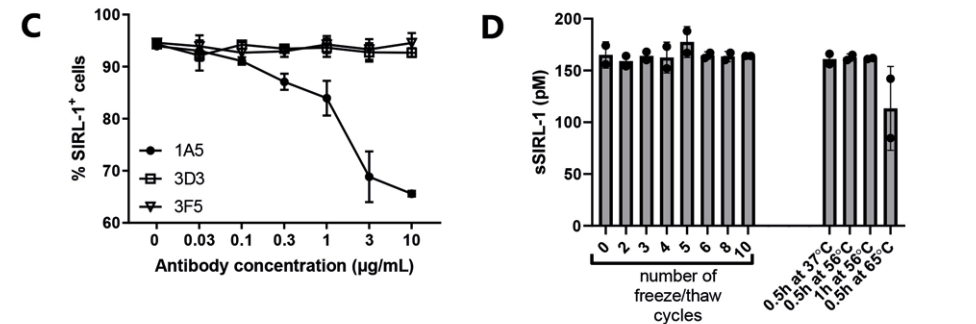
Acknowledgements

5

References

1. Steevels TA, Meyaard L. Immune inhibitory receptors: essential regulators of phagocyte function. Eur J Immunol. 2011;41(3):575-87.

2. Rumpret M, Drylewicz J, Ackermans LJE, Borghans JAM, Medzhitov R, Meyaard L. Functional categories of immune inhibitory receptors. Nat Rev Immunol. 2020.

3. Gu D, Ao X, Yang Y, Chen Z, Xu X. Soluble immune checkpoints in cancer: production, function and biological significance. J Immunother Cancer. 2018;6(1):132.

4. Ohnishi H, Kobayashi H, Okazawa H, Ohe Y, Tomizawa K, Sato R, et al. Ectodomain shedding of SHPS-1 and its role in regulation of cell migration. J Biol Chem. 2004;279(27):27878-87.

5. Fornasa G, Groyer E, Clement M, Dimitrov J, Compain C, Gaston AT, et al. TCR stimulation drives cleavage and shedding of the ITIM receptor CD31. J Immunol. 2010;184(10):5485-92.

6. Nielsen C, Ohm-Laursen L, Barington T, Husby S, Lillevang ST. Alternative splice variants of the human PD-1 gene. Cell Immunol. 2005;235(2):109-16.

7. Terahara K, Yoshida M, Taguchi F, Igarashi O, Nochi T, Gotoh Y, et al. Expression of newly identified secretory CEACAM1(a) isoforms in the intestinal epithelium. Biochem Biophys Res Commun. 2009;383(3):340-6.

8. Lebbink RJ, van den Berg MCW, De Ruiter T, Raynal N, van Roon JAG, Lenting PJ, et al. The soluble LAIR-2 antagonizes the collagen/LAIR-1 inhibitory immune interaction. J Immunol. 2008;180:1662-9.

9. Pepin D, Godeny M, Russell D, Mehta P, Lie WR. Profiling of soluble immune checkpoint proteins as potential non-invasive biomarkers in colorectal cancer and sepsis. Journal of Immunology. 2018;200(1).

10. Kong Y, Wang Y, Wu X, Han J, Li G, Hua M, et al. Storm of soluble immune checkpoints associated with disease severity of COVID-19. Signal Transduct Target Ther. 2020;5(1):192.

11. Steevels TAM, Lebbink RJ, Westerlaken GHA, Coffer PJ, Meyaard L. Signal Inhibitory Receptor on Leukocytes-1 (SIRL-1) is a novel functional inhibitory immune receptor expressed on human phagocytes. J Immunol. 2010;184:4741-8.

12. Xie M, Li T, Li N, Li J, Yao Q, Han W, et al. VSTM-v1, a potential myeloid differentiation antigen that is downregulated in bone marrow cells from myeloid leukemia patients. J Hematol Oncol. 2015;8(1):25.

13. Kumar D, Puan KJ, Andiappan AK, Lee B, Westerlaken GH, Haase D, et al. A functional SNP associated with atopic dermatitis controls cell type-specific methylation of the VSTM1 gene locus. Genome Med. 2017;9(1):18.

14. von Richthofen HJ, Gollnast D, van Capel TMM, Giovannone B, Westerlaken GHA, Lutter L, et al. Signal Inhibitory Receptor on Leukocytes-1 is highly expressed on lung monocytes, but absent on mononuclear phagocytes in skin and colon. Cell Immunol. 2020;357:104199.

15. Steevels TA, van Avondt K, Westerlaken GH, Walk J, Bont L, Coffer PJ, et al. Signal Inhibitory Receptor on Leukocytes-1 (SIRL-1) negatively regulates the oxidative burst in human phagocytes. Eur J Immunol. 2013;43:1297-308.

16. Besteman SB, Callaghan A, Hennus MP, Westerlaken GHA, Meyaard L, Bont LL. Signal inhibitory receptor on leukocytes (SIRL)-1 and leukocyte- associated immunoglobulin-like receptor (LAIR)-1 regulate neutrophil function in infants. Clin Immunol. 2020;211:108324.

17. Van Avondt K, van der Linden M, Naccache PH, Egan DA, Meyaard L. Signal Inhibitory Receptor on Leukocytes-1 Limits the Formation of Neutrophil Extracellular Traps, but Preserves Intracellular Bacterial Killing. J Immunol. 2016;196(9):3686-94.

18. Rumpret M, von Richthofen HJ, van der Linden M, Westerlaken GHA, Talavera Ormeno C, van Strijp JAG, et al. Signal inhibitory receptor on leukocytes-1 recognizes bacterial and endogenous amphipathic alpha-helical peptides. FASEB J. 2021;35(10):e21875.

19. Rumpret M, von Richthofen HJ, van der Linden M, Westerlaken GHA, Talavera Ormeno C, Low TY, et al. Recognition of S100 proteins by Signal Inhibitory Receptor on Leukocytes-1 negatively regulates human neutrophils. Eur J Immunol. 2021;51(9):2210-7.

20. Rumpret M, von Richthofen HJ, Peperzak V, Meyaard L. Inhibitory pattern recognition receptors. J Exp Med. 2022;219(1).

21. Guo X, Zhang Y, Wang P, Li T, Fu W, Mo X, et al. VSTM1-v2, a novel soluble glycoprotein, promotes the differentiation and activation of Th17 cells. Cell Immunol. 2012;278(1-2):136-42.

22. Andiappan AK, Puan KJ, Lee B, Yeow PT, Yusof N, Merid SK, et al. Inverse association of FCER1A allergy variant in monocytes and plasmacytoid dendritic cells. The Journal of allergy and clinical immunology. 2021;147(4):1510-3 e8.

23. Stapels DA, Ramyar KX, Bischoff M, von Kockritz-Blickwede M, Milder FJ, Ruyken M, et al. Staphylococcus aureus secretes a unique class of neutrophil serine protease inhibitors. Proceedings of the National Academy of Sciences of the United States of America. 2014;111(36):13187-92.

24. Guarino C, Gruba N, Grzywa R, Dyguda-Kazimierowicz E, Hamon Y, Legowska M, et al. Exploiting the S4-S5 Specificity of Human Neutrophil Proteinase 3 to Improve the Potency of Peptidyl Di(chlorophenyl)-phosphonate Ester Inhibitors: A Kinetic and Molecular Modeling Analysis. J Med Chem. 2018;61(5):1858-70.

25. Olde Nordkamp MJM, van Roon JA, Douwes M, De Ruiter T, Urbanus RT, Meyaard L. Enhanced secretion of Leukocyte-Associated Immunoglobulin-like Receptor (LAIR)-2 and soluble LAIR-1 in rheumatoid arthritis: LAIR-2 is a more efficient antagonist of the LAIR-1-collagen inhibitory interaction than soluble LAIR -1. Arthritis Rheum. 2011;63:3749-57.

26. Geerdink RJ, Pillay J, Meyaard L, Bont L. Neutrophils in respiratory syncytial virus infection: A target for asthma prevention. The Journal of allergy and clinical immunology. 2015;136(4): 838-47.

27. Reusch N, De Domenico E, Bonaguro L, Schulte-Schrepping J, Bassler K, Schultze JL, et al. Neutrophils in COVID-19. Front Immunol. 2021;12:652470.

28. Geerdink RJ, Hennus MP, Westerlaken GHA, Abrahams AC, Albers KI, Walk J, et al. LAIR-1 limits neutrophil extracellular trap formation in viral bronchiolitis. The Journal of allergy and clinical immunology. 2018;141(2):811-4.

29. Pham CT. Neutrophil serine proteases: specific regulators of inflammation. Nat Rev Immunol. 2006;6(7):541-50.

30. Imanaka H, Shimaoka M, Matsuura N, Nishimura M, Ohta N, Kiyono H. Ventilator-induced lung injury is associated with neutrophil infiltration, macrophage activation, and TGF-beta 1 mRNA upregulation in rat lungs. Anesth Analg. 2001;92(2):428-36.

31. Meizlish ML, Pine AB, Bishai JD, Goshua G, Nadelmann ER, Simonov M, et al. A neutrophil activation signature predicts critical illness and mortality in COVID-19. Blood Adv. 2021;5(5): 1164-77.

32. Halbwachs-Mecarelli L, Bessou G, Lesavre P, Lopez S, Witko-Sarsat V. Bimodal distribution of proteinase 3 (PR3) surface expression reflects a constitutive heterogeneity in the polymorphonuclear neutrophil pool. FEBS Lett. 1995;374(1):29-33.

33. Hajjar E, Mihajlovic M, Witko-Sarsat V, Lazaridis T, Reuter N. Computational prediction of the binding site of proteinase 3 to the plasma membrane. Proteins. 2008;71(4):1655-69.
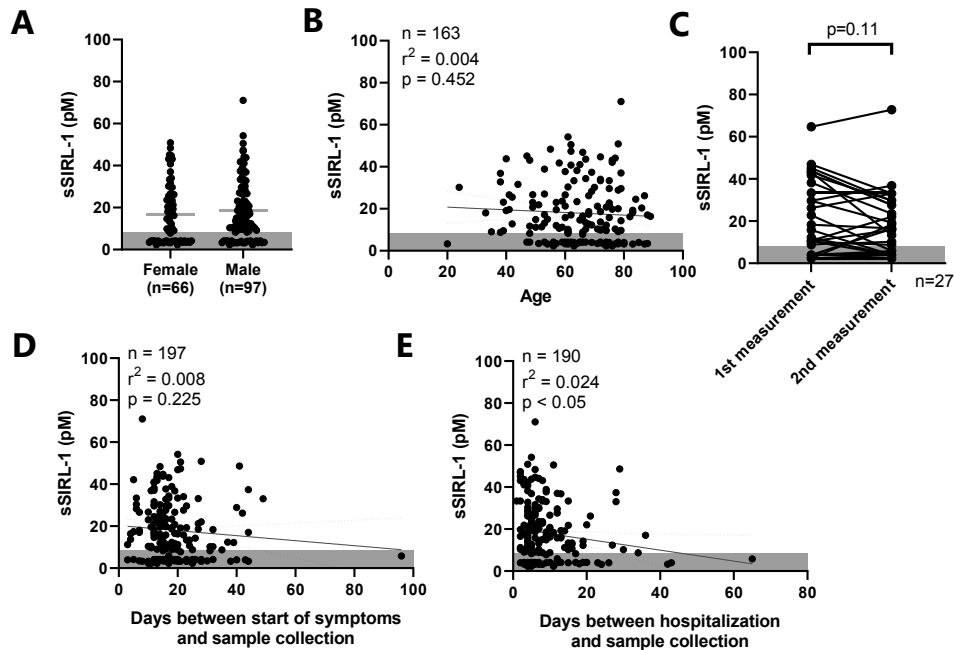
34. Jerke U, Marino SF, Daumke O, Kettritz R. Characterization of the CD177 interaction with the ANCA antigen proteinase 3. Sci Rep. 2017;7:43328.

35. Korkmaz B, Kuhl A, Bayat B, Santoso S, Jenne DE. A hydrophobic patch on proteinase 3, the target of autoantibodies in Wegener granulomatosis, mediates membrane binding via NB1 receptors. J Biol Chem. 2008;283(51):35976-82.

36. Korkmaz B, Jaillet J, Jourdan ML, Gauthier A, Gauthier F, Attucci S. Catalytic activity and inhibition of wegener antigen proteinase 3 on the cell surface of human polymorphonuclear neutrophils. J Biol Chem. 2009;284(30):19896-902.

37. Matsumoto T, Kaneko T, Wada H, Kobayashi T, Abe Y, Nobori T, et al. Proteinase 3 expression on neutrophil membranes from patients with infectious disease. Shock. 2006;26(2):128-33.

38. Jouleh B, Haaland I, Khorsand F, Sandvik R, Kalananthan T, Nielsen R, et al. Levels of proteinase 3 and neutrophil elastase in plasma, BAL and biopsies in COPD. European Respiratory Journal. 2020;56.

39. Sinden NJ, Stockley RA. Proteinase 3 activity in sputum from subjects with alpha-1-antitrypsin deficiency and COPD. Eur Respir J. 2013;41(5):1042-50.

40. Witko-Sarsat V, Halbwachs-Mecarelli L, Schuster A, Nusbaum P, Ueki I, Canteloup S, et al. Proteinase 3, a potent secretagogue in airways, is present in cystic fibrosis sputum. Am J Resp Cell Mol. 1999;20(4):729-36.

41. Seren S, Derian L, Keles I, Guillon A, Lesner A, Gonzalez L, et al. Proteinase release from activated neutrophils in mechanically ventilated patients with non-COVID-19 and COVID-19 pneumonia. Eur Respir J. 2021;57(4).

42. Huang W, Li M, Luo G, Wu X, Su B, Zhao L, et al. The Inflammatory Factors Associated with Disease Severity to Predict COVID-19 Progression. J Immunol. 2021;206(7):1597-608.

43. Guarino C, Legowska M, Epinette C, Kellenberger C, Dallet-Choisy S, Sienczyk M, et al. New selective peptidyl di(chlorophenyl) phosphonate esters for visualizing and blocking neutrophil proteinase 3 in human diseases. J Biol Chem. 2014;289(46):31777-91.

44. Wang D, Li Y, Liu Y, He Y, Shi G. Expression of VSTM1-v2 Is Increased in Peripheral Blood Mononuclear Cells from Patients with Rheumatoid Arthritis and Is Correlated with Disease Activity. PLoS One. 2016;11(1):e0146805.

45. Cogen AL, Yamasaki K, Sanchez KM, Dorschner RA, Lai YP, MacLeod DT, et al. Selective Antimicrobial Action Is Provided by Phenol-Soluble Modulins Derived from Staphylococcus epidermidis, a Normal Resident of the Skin. Journal of Investigative Dermatology. 2010;130(1):192-200.

46. Kretschmer D, Breitmeyer R, Gekeler C, Lebtig M, Schlatterer K, Nega M, et al. Staphylococcus aureus Depends on Eap Proteins for Preventing Degradation of Its Phenol-Soluble Modulin Toxins by Neutrophil Serine Proteases. Front Immunol. 2021;12:701093.

Supplementary information

**Supplementary figure 1. Development of sSIRL-1 ELISA.**

(A) Amino acid sequence of membrane-expressed SIRL-1, recombinant VSTM1-v2 and sSIRL-1^{ecto}. Horizontal colored lines indicate the signal peptide, extracellular domain, transmembrane domain, cytoplasmic domain and His-tag. For sSIRL-1^{ecto}, the sequence of the ectodomain of SIRL-1 minus three amino acids was used. **(B)** cDNA sequence for recombinant sSIRL-1^{ecto} and VSTM1-v2. **(C)** PBMCs were pre-incubated for 2 hours at 37°C with 0.03 – 10 µg/mL of indicated anti-SIRL-1 mAb clones, followed by staining with anti-SIRL-1 clone 1A5-AF647 and flow cytometry analysis. The graph shows the percentage of SIRL-1 expressing cells, n=1, mean ± SD from technical duplicates. **(D)** Human pooled serum was spiked with sSIRL-1^{ecto} and subjected to a maximum of ten freeze-thaw cycles, 0.5 or 1h incubation at 56 °C, or 0.5h incubation at 65 °C. sSIRL-1 concentration was measured by ELISA, n=2.

Supplementary figure 2. sSIRL-1 concentration in hospitalized COVID-19 patients.

sSIRL-1 was measured by ELISA in serum of hospitalized COVID-19 patients at one (n=138) or two (n=27) time points at various intervals, and correlated to sex (A), age (B), number of days between start of symptoms and sample collection (D) or number of days between hospitalization and sample collection (E). Graphs show only the first measurement time point per donor (A-B), compare the first and second measurement time point within the same patient (C), or show all measurement time points (D-E). Each dot represents one donor, the green bars represent the means. The shaded area indicates the lower limit of detection (LLOD), and samples with undetectable sSIRL-1 were given a value of 0.5 x LLOD. Correlations were calculated using simple linear regression, the blue lines represent the best fit line with 95% confidence interval. In C, statistical significance was determined using a Wilcoxon matched-pairs test.
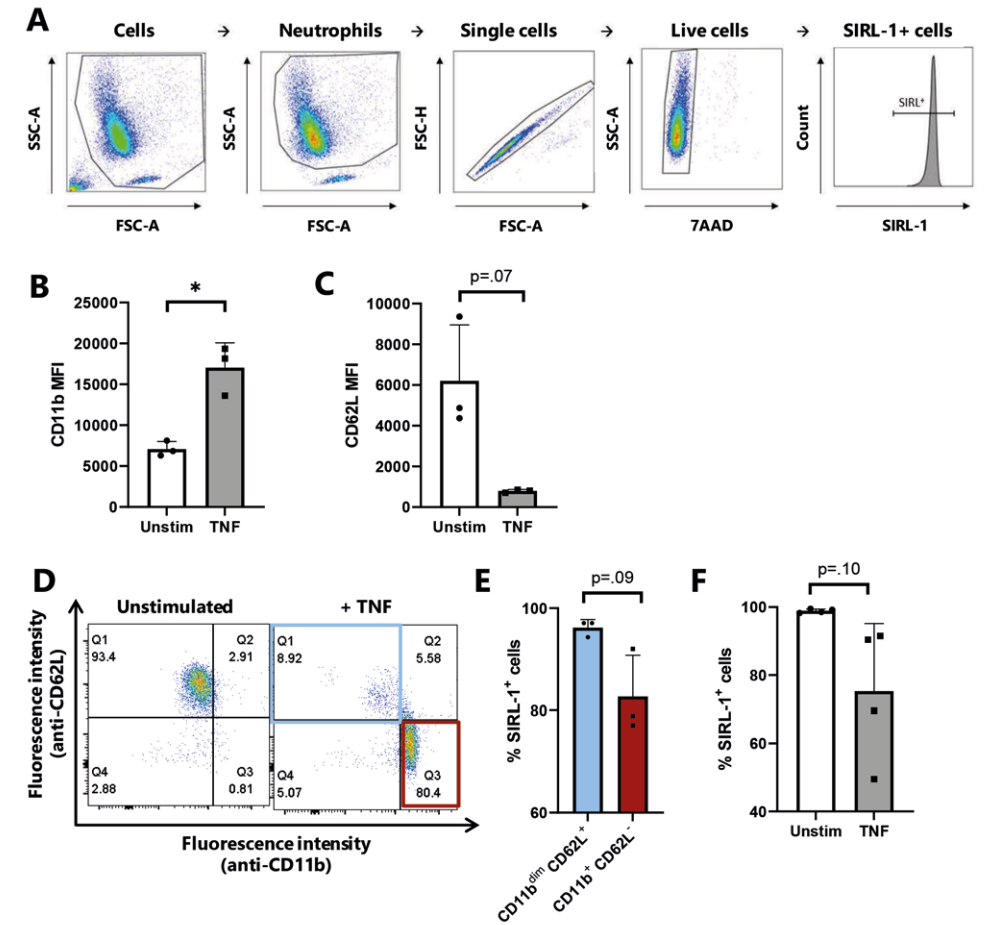
Supplementary figure 3. Gating strategy and activation markers of *in vitro* stimulated neutrophils.

Neutrophils were isolated by ficoll gradient centrifugation, stimulated *in vitro* and analyzed by flow cytometry. **(A)** Single neutrophils were gated using forward scatter (FSC) and sideward scatter (SSC). Viable cells were selected by negative 7AAD staining, followed by selection of SIRL-1+ cells. **(B-F)** Neutrophils were stimulated for 2h (B-E) or 1h (F) with 50 ng/mL TNF and stained for CD11b, CD62L and/or SIRL-1. Shown is the percentage of SIRL-1 positive cells or the median fluorescent intensity (MFI). The percentage of SIRL-1 positive cells was also determined within the CD11b-dim CD62L+ and CD11b+ CD62L- population, representing respectively neutrophils without or with an activated phenotype (D-E). Each symbol represents a donor, n=3-4. Statistical significance was determined using a paired t-test, * $p \leq .05$
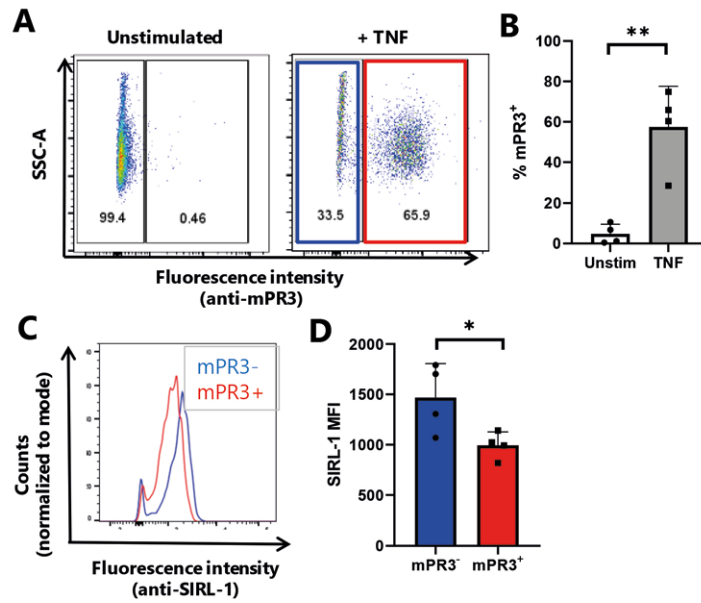
Supplementary figure 4. mPR3 expression on TNF-stimulated neutrophils.

Neutrophils were isolated by ficoll gradient centrifugation, stimulated for 1h with 50 ng/mL TNF, stained for mPR3 and SIRL-1 expression and analyzed by flow cytometry. **(A-B)** Representative dot plot (A) and quantification (B) of mPR3 expression after TNF stimulation **(C-D)** Representative histogram (C) and quantification (D) of SIRL-1 expression in TNF-stimulated mPR3 negative and mPR3 positive cells. Each symbol represents a donor, n=4. Statistical significance was determined using a paired t-test, * p ≤ .05

CHAPTER **6**

VSTM1-v2 does not drive human Th17 cell differentiation: a replication study

Helen J. von Richthofen[1,2¶], **Florianne M.J. Hafkamp**[3¶],
Anouk van Haperen[1,2], **Esther C. de Jong**[3&], **Linde Meyaard** [1,2&]

[1] Center for Translational Immunology, University Medical Center Utrecht, Utrecht
   University, Lundlaan 6, 3584 EA Utrecht, The Netherlands
[2] Oncode Institute, Lundlaan 6, 3584 EA Utrecht, The Netherlands
[3] Department of Experimental Immunology, Amsterdam University Medical
   Center, Amsterdam Institute for Infection & Immunity, University of Amsterdam,
   Meibergdreef 15, 1105 AZ Amsterdam, The Netherlands

¶ These authors contributed equally to this work.
& These authors also contributed equally to this work.

Abstract

Signal inhibitory receptor on leukocytes-1 (SIRL-1) is an immune inhibitory receptor expressed on human myeloid cells. We previously showed that dendritic cell (DC)-driven Th17 cell differentiation of human naive CD4+ T cells requires presence of neutrophils, which is inhibited by SIRL-1 ligation. VSTM1-v2 is a soluble isoform of SIRL-1, which was previously proposed to function as a Th17 polarizing cytokine. Here, we investigated the effect of VSTM1-v2 on DC-driven Th17 cell development. Neutrophils induced DC-driven Th17 cell differentiation, which was not enhanced by VSTM1-v2. Similarly, we found no effect of VSTM1-v2 on cytokine-driven Th17 cell development. Thus, our results do not support a role for VSTM1-v2 in Th17 cell differentiation.

Introduction

Signal inhibitory receptor on leukocytes-1 (SIRL-1), encoded by the gene *VSTM1*, is an immune inhibitory receptor expressed on human granulocytes and monocytes (1-4). We recently described that activated neutrophils shed the ectodomain of SIRL-1, thereby releasing soluble SIRL-1 (sSIRL-1) (5). In addition, SIRL-1 has a soluble isoform named VSTM1-v2, which lacks the exon that encodes the transmembrane domain of SIRL-1 and is therefore predicted to give rise to a secreted protein (6).

VSTM1-v2 mRNA expression has been reported to be increased in peripheral blood mononuclear cells (PBMCs) of rheumatoid arthritis patients compared to controls, and to correlate positively with IL-17 mRNA expression (7). Moreover, recombinant VSTM1-v2 has been shown to induce Th17 cell differentiation and activation, using purified CD4+ T cells that were stimulated with a Th17 cell inducing cytokine cocktail and/or anti-CD3 and anti-CD28 stimulation (6), suggesting that VSTM1-v2 acts as a polarizing cytokine on CD4+ T cells. We previously showed that DC-driven differentiation of human naive CD4+ T cells into Th17 cells requires presence of neutrophils, which is inhibited by SIRL-1 ligation (8).

It is unclear whether VSTM1-v2 also affects DC-driven differentiation into Th17 cells. Here, we tested the effect of VSTM1-v2 on DC-driven and cytokine-driven Th17 cell development and assessed binding of VSTM1-v2 to leukocytes.

Materials and methods

Biological samples

Heparinized blood was obtained from healthy volunteers at the UMC Utrecht or Amsterdam UMC. Samples were collected in accordance with the Institutional Review Board of these institutes (METC 2015_074) and after written consent.

Recombinant proteins

The cDNA sequence, cloning and production of recombinant His-tagged VSTM1-v2 and LAIR-1 ectodomain (sLAIR-1^{ecto}) has been previously described (5). Endotoxins were removed with Triton X-114 (Sigma-Aldrich) and SM-2 beads (Bio-Rad) as previously described (9). Absence of endotoxins (< 1EU/mL) was confirmed using the PyroGene™ Recombinant Factor C Assay (Lonza) according to manufacturer's instructions.

DC-driven Th17 cell differentiation

Isolation and co-cultures of T cells, monocyte-derived DCs (moDCs) and neutrophils were performed as previously described (8). In brief, following CD4^{+} T-cell isolation, CD45RA^{+} naive cells were separated from the CD45RO^{+} memory T cells by positive selection of memory T cells using CD45RO-Phycoerythrin antibody (DAKO) and magnetically-labeled anti-PE beads (Miltenyi Biotec). Naive CD4^{+} T cells were always more than 98% pure. Monocytes were differentiated into moDCs and harvested as immature DCs after 6 days. Co-cultures were initiated in 96-well *Candida albicans* hyphae-coated plates, with 50,000 DCs and 50,000 autologous CD4^{+} naive or memory T cells, with or without 100 ng/mL VSTM1-v2, and for the naive T cell cultures, with or without 100,000 autologous freshly isolated neutrophils. Co-cultures were done in IMDM supplemented with 5% HI-HS (Lonza) and gentamycin (86 μg/mL, Duchefa Biochemie). After 4 days, cells were transferred to 48-well plates (Costar) and refreshed every 2 days with IMDM/5% HS medium containing 10 U/mL IL-2. At 10-12 days of culture, when cells were resting, they were restimulated for 5h with PMA (100 ng/mL), ionomycin (1 μg/mL), and brefeldin A (10 μg/mL) (all Sigma-Aldrich).

Cytokine-driven Th17 cell differentiation

CD4^{+} T cells were isolated from peripheral blood lymphocytes by negative selection using a CD4 T-cell isolation kit II and magnetic cell separation (Miltenyi Biotec). A total of 50,000 CD4^{+} T cells were cultured in IMDM (Thermo Scientific, Gibco) supplemented with 10% FCS (Gibco) and stimulated with plate-bound anti-CD3 (16A9, 1 μg/mL, Sanquin) and soluble anti-CD28 (15E8, 1 μg/mL, Sanquin (10), in the presence of Th17 polarizing cytokines IL-1β (10 ng/mL), IL-6 (50 ng/mL), IL-23 (50 ng/mL), TGF-β (5 ng/mL) and TNF-α (10 ng/mL) and neutralizing antibodies anti-IFN-γ (10 μg/mL) and anti-IL-4 (10 μg/mL). IL-1β, IL-6 and TNF-α were purchased from Miltenyi Biotech, IL-23 and TGF-β from R&D Systems, anti-IFN-γ from U-CyTech and anti-IL-4 from BD Pharmingen. VSTM1-v2 was added at 10 or 100 ng/mL, or medium was added as control. After 4 days, cells were transferred to 24-well plates (Costar) and refreshed every 2 days with IMDM/10% FCS medium containing 10 U/mL recombinant human IL-2 (Novartis AG). After a total culture of 10-12 days, when cells were resting, they were re-stimulated with PMA, ionomycin, and brefeldin A as described above.

Binding assays

Erythrocytes from full blood samples were lysed with Ammonium-Chloride-Potassium (ACK) lysis buffer (155 mM NH_4Cl, 10 mM $KHCO_3$, 0.1 mM EDTA in ddH_2O, pH 7.2-7.4). The remaining leukocytes were incubated with 10 or 50 μg/mL VSTM1-v2 or sLAIR-1[ecto] for 90 minutes at 4°C, after which the cells were stained with anti-Penta-His-AF647

(1 μg/mL; Qiagen) for 30 minutes at 4°C. Between all steps, cells were extensively washed with PBS containing 1% BSA and 0.01% NaN_3. Cells were analyzed by flow cytometry.

Flow cytometry

Cells were acquired on a FACS Canto II (BD Biosciences). Lymphocytes, monocytes and granulocytes were distinguished based on forward scatter (FSC) and sideward scatter (SSC) (Fig 1A). For intracellular IL-17 staining, restimulated T cells were washed with Saponin (Sigma-Aldrich) in PBS-0.5% w/v BSA-0.05% v/v azide and stained with anti-IL-17A-eFluor660. Gating was performed as previously described (8). Flow cytometry analysis was performed using FlowJo software (Treestar, Ashland, OR).

Statistics

Statistical analyses were performed using GraphPad Prism Software, La Jolla, CA, USA, version 8.3.0 for Windows. For each graph, the statistical test and number of biological replicates (n) are described in the figure legends. P values of 0.05 or less were considered significant.

Results

To test the effect of VSTM1-v2 on DC-driven Th17 cell differentiation, we used our previously described co-culture system (8) of naive CD4+ T cells, *Candida albicans*-activated moDCs, and neutrophils (See Fig 1A, upper panel, for a schematic overview). *C. albicans* is a potent Th17 inducing pathogen in DC-driven T cell outgrowth, and patients with genetic errors in IL-17 expression suffer from chronic mucocutaneous candidiasis (11). In line with our previous data, presence of neutrophils promoted the differentiation of naive CD4+ T cells into IL-17+ T cells (Fig 1B, C). However, VSTM1-v2 did not consistently change the percentage of IL-17+ T cells in these cultures (Fig 1C, left panel).

We previously showed that *C. albicans*-activated moDCs also enhance Th17 cell activation of memory CD4+ T cells (8). Therefore, we subsequently tested the effect of VSTM1-v2 on Th17 cell activation from memory CD4+ T cells (see Fig 1A, lower panel for the co-culture set-up). Similar to our previous findings, co-culture of memory CD4+ T cells with *C. albicans*-activated moDCs induced up to 30% of IL-17+ cells, but this was not increased by addition of VSTM1-v2 (Fig 1C, right panel). Taken together, we found no effect of VSTM1-v2 on DC-driven Th17 cell differentiation nor activation.

In the co-culture systems, a direct effect of VSTM1-v2 on Th17 cell development may be blocked if moDCs or granulocytes compete with CD4+ T cells for VSTM1-v2 binding. To rule this out, we assessed binding of VSTM1-v2 to granulocytes, lymphocytes and monocytes in erythrocyte-lysed whole blood (See S1 Fig panel A for the gating strategy). As a negative control, sLAIR-1ecto was used, which was produced in the same way as VSTM1-v2 and has 30% sequence identity with VSTM1-v2. For detection, fluorescently labeled anti-His was used. In comparison to the staining by anti-His alone, we observed no increased binding of VSTM1-v2 to lymphocytes, monocytes, or granulocytes (S1 Fig panel B-E), indicating that VSTM1-v2 does not bind directly to human leukocytes.

Finally, we repeated the same set-up as Guo *et al.* used to show that VSTM1-v2 induced Th17 cell differentiation, by activating total CD4+ T cells with anti-CD3, anti-CD28, and a Th17 polarizing cytokine mix (6). The Th17 polarizing mix increased the percentage of IL-17+ cells, but there was no effect of VSTM1-v2 (Fig 1D). Thus, our data do not support a role for VSTM1-v2 in the differentiation or activation of Th17 cells.
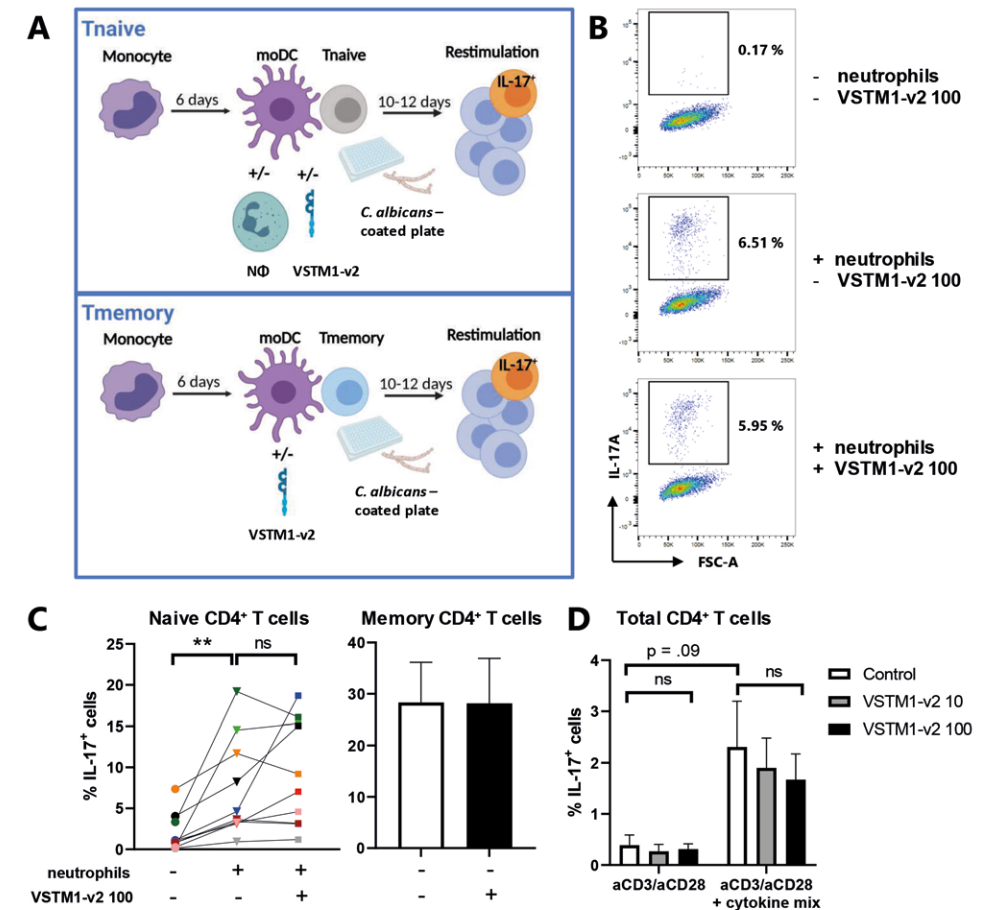

Figure 1. VSTM1-v2 does not enhance Th17 cell differentiation and activation.

CD4+ T cells were stimulated by *C. albicans*-activated moDCs, with or without autologous neutrophils (A-C), or with antibodies and a polarizing cytokine mix (D), with or without addition of 10 or 100 ng/mL VSTM1-v2. Intracellular IL-17 expression was determined by flow cytometry. **(A)** Schematic representation of the co-culture system of moDC-driven Th17 cell differentiation and activation. **(B)** Representative dot plots of the percentage of IL-17+ cells after co-culture of naive CD4+ T cells. The y-axis indicates the fluorescence intensity of the IL-17A staining, while the x-axis indicates the forward scatter (FSC). **(C)** The percentage of IL-17+ cells after co-culture of naive CD4+ T cells (n= 10), each donor represented by a different color, or memory CD4+ T cells (n = 3; mean ± SD). **(D)** The percentage of IL-17+ cells after stimulation of total CD4+ T cells with anti-CD3, anti-CD28, and a Th17 polarizing mix, mean ± SD, n = 3. Statistical significance was determined using a Friedman test with Dunn's correction (C, D). ** p < .01, ns = not significant. Figure A was made using biorender.com.

Discussion

We confirmed our previous observations that neutrophils are required for DC-driven differentiation of naive CD4+ T cells into Th17 cells (8). Mechanistically, we explained this effect by release of elastase from activated neutrophils, which cleaved DC-derived CXCL8 into a Th17-cell inducing agent. SIRL-1 ligation inhibited Th17 cell development, most likely by suppression of neutrophil degranulation and thereby the release of neutrophil elastase (8). Based on those findings, we hypothesized that VSTM1-v2 may revert the suppressive effect of SIRL-1 on Th17 cell development by competing with SIRL-1 for binding to its ligands S100 and LL-37 (12, 13), which are both neutrophil-derived proteins. Of note, we were not able to detect direct binding between SIRL-1 and its ligands (12, 13), possibly due to low affinity or the requirement of an additional binding partner. Therefore we could technically not assess whether VSTM1-v2 competes with this interaction. More importantly, we did not find any effect of VSTM1-v2 on Th17 cell differentiation and activation, unlike the results by Guo *et al.* (6).

We neither observed effects of VSTM1-v2 on DC-driven nor cytokine-driven T cell outgrowth. It is unclear what caused these differential results with the study by Guo *et al.*. Purified VSTM1-v2 had a similar molecular weight as in the study by Guo *et al.*, as assessed by SDS-PAGE (5). We also used a similar Th17 polarizing mix and the same VSTM1-v2 concentrations, but we cultured the cells for 10-12 days before staining them for IL-17 expression, whereas Guo *et al.* found that IL-17 release by total CD4+ T cells was already increased after 72 h stimulation (6). This could indicate that pre-existing Th17 cells within the memory CD4+ T cell population were stimulated to produce more IL-17, rather than amplifying the percentage of IL-17+ cells. However, how VSTM1-v2 would activate IL-17 production by T cells is unclear, since we did not observe any binding to lymphocytes (S1 Fig).

As of now, endogenous expression of VSTM1-v2 has only been shown on mRNA level (6, 7), but not as a protein. We recently described that sSIRL-1 protein is released by ectodomain shedding (5). Using an in-house developed ELISA, we found sSIRL-1 concentration increased in COVID-19 and RSV bronchiolitis patients. Notably, this ELISA can also recognize recombinant VSTM1-v2, and VSTM1-v2 may therefore contribute to the total amount of sSIRL-1 that was found. In future, VSTM1-v2 specific antibodies will allow investigation of endogenous VSTM1-v2 protein expression.

In conclusion, our results do not support a role for VSTM1-v2 in Th17 cell differentiation. Further research is required to elucidate the expression of VSTM1-v2 protein and its functional implications.

Acknowledgments

References

1. Steevels TAM, Lebbink RJ, Westerlaken GHA, Coffer PJ, Meyaard L. Signal Inhibitory Receptor on Leukocytes-1 (SIRL-1) is a novel functional inhibitory immune receptor expressed on human phagocytes. J Immunol. 2010;184:4741-8.

2. Kumar D, Puan KJ, Andiappan AK, Lee B, Westerlaken GH, Haase D, et al. A functional SNP associated with atopic dermatitis controls cell type-specific methylation of the VSTM1 gene locus. Genome Med. 2017;9(1):18.

3. Xie M, Li T, Li N, Li J, Yao Q, Han W, et al. VSTM-v1, a potential myeloid differentiation antigen that is downregulated in bone marrow cells from myeloid leukemia patients. J Hematol Oncol. 2015;8(1):25.

4. von Richthofen HJ, Gollnast D, van Capel TMM, Giovannone B, Westerlaken GHA, Lutter L, et al. Signal Inhibitory Receptor on Leukocytes-1 is highly expressed on lung monocytes, but absent on mononuclear phagocytes in skin and colon. Cell Immunol. 2020;357:104199.

5. von Richthofen HJ, Westerlaken GHA, Gollnast D, Besteman S, Delemarre EM, Rodenburg K, et al. Soluble Signal Inhibitory Receptor on Leukocytes-1 Is Released from Activated Neutrophils by Proteinase 3 Cleavage. J Immunol. 2023.

6. Guo X, Zhang Y, Wang P, Li T, Fu W, Mo X, et al. VSTM1-v2, a novel soluble glycoprotein, promotes the differentiation and activation of Th17 cells. Cell Immunol. 2012;278(1-2):136-42.

7. Wang D, Li Y, Liu Y, He Y, Shi G. Expression of VSTM1-v2 Is Increased in Peripheral Blood Mononuclear Cells from Patients with Rheumatoid Arthritis and Is Correlated with Disease Activity. PLoS One. 2016;11(1):e0146805.

8. Souwer Y, Groot Kormelink T, Taanman-Kueter EW, Muller FJ, van Capel TMM, Varga DV, et al. Human TH17 cell development requires processing of dendritic cell-derived CXCL8 by neutrophil elastase. The Journal of allergy and clinical immunology. 2018;141(6):2286-9 e5.

9. Teodorowicz M, Perdijk O, Verhoek I, Govers C, Savelkoul HF, Tang Y, et al. Optimized Triton X-114 assisted lipopolysaccharide (LPS) removal method reveals the immunomodulatory effect of food proteins. PLoS One. 2017;12(3):e0173778.

10. Bakdash G, Vogelpoel LT, van Capel TM, Kapsenberg ML, de Jong EC. Retinoic acid primes human dendritic cells to induce gut-homing, IL-10-producing regulatory T cells. Mucosal Immunol. 2015;8(2):265-78.

11. Puel A, Cypowyj S, Bustamante J, Wright JF, Liu L, Lim HK, et al. Chronic mucocutaneous candidiasis in humans with inborn errors of interleukin-17 immunity. Science. 2011;332(6025):65-8.

12. Rumpret M, von Richthofen HJ, van der Linden M, Westerlaken GHA, Talavera Ormeno C, van Strijp JAG, et al. Signal inhibitory receptor on leukocytes-1 recognizes bacterial and endogenous amphipathic alpha-helical peptides. FASEB J. 2021;35(10):e21875.

13. Rumpret M, von Richthofen HJ, van der Linden M, Westerlaken GHA, Talavera Ormeno C, Low TY, et al. Recognition of S100 proteins by Signal Inhibitory Receptor on Leukocytes-1 negatively regulates human neutrophils. Eur J Immunol. 2021;51(9):2210-7.

Supplementary information
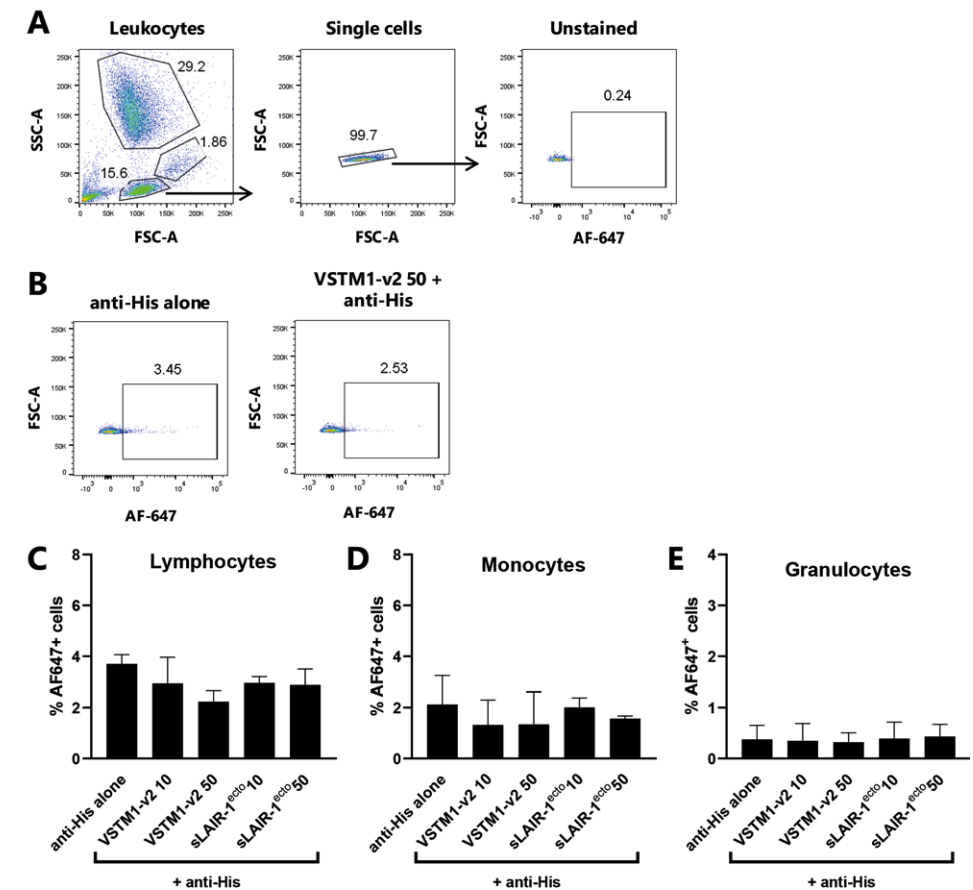
S1 Figure. VSTM1-v2 does not bind to leukocytes.

Erythrocyte-lysed whole blood was incubated with His-tagged VSTM1-v2 or sLAIR-1ecto (10-50 µg/mL), followed by detection with anti-His-AF647. **(A)** Lymphocytes (lower population), monocytes (middle population) and granulocytes (upper population) were gated based on forward scatter (FSC) and sideward scatter (SSC), followed by gating on single cells and AF-647+ cells. **(B)** Shown are representative dot plots of lymphocytes stained with 50 µg/mL VSTM1-v2 and/or anti-His-AF647. **(C-E)** The graphs show the quantification of the percentage of AF647+ cells of lymphocytes (C), monocytes (D), or granulocytes (E). Data are shown as mean ± SD of two donors

CHAPTER **7**

Inhibitory pattern recognition receptors

Matevž Rumpret[1,2], **Helen J. von Richthofen**[1,2], **Victor Peperzak**[1],
Linde Meyaard[1,2]

[1] Center for Translational Immunology, University Medical Center Utrecht,
   Utrecht University, Utrecht, The Netherlands
[2] Oncode Institute, Utrecht, The Netherlands

Abstract

Pathogen- and damage-associated molecular patterns are sensed by the immune system's pattern recognition receptors (PRR) upon contact with a microbe or damaged tissue. In situations such as in contact with commensals or during the occurrence of physiological cell death, the immune system should not respond to these patterns. Hence, immune responses need to be context-dependent, but it is not clear how context to molecular pattern recognition is provided. We explore inhibitory receptors as potential counterparts to activating pattern recognition receptors. We identify a group of inhibitory pattern recognition receptors (iPRRs) that recognize endogenous and microbial patterns associated with danger, homeostasis, or both. We propose that recognition of molecular patterns by iPRRs provides context and helps mediate tolerance to microbes and balance responses to danger signals.

Introduction

Pattern recognition receptors recognize molecular patterns

The immune system needs to recognize and correct deviations from normal physiology, such as harmful contact with a microbe, disruption and damage of healthy tissue, and malignant transformation of cells. To sense the presence of microbes, the immune system employs a set of pattern recognition receptors (PRRs) (1). At present, five classes of PRRs have been defined: the Toll-like receptors (TLR) and the C-type lectin receptors (CLR), which are both localized to cell or endosomal membranes; the cytoplasmic NOD-like receptors (NLR) and RIG-I-like receptors (RLR); and additional cytoplasmic DNA sensors, such as cyclic GMP–AMP synthase (2, 3). PRRs recognize highly conserved components of microbes, termed pathogen-associated molecular patterns (PAMPs) (4, 5). In addition, PRRs sense endogenous molecules associated with damaged and dying cells termed danger- (or damage-) associated molecular patterns (DAMPs). Many factors are currently considered DAMPs, among which S100 proteins, heat-shock proteins, high mobility group box 1 protein (HMGB1), and different glycans such as heparan sulfate (6-8).

The self–non-self model of microbe recognition, first introduced by Frank Macfarlane Burnet and later refined by Charles Janeway, explains how the innate immune system recognizes pathogens through molecular patterns (1, 9). Because pathogens constantly evolve, they cannot be recognized individually as this would require an infinite number of receptors. To circumvent this problem, the immune system recognizes components of microbial cells that are highly conserved (but not identical) among microbes and cannot be subject to quick change or removal by the microbe because they are essential for its survival (10). These groups of structurally similar molecules are called PAMPs. One of the first PAMPs to be discovered was lipopolysaccharide (LPS) of Gram-negative bacteria, which is detected by Toll-like receptor 4 (TLR4), providing activating signals that drive adaptive immunity (11, 12). Soon after, many additional PAMPs were discovered, such as the lipoteichoic acid (LTA) of Gram-positive bacteria (13). Later, Polly Matzinger extended the family of "molecular patterns" by presenting the danger theory of immunity, introducing damage-associated molecular patterns (DAMPs). The term DAMP has since then been used in literature denoting both damage- and danger-associated molecular patterns. Unlike PAMPs, DAMPs are not defined structurally, and there is, following Janeway's argument, little need for that—there is only a finite number of host molecules. Instead, DAMPs are defined contextually: they signal danger, and what is dangerous in one place is not necessarily dangerous in another. Such a model

is not easily addressed experimentally because of this elusive definition of danger (14). As highlighted by Pradeu (14), Matzinger later clarified that while the model is theoretical, the idea behind it is that the immune system responds to damage (8), and damage signals are much easier to define than danger signals. Since then, many more groups of molecular patterns have been put forward, among which are resolution-, metabolism-, commensal-, and homeostasis-associated molecular patterns (HAMPs) (15-19). Under the term "molecular pattern," we now classify groups of molecules that signal the occurrence of a particular event, that elicit similar effects, and that may share common structural features.

Immune responses are context-dependent

The same molecular pattern does not always evoke the same response. Different microbes inevitably colonize barrier tissues such as the skin and gastrointestinal tract, and most of them are not harmful or even provide benefit to the host, yet still express PAMPs. Similarly, while tissue damage and cell death can be pathological, cell death can also be part of normal physiology and tissue renewal. To distinguishes harmless from potentially harmful circumstances, the immune system must correctly interpret the activating signals molecular patterns are delivering, and therefore the threshold for immune system activation needs to vary per context. Tissues that are highly exposed to microbes, like the gut and skin, require a high activation threshold to tolerate most microbes, whereas in the circulation a low activation threshold is required to respond to all microbes (Figure 1). Furthermore, not all tissues can tolerate tissue damage to the same extent. In situations where inflammatory responses result in more damage to the organism than the disturbance itself, not responding to disturbances is the best strategy (20). Following this argument, the threshold for immune activation needs to be higher in organs with low regenerative capacity like the heart or brain, where an inflammatory response can lead to detrimental consequences, versus organs with a high regenerative capacity like the liver (Figure 1). Hence, the immune response needs to be context-dependent, and it is not clear how context to molecular pattern recognition is provided.

Immune inhibitory receptors dampen immune system activation

Inhibitory immune receptors are germline-encoded innate receptors relaying inhibitory signals to immune cells. Much about their functioning has been learned by studying programmed cell death protein 1 (PD-1), cytotoxic T-lymphocyte protein 4 (CTLA-4), and killer cell immunoglobulin-like inhibitory receptors (KIR) on NK cells (21-23). Inhibitory receptors attenuate activating signals coming from
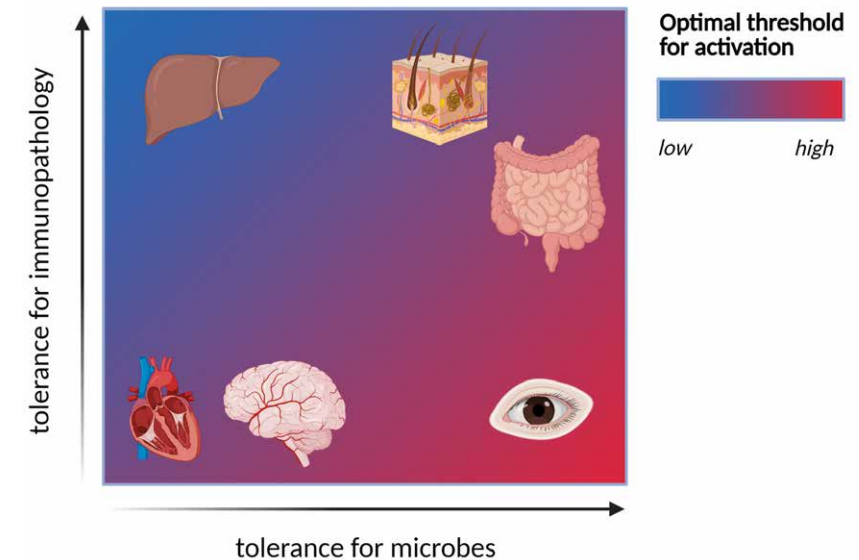

Figure 1. The optimal threshold for activation is context-dependent.
The required threshold for activation of immune cells differs per location and depends on (1) the tolerance of the organ for immune pathology and (2) the tolerance to microbial exposure. Organs with a high regenerative capacity, such as the liver, are more able to deal with immunopathology than organs with low regenerative capacity, such as the heart or the brain. The gut and skin are constantly exposed to microbes, most of which are harmless or beneficial and should be tolerated. The eye can tolerate a certain amount of microbial exposure, and the cost of responding to a microbial stimulus will be high, so a high threshold will ensure the response will only occur when needed. (Figure created with BioRender.com.)

activating receptors and fine-tune the level of activation of an immune cell. Most of them relay the inhibitory signals via one or more tyrosine-based inhibitory motifs (ITIMs) present in their cytoplasmic tails. ITIMs have the consensus sequence V/L/I/SxYxxV/L/I (24). When immune inhibitory receptors are activated by their ligands, the ITIMs recruit tyrosine phosphatases, which dephosphorylate the cytoplasmic tails of activating receptors or key molecules in their signaling pathways (25, 26). The ligands for many inhibitory receptors are still unknown, while some single-molecule ligands are identified for others. We previously argued that immune inhibitory receptors regulate immune responses in different ways. They may set a threshold for immune cell activation by preventing activating receptor signaling in certain contexts, or dampen activating receptor signaling after it has already happened. The mode of action of any inhibitory receptor depends on the expression pattern of the receptor and the availability of its ligand (27). By providing an inhibitory signal,

inhibitory receptors give additional information on the context in which an activating signal is sensed, thereby adjusting the immune response to the specific situation.

Some activating PRRs can under specific circumstances also demonstrate inhibitory functions. For example, TLR4 signaling from the cell membrane typically evokes pro-inflammatory responses, while TLR4 signaling from the endosome also triggers anti-inflammatory responses (28, 29). Here, we explore the concept of inhibitory pattern recognition receptors (iPRRs). We specifically focus on canonical inhibitory receptors that use ITIM-dependent inhibitory signaling pathways to relay their signals, resulting in inhibitory functions. We identify a group of immune inhibitory receptors that recognize DAMPs, HAMPs, and PAMPs, and classify these inhibitory receptors as iPRRs. We show that just like most activating PRRs (3), most iPRRs recognize both microbial and endogenous patterns (Figure 2). We propose that iPRRs constitute the inhibitory counterparts of activating PRRs and provide context to the activating signals coming from activating PRRs.

iPRRs recognize DAMPs

Upon the occurrence of damaged or dying cells, different DAMPs can arise and promote inflammation, leading to tissue repair but also immunopathology (3). Multiple inhibitory receptors could potentially tune DAMP-induced inflammatory responses (Figure 2 and (30-53)). The sialic acid-binding Ig-like lectin (Siglec)-10–CD24 complex recognizes high mobility group box 1 (HMGB1), heat shock protein 70 (Hsp70) and heat shock protein 90 (Hsp90), and limits the immune response to damaged cells (30). It thereby limits harmful inflammatory responses in conditions such as sepsis (54), infection (55), and liver damage. Indeed, CD24$^{-/-}$ mice die of sub-lethal doses of acetaminophen-induced liver injury (30). Siglec-5 recognizes Hsp70 and delivers anti-inflammatory signals to monocytes, which results in decreased production of TNFα and IL-8 in cells stimulated with LPS (36). Similarly, CD85j (leukocyte immunoglobulin-like receptor subfamily B member 1, LILRB1) (37) and signal inhibitory receptor on leukocytes 1 (SIRL-1) (53) recognize S100 proteins, another group of prototypical DAMPs. Blocking SIRL-1 enhances S100-induced release of reactive oxygen species in human neutrophils (53). SIRL-1 additionally recognizes another DAMP, the antimicrobial peptide LL-37 (52). Leukocyte immunoglobulin-like receptor subfamily B member 3 (LILRB3) recognizes a cytokeratin-associated protein, a cytoskeleton protein that is exposed in the extracellular environment after necrotic cell death and is recognized by the activating receptor leukocyte immunoglobulin-like receptor subfamily A member 6 (LILRA6) (38). Thus, several iPRRs can be identified that recognize DAMPs.
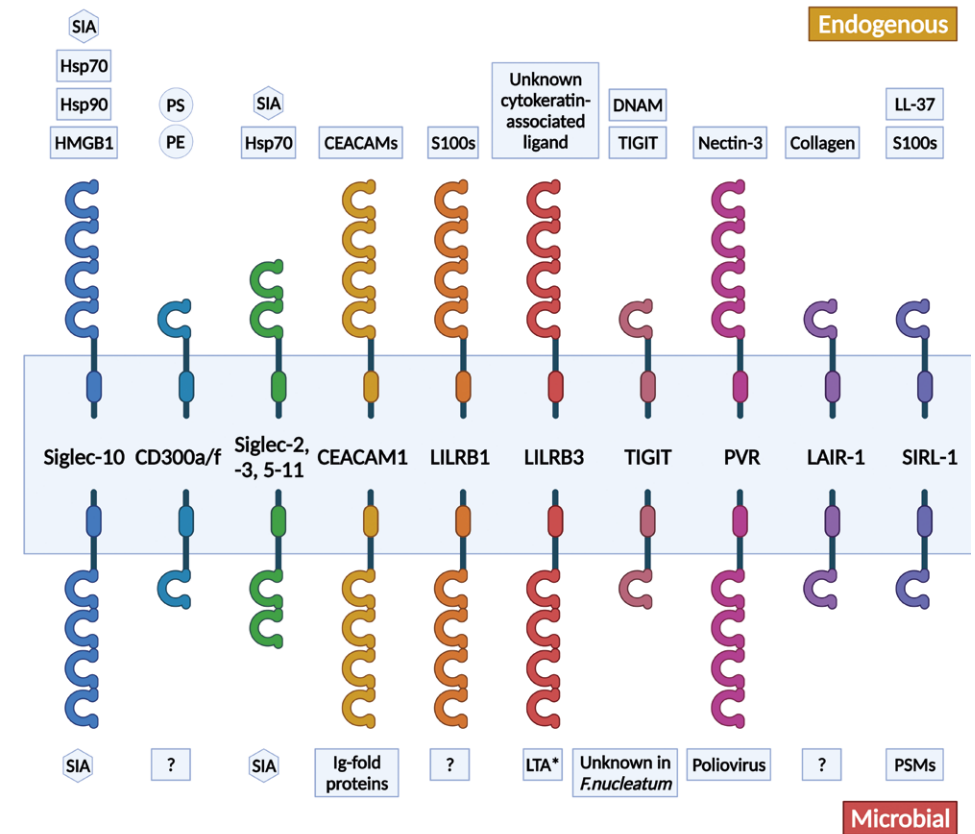

Figure 2. Inhibitory pattern recognition receptors and their endogenous and microbial ligands.

The currently known group of iPRRs consist of CD300a/f, sialic acid-binding Ig-like lectins (Siglecs) 2–3 and 5–11, carcinoembryonic antigen-related cell adhesion molecule 1 (CEACAM1), leukocyte immunoglobulin-like receptor subfamily B members 1 and 3 (LILRB1, LILRB3), T-cell immunoreceptor with Ig and ITIM domains (TIGIT), Poliovirus receptor (PVR), leukocyte-associated immunoglobulin-like receptor (LAIR-1), and signal inhibitory receptor on leukocytes 1 (SIRL-1). The upper part of the figure displays endogenous ligands, and the bottom part the microbial ligands for iPRRs. For most receptors both endogenous and exogenous ligands have been identified. Protein ligands are depicted as rectangles, lipids as circles, and carbohydrates as hexagons. All depicted inhibitory receptors are composed of Ig-domains, and the number of Ig-domains is schematically depicted for each receptor. In humans, most of these receptors are located in the chromosomal region 19q13, except CD300a/f (17q25) and TIGIT (3q13). *LTA is a ligand for the mouse orthologue of the human LILRB3.

Die. Where? How?

Cells can die in either an immunologically silent (apoptosis) or in an immunogenic and pro-inflammatory manner, where the latter can be a controlled (such as necroptosis and pyroptosis) or an uncontrolled (necrosis) process. Apoptotic cells are recognized, engulfed by phagocytes, and degraded intracellularly. In contrast, membranes of cells that die via immunogenic cell death (ICD) are ruptured, and intracellular components are released into the local microenvironment, many of which are regarded as DAMPs by neighboring cells (56). Interestingly, the type of ICD may determine which type of DAMP is released. This is illustrated by the finding that HMGB1 release can occur after both necroptosis and pyroptosis, while release of S100, Hsp70 and Hsp90 only occurs upon necrosis and/or necroptosis, but not in the context of pyroptosis (57). Thus, ICD results in the release of DAMPs and sets off a chain reaction, since DAMPs themselves induce ICD in cells that recognize them. This inflammatory chain reaction can be unwanted and highly dangerous, particularly in locations with low regenerative capacity (Figure 1). Mechanical stress, e.g., in case of brain trauma, can induce both apoptosis as well as ICD via necrosis (58). The balance between these two types of cell death in case of mechanical stress varies between tissues and seems to shift more towards necrosis upon increased levels of stress and duration of stress (58-60). A recent review poses that a certain level of plasticity exists between apoptosis and ICD: inflammasomes, multiprotein oligomers that form intracellularly upon recognition of PAMPs or DAMPs and usually activate ICD, can drive apoptosis when specific molecules (caspase 1 or gasdermin D) are inhibited (56). iPRR could provide this inhibitory signal upon recognition of DAMPs, resulting in the immediate dampening of an inflammatory chain reaction by steering the response away from ICD, towards apoptosis. Consequently, one can imagine that if inhibitory signaling occurs swiftly in sterile stress conditions, such as ischemia–reperfusion injury or trauma, inflammatory responses can be avoided. Importantly, sterile stress conditions do not always result in measurable inflammatory responses, and it is conceivable that cells in specific essential tissues do not respond to the initial release of DAMPs altogether. Since dependence on a rapid switch from ICD towards apoptosis is a risky bet for essential tissues, a more rapid alternative would be if DAMPs that bind iPRRs directly render the cells unresponsive.

iPRRs recognize molecules associated with homeostasis

As opposed to DAMPs, which typically are associated with danger and damage, HAMPs have previously been proposed to inhibit immune activation (17, 61, 62). HAMPs have various properties and mechanisms of action; for example,

lysophospholipids bind G protein-coupled receptors (61), and IL-35 binds cytokine receptors (17). Already before the introduction of the concept of HAMPs, the guard theory of immunity was established in plants. The guard theory proposes that rather than sensing insults such as pathogens directly, the immune system recognizes the consequences of these insults for the organism. This is reflected by changes in the levels of the guard proteins, triggering immune responses (63). Multiple lines of evidence suggest that the foundations of the guard theory also apply to the animal immune system (64). HAMPs in animals and human thus may be seen as a parallel to the preceding guard theory. Here, we identify HAMPs that ligate immune inhibitory receptors.

When cells undergo apoptosis, lipids such as phosphatidylserine (PS) and phosphatidylethanolamine (PE) are exposed on the cell surface and signal tissue-resident immune cells to find and dispose of the dying cells without triggering inflammation (65-67). PS and PE are sensed by inhibitory members of the CD300 family of immune receptors, CD300a and CD300f (34, 35). These interactions primarily result in dampening of mast cell activation by apoptotic cells, preventing inflammatory responses (68). In line with this, CD300a$^{-/-}$ mice develop exacerbated joint inflammation in an antigen-induced arthritis model (69). In addition to apoptotic cells, viable cells can also transiently expose PS and PE, which may arise under inflammatory conditions (3, 65, 70), suggesting that additional layers of regulation may be needed to prevent phagocytosis of non-apoptotic cells. Indeed, it has been shown that CD300a/f ligation by PS and PE also negatively regulates phagocytosis of apoptotic cells (34, 71). It is possible that a similar regulatory circuit is in place to prevent phagocytosis of PS or PE-bearing non-apoptotic cells. Furthermore, all host cells express diverse sialylated glycan structures, and these sialic acids are effectively a molecular pattern associated with "self" and homeostasis. Sialylated glycans are sensed by immune receptors of the Siglec family (reviewed in (31)). Most Siglecs (human Siglec 2–3 and Siglec 5–11) harbor an ITIM motif and are inhibitory receptors. Each Siglec exhibits preferential recognition of a different sialylated glycan. Siglecs participate in immune surveillance and provide the immune system with inhibitory signals to prevent reactivity against "self." It has recently been shown that in addition to cell-surface proteins and lipids, small RNAs can also be modified with glycans and tethered to the cell membrane of diverse cells under homeostatic conditions, emphasizing the role glycans play in the maintenance of homeostasis (72). In line with this, the lack of Siglec signaling is associated with autoimmune disease. Mice double-deficient for Siglec-G and Siglec-2 spontaneously develop systemic lupus erythematosus-like systemic autoimmune disease upon

aging (73). Other mechanisms of host's own molecules preventing the activation of immune system have recently been demonstrated, for example, the inhibitory properties of select endogenous lipids that the interactions between the CD1a and the T-cell receptor, effectively preventing T-cell responses (74). It remains to be determined whether similar molecules can also deliver inhibitory signals to immune cells via inhibitory receptors.

Some molecular patterns elicit activating and inhibitory signals

Several molecular patterns can be recognized by both inhibitory and activating receptors. The inhibitory receptor leukocyte-associated immunoglobulin-like receptor 1 (LAIR-1) recognizes a HAMP present in different transmembrane and extracellular matrix-associated collagens as well as collectins, leading to negative regulation of inflammatory responses, such as airway inflammation during viral infection (48, 49). Collagens are also recognized by the activating receptor osteoclast-associated immunoglobulin-like receptor (OSCAR), through which they can promote inflammation (75, 76). Further, a few Siglec receptors are activating (31), indicating there may be instances where sialylated glycans instigate immune activation. The relative expression of activating and inhibitory receptors on immune cells in a given situation together with potential other environmental clues will thus determine to what extent a cell becomes activated by these molecular patterns.

iPRRs can deliver potent inhibitory signals to immune cells and attenuate or halt immune system activation. Therefore, they are often exploited by tumors to evade the immune system. For instance, many tumors highly express diverse collagens, dampening anti-tumor immune responses through LAIR-1 activation on immune cells (77, 78). Similarly, various tumor types upregulate sialylated ligands for inhibitory Siglec receptors, resulting in a dampened anti-tumor immune response (79-81). CD155, the ligand for inhibitory receptor T-cell immunoreceptor with Ig and ITIM domains (TIGIT), is also upregulated on tumor cells and inhibits T-cell anti-tumor immune responses (82, 83). Upregulation of inhibitory receptor ligands in tumor tissues so appears to be a strategy of immune evasion in cancer.

iPRR recognize microbial molecular patterns

Similar to how occurrence of DAMPs does not always result in inflammation, microbial PAMPs also not always relay inflammation-promoting signals. Most microbes do not behave strictly as either pathogens or commensals. Microbes with high pathogenic potential can also exist as harmless colonizers of the host, and commensal microbes can cause disease when they behave in an atypical way.

Activating PRRs alone cannot differentiate between these situations, and it has thus been suggested that the immune system makes distinctions between pathogenic and non-pathogenic microbes through an integrated system of signals rather than one particular signal (19, 84). We argue that iPRRs may provide these additional signals.

Immune inhibitory receptors have been shown to interact with microbes, but since these interactions have been predominantly studied in experimental models of infection, it is commonly thought that iPRR–microbe interactions mediate immune evasion by the microbe (85). Since most microbes are not strictly pathogens, it is reasonable to think that the interaction of microbial ligands with inhibitory receptors could contribute to symbiosis. Multiple iPRRs recognize microbial ligands (Figure 2). *Staphylococcus aureus*, a bacterium commonly colonizing the human skin and nasal mucosa, interacts with the mouse paired immunoglobulin-like receptor B (PIR-B, orthologue of human LILRB3) through LTA, thereby limiting pro-inflammatory cytokine production. Indeed, PIR-B$^{-/-}$ mice infected with *S. aureus* show decreased survival compared to wild-type mice (39). LTA is a PAMP and an essential component of the cell wall universally expressed not only by *S. aureus* but also by other related less pathogenic species. The inhibitory receptor PIR-B/LILRB3 could thus regulate the host interaction with *S. aureus* in a non-inflammatory context through recognition of PAMPs.

As discussed, endogenous sialic acids are a molecular pattern associated with "self" and homeostasis, and interact with different inhibitory Siglec receptors. Sialic acids present on the surface of group B streptococcus (GBS) likewise interact with inhibitory Siglecs (32, 33). The sialic acid is common to all GBS, which is not a strict pathogen but rather an opportunist. CD33 Siglecs are expressed in skin-resident Langerhans cells, which could allow for interaction between Langerhans cells and GBS, resulting in an inhibitory signal and thus promoting the colonizing lifestyle of GBS. Other inhibitory receptors interacting with bacteria are SIRL-1, which recognizes staphylococcal phenol-soluble modulins (52), and TIGIT, which recognizes a ligand expressed by the oral commensal bacterium *Fusobacterium nucleatum* (50). The functional roles of these interactions are yet to be fully explored.

A particularly prominent binder of microbial ligands is the inhibitory receptor carcinoembryonic antigen-related cell adhesion molecule 1 (CEACAM1). On immune cells, CEACAM1 is restrictively expressed on activated cells, whereas it is constitutively expressed by epithelial cells (86, 87). It binds many different microbial

ligands, such as bacterial Dr adhesins of *Escherichia coli* (40), the Opa protein of *Neisseria meningitidis, Neisseria gonorrhoeae* (41) and commensal *Neisseria* species (88), adhesin UspA1 of *Moraxella catarrhalis* (42), the HopQ adhesin of *Helicobacter pylori* (43), CbpF adhesion of *Fusobacterium sp.* (44, 45), the streptococcal β protein (46), and also an unidentified ligand in the fungus *Candida sp.* (47). Though most of these microbes can be pathogenic, they do not always cause disease. Moreover, the absence of CEACAM1 has been shown in mouse models to predispose to colitis (89, 90). Together, this indicates that CEACAM1 may have a tolerizing function in host-microbe interactions rather than only serving as a means for immune evasion.

Concluding remarks and future perspectives

Here, we identify a group of inhibitory receptors that can be classified as iPRRs. We argue that iPRRs, like their activating counterparts, recognize molecular patterns (see also Supplementary Table 1). This provides context- and location-dependent signals to help shape the immune response. We show that most here identified iPRRs are able to recognize both endogenous and microbial patterns (Figure 2). The relative expression of activating and inhibitory PRRs and the integration of their signals will ultimately determine the strength of an immune response to microbes or damage. This would allow a differential response to tissue damage in different organs, depending on their susceptibility to immunopathology (Figure 1). For example, in tissues that have low regenerative capacity, such as the brain, increased expression of iPRRs could provide a higher activation threshold and prevent that release of DAMPs leads to inflammation and further tissue damage (91). We also point out that endogenous patterns can signal "safety" via iPRRs, to ensure that commonly occurring events such as apoptosis do not trigger the immune system. Similarly, there may be microbial patterns ensuring that harmless microbes colonizing the host do not bring about inflammatory responses (see Figure 3). For example, in the blood, microbial patterns such as LTA are recognized by activating PRRs. In contrast, in other anatomical locations, such as the skin, iPRRs could also signal in response to these patterns, abrogating their potential to trigger inflammatory responses. We argue that the interactions between iPRRs and their microbial ligands may thus be vital for establishing and maintaining commensal–host homeostasis and suggest that studies in this direction are needed to examine this hypothesis. Further exploration of possibly additional iPRRs, their ligands, and their expression patterns will provide a better understanding of the interactions of the host with its microbiota and the contextual regulation of septic and sterile inflammation.
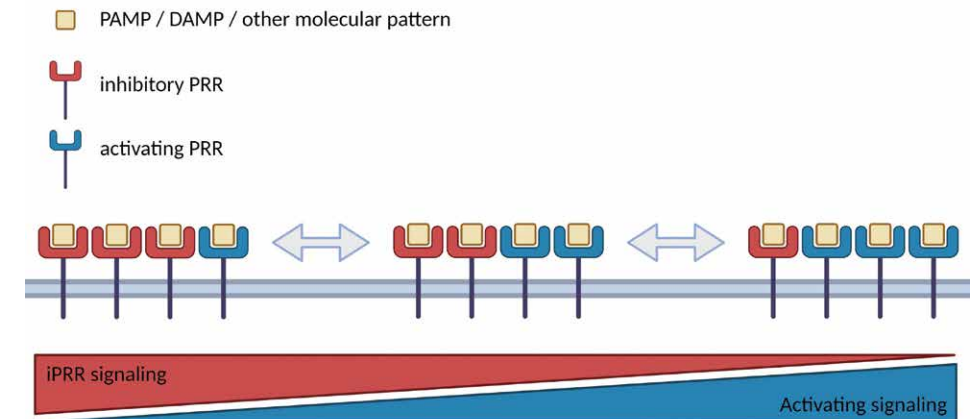

Figure 3. The integration of activating and inhibitory signals determines the outcome of the immune response.

When damage or a dangerous microbe should not be tolerated, DAMPs and PAMPs signal through activating PRRs to mount an immune response. However, when it is more beneficial for the host to tolerate damage or a harmless microbe, then the same DAMP or PAMP, or a different pattern, can concomitantly signal to an iPRR to inhibit the immune response. The relative expression of PRRs and iPRRs and their respective ligands will determine the strength of the resulting immune response. (Figure created with BioRender.com.)

Finally, iPRRs can be exploited to treat or prevent disease. The increased understanding of the function of inhibitory receptors has led to significant advances in the treatment of cancer. PD-1 and CTLA-4 have already proven their potential as therapeutic targets on T cells for cancer immunotherapy (92). Innate cells such as NK cells, innate lymphoid cells, and different myeloid cell types are also important in anti-cancer immune responses. These cells can directly contribute to tumor removal and additionally modulate anti-tumor T-cell responses by steering T-cell activation. Different iPRRs expressed on these cells, such as TIGIT and CD96, are already being explored as additional therapeutic targets (83). With an increased understanding of the properties of iPRRs and their ligands, we expect that more of these receptors will be used as targets for immunotherapy.

References

1. Janeway CA, Jr. Approaching the asymptote? Evolution and revolution in immunology. Cold Spring Harb Symp Quant Biol. 1989;54 Pt 1:1-13.

2. Takeuchi O, Akira S. Pattern recognition receptors and inflammation. Cell. 2010;140(6):805-20.

3. Gong T, Liu L, Jiang W, Zhou R. DAMP-sensing receptors in sterile inflammation and inflammatory diseases. Nat Rev Immunol. 2020;20(2):95-112.

4. Medzhitov R, Janeway CA, Jr. Decoding the patterns of self and nonself by the innate immune system. Science. 2002;296(5566):298-300.

5. Akira S, Uematsu S, Takeuchi O. Pathogen recognition and innate immunity. Cell. 2006;124(4):783-801.

6. Chen GY, Nunez G. Sterile inflammation: sensing and reacting to damage. Nat Rev Immunol. 2010;10(12):826-37.

7. Matzinger P. Tolerance, danger, and the extended family. Annu Rev Immunol. 1994;12:991-1045.

8. Matzinger P. The danger model: a renewed sense of self. Science. 2002;296(5566):301-5.

9. Burnet FM. The clonal selection theory of acquired immunity. Nashville: Vanderbilt University Press; 1959.

10. Bianchi ME, Manfredi AA. Immunology. Dangers in and out. Science. 2009;323(5922):1683-4.

11. Medzhitov R, Preston-Hurlburt P, Janeway CA, Jr. A human homologue of the Drosophila Toll protein signals activation of adaptive immunity. Nature. 1997;388(6640):394-7.

12. Poltorak A, He X, Smirnova I, Liu MY, Van Huffel C, Du X, et al. Defective LPS signaling in C3H/HeJ and C57BL/10ScCr mice: mutations in Tlr4 gene. Science. 1998;282(5396):2085-8.

13. Schwandner R, Dziarski R, Wesche H, Rothe M, Kirschning CJ. Peptidoglycan- and lipoteichoic acid-induced cell activation is mediated by toll-like receptor 2. J Biol Chem. 1999;274(25):17406-9.

14. Pradeu T, Cooper EL. The danger theory: 20 years later. Front Immunol. 2012;3:287.

15. Shields AM, Panayi GS, Corrigall VM. Resolution-associated molecular patterns (RAMP): RAMParts defending immunological homeostasis? Clin Exp Immunol. 2011;165(3):292-300.

16. Wang X, Wang Y, Antony V, Sun H, Liang G. Metabolism-Associated Molecular Patterns (MAMPs). Trends Endocrinol Metab. 2020;31(10):712-24.

17. Li X, Fang P, Yang WY, Wang H, Yang X. IL-35, as a newly proposed homeostasis-associated molecular pattern, plays three major functions including anti-inflammatory initiator, effector, and blocker in cardiovascular diseases. Cytokine. 2019;122:154076.

18. Cario E, Brown D, McKee M, Lynch-Devaney K, Gerken G, Podolsky DK. Commensal-associated molecular patterns induce selective toll-like receptor-trafficking from apical membrane to cytoplasmic compartments in polarized intestinal epithelium. Am J Pathol. 2002;160(1):165-73.

19. Greslehner GP. Not by structures alone: Can the immune system recognize microbial functions? Stud Hist Philos Biol Biomed Sci. 2020;84:101336.

20. Medzhitov R, Schneider DS, Soares MP. Disease tolerance as a defense strategy. Science. 2012;335(6071):936-41.

21. Rowshanravan B, Halliday N, Sansom DM. CTLA-4: a moving target in immunotherapy. Blood. 2018;131(1):58-67.

22. Long EO. Negative signaling by inhibitory receptors: the NK cell paradigm. Immunological Reviews. 2008;224:70-84.

23. Ravetch JV, Lanier LL. Immune inhibitory receptors. Science. 2000;290(5489):84-9.

24. Vivier E, Daeron M. Immunoreceptor tyrosine-based inhibition motifs. Immunol Today. 1997;18(6):286-91.

25. Coxon CH, Geer MJ, Senis YA. ITIM receptors: more than just inhibitors of platelet activation. Blood. 2017;129(26):3407-18.

26. Gergely J, Pecht I, Sarmay G. Immunoreceptor tyrosine-based inhibition motif-bearing receptors regulate the immunoreceptor tyrosine-based activation motif-induced activation of immune competent cells. Immunol Lett. 1999;68(1):3-15.

27. Rumpret M, Drylewicz J, Ackermans LJE, Borghans JAM, Medzhitov R, Meyaard L. Functional categories of immune inhibitory receptors. Nat Rev Immunol. 2020;20(12):771-80.

28. Siegemund S, Sauer K. Balancing pro- and anti-inflammatory TLR4 signaling. Nat Immunol. 2012;13(11):1031-3.

29. Kagan JC. Defining the subcellular sites of innate immune signal transduction. Trends Immunol. 2012;33(9):442-8.

30. Chen GY, Tang J, Zheng P, Liu Y. CD24 and Siglec-10 selectively repress tissue damage-induced immune responses. Science. 2009;323(5922):1722-5.

31. Macauley MS, Crocker PR, Paulson JC. Siglec-mediated regulation of immune cell function in disease. Nat Rev Immunol. 2014;14(10):653-66.

32. Chang YC, Olson J, Beasley FC, Tung C, Zhang J, Crocker PR, et al. Group B Streptococcus engages an inhibitory Siglec through sialic acid mimicry to blunt innate immune and inflammatory responses in vivo. PLoS Pathog. 2014;10(1):e1003846.

33. Carlin AF, Lewis AL, Varki A, Nizet V. Group B streptococcal capsular sialic acids interact with siglecs (immunoglobulin-like lectins) on human leukocytes. J Bacteriol. 2007;189(4):1231-7.

34. Simhadri VR, Andersen JF, Calvo E, Choi SC, Coligan JE, Borrego F. Human CD300a binds to phosphatidylethanolamine and phosphatidylserine, and modulates the phagocytosis of dead cells. Blood. 2012;119(12):2799-809.

35. Choi SC, Simhadri VR, Tian L, Gil-Krzewska A, Krzewski K, Borrego F, et al. Cutting edge: mouse CD300f (CMRF-35-like molecule-1) recognizes outer membrane-exposed phosphatidylserine and can promote phagocytosis. J Immunol. 2011;187(7):3483-7.

36. Fong JJ, Sreedhara K, Deng L, Varki NM, Angata T, Liu Q, et al. Immunomodulatory activity of extracellular Hsp70 mediated via paired receptors Siglec-5 and Siglec-14. EMBO J. 2015;34(22):2775-88.

37. Arnold V, Cummings JS, Moreno-Nieves UY, Didier C, Gilbert A, Barre-Sinoussi F, et al. S100A9 protein is a novel ligand for the CD85j receptor and its interaction is implicated in the control of HIV-1 replication by NK cells. Retrovirology. 2013;10:122.

38. Jones DC, Hewitt CR, Lopez-Alvarez MR, Jahnke M, Russell AI, Radjabova V, et al. Allele-specific recognition by LILRB3 and LILRA6 of a cytokeratin 8-associated ligand on necrotic glandular epithelial cells. Oncotarget. 2016;7(13):15618-31.

39. Nakayama M, Kurokawa K, Nakamura K, Lee BL, Sekimizu K, Kubagawa H, et al. Inhibitory receptor paired Ig-like receptor B is exploited by Staphylococcus aureus for virulence. J Immunol. 2012;189(12):5903-11.

40. Korotkova N, Yang Y, Le Trong I, Cota E, Demeler B, Marchant J, et al. Binding of Dr adhesins of Escherichia coli to carcinoembryonic antigen triggers receptor dissociation. Mol Microbiol. 2008;67(2):420-34.

41. Virji M, Watt SM, Barker S, Makepeace K, Doyonnas R. The N-domain of the human CD66a adhesion molecule is a target for Opa proteins of Neisseria meningitidis and Neisseria gonorrhoeae. Mol Microbiol. 1996;22(5):929-39.

42. Conners R, Hill DJ, Borodina E, Agnew C, Daniell SJ, Burton NM, et al. The Moraxella adhesin UspA1 binds to its human CEACAM1 receptor by a deformable trimeric coiled-coil. EMBO J. 2008;27(12):1779-89.

43. Koniger V, Holsten L, Harrison U, Busch B, Loell E, Zhao Q, et al. Helicobacter pylori exploits human CEACAMs via HopQ for adherence and translocation of CagA. Nat Microbiol. 2016;2:16188.

44. Brewer ML, Dymock D, Brady RL, Singer BB, Virji M, Hill DJ. Fusobacterium spp. target human CEACAM1 via the trimeric autotransporter adhesin CbpF. J Oral Microbiol. 2019;11(1):1565043.

45. Gur C, Maalouf N, Shhadeh A, Berhani O, Singer BB, Bachrach G, et al. Fusobacterium nucleatum supresses anti-tumor immunity by activating CEACAM1. Oncoimmunology. 2019;8(6):e1581531.

46. van Sorge NM, Bonsor DA, Deng L, Lindahl E, Schmitt V, Lyndin M, et al. Bacterial protein domains with a novel Ig-like fold target human CEACAM receptors. EMBO J. 2021:e106103.

47. Klaile E, Muller MM, Schafer MR, Clauder AK, Feer S, Heyl KA, et al. Binding of Candida albicans to Human CEACAM1 and CEACAM6 Modulates the Inflammatory Response of Intestinal Epithelial Cells. mBio. 2017;8(2).

48. Lebbink RJ, Raynal N, de Ruiter T, Bihan DG, Farndale RW, Meyaard L. Identification of multiple potent binding sites for human leukocyte associated Ig-like receptor LAIR on collagens II and III. Matrix Biol. 2009;28(4):202-10.

49. Kumawat K, Geerdink RJ, Hennus MP, Roda MA, van Ark I, Leusink-Muis T, et al. LAIR-1 Limits Neutrophilic Airway Inflammation. Front Immunol. 2019;10:842.

50. Gur C, Ibrahim Y, Isaacson B, Yamin R, Abed J, Gamliel M, et al. Binding of the Fap2 protein of Fusobacterium nucleatum to human inhibitory receptor TIGIT protects tumors from immune cell attack. Immunity. 2015;42(2):344-55.

51. Yu X, Harden K, Gonzalez LC, Francesco M, Chiang E, Irving B, et al. The surface protein TIGIT suppresses T cell activation by promoting the generation of mature immunoregulatory dendritic cells. Nat Immunol. 2009;10(1):48-57.

52. Rumpret M, von Richthofen HJ, van der Linden M, Westerlaken GHA, Talavera Ormeno C, van Strijp JAG, et al. Signal inhibitory receptor on leukocytes-1 recognizes bacterial and endogenous amphipathic alpha-helical peptides. FASEB J. 2021;35(10):e21875.

53. Rumpret M, von Richthofen HJ, van der Linden M, Westerlaken GHA, Talavera Ormeno C, Low TY, et al. Recognition of S100 proteins by Signal Inhibitory Receptor on Leukocytes-1 negatively regulates human neutrophils. Eur J Immunol. 2021;51(9):2210-7.

54. Chen GY, Chen X, King S, Cavassani KA, Cheng J, Zheng X, et al. Amelioration of sepsis by inhibiting sialidase-mediated disruption of the CD24-SiglecG interaction. Nat Biotechnol. 2011;29(5):428-35.

55. Chen W, Han C, Xie B, Hu X, Yu Q, Shi L, et al. Induction of Siglec-G by RNA viruses inhibits the innate immune response by promoting RIG-I degradation. Cell. 2013;152(3):467-78.

56. Bedoui S, Herold MJ, Strasser A. Emerging connectivity of programmed cell death pathways and its physiological implications. Nat Rev Mol Cell Biol. 2020;21(11):678-95.

57. Frank D, Vince JE. Pyroptosis versus necroptosis: similarities, differences, and crosstalk. Cell Death Differ. 2019;26(1):99-114.

58. Vourc'h M, Roquilly A, Asehnoune K. Trauma-Induced Damage-Associated Molecular Patterns-Mediated Remote Organ Injury and Immunosuppression in the Acutely Ill Patient. Front Immunol. 2018;9:1330.

59. Valon L, Levayer R. Dying under pressure: cellular characterisation and in vivo functions of cell death induced by compaction. Biol Cell. 2019;111(3):51-66.

60. Takao S, Taya M, Chiew C. Mechanical stress-induced cell death in breast cancer cells. Biol Open. 2019;8(8).

61. Wang X, Li YF, Nanayakkara G, Shao Y, Liang B, Cole L, et al. Lysophospholipid Receptors, as Novel Conditional Danger Receptors and Homeostatic Receptors Modulate Inflammation-Novel Paradigm and Therapeutic Potential. J Cardiovasc Transl Res. 2016;9(4):343-59.

62. Sun Y, Johnson C, Zhou J, Wang L, Li YF, Lu Y, et al. Uremic toxins are conditional danger- or homeostasis-associated molecular patterns. Front Biosci (Landmark Ed). 2018;23:348-87.

63. Dangl JL, Jones JD. Plant pathogens and integrated defence responses to infection. Nature. 2001;411(6839):826-33.

64. Medzhitov R. Approaching the asymptote: 20 years later. Immunity. 2009;30(6):766-75.

65. Arandjelovic S, Ravichandran KS. Phagocytosis of apoptotic cells in homeostasis. Nat Immunol. 2015;16(9):907-17.

66. Segawa K, Nagata S. An Apoptotic 'Eat Me' Signal: Phosphatidylserine Exposure. Trends Cell Biol. 2015;25(11):639-50.

67. Gordon S, Pluddemann A. Macrophage Clearance of Apoptotic Cells: A Critical Assessment. Front Immunol. 2018;9:127.

68. Nakahashi-Oda C, Tahara-Hanaoka S, Shoji M, Okoshi Y, Nakano-Yokomizo T, Ohkohchi N, et al. Apoptotic cells suppress mast cell inflammatory responses via the CD300a immunoreceptor. J Exp Med. 2012;209(8):1493-503.

69. Valiate BVS, Alvarez RU, Karra L, Queiroz-Junior CM, Amaral FA, Levi-Schaffer F, et al. The immunoreceptor CD300a controls the intensity of inflammation and dysfunction in a model of Ag-induced arthritis in mice. J Leukoc Biol. 2019;106(4):957-66.

70. Ravichandran KS. Find-me and eat-me signals in apoptotic cell clearance: progress and conundrums. J Exp Med. 2010;207(9):1807-17.

71. Ju X, Zenke M, Hart DN, Clark GJ. CD300a/c regulate type I interferon and TNF-alpha secretion by human plasmacytoid dendritic cells stimulated with TLR7 and TLR9 ligands. Blood. 2008;112(4):1184-94.

72. Flynn RA, Pedram K, Malaker SA, Batista PJ, Smith BAH, Johnson AG, et al. Small RNAs are modified with N-glycans and displayed on the surface of living cells. Cell. 2021.

73. Jellusova J, Wellmann U, Amann K, Winkler TH, Nitschke L. CD22 x Siglec-G double-deficient mice have massively increased B1 cell numbers and develop systemic autoimmunity. J Immunol. 2010;184(7):3618-27.

74. Cotton RN, Wegrecki M, Cheng TY, Chen YL, Veerapen N, Le Nours J, et al. CD1a selectively captures endogenous cellular lipids that broadly block T cell response. J Exp Med. 2021;218(7).

75. Barrow AD, Raynal N, Andersen TL, Slatter DA, Bihan D, Pugh N, et al. OSCAR is a collagen receptor that costimulates osteoclastogenesis in DAP12-deficient humans and mice. J Clin Invest. 2011;121(9):3505-16.

76. Schultz HS, Guo L, Keller P, Fleetwood AJ, Sun M, Guo W, et al. OSCAR-collagen signaling in monocytes plays a proinflammatory role and may contribute to the pathogenesis of rheumatoid arthritis. Eur J Immunol. 2016;46(4):952-63.

77. Rygiel TP, Stolte EH, de Ruiter T, van de Weijer ML, Meyaard L. Tumor-expressed collagens can modulate immune cell function through the inhibitory collagen receptor LAIR-1. Mol Immunol. 2011;49(1-2):402-6.

78. Peng DH, Rodriguez BL, Diao L, Chen L, Wang J, Byers LA, et al. Collagen promotes anti-PD-1/PD-L1 resistance in cancer through LAIR1-dependent CD8(+) T cell exhaustion. Nat Commun. 2020;11(1):4520.

79. Jandus C, Boligan KF, Chijioke O, Liu H, Dahlhaus M, Demoulins T, et al. Interactions between Siglec-7/9 receptors and ligands influence NK cell-dependent tumor immunosurveillance. J Clin Invest. 2014;124(4):1810-20.

80. Fraschilla I, Pillai S. Viewing Siglecs through the lens of tumor immunology. Immunol Rev. 2017;276(1):178-91.

81. van de Wall S, Santegoets KCM, van Houtum EJH, Bull C, Adema GJ. Sialoglycans and Siglecs Can Shape the Tumor Immune Microenvironment. Trends Immunol. 2020;41(4):274-85.

82. Braun M, Aguilera AR, Sundarrajan A, Corvino D, Stannard K, Krumeich S, et al. CD155 on Tumor Cells Drives Resistance to Immunotherapy by Inducing the Degradation of the Activating Receptor CD226 in CD8(+) T Cells. Immunity. 2020;53(4):805-23 e15.

83. Dougall WC, Kurtulus S, Smyth MJ, Anderson AC. TIGIT and CD96: new checkpoint receptor targets for cancer immunotherapy. Immunol Rev. 2017;276(1):112-20.

84. Swiatczak B, Rescigno M, Cohen IR. Systemic features of immune recognition in the gut. Microbes Infect. 2011;13(12-13):983-91.

85. Van Avondt K, van Sorge NM, Meyaard L. Bacterial immune evasion through manipulation of host inhibitory immune signaling. PLoS Pathog. 2015;11(3):e1004644.

86. Gray-Owen SD, Blumberg RS. CEACAM1: contact-dependent control of immunity. Nat Rev Immunol. 2006;6(6):433-46.

87. Huang YH, Zhu C, Kondo Y, Anderson AC, Gandhi A, Russell A, et al. CEACAM1 regulates TIM-3-mediated tolerance and exhaustion. Nature. 2015;517(7534):386-90.

88. Toleman M, Aho E, Virji M. Expression of pathogen-like Opa adhesins in commensal Neisseria: genetic and functional analysis. Cell Microbiol. 2001;3(1):33-44.

89. Jin Y, Lin Y, Lin L, Sun Y, Zheng C. Carcinoembryonic antigen related cellular adhesion molecule 1 alleviates dextran sulfate sodium-induced ulcerative colitis in mice. Life Sci. 2016;149:120-8.

90. Nagaishi T, Pao L, Lin SH, Iijima H, Kaser A, Qiao SW, et al. SHP1 phosphatase-dependent T cell inhibition by CEACAM1 adhesion molecule isoforms. Immunity. 2006;25(5):769-81.

91. Ashour D, Delgobo M, Frantz S, Ramos GC. Coping with sterile inflammation: between risk and necessity. Cardiovasc Res. 2021;117(6):e84-e7.

92. Ribas A, Wolchok JD. Cancer immunotherapy using checkpoint blockade. Science. 2018;359(6382):1350-5.

Supplementary information

Supplementary Table 1. Overview of different properties of iPRRs.

iPRR	Expression iPRR	iPRR structure	Signaling pathway	Endogenous molecular pattern	Expression ligand	Microbial molecular pattern	Activating receptor	References
CD300a/f	Broad on immune cells, upregulated on activation	Ig-like	ITIM	Phosphatidylserine, phosphatidylethanolamine	Exposed in programmed cell death	—	Tim4	(1-5)
CEACAM1	Broad on immune, epithelial and endothelial cells	Ig-like	ITIM	CEACAM1 and other CEACAMs	Constitutive	Ig fold proteins	Other CEA-CAMs	(6-14)
LAIR-1	Broad on immune cells, on activation upregulated on neutrophils, downregulated on T cells	Ig-like	ITIM	Collagen	Constitutive	—	OSCAR	(15-17)
LILRB1 (CD85j)	Neutrophil, monocyte, dendritic cell, NK cell, upregulated on activation	Ig-like	ITIM	S100 proteins	Upon cell damage	—	TLR4, RAGE	(18-21)
LILRB3 (CD85a)	Neutrophil, monocyte, DC	Ig-like	ITIM	Cytokeratin-associated	Upon cell damage	Unknown in *S. aureus* (LTA shown for mice ortholog PIR-B)	TLR2/6	(22-26)
PVR	Dendritic cell, upregulated on activation	Ig-like	ITIM	Nectin-3	Constitutive	Poliovirus	—	(27, 28)
Siglec 2, 3, 5–11	Broad on immune cells, differs per receptor	Ig-like	ITIM	Sialic acids	Constitutive	Sialic acids	Siglec 14–16	(29-37)
Siglec 2, 3, 5–11	Broad on immune cells, differs per receptor	Ig-like	ITIM	Hsp70	Upon cell damage	—	TLR4, RAGE	(21, 29-40)
Siglec 10	B cell, eosinophil, monocyte	Ig-like	ITIM	HMGB1, Hsp90	Upon cell damage	—	TLR4, RAGE	(21, 29, 37, 39, 40)
SIRL-1	Neutrophil, monocyte, downregulated on activation	Ig-like	ITIM	LL-37, S100 proteins	Upon cell damage and immune activation	Phenol-soluble modulins of *Staphylococcus*	TLR4, RAGE, FPR2	(21, 41-44)
TIGIT	T cell, NK cell, upregulated on activation	Ig-like	ITIM	DNAM-1, TIGIT	TIGIT upregulated on activation	Unknown in *F. nucleatum*	DNAM-1	(27, 28, 45, 46)

Supplementary references

1. Simhadri VR, Andersen JF, Calvo E, Choi SC, Coligan JE, Borrego F. Human CD300a binds to phosphatidylethanolamine and phosphatidylserine, and modulates the phagocytosis of dead cells. Blood. 2012;119(12):2799-809.

2. Choi SC, Simhadri VR, Tian L, Gil-Krzewska A, Krzewski K, Borrego F, et al. Cutting edge: mouse CD300f (CMRF-35-like molecule-1) recognizes outer membrane-exposed phosphatidylserine and can promote phagocytosis. J Immunol. 2011;187(7):3483-7.

3. Zenarruzabeitia O, Vitalle J, Eguizabal C, Simhadri VR, Borrego F. The Biology and Disease Relevance of CD300a, an Inhibitory Receptor for Phosphatidylserine and Phosphatidylethanolamine. J Immunol. 2015;194(11):5053-60.

4. Alvarez Y, Tang X, Coligan JE, Borrego F. The CD300a (IRp60) inhibitory receptor is rapidly up-regulated on human neutrophils in response to inflammatory stimuli and modulates CD32a (FcgammaRIIa) mediated signaling. Mol Immunol. 2008;45(1):253-8.

5. Segawa K, Nagata S. An Apoptotic 'Eat Me' Signal: Phosphatidylserine Exposure. Trends Cell Biol. 2015;25(11):639-50.

6. Korotkova N, Yang Y, Le Trong I, Cota E, Demeler B, Marchant J, et al. Binding of Dr adhesins of Escherichia coli to carcinoembryonic antigen triggers receptor dissociation. Mol Microbiol. 2008;67(2):420-34.

7. Virji M, Watt SM, Barker S, Makepeace K, Doyonnas R. The N-domain of the human CD66a adhesion molecule is a target for Opa proteins of Neisseria meningitidis and Neisseria gonorrhoeae. Mol Microbiol. 1996;22(5):929-39.

8. Conners R, Hill DJ, Borodina E, Agnew C, Daniell SJ, Burton NM, et al. The Moraxella adhesin UspA1 binds to its human CEACAM1 receptor by a deformable trimeric coiled-coil. EMBO J. 2008;27(12):1779-89.

9. Koniger V, Holsten L, Harrison U, Busch B, Loell E, Zhao Q, et al. Helicobacter pylori exploits human CEACAMs via HopQ for adherence and translocation of CagA. Nat Microbiol. 2016;2:16188.

10. Brewer ML, Dymock D, Brady RL, Singer BB, Virji M, Hill DJ. Fusobacterium spp. target human CEACAM1 via the trimeric autotransporter adhesin CbpF. J Oral Microbiol. 2019;11(1):1565043.

11. Gur C, Maalouf N, Shhadeh A, Berhani O, Singer BB, Bachrach G, et al. Fusobacterium nucleatum supresses anti-tumor immunity by activating CEACAM1. Oncoimmunology. 2019;8(6):e1581531.

12. van Sorge NM, Bonsor DA, Deng L, Lindahl E, Schmitt V, Lyndin M, et al. Bacterial protein domains with a novel Ig-like fold target human CEACAM receptors. EMBO J. 2021:e106103.

13. Klaile E, Muller MM, Schafer MR, Clauder AK, Feer S, Heyl KA, et al. Binding of Candida albicans to Human CEACAM1 and CEACAM6 Modulates the Inflammatory Response of Intestinal Epithelial Cells. mBio. 2017;8(2).

14. Gray-Owen SD, Blumberg RS. CEACAM1: contact-dependent control of immunity. Nat Rev Immunol. 2006;6(6):433-46.

15. Lebbink RJ, Raynal N, de Ruiter T, Bihan DG, Farndale RW, Meyaard L. Identification of multiple potent binding sites for human leukocyte associated Ig-like receptor LAIR on collagens II and III. Matrix Biol. 2009;28(4):202-10.

16. Kumawat K, Geerdink RJ, Hennus MP, Roda MA, van Ark I, Leusink-Muis T, et al. LAIR-1 Limits Neutrophilic Airway Inflammation. Front Immunol. 2019;10:842.

17. An B, Brodsky B. Collagen binding to OSCAR: the odd couple. Blood. 2016;127(5):521-2.

18. Arnold V, Cummings JS, Moreno-Nieves UY, Didier C, Gilbert A, Barre-Sinoussi F, et al. S100A9 protein is a novel ligand for the CD85j receptor and its interaction is implicated in the control of HIV-1 replication by NK cells. Retrovirology. 2013;10:122.

19. Nunez SY, Ziblat A, Secchiari F, Torres NI, Sierra JM, Raffo Iraolagoitia XL, et al. Human M2 Macrophages Limit NK Cell Effector Functions through Secretion of TGF-beta and Engagement of CD85j. J Immunol. 2018;200(3):1008-15.

20. Young NT, Waller EC, Patel R, Roghanian A, Austyn JM, Trowsdale J. The inhibitory receptor LILRB1 modulates the differentiation and regulatory potential of human dendritic cells. Blood. 2008;111(6):3090-6.

21. Prantner D, Nallar S, Vogel SN. The role of RAGE in host pathology and crosstalk between RAGE and TLR4 in innate immune signal transduction pathways. FASEB J. 2020;34(12):15659-74.

22. Jones DC, Hewitt CR, Lopez-Alvarez MR, Jahnke M, Russell AI, Radjabova V, et al. Allele-specific recognition by LILRB3 and LILRA6 of a cytokeratin 8-associated ligand on necrotic glandular epithelial cells. Oncotarget. 2016;7(13):15618-31.

23. Nakayama M, Kurokawa K, Nakamura K, Lee BL, Sekimizu K, Kubagawa H, et al. Inhibitory receptor paired Ig-like receptor B is exploited by Staphylococcus aureus for virulence. J Immunol. 2012;189(12):5903-11.

24. Lewis Marffy AL, McCarthy AJ. Leukocyte Immunoglobulin-Like Receptors (LILRs) on Human Neutrophils: Modulators of Infection and Immunity. Front Immunol. 2020;11:857.

25. Akira S, Uematsu S, Takeuchi O. Pathogen recognition and innate immunity. Cell. 2006;124(4):783-801.

26. Nakayama M, Underhill DM, Petersen TW, Li B, Kitamura T, Takai T, et al. Paired Ig-like receptors bind to bacteria and shape TLR-mediated cytokine production. J Immunol. 2007;178(7):4250-9.

27. Yu X, Harden K, Gonzalez LC, Francesco M, Chiang E, Irving B, et al. The surface protein TIGIT suppresses T cell activation by promoting the generation of mature immunoregulatory dendritic cells. Nat Immunol. 2009;10(1):48-57.

28. Pende D, Castriconi R, Romagnani P, Spaggiari GM, Marcenaro S, Dondero A, et al. Expression of the DNAM-1 ligands, Nectin-2 (CD112) and poliovirus receptor (CD155), on dendritic cells: relevance for natural killer-dendritic cell interaction. Blood. 2006;107(5):2030-6.

29. Macauley MS, Crocker PR, Paulson JC. Siglec-mediated regulation of immune cell function in disease. Nat Rev Immunol. 2014;14(10):653-66.

30. Chang YC, Olson J, Beasley FC, Tung C, Zhang J, Crocker PR, et al. Group B Streptococcus engages an inhibitory Siglec through sialic acid mimicry to blunt innate immune and inflammatory responses in vivo. PLoS Pathog. 2014;10(1):e1003846.

31. Carlin AF, Lewis AL, Varki A, Nizet V. Group B streptococcal capsular sialic acids interact with siglecs (immunoglobulin-like lectins) on human leukocytes. J Bacteriol. 2007;189(4):1231-7.

32. Han S, Collins BE, Bengtson P, Paulson JC. Homomultimeric complexes of CD22 in B cells revealed by protein-glycan cross-linking. Nat Chem Biol. 2005;1(2):93-7.

33. Brown GD, Crocker PR. Lectin Receptors Expressed on Myeloid Cells. Microbiol Spectr. 2016;4(5).

34. Perez-Oliva AB, Martinez-Esparza M, Vicente-Fernandez JJ, Corral-San Miguel R, Garcia-Penarrubia P, Hernandez-Caselles T. Epitope mapping, expression and post-translational modifications of two isoforms of CD33 (CD33M and CD33m) on lymphoid and myeloid human cells. Glycobiology. 2011;21(6):757-70.

35. Arakawa S, Suzukawa M, Ohshima N, Tashimo H, Asari I, Matsui H, et al. Expression of Siglec-8 is regulated by interleukin-5, and serum levels of soluble Siglec-8 may predict responsiveness of severe eosinophilic asthma to mepolizumab. Allergol Int. 2018;67S:S41-S4.

36. Angata T, Kerr SC, Greaves DR, Varki NM, Crocker PR, Varki A. Cloning and characterization of human Siglec-11. A recently evolved signaling molecule that can interact with SHP-1 and SHP-2 and is expressed by tissue macrophages, including brain microglia. J Biol Chem. 2002;277(27):24466-74.

37. Chen GY, Tang J, Zheng P, Liu Y. CD24 and Siglec-10 selectively repress tissue damage-induced immune responses. Science. 2009;323(5922):1722-5.

38. Fong JJ, Sreedhara K, Deng L, Varki NM, Angata T, Liu Q, et al. Immunomodulatory activity of extracellular Hsp70 mediated via paired receptors Siglec-5 and Siglec-14. EMBO J. 2015;34(22):2775-88.

39. Sims GP, Rowe DC, Rietdijk ST, Herbst R, Coyle AJ. HMGB1 and RAGE in inflammation and cancer. Annu Rev Immunol. 2010;28:367-88.

40. Liu Y, Yin H, Zhao M, Lu Q. TLR2 and TLR4 in autoimmune diseases: a comprehensive review. Clin Rev Allergy Immunol. 2014;47(2):136-47.

41. Rumpret M, von Richthofen HJ, van der Linden M, Westerlaken GHA, Talavera Ormeno C, van Strijp JAG, et al. Signal inhibitory receptor on leukocytes-1 recognizes bacterial and endogenous amphipathic alpha-helical peptides. FASEB J. 2021;35(10):e21875.

42. Rumpret M, von Richthofen HJ, van der Linden M, Westerlaken GHA, Talavera Ormeno C, Low TY, et al. Recognition of S100 proteins by Signal Inhibitory Receptor on Leukocytes-1 negatively regulates human neutrophils. Eur J Immunol. 2021;51(9):2210-7.

43. Steevels TA, van Avondt K, Westerlaken GH, Stalpers F, Walk J, Bont L, et al. Signal inhibitory receptor on leukocytes-1 (SIRL-1) negatively regulates the oxidative burst in human phagocytes. Eur J Immunol. 2013;43(5):1297-308.

44. Kretschmer D, Gleske AK, Rautenberg M, Wang R, Koberle M, Bohn E, et al. Human formyl peptide receptor 2 senses highly pathogenic Staphylococcus aureus. Cell Host Microbe. 2010;7(6):463-73.

45. Gur C, Ibrahim Y, Isaacson B, Yamin R, Abed J, Gamliel M, et al. Binding of the Fap2 protein of Fusobacterium nucleatum to human inhibitory receptor TIGIT protects tumors from immune cell attack. Immunity. 2015;42(2):344-55.

46. Dougall WC, Kurtulus S, Smyth MJ, Anderson AC. TIGIT and CD96: new checkpoint receptor targets for cancer immunotherapy. Immunol Rev. 2017;276(1):112-20.

CHAPTER **8**

Sensing context: inhibitory receptors on non-hematopoietic cells

Helen J. von Richthofen[1,2], **Linde Meyaard**[1,2]

[1] Center for Translational Immunology, University Medical Center Utrecht, Oncode Institute, Utrecht University, Utrecht, The Netherlands
[2] Oncode Institute, Utrecht, The Netherlands

Abstract

Similar to immune cells, non-hematopoietic cells recognize microbial and endogenous threats. Their response to these stimuli is dependent on the environmental context. For example, intact intestinal epithelium expresses pattern recognition receptors (PRRs) but should tolerate commensal bacteria, while damaged epithelium should respond promptly to initiate an immune response. This indicates that non-hematopoietic cells possess mechanisms to sense environmental context and to regulate their responses. Inhibitory receptors provide context sensing to immune cells. For instance, they raise the threshold for activation to prevent overzealous immune activation to harmless stimuli. Inhibitory receptors are typically studied on hematopoietic cells, but several of these receptors are expressed on non-hematopoietic cells. Here, we review evidence for the regulation of non-hematopoietic cells by inhibitory receptors, focusing on epithelial and endothelial cells. We explain that inhibitory receptors on these cells can sense a wide range of signals, including cell-cell adhesion, cell-matrix adhesion, and apoptotic cells. More importantly, they regulate various functions on these cells, including immune activation, proliferation, and migration. In conclusion, we propose that inhibitory receptors provide context to non-hematopoietic cells by fine tuning their response to endogenous or microbial stimuli. These findings prompt to investigate the functions of inhibitory receptors on non-hematopoietic cells more systematically.

Introduction

Similar to immune cells, non-hematopoietic cells express pattern recognition receptors and can be in contact with microbial and endogenous patterns (1-4). Their response to these stimuli depends on the situation. For example, exposure of epithelial cells to a certain microbe can be harmless when the epithelial barrier is intact, whereas the same microbe can be dangerous when the barrier is breached. In the latter case, epithelial cells should become activated and produce inflammatory cytokines to recruit immune cells, which in turn kill microbes at the wound interface and contribute to tissue repair (5). Thus, non-hematopoietic cells need to sense the context in which they receive a microbial or endogenous stimulus.

We previously argued that inhibitory receptors can provide context to immune cells by acting as negative feedback receptors or as threshold receptors. Negative feedback receptors are upregulated after activation to terminate the immune response, whereas threshold receptors are expressed on non-activated cells and provide a threshold to prevent unnecessary immune activation, for instance, in response to harmless stimuli (6). We also recently reviewed that multiple inhibitory receptors recognize endogenous and microbial patterns that can indicate danger, homeostasis, or both (7). As such, these inhibitory pattern recognition receptors (iPRRs) can form a regulatory counterpart to activating PRRs. We proposed that regulation by iPRRs may occur mostly in tissues that require a high activation threshold, such as tissues that face continuous microbial exposure (e.g. barrier tissues such as the intestine and skin) or tissues that have low tolerance for immunopathology (e.g. the brain, heart or eyes) (7). Mechanistically, inhibitory receptors usually contain an immunoreceptor tyrosine-based inhibitory motif (ITIM), or in some cases an immunoreceptor tyrosine-based switch motif (ITSM), which becomes phosphorylated upon receptor ligation. This leads to the recruitment of Src homology-2 (SH2) domain- containing inhibitory effectors such as SH2 domain-containing phosphatases (SHP)-1, SHP-2, SH2 domain-containing inositol 5'phosphatase (SHIP), or C-terminal Src kinase (Csk), which in turn inhibit the signaling of activating receptors (8, 9).

Even though inhibitory receptors are almost exclusively studied on hematopoietic cells, several of these receptors are expressed on non-hematopoietic cells. In this review, we examine evidence for the regulation of non-hematopoietic cells by ITIM-bearing inhibitory receptors. Herein, we focus on the regulation of epithelial cells and endothelial cells, for two reasons. Firstly, these cells are located in barrier tissues and thus provide an example of cells which may particularly benefit from regulation by inhibitory receptors. Secondly, studies which have addressed ITIM-dependent signaling on non-hematopoietic cells are sufficiently available for epithelial cells

and endothelial cells, while only limited for other cell types. Since some inhibitory receptors have multiple functions, we only regard ITIM-dependent signaling as an inhibitory receptor function.

Inhibitory receptors on epithelial cells

Epithelial cells express iPRRs

The immune function of epithelial cells comprises two major tasks: i) maintaining tissue integrity to prevent microbial invasion, which requires cell adhesion, proliferation, and migration, and ii) forming the first line of defense of the immune system by secreting inflammatory mediators. All of these functions could potentially be controlled by inhibitory receptors. Indeed, epithelial cells express several inhibitory receptors. They widely express CEACAM1 (also known as CD66a) and PVR (also known as Necl-5 or CD155) (10, 11), while CD300LF expression is restricted to tuft cells, a rare secretory epithelial cell with immune-related functions (12). All three receptors contain one or more intracellular ITIMs and are known to inhibit immune functions of hematopoietic cells, although PVR has been primarily studied as a ligand for other immune receptors (13-15). Of note, these are inhibitory receptors of which expression on epithelial cells has been described in literature. However, RNA sequencing databases such as protein atlas report that some epithelial cell types may express more inhibitory receptors, albeit at lower levels than in immune cells (16). This requires further validation on protein level. In addition, the human genome encodes many uncharacterized genes potentially encoding for ITIM-bearing receptors, which could also be expressed on epithelial cells (9).

CEACAM1, PVR and CD300LF are pleiotropic receptors, each responding to multiple endogenous and microbial patterns ((17, 18) and reviewed in (7)). CEACAM1 binds itself, other CEACAMs and microbial Ig-fold proteins. PVR binds the adhesion molecule Nectin-3, the matrix protein vitronectin, the immune receptors TIGIT, CD96 and DNAM-1, and forms the entry receptor for poliovirus. CD300LF binds phosphatidylserine (PS) and phosphatidylethanolamine (PE) on apoptotic cells and forms the entry receptor for murine norovirus (but not for human norovirus). This ligand repertoire classifies these receptors as iPRRs (7) in agreement with a regulatory role in barrier tissues that are highly exposed to microbial patterns.

Inhibitory receptors on epithelial cells regulate proliferation, immune activation, and migration

Which functions do these inhibitory receptors regulate on epithelial cells? Firstly,

CEACAM1 and PVR both contribute to cell-cell adhesion by interacting *in trans* with respectively CEACAM1 or Nectin-3 on neighboring epithelial cells (19, 20). In addition, PVR can mediate cell-matrix contact by binding to vitronectin (17). For PVR it has not been addressed whether the ITIM is required for cell adhesion, but cell adhesion mediated by CEACAM1 is ITIM-independent (21). However, *trans* homophilic interaction between CEACAM1 on neighbouring cells does induce CEACAM1 ITIM phosphorylation and SHP-2 recruitment (22). This has multiple potential functional consequences. Firstly, CEACAM1 is already known for 25 years to inhibit proliferation of epithelial cells (21, 23, 24). This involves ITIM-mediated signalling: CEACAM1 overexpression in human lung epithelial cells inhibits cell growth in confluent cell layers, whereas cells with overexpression of CEACAM1 in which the tyrosines of both ITIMs have been mutated to phenylalanine to abrogate sigaling (Y459F/Y486F) continue to proliferate and overgrow (25). Secondly, CEACAM1 signalling may affect cell migration, although contradicting findings are reported: CEACAM1 overexpression inhibits migration of MC38 colon epithelial cells in an ITIM dependent manner (26), but others have found that CEACAM1 overexpression enhances migration of HT-29 and Caco-2 colon epithelial cells (27, 28). Thirdly, CEACAM1 can dampen immune activation of epithelial cells, as it inhibits TLR2-induced IL-8 production by airway epithelial cells in response to its endogenous ligand CEACAM8 (29) and its microbial ligands from *Moraxella catarrhalis* and *Neisseria meningitides* (30). Using HEK293T cells, inhibition of the *M. catarrhali*s-induced TLR2 response was shown to require Y459 but not Y486 (30). Notably, the requirement of ITIM-mediated signaling to the function of these receptors is not always specifically addressed, and thus requires further examination. For example, interaction between CEACAM1 and HopQ from *Helicobacter pylori* has been shown to induce ITIM phosphorylation and enhanced IL-8 release (31), but it was not addressed whether ITIM-mediated signaling is responsible for this immune-activating effect.

For PVR and CD300LF, ITIM activation and the functional consequence thereof has to our knowledge not been addressed in epithelial cells. However, studies using fibroblast cell lines with receptor overexpression indicate that these receptors have the capacity for ITIM-mediated signaling in non-hematopoietic cells and may provide hints towards their function on epithelial cells. PVR ligation inhibits fibroblast adhesion to fibronectin while it enhances cell migration, which is abolished by ITIM mutation or co-expression of a dominant negative SHP-2 mutant (32). In line with this, several other studies show that PVR enhances fibroblast migration, albeit without addressing the requirement of ITIM phosphorylation (reviewed in (33)). In addition, PVR has been shown to enhance fibroblast proliferation, which is reversed upon cell-cell contact-induced endocytosis of PVR (34), posing a different potential mechanism by which an inhibitory receptor may

prevent cell overgrowth. However, again the involvement of ITIM signaling was not addressed. CD300LF overexpression in fibroblasts positively regulates phagocytosis of apoptotic cells by recognition of PS (35). Phagocytosis increases even further after Y-->F mutation of Y241, Y289 or Y325, which are the central tyrosines of two ITIMs and an ITSM motif, respectively. In contrast, phagocytosis decreases after mutation of Y276 which is present in a binding site for the PI3K subunit p85α (35). Together, this indicates that CD300LF can simultaneously transmit inhibitory signals via its ITIMs and activating signals via its p85α-binding motif.

In summary, inhibitory receptors may regulate various processes on epithelial cells, including proliferation, immune activation, and migration. However, more studies are needed to specifically address the requirement of ITIM signalling of inhibitory receptors on epithelial cells.

Splice isoform expression affects function and localization of inhibitory receptors.

One factor that may cause variable outcomes of inhibitory receptor ligation is the differential expression of isoforms that do or do not contain intracellular signaling motifs, as a result of alternative splicing. PVRα and CEACAM1-L isoforms contain a long intracellular tail with ITIMs, as opposed to PVRδ and CEACAM1-S isoforms with a short intracellular tail and no ITIMs (reviewed in (36, 37)). CEACAM1-S not only lacks ITIM-mediated signalling, but also interferes with signalling of CEACAM1-L by disrupting the formation of CEACAM1-L-*cis* dimers, which leads to decreased recruitment of SHP-2 (22). Interestingly, differential expression of CEACAM1-L/S isoforms may regulate the function of CEACAM1 in different contexts. For example, a low L:S ratio is found in subconfluent, proliferating cells, whereas a high L:S ratio is found in confluent rat epithelial cells (38). Thus, predominant CEACAM1-L expression may inhibit proliferation in confluent epithelium, while predominant CEACAM1-S expression may counteract the growth-inhibitory effect of CEACAM1-L in proliferating, sub-confluent epithelial layers.

Additionally, the ITIMs of CEACAM1 and PVR act as sorting signal in polarized epithelial cells. CEACAM-S is only localized on the apical surface of epithelial cells, whereas CEACAM-L is localized on the apical and lateral surface (39). For this lateral sorting, Y515 but not Y488 is needed (40). PVRδ is expressed on the apical and basolateral surface of polarized epithelial cells, whereas PVRα is only localized on the basolateral surface, which depends on interaction between the tyrosine in its ITIM motif and the mu1B subunit of the clathrin adaptor complex (41). The localization of ITIM-containing isoforms may indicate that these inhibitory receptors preferentially respond to basolateral ligation such as contact with neighbouring cells. It remains

to be determined whether this also leads to preferential suppression of basolateral activating signals, e.g. due to the limited molecular reach of phosphatases such as SHP-1 (42), or whether basolateral inhibitory receptors can also suppress signals received at the apical side. Importantly, some activating PRRs such as TLR3 and TLR5 are also preferentially expressed on the basolateral side of epithelial cells (43, 44). This may indicate that tissue damage and basolateral pathogen invasion can activate epithelial cells with a double kick: by increased stimulation of activating PRRs, while concurrently releasing the break of inhibitory PRRs.

Additional factors can affect inhibitory receptor function on epithelial cells. For example, CEACAM1 function can be controlled by proteolytic cleavage of its ectodomain and intracellular domain (45, 46), and by altered expression of CEACAM5 and CEACAM6 (25). Taken together, inhibitory receptor function is controlled by a complex interplay of splice isoform expression, subcellular localization, ligand expression and post translational modifications.

Inhibitory receptors provide context to epithelial cells

In conclusion, epithelial cells express inhibitory receptors through which they can sense a wide range of signals which give information on their context, including cell-cell adhesion, cell-matrix adhesion, apoptotic cells, and presence of microbes (Figure 1). Moreover, these receptors have the potential to inhibit cellular processes in epithelial cells such as proliferation and immune activation, as has been shown for CEACAM1. Based on these findings, we propose that inhibitory receptors on epithelial cells can fine tune their responses to external events depending on the context. For example, interaction between CEACAM1 molecules on adjacent cells may indicate that the epithelial barrier is intact, thereby signalling that proliferation or an immune response is not needed. In other words, CEACAM1 may signal a context of safety.

In contrast, pathogens such as *M. catarrhalis* and *N. meningitidis* may exploit this by ligating CEACAM1 to evade immune activation. Similarly, poliovirus and norovirus may benefit from ITIM-mediated immune inhibition via respectively PVR and CD300LF. Pathogens that bind CEACAM1 have also been shown to inhibit exfoliation of infected epithelial cells, by enhancing epithelial cell binding (47, 48). However, this effect is shared by other CEACAMs which do not contain an ITIM, and is therefore most likely mediated by the adhesive properties of CEACAMs rather than ITIM signaling. Notably, CEACAM1 also binds Opa adhesins expressed by commensal Neisseriae species, although the functional consequence of this interaction has not been addressed (49). It would be interesting to investigate if such interactions could also be of benefit to the host, by dampening immune activation to microbes in locations in which an immune response would do more harm than good.
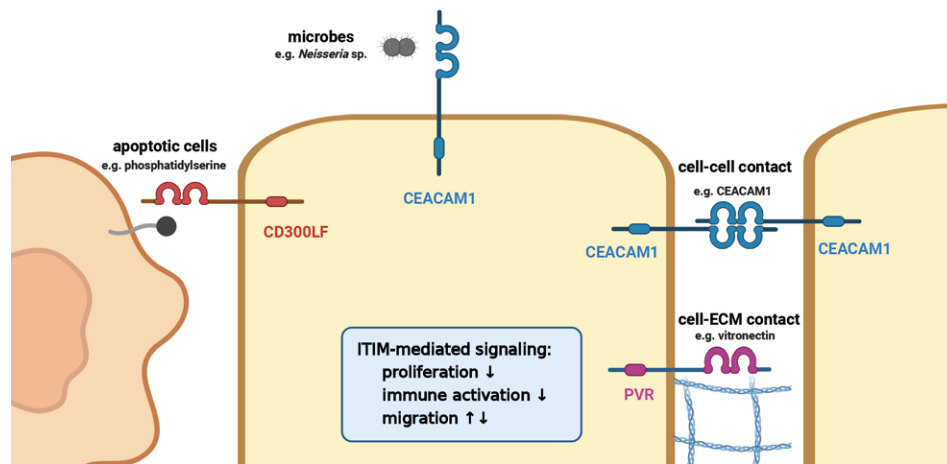
Figure 1.
Inhibitory receptors on epithelial cells can sense several signals such as cell-cell contact (e.g. CEACAM1 with CEACAM1 or other CEACAMs), cell-matrix contact (e.g. PVR – vitronectin), apoptotic cells (e.g. CD300LF – PS / PE) or presence of microbes (e.g. CEACAM1 – *Neisseria* species). These interactions potentially control proliferation, immune activation, and migration. The figure was created with biorender.com.

Inhibitory receptors on endothelial cells

Endothelial cells express inhibitory receptors that recognize cell-cell contact

Just like epithelial cells, endothelial cells have context-dependent immune functions. For instance, they need to maintain vascular integrity, while also allowing leukocyte transmigration during inflammation. Endothelial cells can be exposed to microbial patterns during infection, and to a wide variety of endogenous stimuli such as DAMPs and cytokines (50). Thus, endothelial cells require regulation to ensure appropriate responses to these stimuli, indicating a potential role for inhibitory receptors.

Endothelial cells express several inhibitory receptors, of which PECAM-1 (also known as CD31) is a well-known marker for endothelium (51). In addition, they express CEACAM1 (52), PVR (53), and, in some tissues, SIRPα (also known as SHPS-1) (54, 55). SIRPα and PECAM-1 have extensively been studied for their immune inhibitory function on hematopoietic cells (56, 57). As in epithelial cells, these receptors may signal tissue integrity. All of them interact *in trans* with ligands expressed on neighbouring cells, namely CEACAM1 with CEACAM1, PECAM-1 with PECAM-1, PVR with Nectin-3, and SIRPα with CD47 (57-59). In addition, their ligands are expressed

on leukocytes, indicating potential interaction with transmigrating leukocytes. Lastly, PECAM-1 has been shown to act as a mechanosensor, as it becomes rapidly ITIM phosphorylated and recruits SHP-2 upon fluid sheer stress and direct mechanical pressure (60), although this was not found in primary human endothelial cells *ex vivo* (61). What is the consequence of these interactions?

Inhibitory receptors on endothelial cells regulate endothelial cell migration and leukocyte diapedesis

PECAM-1 resembles CEACAM1 in its function, as *trans* homophilic PECAM-1 and CEACAM1 interactions both contribute to endothelial cell-cell adhesion and vascular integrity (reviewed in (62, 63)). For PECAM-1 this has been shown to be ITIM-independent (64). Conversely, *trans* homophilic PECAM-1 interaction may induce ITIM phosphorylation, as PECAM-1 becomes phosphorylated after binding to immobilized PECAM-1 (65). This has several potential functional outcomes. Firstly, several studies show that PECAM-1 enhances endothelial cell migration (reviewed in (51)), although mixed results are found on whether ITIM signaling positively or negatively contributes to this. Some studies report increased PECAM-1 ITIM phosphorylation in confluent cell cultures and ITIM-mediated *inhibition* of cell migration (66, 67), whereas others show the exact inverse, namely increased ITIM phosphorylation in wounded cell cultures and ITIM-mediated *enhancement* of cell migration (68, 69). Of note, the latter studies used PECAM-1 transfected REN mesothelial cells as a substitute for endothelial cells. In support for pro-migratory effects of inhibitory receptor signaling on endothelial cells, CEACAM1 increases endothelial cell migration in an Y488 dependent manner (70). Similarly, SIRPα increases migration of melanoma and CHO cells via its ITIMs, suggesting it may have a similar function on endothelial cells (71). Thus arguably the most consistent finding is that inhibitory receptor signaling enhances endothelial cell migration. Mechanistically, this has been explained by SHP-2-mediated RhoA regulation, although controversy exists on whether SHP-2 activates (72) or inhibits (73) RhoA, and de-phosphorylation of focal adhesion components such as paxillin, which in turn increases the turnover of focal adhesions (68, 69). Still, increased PECAM-1 tyrosine phosphorylation in wounded cell cultures seems counterintuitive, as one may expect that wounding induces loss of cell-cell contact and thereby *decreased trans* homophilic PECAM-1 ligation. Interestingly though, wounding-induced PECAM-1 ITIM phosphorylation occurs independent of homophilic binding (74), indicating a different ligand for PECAM-1 in this setting.

Secondly, endothelial cell-expressed PECAM-1, PVR and SIRPα all have been shown to facilitate leukocyte transendothelial migration (TEM) upon interaction with their leukocyte-expressed ligands (55, 75-77). Mechanistically, this was suggested

to involve targeting of PECAM-1 towards the membrane engulfing the translocating leukocyte, which required Y663 but not SHP-2 recruitment (78). However, two recent independent studies confirm that PECAM-1 and SIRPα mediate TEM in an ITIM- and SHP-2-dependent manner (55, 79). Remarkably, for PECAM-1 this seems to require its inactivation rather than activation, as contact with leukocytes *decreases* PECAM-1 ITIM phosphorylation and SHP-2 recruitment, while SHP-2 is targeted to VE-cadherin instead (79). As a functional consequence thereof, VE-cadherin is internalized, leading to loosening of endothelial junctions (55, 79). Possibly, these different proposed mechanisms represent distinct steps in how inhibitory receptors mediate TEM. For example, the ITIM may first serve as a sorting signal to target the inhibitory receptor to the membrane engulfing the leukocyte, where it becomes phosphorylated to recruit SHP-2, after which it becomes dephosphorylated to transfer SHP-2 to VE-cadherin. In support, PECAM-1 is itself a substrate of SHP-2 (68).

Inhibitory receptor function may again be affected by differential expression of splice isoforms. In addition to its full-length form with two ITIMs, PECAM-1 contains isoforms that lack one or both ITIMs. In human endothelial cells the full-length form of PECAM1 is predominantly expressed, while murine endothelial cells abundantly express the Δ14,15 isoform which lacks one ITIM (reviewed in (80)). In contrast, SIRPα does not express an ITIM-less isoform but instead an isoform which lacks a large part of the extracellular domain, which may affect its ligation (81).

In summary, inhibitory receptor signaling on endothelial cells has the potential to regulate endothelial cell migration and TEM (Figure 2). Studies on the underlying mechanism are partially conflicting and may be resolved by further investigations that include ITIM mutants, SHP-2 mutants and the monitoring of ITIM phosphorylation across several time points, in addition to controlling factors that may influence inhibitory receptor signaling such as cell density and expression of splice isoforms.

Inhibitory receptors on endothelial cells may protect endothelial integrity

Another special feature of the endothelium is its resistance to cell death, as it needs to withstand high concentrations of inflammatory mediators during inflammation while maintaining its integrity. This becomes evident in patients with allograft rejection, where host effector T cells damage the donor organ while the donor capillary endothelium remains relatively unharmed (82). Remarkably, PECAM-1 is sufficient to confer resistance against TNF and cytotoxic T lymphocytes to vascular endothelium, which requires both of its ITIMs and correlates with SHP-2 recruitment and Erk/Akt pathway activation (83). In addition, both PECAM-1 and PVR inhibit apoptosis induced by serum starvation (65, 84, 85). Together with the ability of inhibitory receptors to
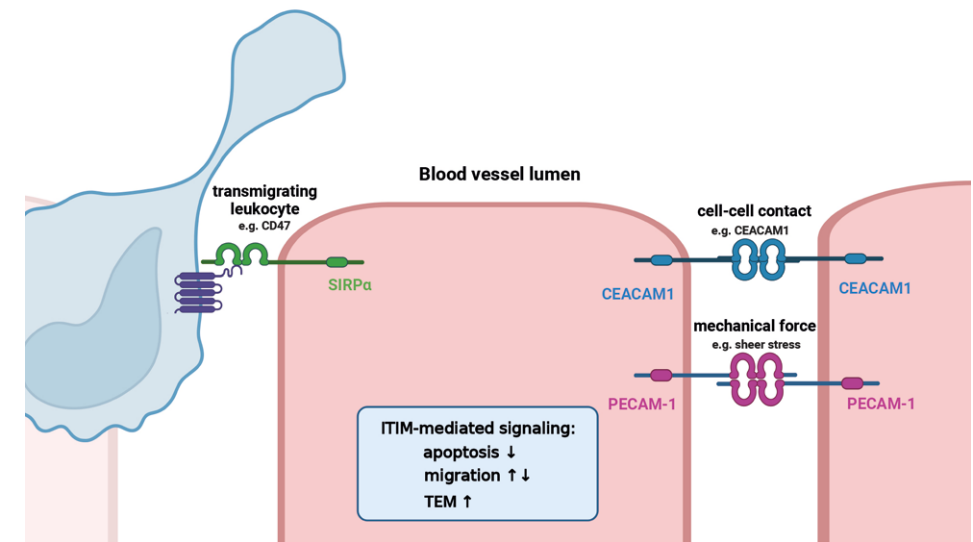

Figure 2.

Inhibitory receptors on endothelial cells can sense contact with neighbouring endothelial cells, transmigrating leukocytes or mechanical force. These interactions potentially control apoptosis, migration, and leukocyte transendothelial migration. The figure was created with biorender.com.

enhance endothelial cell migration, these findings suggest that inhibitory receptors on endothelial cells may protect endothelial integrity, not only by acting as adhesion molecules, but also by inhibiting apoptosis and by enhancing migration in an ITIM-dependent manner. This may be of particular relevance during inflammation or wounding, where endothelial integrity is challenged. In support, mice with endothelial cell-specific PECAM-1 deficiency only have a mild phenotype under homeostatic conditions, but show exaggerated inflammation and vascular permeability in inflammatory disease models, although it remains to be determined whether this phenotype is caused by lack of ITIM signaling ((86) and reviewed in (57)). Perhaps surprising in this regard is the finding that inhibitory receptors mediate TEM, as this is considered a pro-inflammatory function. How and why these functions concur needs to be a topic of future investigation.

Inhibitory receptors on non-hematopoietic cells: role in disease

In line with the regulation of cell growth and migration by inhibitory receptors, several non-hematopoietic malignancies show aberrant inhibitory receptor expression, including CEACAM1 and PVR (reviewed in (87, 88)). Whether expression is preferentially up- or down regulated may depend on the dominant function of the particular receptor in that setting. For example, CEACAM1 expression is abolished in several epithelial malignancies in line with its growth suppressive effects, whereas in other epithelial malignancies CEACAM1 expression is linked to metastatic spread, which may be related to its ability to enhance cell migration (88). Altered expression may also include aberrant isoform expression; malignant cells of non-small cell lung carcinomas patients express predominantly CEACAM-S, whereas healthy-appearing lung epithelial cells of the same patients express predominantly CEACAM1-L (89). Some non-hematopoietic malignancies even express the inhibitory receptor PD1 (90), which is usually exclusively expressed by immune cells. Importantly, these findings indicate that inhibitory receptor blockade in cancer immunotherapy may have side effects on non-hematopoietic cells expressing the targeted receptor, which may concern healthy tissue and/or the non-hematopoietic malignancy itself. Indeed, PD1 blockade has been shown to affect tumour-cell intrinsic PD1 signalling, albeit with dual outcome, with studies indicating enhanced lung carcinoma growth (91) but decreased melanoma growth (92) as a result of tumour-cell intrinsic PD1 blockage.

Not only malignancies but also pathogens can exploit inhibitory receptors on non-hematopoietic cells, such as binding of pathogenic *Neisseria* species to CEACAM1, poliovirus to PVR, and murine norovirus to CD300LF. Similarly, *Clostridium perfringens* and *Streptococcus pneumoniae* have been shown to target PECAM1 to bind to the endothelium and invade underlying tissue (93, 94).

To further understand the role of inhibitory receptors in non-hematopoietic malignancies and infection biology, future studies should differentiate between ITIM-dependent and -independent functions. For example, PVR is also implicated in malignancies due to its function as a ligand of TIGIT on NK cells and T cells, where it inhibits cytotoxic activity towards cancer cells and thereby promotes tumour growth (87). Similarly, it is not always addressed to what extent pathogens use inhibitory receptors for adhesion or also to benefit from ITIM-mediated signalling.

Inhibitory receptors on non-hematopoietic cells in expensive tissues

We focused this review on non-hematopoietic cells that are present in barrier tissues – an environment which is characterized by its high exposure to microbes and other exogenous stimuli. As we previously argued, cells in this environment benefit from a high activation threshold to prevent unnecessary immune activation (7). A high activation threshold may also be beneficial in so called expensive tissues such as the heart, brain, and eyes, which are characterized by a low regenerative capacity and therefore also a low tolerance to immunopathology (7). Notably, non-hematopoietic cells in these tissues do express PRRs. For examples, neurons express TLR2 and TLR4, which contribute to ischemia-induced neuronal cell death (95). Therefore, to prevent overzealous PRR signalling, 'expensive' cells may also be regulated by inhibitory receptors. In support, neurons widely express PD1 and SIRPα (reviewed by (96, 97)), and PD1 ligation in neurons inhibits neuronal excitability and pain via SHP-1 (98). SIRPα and PD1 expression is also found on neurons in the retina (99, 100). Likewise, SIRPα is expressed on human cardiomyocytes (101, 102) and protects against cardiac hypertrophy via inhibition of TLR4 signalling (103). In summary, inhibitory receptors may regulate non-hematopoietic cells in various tissues. This may occur especially in cells or tissues that benefit from a high activation threshold, such as expensive tissues.

Discussion and future perspective

Here, we reviewed evidence for the regulation of non-hematopoietic cells by inhibitory receptors. Based on the described findings, we propose that inhibitory receptors not only provide context to immune cells but also to non-hematopoietic cells. For example, inhibitory receptors on epithelial cells can sense cell-cell contact and thereby signal that an immune response or proliferation is not needed. In contrast, on endothelial cells, sensing of cell wounding by inhibitory receptors may stimulate cell migration to re-establish barrier integrity, indicating cell-specific functions of inhibitory receptors. Seemingly counterintuitive, some of the described inhibitory receptor functions are activating rather than inhibitory, but it should be kept in mind that negative regulation of an inhibitory process leads to a positive outcome. For example, inhibition of cell adhesion leads to enhancement of cell motility and migration. Likewise, at a signaling level, SHP-2 causes activation of ras/ERK/MAPK pathway by dephosphorylating negative regulators of this pathway (reviewed by (104)).

Taken together, there is a clear need to investigate the functions of inhibitory receptors on non-hematopoietic cells more specifically and systematically. Not only because of their potential involvement in disease, but also because some of these receptors are (potential) therapeutic targets as immune checkpoints, such as CEACAM1 and PVR (105-107), which may affect non-hematopoietic cells expressing the same receptor. Importantly, many of the described studies have been done using cancer cell lines, and thus need to be repeated *in vivo*, in primary cells *in vitro (*whenever possible), or in intermediate models such as organoids. Experiments with inhibitory receptors with mutated ITIMs and/or mutants of downstream phosphatases will help clarify the downstream signaling. Lastly, more than sixty inhibitory receptors have been functionally characterized, but over 300 putative ITIM-bearing receptors are encoded in the human genome (9). This raises the possibility that non-hematopoietic cells are regulated by several additional inhibitory receptors that help them to respond appropriately to their environment.

Acknowledgments

References

1. Okun E, Griffioen KJ, Mattson MP. Toll-like receptor signaling in neural plasticity and disease. Trends Neurosci. 2011;34(5):269-81.
2. Leemans JC, Kors L, Anders HJ, Florquin S. Pattern recognition receptors and the inflammasome in kidney disease. Nat Rev Nephrol. 2014;10(7):398-414.
3. McClure R, Massari P. TLR-Dependent Human Mucosal Epithelial Cell Responses to Microbial Pathogens. Front Immunol. 2014;5:386.
4. Szabo G, Dolganiuc A, Mandrekar P. Pattern recognition receptors: a contemporary view on liver diseases. Hepatology. 2006;44(2):287-98.
5. Larsen SB, Cowley CJ, Fuchs E. Epithelial cells: liaisons of immunity. Curr Opin Immunol. 2020;62:45-53.
6. Rumpret M, Drylewicz J, Ackermans LJE, Borghans JAM, Medzhitov R, Meyaard L. Functional categories of immune inhibitory receptors. Nat Rev Immunol. 2020;20(12):771-80.
7. Rumpret M, von Richthofen HJ, Peperzak V, Meyaard L. Inhibitory pattern recognition receptors. J Exp Med. 2022;219(1).
8. Verbrugge A, Rijkers ESK, de Ruiter T, Meyaard L. Leukocyte-associated Ig-like receptor-1 has SH2 domain-containing phosphatase-independent function and recruits C-terminal Src kinase. European Journal of Immunology. 2006;36(1):190-8.
9. Daeron M, Jaeger S, Du Pasquier L, Vivier E. Immunoreceptor tyrosine-based inhibition motifs: a quest in the past and future. Immunological Reviews. 2008;224:11-43.
10. Gray-Owen SD, Blumberg RS. CEACAM1: contact-dependent control of immunity. Nature Reviews Immunology. 2006;6(6):433-46.
11. Iwasaki A, Welker R, Mueller S, Linehan M, Nomoto A, Wimmer E. Immunofluorescence analysis of poliovirus receptor expression in Peyer's patches of humans, primates, and CD155 transgenic mice: implications for poliovirus infection. J Infect Dis. 2002;186(5):585-92.
12. Wilen CB, Lee S, Hsieh LL, Orchard RC, Desai C, Hykes BL, Jr., et al. Tropism for tuft cells determines immune promotion of norovirus pathogenesis. Science. 2018;360(6385):204-8.
13. Kim WM, Huang YH, Gandhi A, Blumberg RS. CEACAM1 structure and function in immunity and its therapeutic implications. Seminars in Immunology. 2019;42.
14. Borrego F. The CD300 molecules: an emerging family of regulators of the immune system. Blood. 2013;121(11):1951-60.
15. Kucan Brlic P, Lenac Rovis T, Cinamon G, Tsukerman P, Mandelboim O, Jonjic S. Targeting PVR (CD155) and its receptors in anti-tumor therapy. Cell Mol Immunol. 2019;16(1):40-52.
16. Karlsson M, Zhang C, Mear L, Zhong W, Digre A, Katona B, et al. A single-cell type transcriptomics map of human tissues. Sci Adv. 2021;7(31).
17. Lange R, Peng X, Wimmer E, Lipp M, Bernhardt G. The poliovirus receptor CD155 mediates cell-to-matrix contacts by specifically binding to vitronectin. Virology. 2001;285(2):218-27.
18. Graziano VR, Walker FC, Kennedy EA, Wei J, Ettayebi K, Strine MS, et al. CD300lf is the primary physiologic receptor of murine norovirus but not human norovirus. Plos Pathogens. 2020;16(4).
19. Sato T, Irie K, Ooshio T, Ikeda W, Takai Y. Involvement of heterophilic trans-interaction of Necl-5/Tage4/PVR/CD155 with nectin-3 in formation of nectin- and cadherin-based adherens junctions. Genes Cells. 2004;9(9):791-9.
20. Benchimol S, Fuks A, Jothy S, Beauchemin N, Shirota K, Stanners CP. Carcinoembryonic antigen, a human tumor marker, functions as an intercellular adhesion molecule. Cell. 1989;57(2):327-34.

21. Luo W, Wood CG, Earley K, Hung MC, Lin SH. Suppression of tumorigenicity of breast cancer cells by an epithelial cell adhesion molecule (C-CAM1): the adhesion and growth suppression are mediated by different domains. Oncogene. 1997;14(14):1697-704.

22. Muller MM, Klaile E, Vorontsova O, Singer BB, Obrink B. Homophilic adhesion and CEACAM1-S regulate dimerization of CEACAM1-L and recruitment of SHP-2 and c-Src. J Cell Biol. 2009;187(4):569-81.

23. Izzi L, Turbide C, Houde C, Kunath T, Beauchemin N. cis-Determinants in the cytoplasmic domain of CEACAM1 responsible for its tumor inhibitory function. Oncogene. 1999;18(40):5563-72.

24. Kunath T, Ordonez-Garcia C, Turbide C, Beauchemin N. Inhibition of colonic tumor cell growth by biliary glycoprotein. Oncogene. 1995;11(11):2375-82.

25. Singer BB, Scheffrahn I, Kammerer R, Suttorp N, Ergun S, Slevogt H. Deregulation of the CEACAM expression pattern causes undifferentiated cell growth in human lung adenocarcinoma cells. PLoS One. 2010;5(1):e8747.

26. Arabzadeh A, Dupaul-Chicoine J, Breton V, Haftchenary S, Yumeen S, Turbide C, et al. Carcinoembryonic Antigen Cell Adhesion Molecule 1 long isoform modulates malignancy of poorly differentiated colon cancer cells. Gut. 2016;65(5):821-9.

27. Ieda J, Yokoyama S, Tamura K, Takifuji K, Hotta T, Matsuda K, et al. Re-expression of CEACAM1 long cytoplasmic domain isoform is associated with invasion and migration of colorectal cancer. International Journal of Cancer. 2011;129(6):1351-61.

28. Jin Y, Lin Y, Lin LJ, Sun Y, Zheng CQ. Carcinoembryonic antigen related cellular adhesion molecule 1 alleviates dextran sulfate sodium-induced ulcerative colitis in mice. Life Sciences. 2016;149:120-8.

29. Singer BB, Opp L, Heinrich A, Schreiber F, Binding-Liermann R, Berrocal-Almanza LC, et al. Soluble CEACAM8 interacts with CEACAM1 inhibiting TLR2-triggered immune responses. PLoS One. 2014;9(4):e94106.

30. Slevogt H, Zabel S, Opitz B, Hocke A, Eitel J, N'Guessan P D, et al. CEACAM1 inhibits Toll-like receptor 2-triggered antibacterial responses of human pulmonary epithelial cells. Nat Immunol. 2008;9(11):1270-8.

31. Javaheri A, Kruse T, Moonens K, Mejias-Luque R, Debraekeleer A, Asche CI, et al. Helicobacter pylori adhesin HopQ engages in a virulence-enhancing interaction with human CEACAMs. Nature Microbiology. 2017;2(1).

32. Oda T, Ohka S, Nomoto A. Ligand stimulation of CD155alpha inhibits cell adhesion and enhances cell migration in fibroblasts. Biochem Biophys Res Commun. 2004;319(4):1253-64.

33. Takai Y, Miyoshi J, Ikeda W, Ogita H. Nectins and nectin-like molecules: roles in contact inhibition of cell movement and proliferation. Nat Rev Mol Cell Biol. 2008;9(8):603-15.

34. Fujito T, Ikeda W, Kakunaga S, Minami Y, Kajita M, Sakamoto Y, et al. Inhibition of cell movement and proliferation by cell-cell contact-induced interaction of Necl-5 with nectin-3. J Cell Biol. 2005;171(1):165-73.

35. Tian L, Choi SC, Murakami Y, Allen J, Morse HC, 3rd, Qi CF, et al. p85alpha recruitment by the CD300f phosphatidylserine receptor mediates apoptotic cell clearance required for autoimmunity suppression. Nat Commun. 2014;5:3146.

36. Bowers JR, Readler JM, Sharma P, Excoffon KJDA. Poliovirus Receptor: More than a simple viral receptor. Virus Research. 2017;242:1-6.

37. Helfrich I, Singer BB. Size Matters: The Functional Role of the CEACAM1 Isoform Signature and Its Impact for NK Cell-Mediated Killing in Melanoma. Cancers (Basel). 2019;11(3).

38. Singer BB, Scheffrahn I, Obrink B. The tumor growth-inhibiting cell adhesion molecule CEACAM1 (C-CAM) is differently expressed in proliferating and quiescent epithelial cells and regulates cell proliferation. Cancer Res. 2000;60(5):1236-44.

39. Sundberg U, Obrink B. CEACAM1 isoforms with different cytoplasmic domains show different localization, organization and adhesive properties in polarized epithelial cells. Journal of Cell Science. 2002;115(6):1273-84.

40. Sundberg U, Beauchemin N, Obrink B. The cytoplasmic domain of CEACAM1-L controls its lateral localization and the organization of desmosomes in polarized epithelial cells. J Cell Sci. 2004;117(Pt 7):1091-104.

41. Ohka S, Ohno H, Tohyama K, Nomoto A. Basolateral sorting of human poliovirus receptor alpha involves an interaction with the mu1B subunit of the clathrin adaptor complex in polarized epithelial cells. Biochem Biophys Res Commun. 2001;287(4):941-8.

42. Clemens L, Kutuzov M, Bayer KV, Goyette J, Allard J, Dushek O. Determination of the molecular reach of the protein tyrosine phosphatase SHP-1. Biophys J. 2021;120(10):2054-66.

43. Stanifer ML, Mukenhirn M, Muenchau S, Pervolaraki K, Kanaya T, Albrecht D, et al. Asymmetric distribution of TLR3 leads to a polarized immune response in human intestinal epithelial cells. Nat Microbiol. 2020;5(1):181-91.

44. Gewirtz AT, Navas TA, Lyons S, Godowski PJ, Madara JL. Cutting edge: bacterial flagellin activates basolaterally expressed TLR5 to induce epithelial proinflammatory gene expression. J Immunol. 2001;167(4):1882-5.

45. Houde C, Roy S, Leung N, Nicholson DW, Beauchemin N. The cell adhesion molecule CEACAM1-L is a substrate of caspase-3-mediated cleavage in apoptotic mouse intestinal cells. J Biol Chem. 2003;278(19):16929-35.

46. Nittka S, Bohm C, Zentgraf H, Neumaier M. The CEACAM1-mediated apoptosis pathway is activated by CEA and triggers dual cleavage of CEACAM1. Oncogene. 2008;27(26):3721-8.

47. Muenzner P, Bachmann V, Zimmermann W, Hentschel J, Hauck CR. Human-restricted bacterial pathogens block shedding of epithelial cells by stimulating integrin activation. Science. 2010;329(5996):1197-201.

48. Muenzner P, Rohde M, Kneitz S, Hauck CR. CEACAM engagement by human pathogens enhances cell adhesion and counteracts bacteria-induced detachment of epithelial cells. J Cell Biol. 2005;170(5):825-36.

49. Toleman M, Aho E, Virji M. Expression of pathogen-like Opa adhesins in commensal Neisseria: genetic and functional analysis. Cell Microbiol. 2001;3(1):33-44.

50. Konradt C, Hunter CA. Pathogen interactions with endothelial cells and the induction of innate and adaptive immunity. Eur J Immunol. 2018;48(10):1607-20.

51. Privratsky JR, Newman PJ. PECAM-1: regulator of endothelial junctional integrity. Cell Tissue Res. 2014;355(3):607-19.

52. Ergun S, Kilik N, Ziegeler G, Hansen A, Nollau P, Gotze J, et al. CEA-related cell adhesion molecule 1: a potent angiogenic factor and a major effector of vascular endothelial growth factor. Mol Cell. 2000;5(2):311-20.

53. Maier MK, Seth S, Czeloth N, Qiu Q, Ravens I, Kremmer E, et al. The adhesion receptor CD155 determines the magnitude of humoral immune responses against orally ingested antigens. Eur J Immunol. 2007;37(8):2214-25.

54. Johansen ML, Brown EJ. Dual regulation of SIRPalpha phosphorylation by integrins and CD47. J Biol Chem. 2007;282(33):24219-30.

55. Ren B, Xia H, Liao Y, Zhou H, Wang Z, Shi Y, et al. Endothelial SIRPalpha signaling controls VE-cadherin endocytosis for thymic homing of progenitor cells. Elife. 2022;11.

56. Logtenberg MEW, Scheeren FA, Schumacher TN. The CD47-SIRPalpha Immune Checkpoint. Immunity. 2020;52(5):742-52.

57. Privratsky JR, Newman DK, Newman PJ. PECAM-1: conflicts of interest in inflammation. Life Sci. 2010;87(3-4):69-82.

58. Devilard E, Xerri L, Dubreuil P, Lopez M, Reymond N. Nectin-3 (CD113) interacts with Nectin-2 (CD112) to promote lymphocyte transendothelial migration. PLoS One. 2013;8(10):e77424.

59. Azcutia V, Stefanidakis M, Tsuboi N, Mayadas T, Croce KJ, Fukuda D, et al. Endothelial CD47 Promotes Vascular Endothelial-Cadherin Tyrosine Phosphorylation and Participates in T Cell Recruitment at Sites of Inflammation In Vivo. Journal of Immunology. 2012;189(5):2553-62.

60. Osawa M, Masuda M, Kusano K, Fujiwara K. Evidence for a role of platelet endothelial cell adhesion molecule-1 in endothelial cell mechanosignal transduction: is it a mechanoresponsive molecule? J Cell Biol. 2002;158(4):773-85.

61. Tryfonos A, Rasoul D, Sadler D, Shelley J, Mills J, Green DJ, et al. Elevated shear rate-induced by exercise increases eNOS ser(1177) but not PECAM-1 Tyr(713) phosphorylation in human conduit artery endothelial cells. Eur J Sport Sci. 2022.

62. Rueckschloss U, Kuerten S, Ergun S. The role of CEA-related cell adhesion molecule-1 (CEACAM1) in vascular homeostasis. Histochem Cell Biol. 2016;146(6):657-71.

63. Lertkiatmongkol P, Liao DY, Mei H, Hu Y, Newman PJ. Endothelial functions of platelet/endothelial cell adhesion molecule-1 (CD31). Current Opinion in Hematology. 2016;23(3):253-9.

64. Privratsky JR, Paddock CM, Florey O, Newman DK, Muller WA, Newman PJ. Relative contribution of PECAM-1 adhesion and signaling to the maintenance of vascular integrity. J Cell Sci. 2011;124(Pt 9):1477-85.

65. Bird IN, Taylor V, Newton JP, Spragg JH, Simmons DL, Salmon M, et al. Homophilic PECAM-1(CD31) interactions prevent endothelial cell apoptosis but do not support cell spreading or migration. Journal of Cell Science. 1999;112(12):1989-97.

66. Gratzinger D, Barreuther M, Madri JA. Platelet-endothelial cell adhesion molecule-1 modulates endothelial migration through its immunoreceptor tyrosine-based inhibitory motif. Biochemical and Biophysical Research Communications. 2003;301(1):243-9.

67. Kim CS, Wang T, Madri JA. Platelet endothelial cell adhesion molecule-1 expression modulates endothelial cell migration in vitro. Lab Invest. 1998;78(5):583-90.

68. Zhu JX, Cao GY, Williams JT, DeLisser HM. SHP-2 phosphatase activity is required for PECAM-1-dependent cell motility. Am J Physiol-Cell Ph. 2010;299(4):C854-C65.

69. O'Brien CD, Cao G, Makrigiannakis A, DeLisser HM. Role of immunoreceptor tyrosine-based inhibitory motifs of PECAM-1 in PECAM-1-dependent cell migration. Am J Physiol Cell Physiol. 2004;287(4):C1103-13.

70. Horst AK, Ito WD, Dabelstein J, Schumacher U, Sander H, Turbide C, et al. Carcinoembryonic antigen-related cell adhesion molecule 1 modulates vascular remodeling in vitro and in vivo. J Clin Invest. 2006;116(6):1596-605.

71. Motegi S, Okazawa H, Ohnishi H, Sato R, Kaneko Y, Kobayashi H, et al. Role of the CD47-SHPS-1 system in regulation of cell migration. EMBO J. 2003;22(11):2634-44.

72. Inagaki K, Yamao T, Noguchi T, Matozaki T, Fukunaga K, Takada T, et al. SHPS-1 regulates integrin-mediated cytoskeletal reorganization and cell motility. EMBO J. 2000;19(24):6721-31.

73. Schoenwaelder SM, Petch LA, Williamson D, Shen R, Feng GS, Burridge K. The protein tyrosine phosphatase Shp-2 regulates RhoA activity. Curr Biol. 2000;10(23):1523-6.

74. Abraham V, Parambath A, Joe DS, DeLisser HM. Influence of PECAM-1 ligand interactions on PECAM-1-dependent cell motility and filopodia extension. Physiol Rep. 2016;4(22).

75. Sullivan DP, Seidman MA, Muller WA. Poliovirus receptor (CD155) regulates a step in transendothelial migration between PECAM and CD99. Am J Pathol. 2013;182(3):1031-42.

76. Reymond N, Imbert AM, Devilard E, Fabre S, Chabannon C, Xerri L, et al. DNAM-1 and PVR regulate monocyte migration through endothelial junctions. Journal of Experimental Medicine. 2004;199(10):1331-41.

77. Muller WA, Weigl SA, Deng XH, Phillips DM. Pecam-1 Is Required for Transendothelial Migration of Leukocytes. Journal of Experimental Medicine. 1993;178(2):449-60.

78. Dasgupta B, Dufour E, Mamdouh Z, Muller WA. A novel and critical role for tyrosine 663 in platelet endothelial cell adhesion molecule-1 trafficking and transendothelial migration. J Immunol. 2009;182(8):5041-51.

79. Arif N, Zinnhardt M, Nyamay'Antu A, Teber D, Bruckner R, Schaefer K, et al. PECAM-1 supports leukocyte diapedesis by tension-dependent dephosphorylation of VE-cadherin. EMBO J. 2021;40(9):e106113.

80. Newman PJ, Newman DK. Signal transduction pathways mediated by PECAM-1: new roles for an old molecule in platelet and vascular cell biology. Arterioscler Thromb Vasc Biol. 2003;23(6):953-64.

81. Shirakabe K, Omura T, Shibagaki Y, Mihara E, Homma K, Kato Y, et al. Mechanistic insights into ectodomain shedding: susceptibility of CADM1 adhesion molecule is determined by alternative splicing and O-glycosylation. Sci Rep-Uk. 2017;7.

82. Thaunat O. Soothing touch of CD31 protects endothelium during cellular immune responses. Proceedings of the National Academy of Sciences of the United States of America. 2015;112(43):13133-4.

83. Cheung K, Ma L, Wang G, Coe D, Ferro R, Falasca M, et al. CD31 signals confer immune privilege to the vascular endothelium. Proceedings of the National Academy of Sciences of the United States of America. 2015;112(43):E5815-24.

84. Evans PC, Taylor ER, Kilshaw PJ. Signaling through CD31 protects endothelial cells from apoptosis. Transplantation. 2001;71(3):457-60.

85. Kinugasa M, Amano H, Satomi-Kobayashi S, Nakayama K, Miyata M, Kubo Y, et al. Necl-5/poliovirus receptor interacts with VEGFR2 and regulates VEGF-induced angiogenesis. Circ Res. 2012;110(5):716-26.

86. Maas M, Stapleton M, Bergom C, Mattson DL, Newman DK, Newman PJ. Endothelial cell PECAM-1 confers protection against endotoxic shock. Am J Physiol Heart Circ Physiol. 2005;288(1):H159-64.

87. Molfetta R, Zitti B, Lecce M, Milito ND, Stabile H, Fionda C, et al. CD155: A Multi-Functional Molecule in Tumor Progression. Int J Mol Sci. 2020;21(3).

88. Calinescu A, Turcu G, Nedelcu RI, Brinzea A, Hodorogea A, Antohe M, et al. On the Dual Role of Carcinoembryonic Antigen-Related Cell Adhesion Molecule 1 (CEACAM1) in Human Malignancies. J Immunol Res. 2018;2018:7169081.

89. Wang L, Lin SH, Wu WG, Kemp BL, Walsh GL, Hong WK, et al. C-CAM1, a candidate tumor suppressor gene, is abnormally expressed in primary lung cancers. Clinical Cancer Research. 2000;6(8):2988-93.

90. Yao H, Wang H, Li C, Fang JY, Xu J. Cancer Cell-Intrinsic PD-1 and Implications in Combinatorial Immunotherapy. Front Immunol. 2018;9:1774.

91. Du S, McCall N, Park K, Guan Q, Fontina P, Ertel A, et al. Blockade of Tumor-Expressed PD-1 promotes lung cancer growth. Oncoimmunology. 2018;7(4):e1408747.

92. Kleffel S, Posch C, Barthel SR, Mueller H, Schlapbach C, Guenova E, et al. Melanoma Cell-Intrinsic PD-1 Receptor Functions Promote Tumor Growth. Cell. 2015;162(6):1242-56.

93. Bruggisser J, Tarek B, Wyder M, Muller P, von Ballmoos C, Witz G, et al. CD31 (PECAM-1) Serves as the Endothelial Cell-Specific Receptor of Clostridium perfringens beta-Toxin. Cell Host & Microbe. 2020;28(1):69-+.

94. Iovino F, Engelen-Lee JY, Brouwer M, van de Beek D, van der Ende A, Valls Seron M, et al. pIgR and PECAM-1 bind to pneumococcal adhesins RrgA and PspC mediating bacterial brain invasion1. J Exp Med. 2017;214(6):1619-30.

95. Tang SC, Arumugam TV, Xu X, Cheng A, Mughal MR, Jo DG, et al. Pivotal role for neuronal Toll-like receptors in ischemic brain injury and functional deficits. Proceedings of the National Academy of Sciences of the United States of America. 2007;104(34):13798-803.

96. Zhao J, Roberts A, Wang Z, Savage J, Ji RR. Emerging Role of PD-1 in the Central Nervous System and Brain Diseases. Neurosci Bull. 2021;37(8):1188-202.

97. Matozaki T, Murata Y, Okazawa H, Ohnishi H. Functions and molecular mechanisms of the CD47-SIRPalpha signalling pathway. Trends Cell Biol. 2009;19(2):72-80.

98. Chen G, Kim YH, Li H, Luo H, Liu DL, Zhang ZJ, et al. PD-L1 inhibits acute and chronic pain by suppressing nociceptive neuron activity via PD-1. Nat Neurosci. 2017;20(7):917-26.

99. Mi ZP, Jiang P, Weng WL, Lindberg FP, Narayanan V, Lagenaur CF. Expression of a synapse-associated membrane protein, P84/SHPS-1, and its ligand, IAP/CD47, in mouse retina. J Comp Neurol. 2000;416(3):335-44.

100. Chen L, Sham CW, Chan AM, Francisco LM, Wu Y, Mareninov S, et al. Role of the immune modulator programmed cell death-1 during development and apoptosis of mouse retinal ganglion cells. Investigative ophthalmology & visual science. 2009;50(10):4941-8.

101. Dubois NC, Craft AM, Sharma P, Elliott DA, Stanley EG, Elefanty AG, et al. SIRPA is a specific cell-surface marker for isolating cardiomyocytes derived from human pluripotent stem cells. Nature Biotechnology. 2011;29(11):1011-U82.

102. Skelton RJ, Costa M, Anderson DJ, Bruveris F, Finnin BW, Koutsis K, et al. SIRPA, VCAM1 and CD34 identify discrete lineages during early human cardiovascular development. Stem Cell Res. 2014;13(1):172-9.

103. Jiang DS, Zhang XF, Gao L, Zong J, Zhou H, Liu Y, et al. Signal regulatory protein-alpha protects against cardiac hypertrophy via the disruption of toll-like receptor 4 signaling. Hypertension. 2014;63(1):96-104.

104. Dempke WCM, Uciechowski P, Fenchel K, Chevassut T. Targeting SHP-1, 2 and SHIP Pathways: A Novel Strategy for Cancer Treatment? Oncology-Basel. 2018;95(5):257-69.

105. Gorvel L, Olive D. Targeting the "PVR-TIGIT axis" with immune checkpoint therapies. F1000Res. 2020;9.

106. Lee JC, Yang WS, Park HY, Nam HM, Cho HJ, Oh MY, et al. Preclinical Characterization and Development of Mg1124, a Novel Immune Checkpoint Inhibitor Targeting Ceacam1 for Nsclc Patients. Journal for Immunotherapy of Cancer. 2020;8:A119-A.

107. Chiang EY, Mellman I. TIGIT-CD226-PVR axis: advancing immune checkpoint blockade for cancer immunotherapy. Journal for Immunotherapy of Cancer. 2022;10(4).

CHAPTER **9**

General discussion

Inhibitory immune receptors regulate the immune system by inhibiting the signaling of activating immune receptors. Our group previously proposed that inhibitory receptors can be divided in three functional groups based on expression: 1) negative feedback receptors, which are upregulated after activation and provide negative feedback to terminate immune responses, 2) threshold receptors, which are constitutively expressed and put a threshold to prevent immune activation in response to harmless stimuli, and 3) disinhibition receptors, which are constitutively expressed but downregulated after activation to facilitate a strong immunological response once the activation threshold has been exceeded (1).

Regulation of inhibitory receptors by proteolytic cleavage

In order to respond promptly to infection, the downregulation of disinhibition receptors probably has to occur rapidly. As opposed to the relatively slow outcome of altered transcription, proteolytic cleavage of receptors can meet this requirement (Figure 1A). Indeed, ectodomain shedding of inhibitory receptors is typically observed within 30-120 minutes after cell activation (2-4). Ectodomain shedding has been described for several inhibitory receptors, including SIRPα (2, 3, 5), PECAM-1 (6, 7), and LAIR-1 (4, 8). We now show that downregulation of SIRL-1 also occurs via proteolytic cleavage (**Chapter 5**).

In addition to the regulation of surface expression, some evidence exists that proteolytic cleavage can also regulate signal transduction of inhibitory receptors (Figure 1A). For example, in inflammatory disease patients, neutrophils (but not monocytes) express SIRPα of which the ITIM-containing cytoplasmic domain is cleaved, which abolishes the inhibitory signaling capacity of SIRPα (9). Further investigation revealed this occurs in a serine-protease dependent manner (9). Similarly, apoptosis induces cleavage of the ITIM-containing intracellular domain of CEACAM-1 (10). Together, this suggests that proteolytic cleavage is a common mechanism to downregulate inhibitory receptor signaling upon cell activation.

The remaining fragments of inhibitory receptor cleavage may acquire novel functions

Upon ectodomain shedding, the released soluble ectodomain may still bind ligand and become a decoy receptor (Figure 1B) (11). However, proteolytic cleavage might alter the ectodomain to such an extent that ligand binding does not occur anymore. For example, shed SIRPα does not compete with the interaction between SIRPα-Fc and its ligand CD47 (2). Similarly, recombinant soluble LAIR-1 ectodomain does not efficiently compete with the interaction between membrane-expressed LAIR-1 and its ligand collagen (8). Another potential explanation for such findings is that

shed ectodomains are likely monomeric and may thus not be able to outcompete an interaction between a multimeric ligand and a surface receptor in high density. Whether shed SIRL-1 functions as decoy receptor remains to be elucidated.
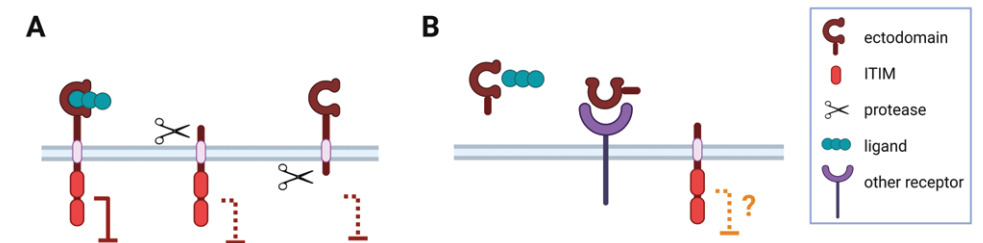

Figure 1. Regulation of inhibitory receptors by proteolytic cleavage.
(A) Proteolytic cleavage can abrogate inhibitory receptor signaling by targeting the ectodomain or the intracellular domain of the receptor. **(B)** The remaining fragments may acquire novel functions, such as competition for ligand binding, becoming a ligand for another receptor, or mediating signaling via the remaining stalk (as depicted from left to right).

Notably, it is mostly assumed that ectodomain shedding completely abrogates the signaling capacity of the receptor, but the remaining membrane-anchored fragment may also retain or acquire novel possibilities for signaling (Fig 1B). For example, PECAM-1 ectodomain shedding was shown to generate a membrane-anchored fragment which inhibited endothelial cell proliferation, whereas full-length PECAM-1 does not have this effect (12). ITIM phosphorylation of full-length and truncated PECAM-1 was similar, but truncated PECAM-1 recruited more SHP-2 than full-length PECAM-1, suggesting that proteolytic cleavage induced a conformational change which favored SHP-2 binding (12).

The released ectodomain can in theory also acquire a completely novel function, for example by becoming a ligand for another receptor (11). This was suggested for VSTM1-v2, a soluble form of SIRL-1. Of note, VSTM1-v2 is a product of alternative splicing rather than ectodomain shedding (13). VSTM1-v2 was shown to induce differentiation of Th17 cells, suggestively by binding directly to T cells (13). However, we did not find any effect of VSTM1-v2 on Th17 cell differentiation, nor did we detect binding of VSTM1-v2 to T cells (**Chapter 6**). To our knowledge, no other examples have been described of shed inhibitory receptors that become ligands for another receptor.

In conclusion, next to being a rapid way of downregulation of inhibitory receptor expression and function, proteolytic cleavage may result in the generation of soluble

or membrane-anchored fragments which are biologically active and may counteract the action of the full-length receptor.

Receptor downregulation: shedding or internalization?

Receptor downregulation can also occur via internalization, as has been demonstrated for several inhibitory receptors from the C-type lectin (CLR) and Siglec families, including CLEC4A (14), CLEC12A (15), and CD33 (Siglec3) (16, 17). Interestingly, internalization of Siglecs occurs in an ITIM-dependent manner, suggestive that this may be a feature shared by other ITIM-bearing receptors (16-18). On a critical note, receptor internalization can also be a method for antigen uptake rather than for receptor downregulation. For instance, the inhibitory receptor CD22 (Siglec2) is efficiently recycled to the cell surface upon internalization, while only its cargo is released intracellularly (19). Still, when it comes to receptor downregulation, why would a cell 'choose' shedding versus internalization? The speed of internalization is similar or somewhat faster compared to ectodomain shedding (e.g. within 15-60 minutes) (17). However, shedding mostly occurs upon activation-induced protease release, while internalization usually occurs upon receptor ligation (14, 16, 17). Thus, internalization might primarily take place to downregulate an inhibitory receptor that also already initiated signaling, while proteolytic cleavage can occur independent of that.

Disinhibition receptors may alter population dynamics

Taken together, multiple mechanisms can lead to rapid downregulation of disinhibition receptors. We already argued that disinhibition receptors enable optimal cell responses (1): they are constitutively expressed on resting cells which provides an activation threshold to prevent a cell from responding to weak, sub-threshold stimulation. In contrast, they are downregulated when stimulation exceeds the activation threshold, which allows an efficient response (1). One may speculate that disinhibition receptors not only mediate optimal responses on a single cell level, but also on a population level. Arguably, in a system with only activating receptors, cells that encounter a disturbance will all become activated to a varying extent in response to a gradient of activating stimuli (Figure 2A). However, when an anti-microbial response may lead to death of the effector cell as is often the case for neutrophils (20), it might be better to fully utilize the effector mechanisms of some cells, while not using the effector mechanisms of other cells to save resources. This is what disinhibition receptors could facilitate: the part of the population with sub-threshold stimulation is spared (e.g. newly infiltrating cells), while the part of the population which exceeds the stimulation threshold (e.g. the cells which are closest to the disturbance) fully utilize their antimicrobial functions (Figure 2B). When an infection
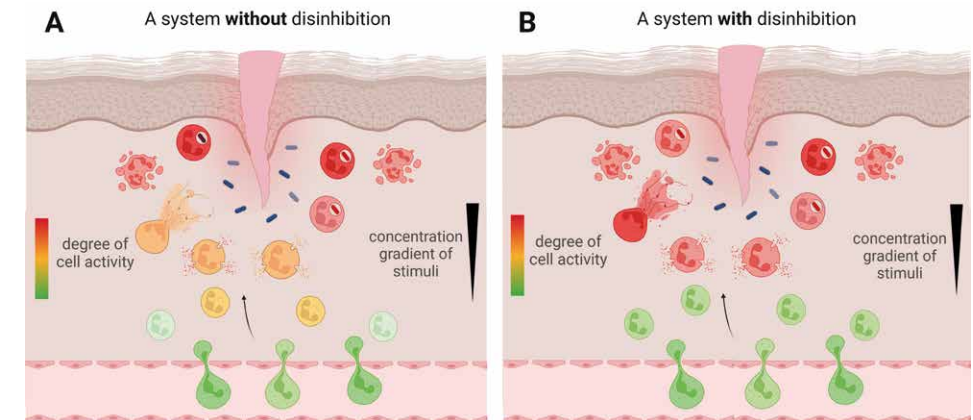

Figure 2. Disinhibition receptors may alter population dynamics.
(A) In a system without disinhibition receptors, cells become activated to varying degrees in response to a concentration gradient of activating stimuli. **(B)** In a system with disinhibition receptors, some cells exceed the activation threshold and become fully activated for an efficient response, while some cells do not exceed the activation threshold and are (at least provisionally) spared. This model requires experimental validation.

is ongoing, the cells which have been spared may still exceed the activation threshold at a later time point or when moving closer to the infection. However, when the infection is almost cleared, cells may remain below the activation threshold and allow termination of the inflammatory response. As such, disinhibition receptors may mediate optimal responses on a population level. This requires further experimental validation.

Inhibitory receptors require clustering for signal transduction

Immune receptors generally require ligand-induced oligomerization or clustering in order to be activated (21, 22). The same has been demonstrated for inhibitory receptors (23, 24). One of the reasons for this is thought to be that clustering brings receptors in close proximity, increasing the likelihood of interaction between them and their signaling partners (25). Receptor clustering can be achieved by recognition of multivalent ligands, for example a ligand that self-assembles into an oligomer or polymer, or a ligand which binds in multiple copies to a scaffold (26, 27). Such a scaffold can be a cell membrane, extracellular matrix, or a large extracellular molecule. *In vitro*, scaffolds are typically mimicked by immobilizing a ligand or agonistic antibody on a plastic cell culture plate. This is also how we identified S100 proteins, LL-37 and α-type phenol-soluble modulins (PSMs) from staphylococci as SIRL-1 ligands (**Chapter 3, 4**).

S100 proteins are functionally diverse but share a conserved structure which consists of two calcium-binding EF-hand domains (28). LL-37 and PSMs have an amphipathic α-helical structure and share several other features, such as cytolytic activity, the propensity to form fibrils, and the ability to ligate the immune activating receptor FPR2 (29-31). LL-37 and PSMs are small peptides (between 20-40 amino acids), indicating that they are unlikely to contain multiple SIRL-1 binding sites within themselves. So, assuming that SIRL-1 requires clustering for efficient ligation, how do these ligands cluster SIRL-1 *in vivo*?

How is SIRL-1 clustered *in vivo*?

Before discussing potential modes of SIRL-1 clustering, it is important to point out that we were not able to detect direct binding between SIRL-1 and its ligands, neither using cell-based assays nor using assays with purified recombinant proteins (**Chapter 3, 4**). On one hand, this might be caused by technical difficulties related to cytolytic activity and fibril formation of PSMs and LL-37. For example, during isothermal titration calorimetry experiments, it could not be distinguished whether a temperature change occurred as a result of binding between SIRL-1 and PSM**α**3, or as a result of PSMα3 fibrillation (data not shown). Alternatively, the lack of direct binding between SIRL-1 and its ligands could indicate that an additional binding partner is required, for example a serum-based or membrane-expressed protein which is lacking in purified assays (Figure 3). Such a binding partner may also provide a scaffold to facilitate receptor clustering, although a potential binding partner and scaffold may also be separate molecules.

Clustering of SIRL-1 may occur in various ways, first of all by ligand multimerization (Figure 3). PSMs from *S. aureus* can self-assemble into amyloid or amyloid-like fibrils (32, 33). These fibrils show remarkable diversity, with PSMα1 and PSMα4 forming canonical cross-β fibrils, whereas PSMα3 forms recently discovered cross-α fibrils, of which the main difference is the stacking of β-strands versus α-helices perpendicular to the fibril axis (34). In contrast, PSMs from *S. epidermidis* do not form fibrils (35). LL-37 is found as monomer, dimer and tetramer, while it can also form fiber-like structures in the presence of lipids (31). S100 protein family members usually exist as homo- or heterodimers, but they can form higher-order oligomers under the influence of calcium (reviewed in (28)). Some S100 proteins have also been shown to form amyloid fibrils (36, 37), although it remains to be determined whether these are functional.

Secondly, several interactions between SIRL-1 ligands and potential scaffolds have been described, such as interactions between PSMs or LL-37 with extracellular DNA (38, 39) or NETs (40). PSMs also form an important component of *Staphylococcal*
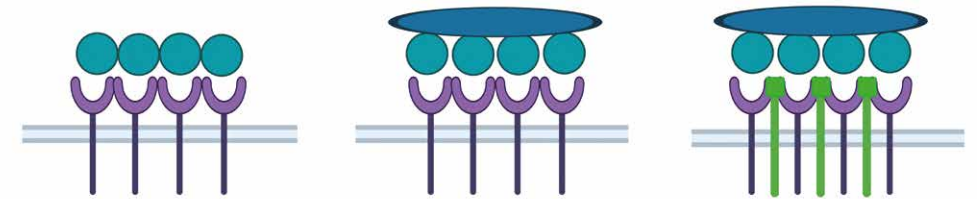

Figure 3. Potential mechanisms for SIRL-1 clustering.
Clustering might be induced by ligand self-assembly into an oligomer, by binding of several ligand copies to a scaffold, and/or might require an additional binding partner (as depicted from left to right)

biofilms (33, 35, 41). In addition, PSMs and LL-37 can interact with and integrate into plasma membranes (42-45), which gives them their cytolytic properties, but it is questionable whether such integration leaves enough of the molecule exposed to still bind SIRL-1. The same holds true for binding of PSMs to serum-based lipoproteins (46), since high density lipoprotein in plasma was shown to abolish PSMα3-induced FPR2 activation (47).

We tested some of these potential forms of ligand-induced clustering of SIRL-1. PSMα3 spontaneously assembles into fibrils when dissolved in water (32), but soluble PSMα3 did not activate SIRL-1 reporter cells (data not shown). Similarly, soluble LL-37 and S100A8/9 did not induce activation of SIRL-1 reporter cells. Lastly, SIRL-1 reporter cells were not activated by soluble PSMα3 combined with low density lipoprotein, DNA, or human serum (data not shown). However, we did not confirm whether fibrillation, oligomerization or complex formation indeed occurred in these experimental settings. Notably, SIRL-1 reporter cells might not be an appropriate system to study ligand-induced clustering, as these cells express a SIRL-1 chimera rather than native SIRL-1 (Chapter 3) and might therefore have altered clustering requirements.

In conclusion, the mechanism of SIRL-1 clustering requires further investigation. Even though different PSMs, S100 proteins and LL-37 induce a similar degree of SIRL-1 reporter cell activation *in vitro* (Chapter 3, 4), the extent at which they can ligate SIRL-1 *in vivo* may differ, depending on what type of quaternary structure these ligands form. Potential binding to a scaffold may also determine the context in which receptor ligation occurs (e.g. a scaffold such as extracellular DNA will only be available upon tissue damage). Together, these open questions underscore the limitation of using plate-immobilization for ligand identification, despite its common usage and convenience.

Microbial ligands of inhibitory receptors: immune evasion or tolerance?

Several inhibitory receptors have been shown to interact with microbial ligands (**Chapter 7, 8**, and reviewed in (48)). In this thesis we extend this by showing that *S. aureus* can interact with SIRL-1 in two ways: as mentioned above, it can ligate SIRL-1 by secreting α-type PSMs (Chapter 4). At the same time, *S. aureus* can prevent shedding
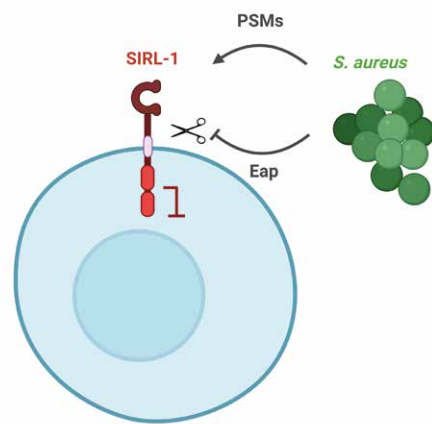

Figure 4.

The interaction between *S. aureus* and SIRL-1 occurs via two ways: *S. aureus* activates SIRL-1 via the secretion of PSMs, while at the same time maintaining SIRL-1 expression by preventing shedding via Eap.

of SIRL-1 via its protease inhibitor Eap (**Chapter 5**; Figure 4). SIRL-1 also recognizes PSMs from all other Staphylococcus species that we tested (**Chapter 4**), although Eap is only expressed by *S. aureus*. So far, inhibitory receptor - microbial interactions have been regarded as pathogenic strategies for immune evasion, and thus as detrimental for the host. However, interaction between an inhibitory receptor and a microbial ligand may also be beneficial for the host, if it prevents immune activation in response to a harmless commensal microbe. Especially when the damage caused by the immune response outweighs the damage caused by the microbe, tolerance can be an effective host defense strategy (49). Some examples of potentially beneficial inhibitory receptor – microbial interactions have been found. For instance, CEACAM1 binds Opa adhesins expressed by pathogenic *Neisseriae* (50) but also by commensal *Neisseriae* (51), although the functional outcome of the latter interaction has not been investigated.

Importantly, the difference between a pathogen and commensal is not black and white but rather a continuous scale. The *Staphylococcus* genus is a typical example of that: most staphylococci are opportunistic microbes that live a commensal lifestyle but cause occasional infections when the conditions become favorable for it (52, 53). For instance, *S. epidermidis* colonizes the skin of virtually all individuals, but it usually

only causes infections under specific circumstances such as on implanted medical devices (52, 54). In contrast, *S. aureus* is the most pathogenic staphylococcus, with its ability to cause fatal infections (55) and its various mechanisms for immune evasion (56). Still, *S. aureus* colonizes the upper respiratory tract (URT) of approximately 30% of the human population without causing symptoms (57, 58).

Considering the opportunistic lifestyle of staphylococci, is interaction between SIRL-1 and PSMs likely to be detrimental or beneficial to the host? Suggestively, our group previously described an association between lack of SIRL-1 expression on monocytes (related to the rs612529 SNP in the promoter region of VSTM1, the gene encoding SIRL-1) and an increased risk of the inflammatory skin disease atopic dermatitis (AD) (59). This led to the hypothesis that interaction between SIRL-1 and staphylococci is beneficial by preventing excessive immune responses in the skin. Due to the lack of an animal model with SIRL-1 expression, we could so far not experimentally address this hypothesis, nor could we confirm whether lack of SIRL-1 expression on monocytes indeed plays a causal role in AD. Instead, we will speculate on the answers to these questions by first discussing the contexts in which SIRL-1 and its microbial ligands may meet, with a focus on skin.

Where does SIRL-1 meet PSMs?

Somewhat surprisingly, we found that SIRL-1 expression is almost absent in healthy skin (**Chapter 2**). We did find SIRL-1 expression on eosinophils in the intestine and on monocytes and granulocytes in the lung (**Chapter 2**), but those sites are not typically colonized by staphylococci. In contrast, staphylococci are abundantly present in the URT (60), thus it would be relevant to determine SIRL-1 expression there in steady state conditions.

During inflammation, neutrophils and monocytes (which highly express SIRL-1 (59, 61)) are recruited from the circulation. However, we found no SIRL-1 expressing cells in AD lesional skin (**Chapter 2**), even though AD skin contains increased numbers of neutrophils and monocytes (62, 63). In contrast, we found several SIRL-1^{+} cells and elastase[+] granulocytes in skin from an AD patient 24 h after an atopy patch test (**Chapter 2**). Together, this suggests that SIRL-1 may be expressed for a short time frame by newly recruited cells in inflamed skin (or any other inflamed tissue with cell infiltration), followed by its downregulation. Neutrophils shed SIRL-1 with proteinase 3 (PR3) (**Chapter 5**), and monocytes could potentially do the same, as they can express PR3 (64, 65). In support, monocytes downregulate SIRL-1 expression within two hours after activation *in vitro* (66). Additionally, SIRL-1 expression might be downregulated on a transcriptional level, as shown by the low levels of SIRL-1 mRNA in Mo-MΦ in skin compared to PBMCs (**Chapter 2**).

If SIRL-1 expressing cells infiltrate the skin, which ligands do they meet there? Healthy skin is abundantly colonized by coagulase-negative staphylococci (CoNS) such as *S. epidermidis*, *S. capitis* and *S. homini*, while *S. aureus* is only present in less than 5% of the healthy population (67). In contrast, *S. aureus* colonizes the skin in more than 90% of AD patients (67), and the degree of *S. aureus* colonization correlates with the severity of AD (68). The production of PSMs by different staphylococci has to our knowledge not been compared in skin, but *S. epidermidis* δ-Toxin (an α-type PSM that ligates SIRL-1) can be abundantly detected in the epidermis of healthy human skin (40). In culture, *S. aureus* produces mostly δ-toxin and other α-type PSMs, while *S. epidermidis* produces mostly δ-toxin and β-type PSMs, although differences between strains exist (69). The endogenous ligands of SIRL-1 are also expressed in the skin. Several S100 proteins such as S100A7, S100A8, S100A9 and S100A12 are readily detected in healthy epidermis and upregulated upon tissue damage or inflammation (reviewed in (70)). LL-37 is barely detectable in healthy skin, but expressed upon skin damage (71). Notably, S100 proteins and LL-37 have pro-inflammatory effects, which is why they are considered DAMPs (72, 73). Likewise, PSMs have pro-inflammatory effects in skin; for instance, sub-cytolytic concentrations of *S. aureus* PSMs induce cytokine production by keratinocytes (74) and degranulation of mast cells (75), resulting in skin inflammation. Thus, even though the isolated effect of the interaction between SIRL-1 and its ligands is inhibitory, the net effect of these compounds on skin can be pro-inflammatory. This is also illustrated by the results in **Chapter 3**, which show that S100A6 induces ROS production by neutrophils, while ROS production is enhanced even further when SIRL-1 is blocked.

In summary, SIRL-1 is not expressed in healthy skin but might be expressed on cells that have been recently recruited to inflamed skin, where it can interact with a variety of its ligands including PSMs. SIRL-1 – PSM interactions might also take place in other inflamed tissues which are colonized by staphylococci, such as the URT. As discussed, it is not clear yet whether SIRL-1 ligands differ in their ability to cluster SIRL-1 *in vivo*. Therefore it remains to be determined whether potential changes in ligand composition, e.g. due to shifts in staphylococcal colonization, are relevant for the function of SIRL-1.

Is interaction between SIRL-1 and staphylococcal PSMs beneficial to the host?

Considering the expression of SIRL-1 and its microbial ligands, how likely is it that this interaction is beneficial to the host? We will differentiate herein between different scenarios. In injured but otherwise healthy skin, SIRL-1 on infiltrating monocytes or granulocytes may respond to PSMs from CoNS such as *S. epidermidis*. This raises the

activation threshold of these cells and inhibits their activation, similar to the model in Fig 2B. However, if the degree of stimulation transcends the activation threshold of the infiltrating cells, for example because *S. epidermidis* is invading underlying tissue, SIRL-1 is shed. All in all, this can be seen as beneficial: during mild inflammatory conditions *S. epidermidis* is tolerated via SIRL-1 - PSM interaction to prevent excessive responses and limit immunopathology, while during strong inflammatory conditions SIRL-1 is shed and neutrophils can efficiently clear the infection. Notably, some CoNS strains kill *S. aureus* and thereby counteract its colonization. A clinical trial is currently investigating the effect of CoNS as topical AD treatment (76, 77). Thus, the interaction between SIRL-1 and PSMs might not only be beneficial to limit immunopathology, but also to facilitate survival of commensal staphylococci at the expense of more pathogenic species.

Judging the outcome of the interaction between SIRL-1 and *S. aureus* PSMs is more complex. Such an interaction may occur in injured tissue that is colonized by *S. aureus,* such as skin of AD patients or the URT. Already during mild tissue damage, one may argue that it is not beneficial for the host to tolerate *S. aureus,* due to its high virulence and the (small) risk it poses for life-threatening infections (55). Moreover, if the infection becomes more severe, *S. aureus* could use Eap to prevent shedding of SIRL-1 and maintain the high activation threshold of immune cells to evade their antimicrobial response. This would be detrimental for the host. On the other hand, AD is characterized by a vicious cycle of defective barrier integrity, excessive *S. aureus* colonization, and an excessive immune response. Thus one may also argue that interaction between SIRL-1 and *S. aureus* PSMs in AD skin may dampen the already excessive immune response, and in that sense be beneficial. How these opposing scenarios combine *in vivo* has to be experimentally addressed.

In conclusion, the fluidity between commensalism and pathogenicity makes it challenging to clearly determine whether interaction between an inhibitory receptor and a microbial ligand is beneficial or detrimental to the host. Therefore, the outcome of such interactions can only be interpreted within each specific context and depends on the location of microbial exposure and the virulence of a certain strain. Still, we propose that interaction between SIRL-1 and PSMs from CoNS such as *S. epidermidis* is beneficial for the host and allows tolerance of a mostly harmless microbe. Importantly, studies on inhibitory receptor – microbial interactions typically focus on pathogens, while interactions with commensals remain largely unexplored. Arguably, this creates a bias towards outcomes of inhibitory receptors that are used for immune evasion rather than tolerance.

A potential role for SIRL-1 in atopic dermatitis

Given what we have learned about SIRL-1 from our studies, could absence of SIRL-1 play a causal role in AD? The lack of SIRL-1 expression in healthy skin makes it unlikely that SIRL-1 has a regulatory role in skin under homeostatic conditions. However, it is conceivable that brief SIRL-1 expression on tissue infiltrating monocytes may dampen their immune activation. This may be especially relevant when inflammation has already caused considerable tissue damage, resulting in a high concentration of S100 proteins and LL-37 and perhaps PSMs. Lack of such regulation on monocytes from individuals with rs612529 SNP may lead to a hyper inflammatory response such as in AD. Importantly, the regulation of monocytes by SIRL-1 requires further investigation, as inhibition of Fc-receptor-mediated ROS production is the only confirmed function (59, 66). However, SIRL-1 may also regulate other monocyte functions, such as cytokine production, migration, or differentiation into macrophages. Suggestively, low SIRL-1 expression on monocytes (possibly as a result of the rs612529 SNP, but this was not addressed) has been described as prognostic factor for major adverse cardiac events in coronary heart disease patients (78), a disease which is characterized by excessive monocyte infiltration and macrophage activity in atherosclerotic plaques (79). Since macrophage and monocyte numbers are also increased in AD skin (63, 80), it would be interesting to test whether individuals with rs612529C/C genotype have relatively more monocyte recruitment to inflamed skin than individuals with rs612529T/T genotype. Importantly, if SIRL-1 would regulate migration or macrophage differentiation, then SIRL-1 may have an impact beyond the time frame in which it is expressed.

Taken together, lack of SIRL-1 on monocytes probably does not initiate skin inflammation, but instead it might drive already existing inflammation. To further investigate this, future studies should further address 1) the dynamics of SIRL-1 expression on tissue-infiltrating monocytes in healthy and AD skin, and 2) potential regulatory roles of SIRL-1 on monocytes and macrophages. Such studies may also lead to better understanding of the function of SIRL-1 on monocytes in the lung.

Interactions between inhibitory receptors and homeostasis-associated molecular patterns (HAMPs) signal safety

Taken together, SIRL-1 can be seen as an inhibitory pattern recognition receptor (iPRR) that recognizes danger patterns (S100/LL-37) and microbial patterns. This finding prompted us to investigate whether inhibitory receptors can also recognize molecular patterns related to safety, so called homeostasis-associated molecular patterns (HAMPs). In **Chapter 7**, we discuss several potential examples of inhibitory receptors that recognize HAMPs, such as the interactions between CD300LF and phosphatidylserine, between Siglecs and sialylated glycans, or between LAIR-1 and collagen, which may signal respectively physiological cell death, "self", or an intact extracellular matrix. Sensing of safety might be especially important in epithelial barriers, which are continuously colonized by microbes and thus require a high activation threshold. Indeed, we also describe examples of inhibitory receptors on epithelial cells which recognize potential safety signals, such as trans homophilic CEACAM1 interactions which may indicate epithelial integrity (**Chapter 8**). We hypothesize that the combination of microbial signaling by activating PRRs and safety signaling by inhibitory PRRs might together lead to optimal discrimination between commensal and pathogenic colonization. As long as a microbe has a commensal lifestyle and does not invade host tissue, inhibitory PRRs such as CEACAM1 will detect epithelial integrity and provide a threshold for activation (Figure 5). At the same time, the degree of activating PRR stimulation will be only moderate, especially for PRRs that are preferentially expressed on the basolateral side of epithelial cells such as TLR3 and TLR5 (81). However, once a pathogen adopts a pathogenic lifestyle and invades the epithelial barrier, the inhibitory safety signaling is abrogated (Figure 5). Concomitantly, the degree of activating PRR stimulation will increase, which together leads to a strong immune response by the epithelium. Thus, we propose that inhibitory receptors in this system can give context to microbial signals, and allow for a more efficient immune response once a situation of safety turns into danger.
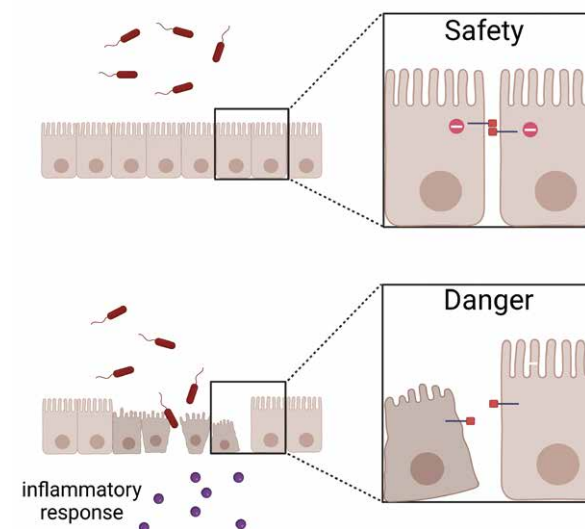

Figure 5. Proposed model on how inhibitory receptors signal a context of safety.

When barrier integrity is sensed by inhibitory PRRs such as CEACAM1, epithelial cell activation in response to bacterial colonization is dampened. In contrast, when the barrier is breached, the loss of inhibitory signaling will lead to an inflammatory response by the epithelium. Thus, inhibitory receptor ligation signals safety, while lack thereof signals danger. In addition to that, a breached epithelial barrier will lead to increased signaling of activating PRRs with basolateral localization (not depicted in this figure).

Future perspectives

In this thesis, we investigated various aspects of inhibitory receptor biology, including regulation of expression, ligand repertoires, microbial interactions, and the function of inhibitory receptors on immune cells and non-immune cells. We show that several inhibitory receptors can indicate situations of danger or safety. As such, we propose that inhibitory receptors can provide environmental context to immune cells and non-hematopoietic cells to ensure appropriate responses to their surroundings.

We hypothesized that tissues with high microbial exposure or a low capacity for regeneration might particularly require a high activation threshold and therefore benefit from regulation by inhibitory receptors (**Chapter 7**). Future studies should validate whether inhibitory receptors are indeed differentially expressed on immune cells or non-hematopoietic cells in certain tissues, depending on their proposed activation threshold. For example, how does the expression of inhibitory receptors on cells in immune privileged tissues such as the brain, eyes, or testis compare to tissues with high generation capacity such as the liver? And does inhibitory receptor expression contribute to tissue-dependent immune responses?

To gain better understanding of the requirements of ITIM signaling in these tissues, future studies should include measurements on different splice isoforms that do or do not contain intracellular ITIMs, and if possible, perform functional experiments with ITIM mutants and mutants of downstream effectors. We also want to point out that, even though the term "immune inhibitory receptor" is in most cases appropriate, it can also be misleading. As we reviewed, inhibitory receptors do not only regulate immune activation but also several other cellular processes, and the outcome of this regulation is not always inhibitory (**Chapter 8**). Therefore, we would like to encourage to look with an open eye at inhibitory receptor biology.

Increased understanding of inhibitory receptors will further pave the way for the development of drugs that target these receptors in disease. We recently developed a bioinformatics pipeline in which we identified around 400 putative ITIM-bearing receptors (manuscript in preparation). Further characterization of these receptors will provide a wealth of information and potential therapeutic targets.

Acknowledgements

The figures in this chapter were created with BioRender.com .

References

1. Rumpret M, Drylewicz J, Ackermans LJE, Borghans JAM, Medzhitov R, Meyaard L. Functional categories of immune inhibitory receptors. Nat Rev Immunol. 2020;20(12):771-80.
2. Ohnishi H, Kobayashi H, Okazawa H, Ohe Y, Tomizawa K, Sato R, et al. Ectodomain shedding of of SHPS-1 and its role in regulation of cell migration. J Biol Chem. 2004;279(27):27878-87.
3. Londino JD, Gulick D, Isenberg JS, Mallampalli RK. Cleavage of Signal Regulatory Protein alpha (SIRPalpha) Enhances Inflammatory Signaling. J Biol Chem. 2015;290(52):31113-25.
4. Ouyang W, Xue J, Liu J, Jia W, Li Z, Xie X, et al. Establishment of an ELISA system for determining soluble LAIR-1 levels in sera of patients with HFRS and kidney transplant. J Immunol Methods. 2004;292(1-2):109-17.
5. Stenberg A, Sehlin J, Oldenborg PA. Neutrophil apoptosis is associated with loss of signal regulatory protein alpha (SIRP alpha) from the cell surface. J Leukocyte Biol. 2013;93(3):403-12.
6. Wang SZ, Smith PK, Lovejoy M, Bowden JJ, Alpers JH, Forsyth KD. Shedding of L-selectin and PECAM-1 and upregulation of Mac-1 and ICAM-1 on neutrophils in RSV bronchiolitis. Am J Physiol. 1998;275(5):L983-9.
7. Eugenin EA, Gamss R, Buckner C, Buono D, Klein RS, Schoenbaum EE, et al. Shedding of PECAM-1 during HIV infection: a potential role for soluble PECAM-1 in the pathogenesis of NeuroAIDS. J Leukoc Biol. 2006;79(3):444-52.
8. Olde Nordkamp MJ, van Roon JA, Douwes M, de Ruiter T, Urbanus RT, Meyaard L. Enhanced secretion of leukocyte-associated immunoglobulin-like receptor 2 (LAIR-2) and soluble LAIR-1 in rheumatoid arthritis: LAIR-2 is a more efficient antagonist of the LAIR-1-collagen inhibitory interaction than is soluble LAIR-1. Arthritis Rheum. 2011;63(12):3749-57.
9. Zen K, Guo Y, Bian Z, Lv Z, Zhu D, Ohnishi H, et al. Inflammation-induced proteolytic processing of the SIRPalpha cytoplasmic ITIM in neutrophils propagates a proinflammatory state. Nat Commun. 2013;4:2436.
10. Houde C, Roy S, Leung N, Nicholson DW, Beauchemin N. The cell adhesion molecule CEACAM1-L is a substrate of caspase-3-mediated cleavage in apoptotic mouse intestinal cells. J Biol Chem. 2003;278(19):16929-35.
11. Lichtenthaler SF, Lemberg MK, Fluhrer R. Proteolytic ectodomain shedding of membrane proteins in mammals-hardware, concepts, and recent developments. EMBO J. 2018;37(15).
12. Ilan N, Mohsenin A, Cheung L, Madri JA. PECAM-1 shedding during apoptosis generates a membrane-anchored truncated molecule with unique signaling characteristics. FASEB J. 2001;15(2):362-72.
13. Guo X, Zhang Y, Wang P, Li T, Fu W, Mo X, et al. VSTM1-v2, a novel soluble glycoprotein, promotes the differentiation and activation of Th17 cells. Cell Immunol. 2012;278(1-2):136-42.
14. Meyer-Wentrup F, Cambi A, Joosten B, Looman MW, de Vries IJM, Figdor CG, et al. DCIR is endocytosed into human dendritic cells and inhibits TLR8-mediated cytokine production. J Leukocyte Biol. 2009;85(3):518-25.
15. Gagne V, Marois L, Levesque JM, Galarneau H, Lahoud MH, Caminschi I, et al. Modulation of monosodium urate crystal-induced responses in neutrophils by the myeloid inhibitory C-type lectin-like receptor: potential therapeutic implications. Arthritis Res Ther. 2013;15(4):R73.
16. Walter RB, Raden BW, Kamikura DM, Cooper JA, Bernstein ID. Influence of CD33 expression levels and ITIM-dependent internalization on gemtuzumab ozogamicin-induced cytotoxicity. Blood. 2005;105(3):1295-302.
17. Walter RB, Raden BW, Zeng R, Hausermann P, Bernstein ID, Cooper JA. ITIM-dependent endocytosis of CD33-related Siglecs: role of intracellular domain, tyrosine phosphorylation, and the tyrosine phosphatases, Shp1 and Shp2. J Leukoc Biol. 2008;83(1):200-11.

18. Tateno H, Li H, Schur MJ, Bovin N, Crocker PR, Wakarchuk WW, et al. Distinct endocytic mechanisms of CD22 (Siglec-2) and Siglec-F reflect roles in cell signaling and innate immunity. Mol Cell Biol. 2007;27(16):5699-710.

19. O'Reilly MK, Tian H, Paulson JC. CD22 Is a Recycling Receptor That Can Shuttle Cargo between the Cell Surface and Endosomal Compartments of B Cells. J Immunol. 2011;186(3):1554-63.

20. Perez-Figueroa E, Alvarez-Carrasco P, Ortega E, Maldonado-Bernal C. Neutrophils: Many Ways to Die. Frontiers in Immunology. 2021;12.

21. Dustin ML, Groves JT. Receptor Signaling Clusters in the Immune Synapse. Annu Rev Biophys. 2012;41:543-56.

22. Li M, Yu Y. Innate immune receptor clustering and its role in immune regulation. J Cell Sci. 2021;134(4).

23. Pageon SV, Cordoba SP, Owen DM, Rothery SM, Oszmiana A, Davis DM. Superresolution Microscopy Reveals Nanometer-Scale Reorganization of Inhibitory Natural Killer Cell Receptors upon Activation of NKG2D. Sci Signal. 2013;6(285).

24. Yokosuka T, Takamatsu M, Kobayashi-Imanishi W, Hashimoto-Tane A, Azuma M, Saito T. Programmed cell death 1 forms negative costimulatory microclusters that directly inhibit T cell receptor signaling by recruiting phosphatase SHP2. J Exp Med. 2012;209(6):1201-17.

25. Cebecauer M, Spitaler M, Serge A, Magee AI. Signalling complexes and clusters: functional advantages and methodological hurdles. J Cell Sci. 2010;123(3):309-20.

26. Mammen M, Choi SK, Whitesides GM. Polyvalent Interactions in Biological Systems: Implications for Design and Use of Multivalent Ligands and Inhibitors. Angew Chem Int Ed Engl. 1998;37(20):2754-94.

27. Cairo CW, Gestwicki JE, Kanai M, Kiessling LL. Control of multivalent interactions by binding epitope density. J Am Chem Soc. 2002;124(8):1615-9.

28. Fritz G, Botelho HM, Morozova-Roche LA, Gomes CM. Natural and amyloid self-assembly of S100 proteins: structural basis of functional diversity. FEBS J. 2010;277(22):4578-90.

29. Otto M. Phenol-soluble modulins. Int J Med Microbiol. 2014;304(2):164-9.

30. Kahlenberg JM, Kaplan MJ. Little peptide, big effects: the role of LL-37 in inflammation and autoimmune disease. J Immunol. 2013;191(10):4895-901.

31. Sancho-Vaello E, FranOois P, Bonetti EJ, Lilie H, Finger S, Gil-Ortiz F, et al. Structural remodeling and oligomerization of human cathelicidin on membranes suggest fibril-like structures as active species. Sci Rep-Uk. 2017;7.

32. Tayeb-Fligelman E, Tabachnikov O, Moshe A, Goldshmidt-Tran O, Sawaya MR, Coquelle N, et al. The cytotoxic Staphylococcus aureus PSMalpha3 reveals a cross-alpha amyloid-like fibril. Science. 2017;355(6327):831-3.

33. Schwartz K, Syed AK, Stephenson RE, Rickard AH, Boles BR. Functional amyloids composed of phenol soluble modulins stabilize Staphylococcus aureus biofilms. PLoS Pathog. 2012;8(6):e1002744.

34. Salinas N, Colletier JP, Moshe A, Landau M. Extreme amyloid polymorphism in Staphylococcus aureus virulent PSMalpha peptides. Nat Commun. 2018;9(1):3512.

35. Le KY, Villaruz AE, Zheng Y, He L, Fisher EL, Nguyen TH, et al. Role of Phenol-Soluble Modulins in Staphylococcus epidermidis Biofilm Formation and Infection of Indwelling Medical Devices. J Mol Biol. 2019;431(16):3015-27.

36. Vogl T, Gharibyan AL, Morozova-Roche LA. Pro-Inflammatory S100A8 and S100A9 Proteins: Self-Assembly into Multifunctional Native and Amyloid Complexes. Int J Mol Sci. 2012;13(3):2893-917.

37. Botelho HM, Leal SS, Cardoso I, Yanamandra K, Morozova-Roche LA, Fritz G, et al. S100A6 Amyloid Fibril Formation Is Calcium-modulated and Enhances Superoxide Dismutase-1 (SOD1) Aggregation. J Biol Chem. 2012;287(50):42233-42.

38. Schwartz K, Ganesan M, Payne DE, Solomon MJ, Boles BR. Extracellular DNA facilitates the formation of functional amyloids in Staphylococcus aureus biofilms. Mol Microbiol. 2016;99(1):123-34.

39. Lande R, Gregorio J, Facchinetti V, Chatterjee B, Wang YH, Homey B, et al. Plasmacytoid dendritic cells sense self-DNA coupled with antimicrobial peptide. Nature. 2007;449(7162):564-9.

40. Cogen AL, Yamasaki K, Muto J, Sanchez KM, Crotty Alexander L, Tanios J, et al. Staphylococcus epidermidis antimicrobial delta-toxin (phenol-soluble modulin-gamma) cooperates with host antimicrobial peptides to kill group A Streptococcus. PLoS One. 2010;5(1):e8557.

41. Marinelli P, Pallares I, Navarro S, Ventura S. Dissecting the contribution of Staphylococcus aureus alpha-phenol-soluble modulins to biofilm amyloid structure. Sci Rep. 2016;6:34552.

42. Duong AC, Cheung GY, Otto M. Interaction of phenol-soluble modulins with phosphatidylcholine vesicles. Pathogens. 2012;1(1):3-11.

43. Drab E, Sugihara K. Cooperative Function of LL-37 and HNP1 Protects Mammalian Cell Membranes from Lysis. Biophys J. 2020;119(12):2440-50.

44. Sood R, Domanov Y, Pietiainen M, Kontinen VP, Kinnunen PKJ. Binding of LL-37 to model biomembranes: Insight into target vs host cell recognition. Bba-Biomembranes. 2008;1778(4):983-96.

45. Verdon J, Girardin N, Lacombe C, Berjeaud JM, Hechard Y. delta-hemolysin, an update on a membrane-interacting peptide. Peptides. 2009;30(4):817-23.

46. Surewaard BG, Nijland R, Spaan AN, Kruijtzer JA, de Haas CJ, van Strijp JA. Inactivation of staphylococcal phenol soluble modulins by serum lipoprotein particles. PLoS Pathog. 2012;8(3):e1002606.

47. Hommes JW, Kratofil RM, Wahlen S, de Haas CJC, Hildebrand RB, Hovingh GK, et al. High density lipoproteins mediate in vivo protection against staphylococcal phenol-soluble modulins. Sci Rep. 2021;11(1):15357.

48. Van Avondt K, van Sorge NM, Meyaard L. Bacterial immune evasion through manipulation of host inhibitory immune signaling. PLoS Pathog. 2015;11(3):e1004644.

49. Medzhitov R, Schneider DS, Soares MP. Disease tolerance as a defense strategy. Science. 2012;335(6071):936-41.

50. Virji M, Watt SM, Barker S, Makepeace K, Doyonnas R. The N-domain of the human CD66a adhesion molecule is a target for Opa proteins of Neisseria meningitidis and Neisseria gonorrhoeae. Mol Microbiol. 1996;22(5):929-39.

51. Toleman M, Aho E, Virji M. Expression of pathogen-like Opa adhesins in commensal Neisseria: genetic and functional analysis. Cell Microbiol. 2001;3(1):33-44.

52. Becker K, Heilmann C, Peters G. Coagulase-negative staphylococci. Clin Microbiol Rev. 2014;27(4):870-926.

53. Krismer B, Weidenmaier C, Zipperer A, Peschel A. The commensal lifestyle of Staphylococcus aureus and its interactions with the nasal microbiota. Nat Rev Microbiol. 2017;15(11):675-87.

54. Otto M. Staphylococcus epidermidis - the 'accidental' pathogen. Nature Reviews Microbiology. 2009;7(8):555-67.

55. Peschel A, Otto M. Phenol-soluble modulins and staphylococcal infection. Nat Rev Microbiol. 2013;11(10):667-73.

56. Howden BP, Giulieri SG, Wong Fok Lung T, Baines SL, Sharkey LK, Lee JYH, et al. Staphylococcus aureus host interactions and adaptation. Nat Rev Microbiol. 2023.

57. Wertheim HFL, Melles DC, Vos MC, van Leeuwen W, van Belkum A, Verbrugh HA, et al. The role of nasal carriage in Staphylococcus aureus infections. Lancet Infect Dis. 2005;5(12):751-62.

58. Muthukrishnan G, Lamers RP, Ellis A, Paramanandam V, Persaud AB, Tafur S, et al. Longitudinal genetic analyses of Staphylococcus aureus nasal carriage dynamics in a diverse population. BMC Infect Dis. 2013;13:221.

59. Kumar D, Puan KJ, Andiappan AK, Lee B, Westerlaken GH, Haase D, et al. A functional SNP associated with atopic dermatitis controls cell type-specific methylation of the VSTM1 gene locus. Genome Med. 2017;9(1):18.

60. Natalini JG, Singh S, Segal LN. The dynamic lung microbiome in health and disease. Nat Rev Microbiol. 2022:1-14.

61. Steevels TA, Lebbink RJ, Westerlaken GH, Coffer PJ, Meyaard L. Signal inhibitory receptor on leukocytes-1 is a novel functional inhibitory immune receptor expressed on human phagocytes. J Immunol. 2010;184(9):4741-8.

62. Choy DF, Hsu DK, Seshasayee D, Fung MA, Modrusan Z, Martin F, et al. Comparative transcriptomic analyses of atopic dermatitis and psoriasis reveal shared neutrophilic inflammation. J Allergy Clin Immun. 2012;130(6):1335-+.

63. Baran W, Oehrl S, Ahmad F, Dobel T, Alt C, Buske-Kirschbaum A, et al. Phenotype, Function, and Mobilization of 6-Sulfo LacNAc-Expressing Monocytes in Atopic Dermatitis. Front Immunol. 2018;9:1352.

64. Ralston DR, Marsh CB, Lowe MP, Wewers MD. Antineutrophil cytoplasmic antibodies induce monocyte IL-8 release. Role of surface proteinase-3, alpha1-antitrypsin, and Fcgamma receptors. J Clin Invest. 1997;100(6):1416-24.

65. Ohlsson S, Hellmark T, Pieters K, Sturfelt G, Wieslander J, Segelmark M. Increased monocyte transcription of the proteinase 3 gene in small vessel vasculitis. Clin Exp Immunol. 2005;141(1):174-82.

66. Steevels TA, van Avondt K, Westerlaken GH, Stalpers F, Walk J, Bont L, et al. Signal inhibitory receptor on leukocytes-1 (SIRL-1) negatively regulates the oxidative burst in human phagocytes. Eur J Immunol. 2013;43(5):1297-308.

67. Grice EA, Segre JA. The skin microbiome. Nat Rev Microbiol. 2011;9(4):244-53.

68. Kong HH, Oh J, Deming C, Conlan S, Grice EA, Beatson MA, et al. Temporal shifts in the skin microbiome associated with disease flares and treatment in children with atopic dermatitis. Genome Res. 2012;22(5):850-9.

69. Cheung GY, Rigby K, Wang R, Queck SY, Braughton KR, Whitney AR, et al. Staphylococcus epidermidis strategies to avoid killing by human neutrophils. PLoS Pathog. 2010;6(10):e1001133.

70. Lesniak W, Graczyk-Jarzynka A. The S100 proteins in epidermis: Topology and function. Biochim Biophys Acta. 2015;1850(12):2563-72.

71. Schauber J, Dorschner RA, Coda AB, Buechau AS, Brouha B, Liu PT, et al. Injury enhances TLR2 function and antimicrobial peptide expression through a vitamin D dependent mechanism. Journal of Investigative Dermatology. 2007;127:S130-S.

72. Reinholz M, Ruzicka T, Schauber J. Cathelicidin LL-37: an antimicrobial peptide with a role in inflammatory skin disease. Ann Dermatol. 2012;24(2):126-35.

73. Foell D, Wittkowski H, Vogl T, Roth J. S100 proteins expressed in phagocytes: a novel group of damage-associated molecular pattern molecules. J Leukoc Biol. 2007;81(1):28-37.

74. Damour A, Robin B, Deroche L, Broutin L, Bellin N, Verdon J, et al. Phenol-soluble modulins alpha are major virulence factors of Staphylococcus aureus secretome promoting inflammatory response in human epidermis. Virulence. 2021;12(1):2474-92.

75. Nakamura Y, Oscherwitz J, Cease KB, Chan SM, Munoz-Planillo R, Hasegawa M, et al. Staphylococcus delta-toxin induces allergic skin disease by activating mast cells. Nature. 2013;503(7476):397-401.

76. Nakatsuji T, Hata TR, Tong Y, Cheng JY, Shafiq F, Butcher AM, et al. Development of a human skin commensal microbe for bacteriotherapy of atopic dermatitis and use in a phase 1 randomized clinical trial. Nat Med. 2021;27(4):700-9.

77. Nakatsuji T, Chen TH, Narala S, Chun KA, Two AM, Yun T, et al. Antimicrobials from human skin commensal bacteria protect against Staphylococcus aureus and are deficient in atopic dermatitis. Sci Transl Med. 2017;9(378).

78. Wang XF, Xu MC, Mao CY, En Z, He Q, Qu XQ, et al. Predictive and prognostic value of v-set and transmembrane domain-containing 1 expression in monocytes for coronary artery disease. Rev Cardiovasc Med. 2021;22(3):1009-17.

79. Barrett TJ. Macrophages in Atherosclerosis Regression. Arterioscler Thromb Vasc Biol. 2020;40(1):20-33.

80. Kiekens RCM, Thepen T, Oosting AJ, Bihari IC, Van De Winkel JGJ, Bruijnzeel-Koomen CAFM, et al. Heterogeneity within tissue-specific macrophage and dendritic cell populations during cutaneous inflammation in atopic dermatitis. Brit J Dermatol. 2001;145(6):957-65.

81. Yu S, Gao N. Compartmentalizing intestinal epithelial cell toll-like receptors for immune surveillance. Cell Mol Life Sci. 2015;72(17):3343-53.

9

CHAPTER **10**

Appendix

English Summary

The immune system is able to maintain health by distinguishing safe situations from dangerous situations. Safe situations are for example the presence of commensal (harmless) microbes, an intact barrier tissue, or regular cell renewal. In contrast, dangerous situations include the invasion of pathogenic microbes, excessive tissue damage, or the formation of cancer cells. The immune system detects such dangerous situations with an orchestra of immune cell types, which each have their specific functions. Immune cells can be roughly divided into two main groups: cells from the innate immune system and cells from the adaptive immune system. In this thesis we focus mostly on innate immune cells, which include granulocytes (consisting of neutrophils, eosinophils, and basophils), monocytes, macrophages, mast cells, dendritic cells, γδ T cells and innate lymphoid cells such as natural killer cells. One important group of receptors that these cells express are pattern recognition receptors (PRRs). These PRRs are used to recognize general patterns that are associated with pathogens or dangers. For example, some pathogen-associated molecular patterns (PAMPs) are components from bacterial cell walls, while danger-associated molecular patterns (DAMPs) are typically patterns that are released from damaged cells. Upon recognition of these patterns, innate immune cells rapidly become activated and use various tactics to eradicate the disturbance. Examples of these tactics are the phagocytosis ("eating") of pathogens, or the production of reactive oxygen species (ROS) or other toxic molecules to kill pathogens. The downside of this innate immune response is that it is somewhat unspecific, and therefore not only eradicates the pathogen but often also damages the surrounding tissue. Therefore it is highly important that the strength of the immune response is appropriate: a too strong immune response damages healthy tissue, while a too weak immune response can lead to survival of pathogens or cancer cells. This also means that it is very important that the immune system does not accidentally respond to safe situations. In some cases, the distinction between danger and safety is not easily made. For example, PAMPs are not only expressed by pathogens but also by commensal (harmless) microbes. This suggests that the innate immune system has additional mechanisms to distinguish danger from safety. Taken together, the immune system protects the host against danger, but its activity also forms a risk, which is why it needs to be tightly regulated.

One of the ways by which the activity of the immune system is regulated is by the expression of inhibitory receptors. These receptors can block the signaling of activating receptors (such as PRRs). Inhibitory receptors which are expressed continuously on immune cells can prevent that cells become activated in response to harmless stimuli. On the other hand, inhibitory receptors which are upregulated on activated immune cells can help the immune system to calm down once a dangerous situation has been resolved. The human genome encodes more than 300 of these inhibitory receptors, but only about sixty of them have been characterized.

In **Chapter 2,** we focus on one of these inhibitory receptors, named Signal Inhibitory Receptor on Leukocytes-1 (SIRL-1). Previous studies had already shown that SIRL-1 is highly expressed on monocytes and granulocytes in human blood. In this chapter, we extend this knowledge by determining the expression of SIRL-1 outside the blood, namely in the barrier tissues skin, lung, and intestine. We measure high SIRL-1 expression on nearly all granulocytes in these tissues and on monocytes in the lung, while expression is virtually absent on monocyte-derived cells in skin and colon. We conclude that SIRL-1 is differentially expressed on cell subsets in barrier tissues, and that regulation of monocytes by SIRL-1 may be particularly relevant in the lungs.

In **Chapter 3,** we are the first to identify endogenous ligands of SIRL-1, namely S100 proteins. Various S100 proteins are released upon tissue damage and induce immune activation via activating receptors, and are therefore considered DAMPs. Here, we show that S100 proteins activate SIRL-1. Previous studies had already demonstrated that SIRL-1 ligation with an agonistic antibody inhibits ROS production. We confirm here that S100 protein S100A6 also dampens ROS production via SIRL-1. In conclusion, we show that SIRL-1 recognizes the S100 protein family of DAMPs, which may provide negative feedback to activated neutrophils to limit damage caused by the immune response.

In **Chapter 4**, we describe that SIRL-1 is also ligated by phenol-soluble modulins (PSMs) from *Staphylococci* and by the endogenous cathelicidin LL-37. These ligands have multiple similarities, such as an amphipathic α-helical structure, cytotoxic properties and the ability to ligate the immune activating receptor FPR2. Based on their structure, we design synthetic peptides with an amphipathic α -helical structure that specifically ligate SIRL-1 but not FPR2, showing potential ways to specifically target SIRL-1. Based on these findings, we propose that SIRL-1 recognizes amphipathic α-helical patterns.

In **Chapter 5,** we show that SIRL-1 is shed from activated neutrophils, resulting in the release of soluble SIRL-1. In line with this, we measure increased concentration

of soluble SIRL-1 in serum of patients with COVID-19, a disease which is characterized by excessive neutrophil activation. We also delve into the mechanism of SIRL-1 shedding, and show that SIRL-1 is shed by a serine protease that is released from activated neutrophils, namely proteinase 3. Finally, we demonstrate that the shedding of SIRL-1 is prevented by the protease inhibitor Eap from *S. aureus.* Taken together, we propose that shedding of SIRL-1 might be a way to release the break of activated neutrophils, thereby allowing them to be fully active during an anti-microbial response. S*. aureus* may counteract this process to evade immune activation.

In **Chapter 6**, we investigate VSTM1-v2, a soluble splice variant of SIRL-1. We follow-up on a previous study which showed that VSTM1-v2 induces activation of Th17 cells. However, using different cell culture systems, we show that VSTM1-v2 does not enhance differentiation nor activation of Th17 cells. Thus, our data do not support a role for VSTM1-v2 in Th17 cell activation.

In **Chapter 7**, we explore inhibitory receptors as potential regulatory counterparts for activating pattern recognition receptors (PRRs). As mentioned above, activating PRRs recognize molecular patterns associated with microbes or tissue damage, which leads to immune activation. However, in some contexts such immune activation is not required, for example when sensing microbial patterns from harmless microbes or physiological cell death. Thus, immune responses needs to be context dependent. Based on literature, we describe several inhibitory receptors that recognize molecular patterns that are related to danger or homeostasis. We propose that these inhibitory pattern recognition receptors (iPRRs) provide context to immune cells to mediate appropriate responses to molecular patterns.

In **Chapter 8**, we review evidence for a regulatory role of inhibitory receptors on non-immune cells (so called non-hematopoietic cells), focusing on epithelial and endothelial cells. Similar to immune cells, non-hematopoietic cells need to sense the context in which they receive microbial or endogenous stimuli. We hypothesize that inhibitory receptors provide such context to non-hematopoietic cells. Indeed, we explain that inhibitory receptors on epithelial cells can recognize ligands on neighboring cells, resulting in inhibition of immune activation and inhibition of proliferation. We propose that these inhibitory receptors signal a situation of safety (namely intact epithelium), conveying to a cell that it does not need to become activated. This topic is largely unexplored and requires further investigation.

Altogether, we conclude that some inhibitory receptors, including SIRL-1, recognize patterns that indicate danger or safety. In this way, inhibitory receptors can provide additional information to a cell about the context in which it is receiving other stimuli. By putting forward these novel concepts, we aim to prompt further research that addresses these concepts experimentally. This will lead to increased understanding of inhibitory receptor biology and to improved therapeutic targeting of these receptors in disease.

Nederlandse samenvatting

Het immuunsysteem is in staat om ons lichaam gezond te houden door veilige situaties te onderscheiden van gevaarlijke situaties. Veilige situaties zijn bijvoorbeeld de aanwezigheid van onschadelijke microben, intact weefsel of normale celdeling. Gevaarlijke situaties zijn daarentegen het binnen dringen van ziekteverwekkers, overmatige weefselschade of de vorming van kankercellen. Het immuunsysteem herkent zulke gevaarlijke situaties met allerlei immuun cellen, die elk hun specifieke functies hebben. Immuun cellen kunnen grofweg in twee hoofdgroepen worden verdeeld: cellen van het aangeboren immuunsysteem en cellen van het adaptieve immuunsysteem. In dit proefschrift richten wij ons vooral op aangeboren immuun cellen, die onder andere bestaan uit granulocyten (bestaande uit neutrofielen, eosinofielen en basofielen), monocyten, macrofagen, mestcellen, dendritische cellen, γδ T cellen, en aangeboren lymfoïde cellen zoals "natural killer" cellen. Deze cellen hebben onder andere bepaalde patroonherkenningsreceptoren op hun oppervlak (zogenaamde PRR's) waarmee ze patronen kunnen herkennen die wijzen op de aanwezigheid van een ziekteverwekker of gevaar. Patronen die wijzen op ziekteverwekkers (zogenaamde PAMP's) zijn bijvoorbeeld bestanddelen van bacteriële celwanden, terwijl patronen die laten zien dat er gevaar is (zogenaamde DAMP's) vaak moleculen zijn die vrijkomen uit beschadigde lichaamscellen. Na herkenning van deze patronen worden aangeboren immuun cellen snel geactiveerd en gebruiken ze verschillende tactieken om de verstoring op te lossen. Voorbeelden hiervan zijn de fagocytose ("opeten") van ziekteverwekkers, of de productie van zuurstofradicalen of andere giftige moleculen om ziekteverwekkers te doden. Het nadeel van deze aangeboren immuunrespons is dat hij niet zo specifiek is, en dus niet alleen de ziekteverwekker uitroeit, maar vaak ook het omringende weefsel beschadigt. Daarom moet de sterkte van de immuunrespons precies passend zijn: een te sterke immuunrespons beschadigt gezond weefsel, terwijl een te zwakke immuunrespons juist kan leiden tot het overleven van ziekteverwekkers of kankercellen. En daarom is het ook heel belangrijk dat het immuunsysteem niet per ongeluk reageert op veilige situaties. In sommige gevallen is het niet zo makkelijk om het onderscheid te maken tussen gevaarlijke situaties en veilige situaties. PAMP's die wijzen op de aanwezigheid van ziekteverwekkers komen bijvoorbeeld ook voor op onschadelijke microben waarop het immuun systeem niet hoeft te reageren. Dit suggereert dat het aangeboren immuunsysteem in dit soort situaties nog meer manieren nodig heeft om een gevaarlijke van een veilige situatie te onderscheiden. Kortom, het immuunsysteem beschermt ons tegen gevaar, maar het vormt ook een risico en moet daarom strak worden gereguleerd.

Eén van de manieren waarop de activiteit van het immuunsysteem wordt gereguleerd is door remmende receptoren. Deze receptoren kunnen de signalering van activerende receptoren (zoals PRR's) remmen. Remmende receptoren die standaard op immuun cellen zitten kunnen ervoor zorgen dat deze cellen niet te makkelijk geactiveerd worden door onschadelijke prikkels. Remmende receptoren die juist met name op geactiveerde immuun cellen zitten kunnen ervoor zorgen dat het immuun systeem weer tot rust wordt gebracht nadat een gevaarlijke situatie is opgelost. Het menselijk lichaam bevat naar schatting meer dan driehonderd verschillende remmende receptoren, maar slechts ongeveer zestig ervan zijn onderzocht.

In **hoofdstuk 2** richten wij ons op één van deze remmende receptoren, genaamd Signal Inhibitory Receptor on Leukocytes-1 (SIRL-1). Uit eerdere studies was al gebleken dat SIRL-1 in hoge mate voorkomt op monocyten en granulocyten in menselijk bloed. In dit hoofdstuk breiden we deze kennis uit door te kijken of SIRL-1 buiten het bloed voorkomt, namelijk in de barrièreweefsels huid, long en darm. We zien veel SIRL-1 op bijna alle granulocyten in deze weefsels en op monocyten in de long, terwijl we bijna geen SIRL-1 meten op van monocyten afgeleide cellen in huid en darm. We concluderen dat SIRL-1 verschillend voorkomt op diverse types cellen in barrièreweefsels, en dat regulering van monocyten door SIRL-1 met name relevant kan zijn in de longen.

In **hoofdstuk 3** laten we zien dat SIRL-1 geactiveerd ('geligeerd') wordt door S100 eiwitten. Verschillende S100 eiwitten komen vrij bij weefselschade en worden daarom beschouwd als DAMPs. Eerdere studies hadden al aangetoond dat SIRL-1 ligatie met een activerend antilichaam ervoor zorgt dat productie van zuurstofradicalen door neutrofielen wordt geremd. Hier laten we zien dat S100 eiwitten hetzelfde kunnen doen. Onze conclusie is dat SIRL-1 S100-eiwitten herkent, en we stellen voor dat dit belangrijk zou kunnen zijn om neutrofielen te remmen als er al veel weefselschade is, om verdere schade door het immuunsysteem te beperken.

In **hoofdstuk 4** beschrijven we dat SIRL-1 ook wordt geactiveerd door bepaalde peptiden die door Stafylokokken uitgescheiden worden, zogenaamde phenol-soluble modulins (PSMs), en door een lichaamseigen peptide genaamd cathelicidin LL-37. Deze liganden hebben veel overeenkomsten, zoals een amfipatische α-helicale structuur (dat wil zeggen dat ze een α-helix vormen die aan één kant hydrofiel is en aan de andere kant hydrofoob), het vermogen cellen te doden, en het vermogen om de activerende receptor FPR2 te ligeren. Op basis van hun structuur lukt het ons om synthetische peptiden te ontwerpen die specifiek SIRL-1 maar niet FPR2

ligeren. Dit laat zien dat het in theorie mogelijk is om specifiek SIRL-1 te beïnvloeden. We concluderen dat SIRL-1 een remmende receptor is die patronen herkent met amfipatische α-helicale structuur.

In **hoofdstuk 5** laten we zien dat SIRL-1 wordt verwijderd van het oppervlakte van geactiveerde neutrofielen, waardoor oplosbaar SIRL-1 vrijkomt. In overeenstemming hiermee meten we een verhoogde concentratie oplosbaar SIRL-1 in het bloed van patiënten met COVID-19, een ziekte die gekenmerkt worden door overmatige neutrofielen activatie. We onderzoeken ook op welke manier SIRL-1 verwijdert wordt, en tonen aan dat SIRL-1 wordt afgeknipt door een protease die vrijkomt uit geactiveerde neutrofielen, namelijk proteïnase 3. Tenslotte tonen wij aan dat het knippen van SIRL-1 wordt voorkomen door de proteaseremmer Eap van de bacterie *S. aureus*. Al met al stellen wij voor dat het afwerpen van SIRL-1 door cellen een manier zou kunnen zijn om de remming van SIRL-1 op geactiveerde neutrofielen tegen te gaan, waardoor zij volledig actief kunnen zijn tijdens een antimicrobiële respons. *S. aureus* kan dit proces tegenwerken om immuun activatie te ontwijken.

In **hoofdstuk 6** onderzoeken we VSTM1-v2, een oplosbare variant van SIRL-1. We volgen een eerdere studie op waaruit bleek dat VSTM1-v2 de activering van Th17 cellen induceert, een cel type van het adaptieve immuun systeem. Met behulp van verschillende celkweeksystemen tonen wij echter aan dat VSTM1-v2 de differentiatie of activering van Th17 cellen niet bevordert. Onze resultaten ondersteunen dus niet de eerder gevonden resultaten.

In **hoofdstuk 7** onderzoeken we remmende receptoren als potentiële regulerende tegenhangers voor activerende patroonherkenningsreceptoren (PRR's). Zoals hierboven beschreven, herkennen activerende PRR's bepaalde patronen die wijzen op de aanwezigheid van microben of weefselschade, wat leidt tot immuun activatie. In sommige situaties is immuun activatie echter niet wenselijk, bijvoorbeeld bij de herkenning van onschadelijke microben of geplande celdood. De immuunrespons moet dus contextafhankelijk zijn. Op basis van de literatuur beschrijven we dat verschillende remmende receptoren ook patronen kunnen herkennen, die wijzen op de aanwezigheid van gevaar of juist veiligheid. Wij stellen voor dat remmende patroonherkenningsreceptoren op deze manier context bieden aan immuun cellen, om ervoor te zorgen dat ze op gepaste wijze reageren op hun omgeving.

In **hoofdstuk 8** bespreken we met behulp van een literatuuronderzoek of remmende receptoren ook cellen reguleren die buiten het immuun systeem vallen (zogenaamde niet-hematopoëtische cellen). Daarbij concentreren we ons op epitheel- en endotheelcellen. Net als immuun cellen moeten niet-hematopoëtische cellen de context aanvoelen waarin zij microbiële of lichaamseigen prikkels ontvangen. We stellen de hypothese dat remmende receptoren deze context bieden. Wij leggen bijvoorbeeld uit dat remmende receptoren op epitheel liganden herkennen op naburige cellen, wat zou kunnen signaleren dat de barrière van het epitheel intact is. Dit zorgt er vervolgens voor dat immuun activatie en celdeling van epitheelcellen geremd wordt. Je zou dus kunnen zeggen dat deze remmende receptoren een veilige situatie herkennen (namelijk intact epitheel), en zo laten zien dat een immuun respons of celdeling niet nodig is. Dit is een onderwerp dat verder onderzocht moet worden.

Al met al concluderen we dat sommige remmende receptoren, waaronder SIRL-1, patronen kunnen herkennen die wijzen op gevaar of juist op veiligheid. We stellen voor dat remmende receptoren op deze manier extra informatie geven aan een cel over de context waarin deze zich bevindt, zowel bij immuun cellen en bij cellen die buiten het immuun systeem vallen. Door deze nieuwe concepten naar voren te brengen willen we verder onderzoek hiernaar stimuleren. Dit zal leiden tot een beter begrip van de functie van remmende receptoren en tot een betere therapeutische aanpak van deze receptoren bij ziekte.

Curriculum vitae

Helen Juliette von Richthofen was born on the 16th of February 1989 in Berlin-Wilmersdorf, Germany. From the age of six, she lived in the Netherlands. After finishing her secondary education at the Werkplaats Kindergemeenschap in Bilthoven, she spent one year in Canada and Iceland to train Icelandic horses. In 2008, she started studying Psychobiology at the University of Amsterdam. During her studies, she also participated in an interdisciplinary honors program, and every summer she went back to Iceland for two months to train horses. In 2011, she moved to Stockholm for six months to do a research internship at the Karolinska Institute, where she studied the dopaminergic response of Fmr1 knockout mice in the lab of Gilberto Fisone. After obtaining her BSc degree with honors, Helen started working as a teaching assistant for immunology courses at the University of Amsterdam, which sparked her interest in immunology. Therefore, she decided to pursue a Master's degree in Biomedical Sciences at the University of Amsterdam, with a focus on Infection and Immunity. Her research internships took place at the Netherlands Cancer Institute in the group of Sjaak Neefjes, and at Sanquin Blood Supply in the group of Sacha Zeerleder. In 2015, she obtained her MSc degree with honors. Subsequently, she traveled for 1,5 years in Asia where she volunteered at reforestation and sustainable farming projects.

In 2017, Helen started a PhD at the Center for Translational Immunology at the UMC Utrecht under the supervision of Linde Meyaard. During her PhD, she investigated immune regulation by inhibitory receptors in blood and barrier tissues, with a focus on the inhibitory receptor SIRL-1. In 2020, she was granted the Infection & Immunity Boost grant, together with Marcel de Zoete, to study whether inhibitory receptors regulate the epithelial response to commensal microbes.

In May 2023, Helen started working as a scientist at Neogene Therapeutics in Amsterdam, to develop T cell therapies against solid cancers. She lives in Zeist, together with her husband Ahmed Mostafa and their cat Dimitri.

List of publications

This thesis

- **von Richthofen HJ**, Westerlaken GHA, Gollnast D, Besteman S, Delemarre EM, Rodenburg K, Moerer P, Stapels DAC, Andiappan AK, Rötzschke O, Nierkens S, Leavis HL, Bont LJ, Rooijakkers SHM, Meyaard L. Soluble Signal Inhibitory Receptor on Leukocytes-1 Is Released from Activated Neutrophils by Proteinase 3 Cleavage. J Immunol. 2023;210(4):389-97.

- **von Richthofen HJ**, Meyaard L. Sensing context: Inhibitory receptors on non-hematopoietic cells. Eur J Immunol. 2023:e2250306.

- **von Richthofen HJ***, Hafkamp FMJ*, van Haperen A, de Jong EC#, Meyaard L#. VSTM1-v2 does not drive human Th17 cell differentiation: A replication study. PLoS One. 2023;18(4):e0284404.

- Rumpret M, **von Richthofen HJ**, Peperzak V, Meyaard L. Inhibitory pattern recognition receptors. J Exp Med. 2022;219(1).

- Rumpret M, **von Richthofen HJ***, van der Linden M*, Westerlaken GHA, Talavera Ormeno C, Low TY, Ovaa H, Meyaard L. Recognition of S100 proteins by Signal Inhibitory Receptor on Leukocytes-1 negatively regulates human neutrophils. Eur J Immunol. 2021;51(9):2210-7.

- Rumpret M, **von Richthofen HJ**, van der Linden M, Westerlaken GHA, Talavera Ormeno C, van Strijp JAG, Landau M, Ovaa H, van Sorge NM, Meyaard L. Signal inhibitory receptor on leukocytes-1 recognizes bacterial and endogenous amphipathic alpha-helical peptides. FASEB J. 2021;35(10):e21875.

- **von Richthofen HJ**, Gollnast D, van Capel TMM, Giovannone B, Westerlaken GHA, Lutter L, Oldenburg B, Hijnen D, van der Vlist M, de Jong EC, Meyaard L. Signal Inhibitory Receptor on Leukocytes-1 is highly expressed on lung monocytes, but absent on mononuclear phagocytes in skin and colon. Cell Immunol. 2020;357:104199.

* These authors contributed equally to this work
# These authors also contributed equally to this work

Other publications

- Singh A, Miranda-Bedate A*, **von Richthofen HJ***, van der Vlist M, Kuhn R, Yermanos A, Kuball J, Keşmir Ç, Ramos MIP, Meyaard L. Novel bioinformatics pipeline for the identification of immune inhibitory receptors as potential therapeutic targets. In preparation.
- Falkenburg WJJ, **von Richthofen HJ**, Rispens T. On the origin of rheumatoid factors: Insights from analyses of variable region sequences. Semin Arthritis Rheum. 2019;48(4):603-10.
- Falkenburg WJJ, **von Richthofen HJ**, Koers J, Weykamp C, Schreurs MWJ, Bakker-Jonges LE, Haagen IA, Lems WF, Hamann D, van Schaardenburg D, Rispens T. Clinically relevant discrepancies between different rheumatoid factor assays. Clin Chem Lab Med. 2018;56(10):1749-58.
- Marsman G, **von Richthofen H**, Bulder I, Lupu F, Hazelzet J, Luken BM, Zeerleder S. DNA and factor VII-activating protease protect against the cytotoxicity of histones. Blood Adv. 2017;1(26):2491-502.
- van Rijt L, **von Richthofen H**, van Ree R. Type 2 innate lymphoid cells: at the cross-roads in allergic asthma. Semin Immunopathol. 2016;38(4):483-96.
- Juczewski K, **von Richthofen H**, Bagni C, Celikel T, Fisone G, Krieger P. Somatosensory map expansion and altered processing of tactile inputs in a mouse model of fragile X syndrome. Neurobiol Dis. 2016;96:201-15.

* These authors contributed equally to this work

Acknowledgements

stuk of honderd mooie grafiekjes uit). **Inês**, I don't remember how many evenings I turned my office chair and said "Inês… can I ask you a question?" and you always patiently answered "yes". Thank you so much! I hope these questions were not the reason you moved to another office. ;-) **Kuldeep**, it was fun being office neighbors ("work like a dog, get dog data"). **Michiel**, bedankt voor al je wetenschappelijke input – ik bewonder je snelle denken! We waren ook een goed film editing team - ik moet alleen nog even verder oefenen met zingen. **Ellen**, bedankt dat je me een inkijkje hebt gegeven in het werk van een arts. **Laura**, bedankt voor alle koffie pauzes en het trekken van de green team. **Natalie**, we hebben (nog) geen proeven gedaan samen, maar het was heel leuk om te brainstormen over hoe we onderzoek naar RSV en inhibitory receptors op neus epitheel kunnen combineren. **Eveline**, bedankt voor je hulp met het verzamelen van de COVID-19 samples. **Eline**, ik bewonder je oog-hand coördinatie. Bedankt voor de online crochet les ("arggg hoe dan?!"), het was een perfecte lockdown activiteit. **Anouk**, **Tamara**, **Jop**, en **Saskia**, bedankt voor jullie waardevolle bijdrages aan mijn projecten. Het was heel leuk en leerzaam om jullie stage begeleider te zijn en ik wens jullie veel succes in jullie toekomstige carrières! Alle andere Bonte Meyaardjes - **Klasina, Ruben, Lobke, Tiago, Suraya, Jonne, Rianne**, **Saskia, Dorine, Pauline**, **Anna**, **Susanna, Floor, Amie** en iedereen die een tijdje onderdeel was van onze groep – bedankt voor het delen van successen en "verrassingen", voor de muziek en het gelach in het lab, voor de lunch parades, voor het dragelijk maken van labjournaal dagen door middel van gezelschap en koekjes, en voor een helpende hand tijdens zo veel momenten.

Ik ben ontzettend dankbaar voor mijn paranimfen Matevž & Sjanna - jullie waren een essentieel onderdeel van mijn PhD. **Matevž**, being partners in crime on the SIRL-1 ligand projects was the best thing ever. The countless brainstorm sessions, staring at miserable ROS graphs, sharing hopes and frustrations (how many ligands can one *#@ receptor have?!), making cynical jokes to deal with those frustrations, being frequent visitors of the PMC restaurant, hiding my chocolate at my own request (with no success), teaching me some important Slovenian words (you know which ones), all the random (Rupaul / KPK) quotes - these are just some of the many memories which still bring a big smile to my face whenever I think about them! **Sjanna**, bedankt voor alle gezelligheid en lol, voor het op pijl houden van onze chocolade inname, voor het delen van de havermelkfilosofie, voor lach kicks over shorbet ice cream, voor no-gossip sessies en sinterklaas gedichten, en natuurlijk voor het delen van zo veel sputum samples (dat ene blaadje met al die nummers en kleurtjes zie ik nog steeds helder voor me :-)). Ik ben zo blij dat jullie aan mijn zijde zullen staan tijdens de grand finale van dit avontuur. Heel erg bedankt voor jullie hulp en vriendschap!

I want to sincerely thank all the scientists I collaborated with and who provided essential input to this thesis. **Esther de Jong**, **Toni van Capel** en **Florianne Hafkamp**, bedankt voor jullie belangrijke bijdrages aan de SIRL-1 expressie en VSTM1-v2 stukken. Florianne, onze samenwerking verliep altijd zeer soepel (behalve al die geweigerde powerpoints van het AUMC), dank je wel voor je inzet en co-culture expertise! **Barbara Giovannone**, thank you for introducing me to the world of skin immunology. **Jos van Strijp** en **Nina van Sorge**, bedankt voor jullie bijdrages aan het SIRL-1 – PSM project. **Huib Ovaa** en **Sjaak Neefjes,** bedankt voor de gedachtewisseling over de SIRL-1 liganden. **Cami Talavera Ormeño**, thank you for synthesizing the peptides. **Suzan Rooijakkers** en **Helen Leavis**, bedankt voor jullie bijdrages aan het soluble SIRL-1 project. **Marcel de Zoete**, het was super leuk om samen met jou een beursaanvraag te schrijven, bedankt voor die kans en de samenwerking! **Victor Peperzak**, bedankt voor je bijdrage aan het pattern recognition receptor project. **Anand Andiappan**, **Olaf Rötzschke** and **Mihai Netea,** thank you for providing scientific input and serum samples to measure soluble SIRL-1. **Hans Clevers**, **Jens Puschhof, Ninouk Akkermans, Charelle Boot,** en **Maarten Geurts**, bedankt voor de samenwerking en jullie expertise op het gebied van organoids en CRISPR technologie.

All other **CTI members**, thank you for providing valuable input during meetings, for vital sugar boosts during cake om de week, and for many chats in the corridor and behind FACS machines. **Marlot** en **Rianne,** altijd leuk om met jullie in de koffiekamer te zijn! **Office roomies**, thank you for the time we shared. During covid times, it became extra clear how much support there is in sharing a workspace. I'm happy to see that the office togetherness is back to what it was and better. **Maarten** en **Maarten**, jullie discussies waren een fenomeen, en ik heb ze zeker gemist toen jullie er niet meer waren!

CFF team, dankzij jullie kunnen we FACSen! **Jeroen**, bedankt voor je hulp met de Image stream. **Saskia**, **Mareille**, **Yvonne, Sigrid, Gerrit, Martin**, **Margje**, zonder jullie geen CTI! Bedankt voor al jullie ondersteuning.

Iets verder terug in de tijd: **Jolanda** en **Irma**, jullie enthousiasme voor immunologie en lab werk was aanstekelijk en heeft ervoor gezorgd dat ik nu ben waar ik ben. Veel dank daarvoor! Bij elke ELISA grafiek denk ik nog steeds "niet rekenen zonder tekenen". :-)

Sandies, ik voel me een ontzettende geluksvogel dat ik Sandwijck als thuisbasis had tijdens mijn PhD, en jullie als huisgenoten! Bedankt voor al jullie ondersteuning in de vorm van ontelbare bordjes eten die 's avonds voor me klaar stonden, het aanhoren van lab verhalen ("ja en dan heb je dus cellen en die worden groen"), de avondwandelingen over het landgoed, en het verzorgen van de Dimster als ik weer eens laat thuis was. Boven alles ben ik jullie dankbaar voor alle warmte en gekkigheid die ervoor zorgden dat ik me thuis voelde. Ik mis nog steeds de chaotische afwas sessies (de tupperware mis ik trouwens niet) en hoop nog vaak langs te komen om wolkendroom voor jullie te maken.

Ricky-Ann, bedankt dat je je paarden zo gul met ons deelt. Na menig mislukt experiment ("de cellen waren dood") maakte een rit op Ljómur weer alles goed. Wie naar een ponyclub voor volwassenen gaat heeft verder geen therapie nodig!

Claudia, bedankt voor je prachtige ontwerp van dit boekje. Ik ben erg blij met het resultaat en vind het heel leuk dat het ontwerp zo "in de familie" blijft. Hopelijk heeft het boekje nog vele duurzame jaren voor zich!

Mijn lieve **vriendinnen en vrienden**; vele liters thee, bos wandelingen, sauna bezoeken, vegan tosti's, advies van Gaudí, hoepels, geknutselde collages, en goede gesprekken zorgden ervoor dat ik alles wat met dit proefschrift te maken had even kon vergeten (noem niet het verboden woord!), om daarna weer met frisse energie verder te gaan. Soms zagen we elkaar meer, soms minder, maar het is zo fijn om te weten dat jullie er zijn! Bedankt voor alles!

Tot slot wil ik mijn thuisbasis heel erg bedanken, daar waar alles begint. **Mama**, bedankt dat je mijn grootste supporter bent en me altijd het vertrouwen geeft dat ik het kan. Zonder jou was ik nergens! **Papa**, danke für deine Ratschläge und für dein Vertrauen in mich. Du wohnst zwar weit weg, aber ich weiß dass du immer für mich da bist. **Joyce** en **Jasper**, het is zo fijn om een broer en zus te hebben die dezelfde taal spreken, letterlijk en figuurlijk. Bedankt voor al jullie steun en liefde!

Ahmed, habibi. I received one particularly big blessing during the time of my PhD – you! Thank you for your patience, support, and love. It takes courage to marry someone who is trying to finalize a PhD. ;-) I look so much forward to our lives together!